Geochemistry And Origin Of Late Archean-Early Proterozoic Volcanics Of The Kaapvaal Craton, South Africa

by

Henry Clay Crow 111

Submitted in Partial Fulfillment
of the Requirements for the Degree of
Doctor of Philosophy in Geochemistry

New Mexico Institute of Mining and Technology
Socorro, New Mexico
July 1988

TABLE OF CONTENTS

LIST OF TABLES

LIST OF FIGURES

ACKNOWLEDGMENTS

First, I would like to thank Dr. K.C. Condie, my advisor, for his support and guidance throughout this project. Also, thanks go out to Dave Wronkiewicz for extensive help in the field, without which I might still be wandering about the Drakensberg.

African Selection Trust Exploration, Anglo American Corporation and Johannesburg Consolidated Investment Company kindly provided core samples. Dr.s N.V. Armstrong, D.R. Hunter and A.H. Wilson of the University of Natal, South Africa helped greatly by providing most of the Pongola volcanic samples used in this study. Dr. T.S. McCarthy of the University of the Witwatersrand, South Africa kindly acted as adjunct advisor during our (Wronkiewicz and I) stay in South Africa. Tim Hewitt, Kevin Palmer and Russ Myers (three of Dr. McCarthy's students) were very helpful with core stratigraphy and logistics, as well as increasing our general knowledge of South African geology. And thanks to the "Bowery Boys" (Nick Lindsey and Ian ?) for the use of the crib and bar.

I would like to acknowledge Terry Spell and Mike Knoper for providing many hours of stimulating conversation on geology and for their support. Also, Mike Knoper wrote and provided MODULUS, a computer program for geochemical modeling, without which I would still be at the computer terminal.

I want to also thank my remaining committee members, Dr.s Marshall Reiter, James Robertson, Paul Sylvester and James Smoake.

Last, but not least, I want to acknowledge the support of my family.

This project was supported by NSF grant EAR-8742013 (to Dr. K.C. Condie).

ABSTRACT

The intermittent volcanic activity on the Kaapvaal craton over the last 3 Ga provides a means by which the mantle sources and tectonic settings can be evaluated with time. In this study cratonic and rift successions consisting of the Pongola, Dominion, Ventersdorp, Transvaal and Waterberg suitesare examined. Pongola volcanics (3.0 Ga)(Nsuze Group) are a possible rift related assemblage ranging in composition from basalt to rhyolite. Volcanics of the Dominion Group (2.8 Ga) (Rhenosterhoek Formation) are predominantly basaltic andesites and andesite and represent the protobasinal phase of the Witwatersrand basin. The largest volcanic unit of the Kaapvaal craton occurs in the Ventersdorp Supergroup (2.7 Ga) and consists of volcanics ranging in composition from basaltic komatiite (picrite) to andesite with some rhyolitic differentiates (Makwassie Formation). The Transvaal Supergroup (2.1-2.3 Ga) represents a cratonic assemblage which consists predominantly of sediments. Also present are four volcanic formations ranging in composition from basalt to andesite. The Soutpansberg Group of the Waterberg Supergroup (1.8 Ga) is a rift-related suite which contains abundant basaltic volcanics with a minor amount of rhyolite.

All volcanic rocks of the Kaapvaal craton comprise a chiefly tholeiitic suite with minor calc-alkaline affinities. Most have incompatible trace element characteristics similar to modern subduction-related magmas that include depletion in Ta-Nb relative to Th and LREE. An exception is the Machadodorp volcanics which are depleted in LILE and have relatively flat chondrite-normalized REE patterns similar to MORB. The affinity of Kaapvaal volcanics to volcanics from continental-margin arc systems is also apparent on various tectonic discrimination diagrams.

Geochemical modeling suggests that the most primitive mafic volcanics can be produced by 5-20% batch melting of a mantle garnet lherzolite. The more felsic volcanics are the product of olivine-plagioclase dominated shallow fractional crystallization. Exceptions are the Rhenosterhoek, Dullstroom and Hekpoort volcanics in which olivine-clinopyroxene dominated fractional crystallization occurs (<20 km). Enrichment in Th and La/Yb ratios, particularly in Nsuze and Hekpoort volcanics, may result from crustal contamination.

Mantle source evaluation using immobile trace element ratios (such as Th/Yb, Ta/Yb and Zr/Y) and normalized abundances suggests that the Kaapvaal mantle source is relatively homogeneous. Most Kaapvaal volcanics tap a subcontinental lithosphere mantle source which possesses a variably enriched SZC. The SZC is either the product of contemporaneous subduction or inherited from subduction prior to 3.0 Ga, possibly during greenstone belt formation. Volcanics with little or no SZC (Machadodorp Formation) may be derived from a different source or a different portion of the subcontinental lithosphere.

INTRODUCTION

Geochemical studies have shown that important changes in volcanic and sediment composition occur at the Archean-Proterozoic boundary (2.5 Ga) and these are interpreted to reflect changes in mantle and/or crustal composition (Condie, 1985; Taylor and McLennan, 1985). Going from older to younger, some of these changes include decreases in average compatible element (Ni, Co and Cr) contents of pelites and basalts, increases in initial strontium isotopic ratios of granitic rocks and increases in partially compatible and incompatible trace element composition of basalts. The trace element enrichments in basalts may reflect an increase in enriched mantle sources in the Proterozoic due to recycling of ancient enriched mantle or continental sediments (Condie, 1985). Alternatively, a sampling bias may be responsible for the apparent geochemical changes. In particular, samples of Archean greenstone belt volcanics (environment of deposition uncertain) may not be readily comparable to Proterozoic supracrustal volcanics deposited in a continental environment.

Identification and evaluation of geochemical changes across the Archean-Proterozoic boundary may prove significant in terms of understanding crust-mantle evolution and in terms of changing tectonic settings. In order to examine crust-mantle geochemical evolution, it is necessary to study a succession of rocks with the following characteristics: 1) the succession must span the Archean-Proterozoic boundary, 2) it must contain mafic volcanic rocks of similar bulk chemical composition, and 3) it must not be highly metamorphosed, altered or deformed. The Late Archean and Early Proterozoic successions on the Kaapvaal craton in South Africa meet all these requirements. To further document and understand the evolution of mantle sources of basaltic magma across the Archean-Proterozoic boundary, this dissertation reports new geochemical results from volcanics in the Precambrian Kaapvaal successions. A total of 253 sample analyses are presented.

In South Africa, stabilization of the Kaapvaal craton began just prior to 3.0 Ga and a major unconformity between granite-greenstone terranes and younger supracrustals begins with the development of the Pongola basin (3.0 Ga) on the craton's southeast margin. Basin development migrated northwestward on the Kaapvaal craton with time (Fig. 1a) and formed, sequentially, the Witwatersrand (2.8-2.75 Ga), Ventersdorp (2.75-2.7 Ga) and Transvaal (2.3-2.1 Ga) basins (Fig. 2). This basin migration is thought to be

Figure 1. a, Generalized geologic map of southern Africa showing major Precambrian domains and basins. After Anhaeusser (1973). b, generalized geologic map of southern Africa showing Precambrian basin locations and study areas. Study areas: red= Pongola; green= Dominion; brown= Ventersdorp; blue= Transvaal; purple= Soutpansberg. After Tankard et al., 1982. Heavy dashed line= proposed extent of Kaapvaal craton.

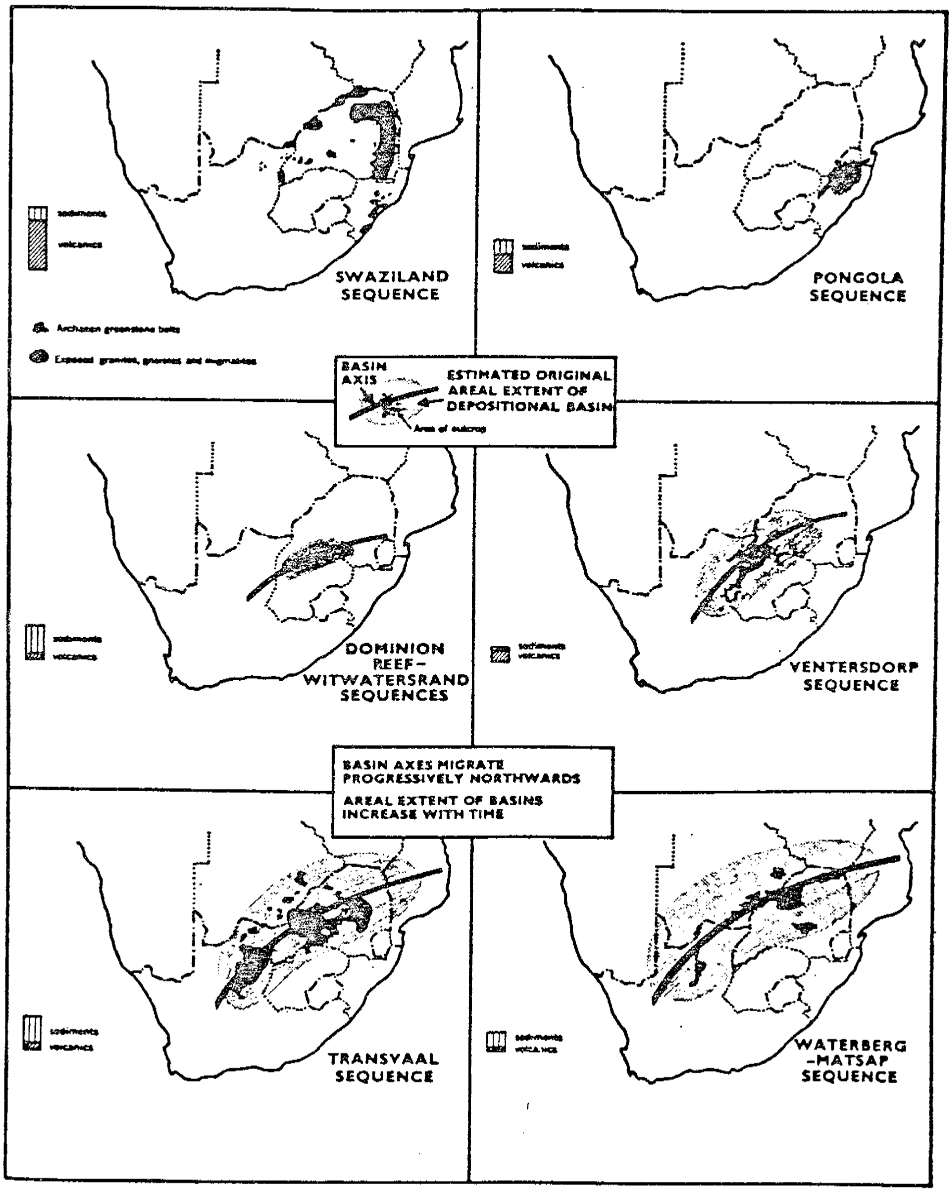
SWAZILAND SEQUENCE
PONGOLA SEQUENCE
BASIN AXIS
ESTIMATED ORIGINAL AREAL EXTENT OF DEPOSITIONAL BASIN
DOMINION REEF-WITWATERSRAND SEQUENCES
VENTERSDORP SEQUENCE
BASIN AXES MIGRATE PROGRESSIVELY NORTHWARDS
AREAL EXTENT OF BASINS INCREASE WITH TIME
TRANSVAAL SEQUENCE
WATERBERG -MATSAP SEQUENCE

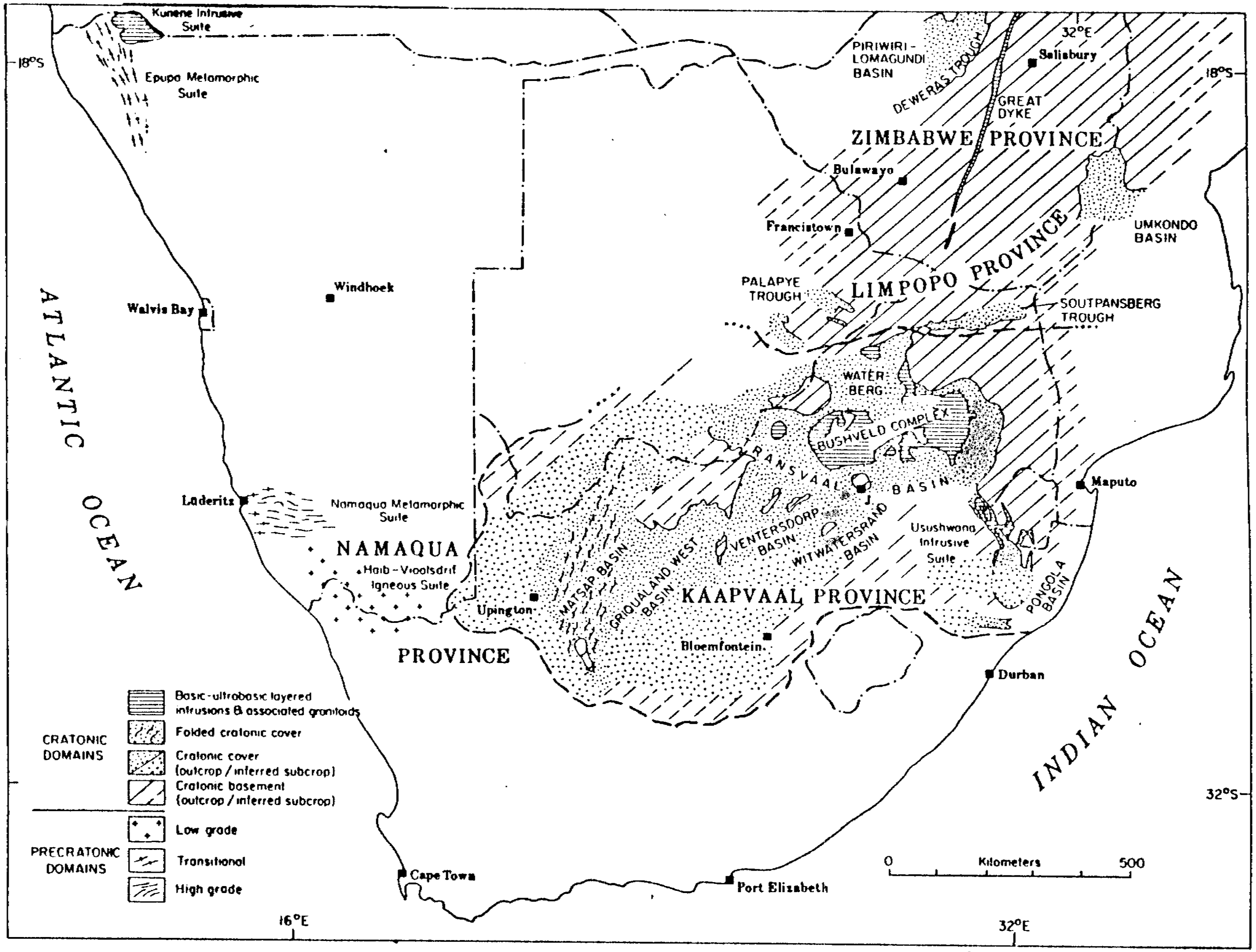

Kunene Intrusive Suite
Epupo Metamorphic Suite
18°S
ATLANTIC OCEAN
Walvis Bay
Windhoek
Lüderitz
Namaqua Metamorphic Suite
NAMAQUA
Haib-Vioolsdrif Igneous Suite
PROVINCE
Upington
Cape Town
Port Elizabeth
Bloemfontein
Durban
Maputo
INDIAN OCEAN
PIRIWIRI-LOMAGUNDI BASIN
DEWERAS TROUGH
32°E
Salisbury
GREAT DYKE
ZIMBABWE PROVINCE
Bulawayo
Francistown
UMKONDO BASIN
PALAPYE TROUGH
LIMPOPO PROVINCE
SOUTPANSBERG TROUGH
WATER BERG
BUSHVELD COMPLEX
TRANSVAAL BASIN
VENTERSDORP BASIN
WITWATERSRAND BASIN
Usushwana Intrusive Suite
PONGOLA BASIN
MATSAP BASIN
GRIQUALAND WEST BASIN
KAAPVAAL PROVINCE
CRATONIC DOMAINS
Basic-ultrabasic layered intrusions & associated granitoids
Folded cratonic cover
Cratonic cover (outcrop / inferred subcrop)
Cratonic basement (outcrop / inferred subcrop)
PRECRATONIC DOMAINS
Low grade
Transitional
High grade
0 Kilometers 500
16°E
32°E
32°S

Figure 2. Generalized stratigraphic columns of Precambrian basins on the Kaapvaal craton. After Armstrong et al. (1986); Watchorn (1980); Winter (1976); Button (1973); Barker (1979).

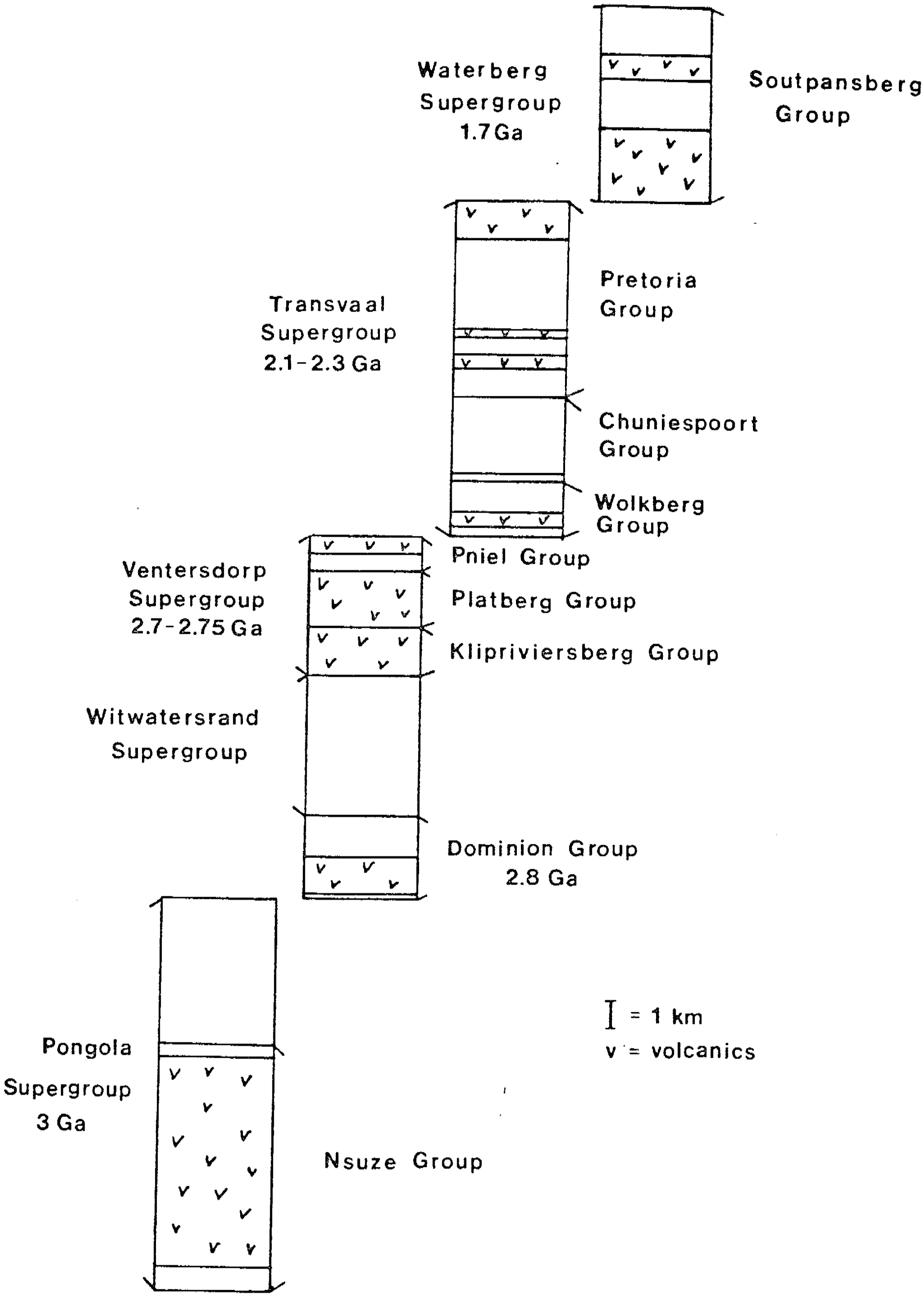
Waterberg
Supergroup
1.7 Ga
Soutpansberg
Group
Transvaal
Supergroup
2.1-2.3 Ga
Pretoria
Group
Chuniespoort
Group
Wolkberg
Group
Ventersdorp
Supergroup
2.7-2.75 Ga
Pniel Group
Platberg Group
Klipriviersberg Group
Witwatersrand
Supergroup
Dominion Group
2.8 Ga
Pongola
Supergroup
3 Ga
Nsuze Group
= 1 km
v = volcanics

the result of earlier granite emplacement which followed the same northwestern trend (Hunter, 1974). Thus, diachronous basin development resulted from and directly followed cratonization.

There are several advantages to studying volcanics on the Kaapvaal craton. One of the most important is that the stratigraphy is well known. Stratigraphic correlation on a craton-wide scale can reduce errors in sampling and facilitates a broad study such as this one. In addition, previous structural and petrologic studies are available for all units. The low grade of metamorphism (greenschist facies) and relatively small degrees of alteration of the volcanics examined are also attractive features for a geochemical study of these rocks. At this grade of metamorphism, element mobility is typically restricted to large ion lithophile elements (LILE) (K, Rb, Ba, Th) and occasionally light REE (La, Ce) while elements such as Y, Yb, Zr, Nb, Ta, Hf, Ti and Ni are immobile (Merriman et al., 1986; Ludden and Gelinas, 1982; Ludden and Thompson, 1979; Menzies et al., 1979; Floyd and Winchester, 1978; Humphris et al., 1978).

Another characteristic feature of the Kaapvaal successions is their relatively small amount of deformation. Typically, rocks of Archean age are highly folded and faulted. On the Kaapvaal craton, however, most supracrustal successions are relatively flat-lying and undeformed. The Pongola Supergroup (3.0 Ga) consists of relatively flat-lying rocks with dips generally less than 30 degrees. Rocks of the Witwatersrand (Dominion Group and Ventersdorp Supergroup) and Soutpansberg basins show evidence of normal faulting and minor folding, but again, they are only mildly deformed and show primary structures and relict mineral assembleges. In the case of the volcanics and sediments of the Transvaal Supergroup, faulting and folding are minimal.

Rocks examined in this study are from one geographical region (Fig. 1a,b). This is an advantage of great importance since speculation as to possible correlations between units, in terms of both space and time, are minimized. The study area (Fig. 1b) is in northeastern South Africa and extends from the central Kaapvaal craton (Dominion, Ventersdorp basins and a portion of the Transvaal basin), northward to the Limpopo Province (Soutpansberg basin) and eastward to the Kaapvaal cratons eastern margin (Pongola basin). Samples from the central Kaapvaal craton are from drillcore while those toward the north and east are from outcrop.

This study of Precambrian volcanics erupted on the Kaapvaal craton presents results on the geochemistry of a succession of relatively undeformed and only mildly metamorphosed volcanic rocks which span a time period of over 1 billion years. A combination of computer modeling and graphical methods are employed to develop geochemical models for the extent of crustal contamination, the petrogenesis within each suite, the tectonic setting(s), and the composition of possible mantle sources and how all of these apparently changed with time.

Geochemical results are discussed in terms of rock classification, tectonic discrimination diagrams and petrogenetic modeling for each stratigraphic unit containing major volcanic components in the four Kaapvaal basin successions. A final discussion presents tectonic models and evaluates mantle source(s) with time. Sample locations, analytical methods and analytical results are given in Appendices A, B, and C, respectively. The correlation of Dominion Group and Ventersdorp Supergroup core samples are given in Appendix D. In addition, methods of computer modeling and the distribution coefficients used in that modeling are given in Appendices E and F, respectively.

GEOLOGIC SETTING

Pongola Supergroup

Of the numerous relatively undeformed supracrustal sequences of this study deposited on the Kaapvaal craton, the oldest is the Pongola Supergroup. It is deposited on what appears to be the eastern margin of the craton (Fig. 3) shortly after cratonization at approximately 3000 Ma (Hunter, 1981). The Pongola Supergroup consists of the Nsuze and Mozaan Groups and attains a total thickness of up to 14 km (Armstrong et al., 1986). The Nsuze Group (up to 8.8 km thick) consists of sediments and volcanics, the latter of which range in composition from basalt to rhyolite. The Mozaan Group conformably overlyies the Nsuze Group in the north and is composed chiefly of shales, quartz arenites, conglomerates and minor intercalations of banded iron formation. Toward the southeast, these sediments rest on successively older units in the Nsuze Group (Button, 1981). Age determinations from the Pongola Supergroup are summarized in Hegner et al.(1984) and range from approximately 2900 to 3100 Ma. According to these authors, the best estimate of the crystallization age of Nsuze rhyolite is 2940 $\pm$ 22 Ma (U-Pb zircon age, concordia intercept), somewhat

Figure 3. Generalized geologic map and stratigraphic columns of the Pongola Supergroup, South Africa. Major exposures of both pre- and post-Pongola plutons are also shown. Geology after Button (1981).

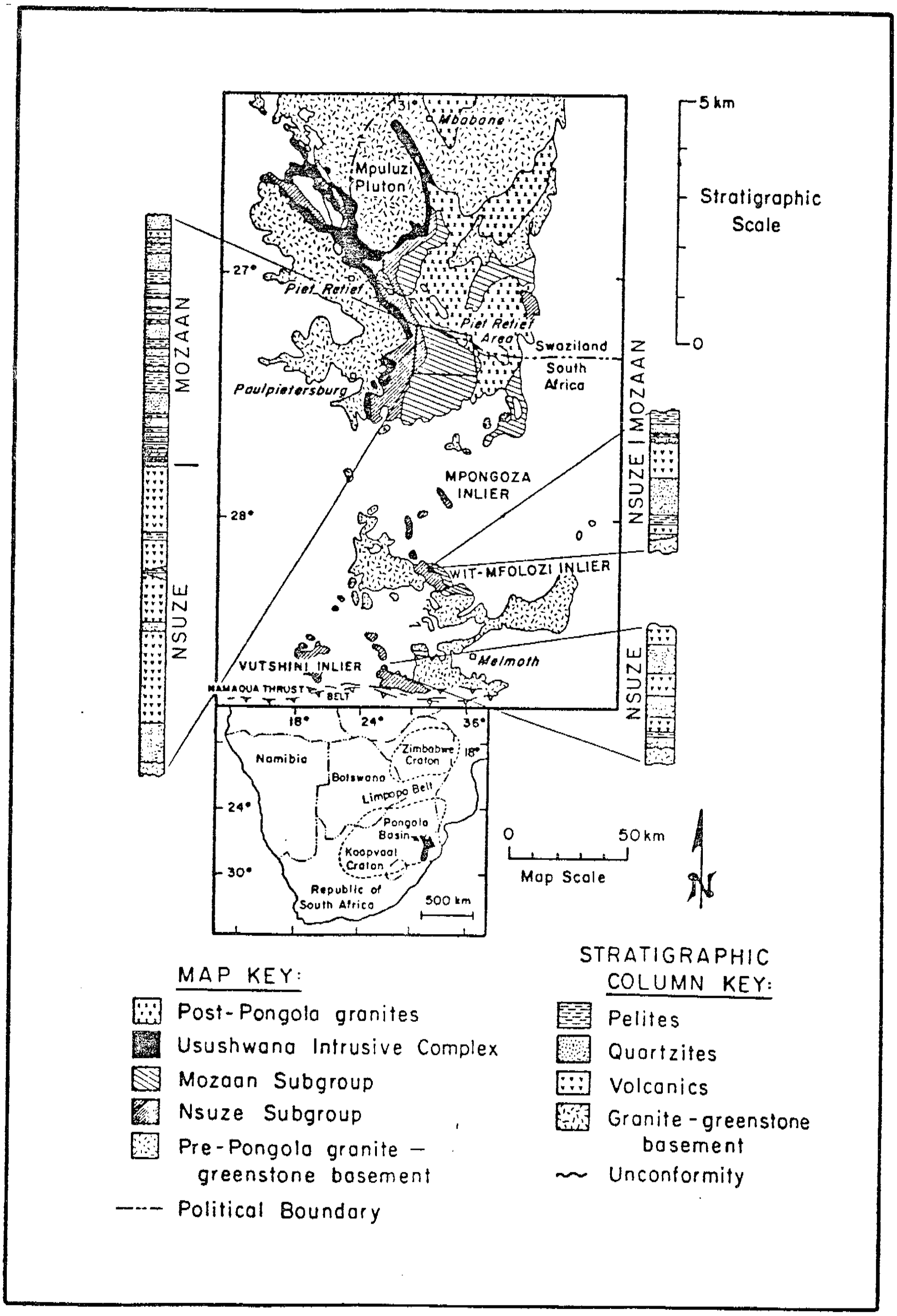
31°
Mbabane
Mpuluzi Pluton
5 km
Stratigraphic Scale
0
27°
Piet Retief
Piet Retief Area
Swaziland
South Africa
Paulpietersburg
MOZAAN
NSUZE
NSUZE | MOZAAN
MPONGOZA INLIER
28°
WIT-MFOLOZI INLIER
Melmoth
VUTSHINI INLIER
NAMAQUA THRUST BELT
18°
24°
36°
Zimbabwe Craton
Namibia
Botswana
Limpopo Belt
Pongola Basin
Kaapvaal Craton
30°
Republic of South Africa
500 km
0
50 km
Map Scale
N
MAP KEY:
Post-Pongola granites
Usushwana Intrusive Complex
Mozaan Subgroup
Nsuze Subgroup
Pre-Pongola granite — greenstone basement
Political Boundary
STRATIGRAPHIC COLUMN KEY:
Pelites
Quartzites
Volcanics
Granite - greenstone basement
Unconformity

younger than the basement upon which it rests (~3000 Ma).

The Nsuze Group occurs in a roughly north-south trending basin that formed on the southeastern flank of the Mpuluzi pluton (Lochiel granite)(Armstrong et al., 1982) in northern Natal and southeastern Transvaal Provinces of South Africa and adjacent Swaziland (Fig. 3). Estimates derived from preserved outcrops of the Pongola Supergroup suggest a minimum depositional basin size of 32,500 km^2 (Button, 1981). The contact with the underlying granitic basement is nonconformable in the west and is masked on the east and north by younger intrusions.

The Nsuze Group is subdivided into 3 formations (Armstrong et al., 1986): these are, from oldest to youngest, the Montonga, Bivane and Roodewal. The Montonga Formation is composed of quartz wackes, quartz and arkosic arenites, local conglomerates of fluvial origin, lava flows, air-fall tuffs and volcanogenic sediments. The overlying Bivane Formation consists of a thick (7500 m) succession of volcanics ranging from basalt to rhyolite in composition with local quartz wacke lenses. The uppermost Roodewal Formation is composed of predominantly volcanogenic sediments intercalated with lavas, tuffs, sandstones and argillites.

All rocks in the Nsuze Group are recrystallized to greenschist-facies mineral assemblages. In mafic igneous rocks the minerals include tremolite-actinolite, plagioclase, magnetite, quartz, chlorite, epidote and sphene. Plagioclase is commonly saussuritized (Armstrong et al., 1986). The succession is only mildly deformed and consists of domes and basins with dips generally less than 30^0 (Button, 1981). Comparable ages from various isotopic systems on the Usushwana Complex (2.9 Ga) which intrudes the Pongola Supergroup indicate that no large scale regional metamorphism has occurred in the eastern Kaapvaal craton since 2.9 Ga. Only in the southernmost outcrops is the Nsuze Group highly deformed and metamorphosed as a result of tectonism due to its proximity to the Namaqua-Natal mobile belt.

Individual lava flows in the Nsuze Group represent primarily subaerial eruptions and are generally less than 50 m thick and extend laterally for a maximum of 10 km (Armstrong et al., 1982). Mafic to intermediate lavas are amygdaloidal and porphyritic, and flow-contact breccias are common. Pillows are limited to outcrops in the White-Mfolozi inlier (Tankard et al., 1982).

Opinions as to the tectonic setting of the Pongola Supergroup vary considerably. Based on apparent bimodal silica contents in Nsuze volcanics and the presence of rift-related sediments (conglomerates and arkoses) in both the Mozaan and Nsuze Groups, Burke et al. (1985) suggest that the Pongola Supergroup was deposited in an intracratonic rift. Hegner et al. (1984) consider the Pongola Supergroup to have formed in a rift-related intracratonic basin, which they suggest represents a failed greenstone belt. The absence of alkaline volcanics in the Pongola Supergroup, however, led Armstrong et al. (1986) to conclude that the tectonic setting of the Pongola Supergroup has no modern analogue. Tankard et al. (1982) rely on calc-alkaline-type REE patterns for their interpretation of the Pongola Supergroup as a remnant of a volcanic arc. The presence of granitic basement and a thick sequence of quartz arenites at the base of the Nsuze Group suggest that this arc is restricted to a continental setting.

Dominion Group

Volcanic and sedimentary rocks of the Dominion Group (2.8 Ga) rest unconformably on granitic basement (Van Niekerk and Burger, 1969; Watchorn, 1980; 1981). The succession represents the protobasinal phase of the overlying Witwatersrand Supergroup (Tankard et al., 1982). Although the Dominion Group was probably deposited in a graben or half graben (Pretorius, 1976), the tectonic setting still remains a subject of considerable debate. Among the leading contenders for the tectonic setting are various continental rift and arc models (Tankard et al., 1982; Burke et al., 1986).

The Dominion Group (<3000 m thick) occupies an area of approximately 15,000 km^2 in the western Orange Free State and southwestern Transvaal (Fig. 4). It is exposed in several places west of Klerksdorp and along the southeastern limb of the Varkenskraal anticline south of Ventersdorp. The stratigraphy of the Dominion Group is reasonably well known from both surface and drillcore data. Samples for this study are taken from three drillcores located along the Varkenskraal anticline, two from north of Klerksdorp (BBS, BSF) and the third (BTF), from south of Ventersdorp (Fig. 4). Geochemical correlation of the three cores is based on statistical analysis (Appendix D).

The Dominion Group consists of three formations which are, from oldest to youngest, the Rhenosterspruit, Rhenosterhoek, and Syferfontein (Whiteside, 1970; Watchorn, 1980; 1981; South African Committee on Stratigraphy, 1980 [SACS]). The Rhenosterspruit Formation consists of up to 100 m of feldspathic sandstone and quartzite with minor

Figure 4. Maps showing distribution of major outcrops (stipple a) and of probable subsurface extent (stipple b) of the Dominion Group in South Africa (after Watchorn, 1980; 1981 and Tankard et al., 1982). Locations of the three drillcores (BSF, BBS, BTF) used in this study are also noted in a.

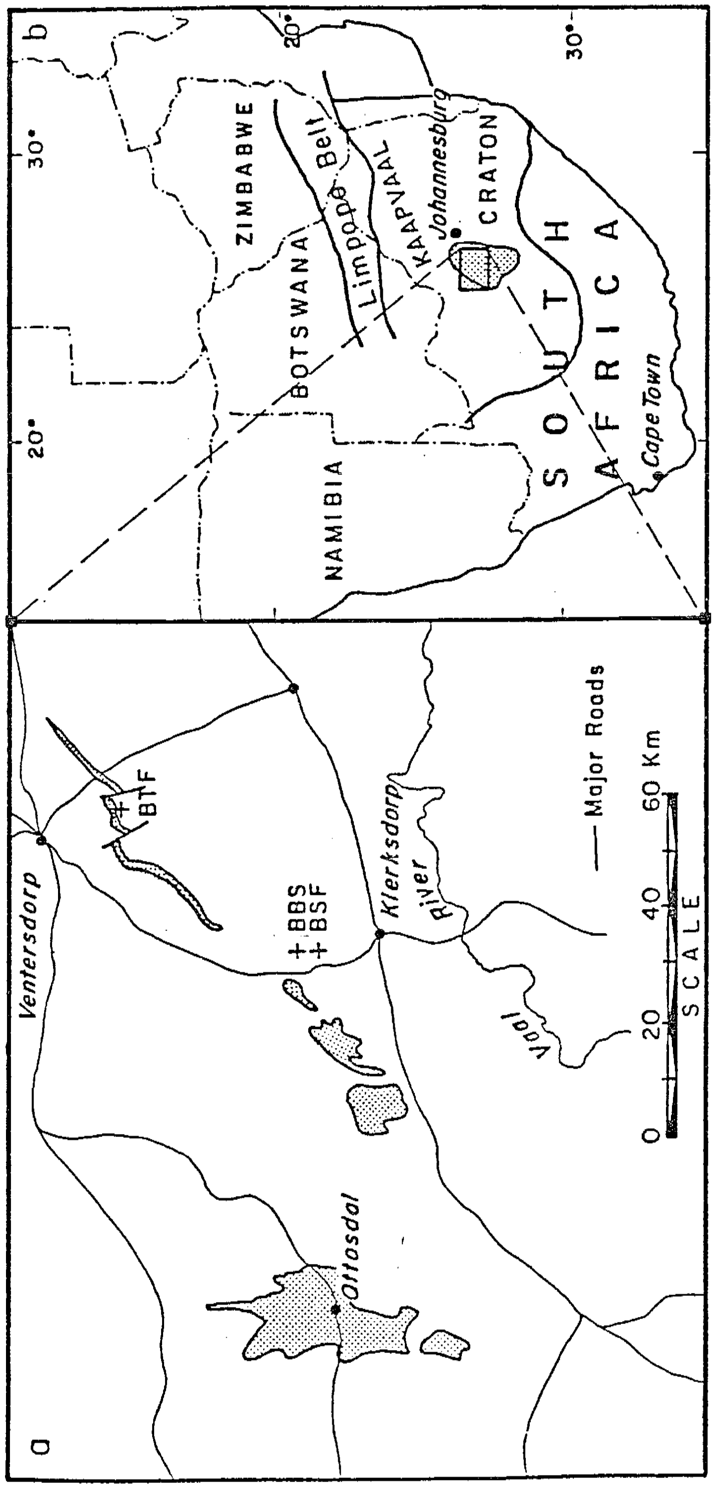

a
Ventersdorp
BTF
BBS
BSF
Klerksdorp
Vaal
River
Ottosdal
Major Roads
0
20
40
60 Km
SCALE
b
ZIMBABWE
BOTSWANA
NAMIBIA
Limpopo Belt
KAAPVAAL
CRATON
Johannesburg
SOUTH
AFRICA
Cape Town
20°
30°

conglomerate beds near the base and an increasing proportion of intercalated lavas and tuffs near the top (Watchorn, 1980). In the drillcores used in this study, the Rhenosterspruit Formation ranges from 0 to 5 m thick and consists entirely of feldspathic quartzites that rest unconformably on older Archean basement (Fig. 5). The conformably overlying Rhenosterhoek Formation contains upward of 1100 m of basaltic andesite and andesite lavas with minor felsic porphyries. Within each core separate flows can be recognized by amygdaloidal and, in some cases, brecciated flow tops. A widespread brecciated lava located 200-300 m from the base of the Rhenosterhoek Formation (SACS, 1980) is observed in all three of the cores (Fig. 5). Although the formation is comprised mainly of flows, minor tuffs occur near the top of the sections. Paleosols, indicative of periods of volcanic quiescence, are also described in the Rhenosterhoek (Button and Tyler, 1981; Grandstaff et al., 1986). In this study, paleosols were found only in core BTF (Fig. 5). The Syferfontein Formation consists of up to 1500 m of mainly felsic porphyries and conformably overlies the Rhenosterhoek Formation (Whiteside, 1970). It also includes a small amount of basaltic to andesitic flows as well as felsic tuffs and breccias. This formation does not occur in the cores used in this study and, with exception of one

Figure 5. Generalized stratigraphic sections of the Rhenosterhoek Formation from the three drillcores used in this study (locations shown on Fig. 4a). Clastic sediments are the Rhenosterspruit Formation.

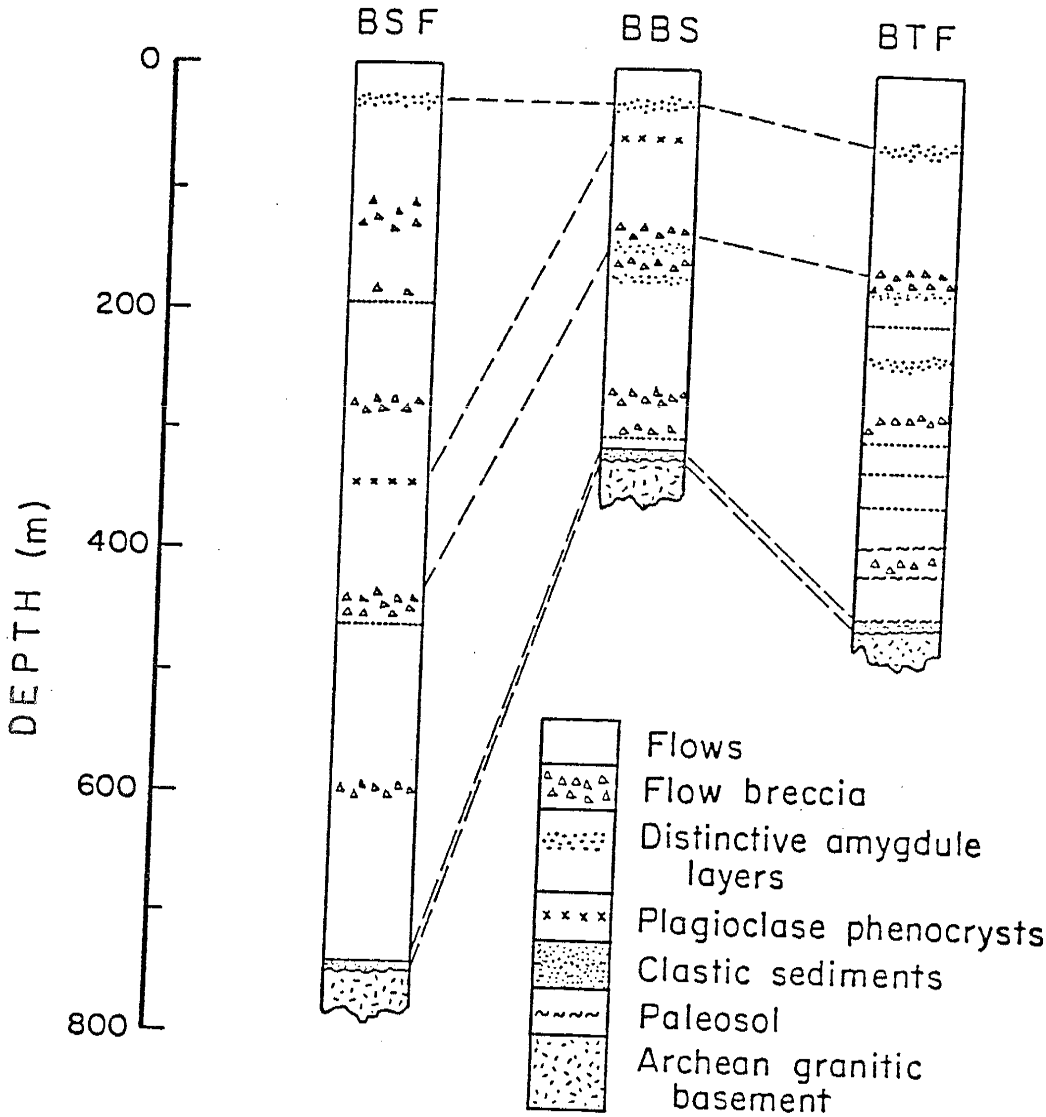
BSF
BBS
BTF
0
200
400
600
800
DEPTH (m)
Flows
Flow breccia
Distinctive amygdule layers
Plagioclase phenocrysts
Clastic sediments
Paleosol
Archean granitic basement

surface sample, Syferfontein volcanics have not been analyzed.

Ventersdorp Supergroup

The Ventersdorp Supergroup represents the largest and most widespread occurrence of volcanic rocks on the Kaapvaal craton (Fig. 6). It appears to have been deposited near the center of the craton and consists of a 5 km thick sequence of subaerial volcanic rocks with small amounts of sediment. The lowermost portion of the supergroup, the Klipriviersberg Group, bears a remarkable resemblance to young flood basalts (Wyatt, 1976) in terms of thickness and lateral extent.

The Ventersdorp Supergroup occupies a large northeast-southwest trending basin which covers an area of over 200,000 km^2 (Fig. 6). The contact between the Ventersdorp and the underlying Witwatersrand Supergroup is conformable in the vicinity of Johannesburg, along the northeastern margin of the Ventersdorp basin (Tankard et al., 1982). In the western part of the basin, the contact becomes unconformable with a 5 degree angular discordance. Here the succession is underlain by the Dominion Group and Archean granite-greenstone basement (Hunter et al., 1981; Stanistreet et al., 1986). The Ventersdorp succession has not

Figure 6. Map showing the outcrop distribution (black)and probable subsurface extent (v-pattern) of the Ventersdorp Supergroup in South Africa (after Hunter, 1981). Locations of drillcores used in this study are also shown.

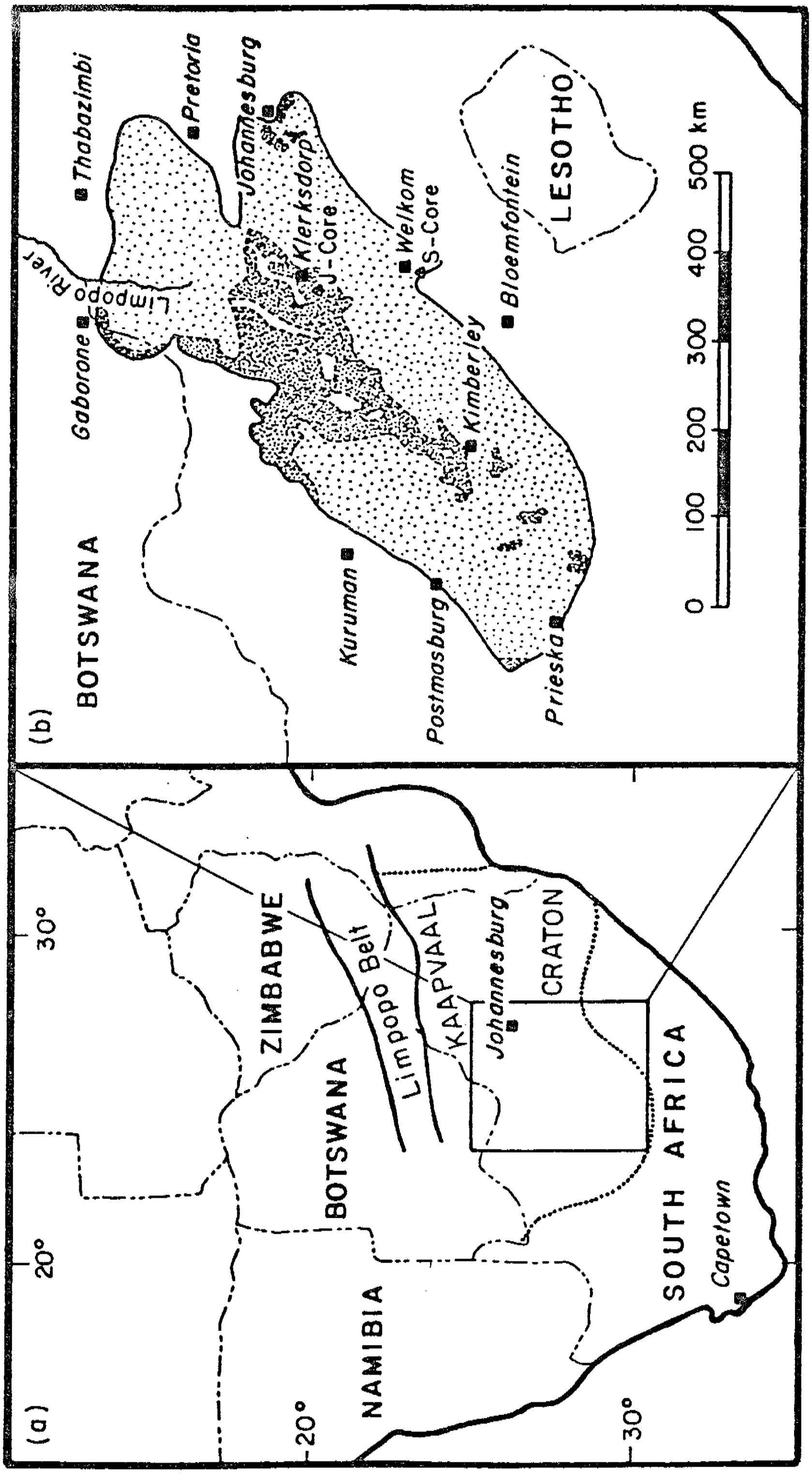
(a)
ZIMBABWE
BOTSWANA
NAMIBIA
SOUTH AFRICA
Limpopo Belt
KAAPVAAL
CRATON
Johannesburg
Capetown
20°
30°
20°
30°
(b)
BOTSWANA
LESOTHO
Thabazimbi
Pretoria
Johannesburg
Gaborone
Limpopo River
Klerksdorp
J-Core
Welkom
S-Core
Bloemfontein
Kimberley
Kuruman
Postmasburg
Prieska
0 100 200 300 400 500 km

undergone major deformation and metamorphic grade is generally lower greenschist facies.

Ventersdorp volcanics are divided into 3 groups: these are, from oldest to youngest, the Klipriviersberg, Platberg and Pniel Groups (Table 1)(Winter, 1976). The mafic to ultramafic lavas of the Klipriviersberg Group are laterally extensive and geochemically correlative from the Evander gold fields in the east to the Klerksdorp gold fields in the west (Myers et al., 1986). The scarcity of sediments and paleosols in the Klipriviersberg Group suggests rapid extrusion of lavas. The conformably overlying Platberg Group is also laterally extensive and outside the Klipriviersberg basin it rests unconformably on steeply dipping older strata. Burke et al. (1985) suggest that the lavas and immature sediments of the Platberg Group were deposited in active fault troughs. The deposition of the unconformably overlying Pniel Group follows a period of extensive erosion and it overlaps most of the older Ventersdorp units.

Poor surface exposures and low relief result in a minimum number of surface outcrops available for sampling and hence, of the 92 samples analyzed, 76 are from two drillcores (Fig. 6; Table 1): 1) the J-core from southwest of Klerksdorp contains the entire Ventersdorp Supergroup with exception of the Alberton

TABLE 1. Stratigraphy of the Ventersdorp Supergroup, South Africa

Group	Formation	Thickness(m)*	Lithology
Pniel Group	Allanridge	(100, 0)	Porphyritic lava, occasionally amygdaloidal
	Bothaville	(20. 0)	Conglomerate, sandstone, shale and limestone
Platberg Group	Rietgat	(210, 0)	Amygdaloidal, porphyritic basaltic andesite; minor siltstone and shale
	Makwassie	(200. 0)	Predominantly felsic porphyritic lava
	Goedgenoeg	(260, 0)	Amygdaloidal, porphyritic basaltic andesite
	Kameeldoorns	(15, 0)	Conglomerate, debris flow deposits, arkose, siltstone and carbonate
Klipriviersberg Group	Edenville	(0, 400)	Fine-grained basalt and basaltic komatiite; scattered amygdules
	Loraine	(690, 335)	Fine-grained basalt and basaltic komatiite; scattered amygdules
	Jeannette	(100, 270)	Numerous thin amygdaloidal basalt flows
	Orkney	(400, 150)	Fine-grained basalt; scattered amygdules
	Alberton	(0, 0)	Amygdaloidal lava
	Westonaria	(0, 0)	Fine-grained basaltic komatiite

* values for J and S cores, respectively
(lithologies after Winter, 1976; Hunter, 1981; Bowen et al., 1986)

and Westonaria Formations which were only locally deposited, and 2) the S-core from southwest of Welkom which includes only the Klipriviersberg Group. The distance between the two cores is about 120 km. Samples of the Meredale Member were collected from outcrops in the Klipriviersberg Hills south of Johannesburg.

Numerous ages have been suggested for the Ventersdorp Supergroup. Rb-Sr isochron dates and U-Pb zircon dates from the Makwassie Formation (upper Ventersdorp) range from 2460 Ma to 2695 Ma (Coertze et al., 1978; Tyler, 1979). Recent results obtained from ion microprobe studies of zircons yield U-Pb dates of 2699 $\pm$ 16 Ma and about 2750 Ma for the Makwassie Formation and the Klipriviersberg lavas, respectively (Armstrong, 1986; Phillips, 1986). These latter dates may approximately bracket the time span of eruption of Ventersdorp lavas. The origin and tectonic significance of Ventersdorp lavas are important in terms of the evolution of the Kaapvaal craton. Geological evidence supports a continental rift tectonic setting. Whether such a rift developed within the craton or as a foreland basin related to southward dipping subduction, however, remains a topic of discussion (Burke et al, 1985; Schweitzer and Kroner, 1985; Stanistreet et al., 1986).

Klipriviersberg Group

The Klipriviersberg Group (KB) is comprised chiefly of subaerially erupted mafic lavas which reach a maximum thickness of about 1800 m (Table 1). The Westonaria Formation, the lowermost formation in the KB Group, is approximately 80m thick and consists of fine-grained basaltic and basaltic komatiite lavas that cover a wide area in the Witwatersrand basin (Winter, 1976). The komatiitic Meredale Member is only locally deposited and is the least altered part of the Westonaria Formation. The overlying Alberton, Orkney, Jeannette, Loraine and Edenville Formations are composed almost entirely of volcanic rocks and show a progressively more primitive character (increasing Ni, Cr and Mg number) with increasing stratigraphic height. The lower Alberton, Orkney, and Jeannette Formations are basaltic in character while the Loraine and Edenville Formations contain basalts and subordinate basaltic komatiites or picrites.

In the drillcores used in this study, formations in the Klipriviersberg Group show variable thicknesses (Table 1). The Edenville Formation does not occur in the J-core and the Alberton and Westonaria Formations are absent in both cores. Correlation of the Orkney, Jeannette and Loraine Formations between cores is based on textural and geochemical similarities (Appendix D).

Meredale lavas consist of long needles of tremolite-actinolite that replace pyroxenes or olivine and resemble spinifex textures observed in komatiites (McIver et al., 1982). The groundmass is extremely fine-grained and chloritic and may represent devitrified glass. In general, KB lavas are composed of fine-grained greenschist-facies metamorphic assemblages of actinolite-tremolite, chlorite, plagioclase, epidote, sphene and calcite. Relict ophitic textures are present and characterized by altered and embayed plagioclase with interstitial actinolite-chlorite-epidote (altered clinopyroxene). Relict clinopyroxene occurs in some porphyritic samples.

The presence of chloritoid and pyrophyllite in the shaly units of the Witwatersrand Supergroup which underlies the Ventersdorp Supergroup suggests metamorphic temperatures of 350 ± 50^{0}C and pressures of 1 to 2 kb (Phillips, 1986).

Platberg Group

The Platberg Group consists of 3 formations which are, from oldest to youngest, the Kameeldoorns, Makwassie and Rietgat Formations (SACS, 1980) (Table 1). In addition, a sequence of mafic to intermediate lavas is frequently present between the sediments of the Kameeldoorns Formation and the more felsic lavas of the Makwassie Formation. Following the nomenclature of Bowen et al. (1986), these lavas are designated as the Goedgenoeg Formation (Table 1). The Kameeldoorns Formation is composed of conglomerates and debris flow deposits that grade basinward into arkoses, siltstones and carbonates. In the study area, this formation attains a thickness of only 15 m. As noted by Bowen et al. (1986), the Rietgat and Goedgenoeg Formations are compositionally similar. The lavas of these formations are fine to medium-grained and porphyritic with plagioclase as the most common phenocryst. Abundant quartz-chlorite filled amygdules occur in thin, repetitious zones often associated with breccias and may represent the tops of flows. Chlorite alteration is also common in some of these zones. The volcanics of the Makwassie Formation are predominantly felsic quartz porphyries which may have erupted as lava flows (Winter, 1976; Grobler et al., 1982). Evidence such as fragmented phenocrysts and possible relict fiamme are suggestive of an ash flow origin for some of the units (Bowen, 1984; Bowen et al., 1986).

Pniel Group

The Pniel Group comprises the uppermost part of the Ventersdorp Supergroup and includes two formations: the Bothaville and Allanridge (Table 1). The Bothaville Formation includes a cyclic sequence of basal conglomerates which grade upward into sandstones, shales and limestones (Hunter, 1981). These sediments are the most mature of Ventersdorp sediments and lack the rapid facies changes characteristic of Platberg sediments (Burke et al., 1985). The environment of deposition has been described as an alluvial plain or fan (Tankard et al., 1982).

The conformably overlying Allanridge Formation contains intermediate volcanics, reported by Visser et al. (1976) to be pillowed near the base. The lava flows are fine to medium-grained and locally amygdaloidal. In thin section, Allanridge volcanics have relict hyalo-ophitic textures and contain abundant altered and embayed relict plagioclase phenocrysts, altered glass, clinopyroxene pseudomorphs (replaced by actinolite-chlorite-epidote) and occasional relict clinopyroxene.

Transvaal Supergroup

The Transvaal Supergroup represents the least deformed and most widespread sequence of this study.

This 12 km thick sequence was deposited in the south-central to northeastern portions of the Kaapvaal craton (Fig. 7a) and contains both subaerial and subaqueous volcanics and sediments consisting of wackes, arkoses, siltstones, shales, conglomerates and chemical sediments. Ages from the Transvaal Supergroup range from 2300 to 2100 Ma. A Rb-Sr whole rock date of 2263 ± 85 Ma is reported on the Timeball Hill Formation (Hamilton, 1977), a shale unit in the lower Pretoria Group. A slightly younger date of 2224 ± 21 Ma (Rb-Sr; whole rock) is given for the Hekpoort Formation (D. Crampton, unpublished data, 1972; in Tankard, 1982). The lower age limit is constrained by a 2095 ± 24 Ma date (Rb-Sr; whole rock) for the Bushveld Complex which intrudes the Transvaal rocks (Hamilton, 1977). Similarly, in the north Cape Province the unconformably overlying Matsap Group yields a date of 2070 ± 70 Ma by Rb-Sr whole rock analysis.

The Transvaal Supergroup occupies two large basins covering some 500,000 km^2 (250,000 km^2 preserved) in the northwest Cape Province, Transvaal Province and eastern Botswana (Fig. 7a). The two basins are separated by a north-northwest trending arch composed primarily of Ventersdorp lavas (Hunter, 1981). In

Figure 7. a= Map showing the distribution of the Transvaal Supergroup and Soutpansberg Group in South Africa; b= Stratigraphy of the Transvaal and Soutpansgerg sequences, South Africa. v pattern= volcanic units.

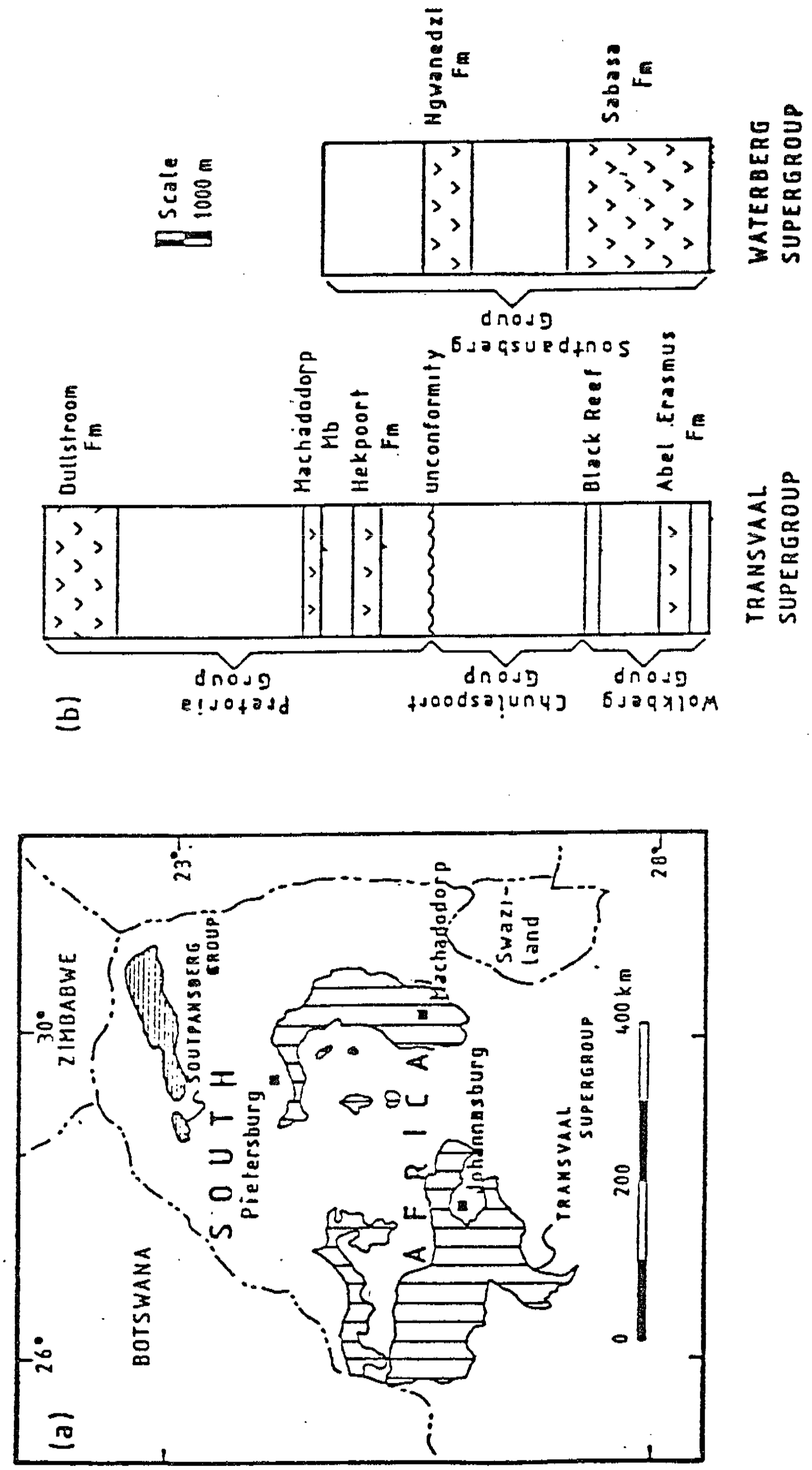
(a)
26°
30°
23°
28°
BOTSWANA
ZIMBABWE
SOUTPANSBERG GROUP
SOUTH AFRICA
Pietersburg
Machadodorp
Johannesburg
Swaziland
TRANSVAAL SUPERGROUP
0
200
400 km
(b)
Dullstroom Fm
Machadodorp Mb
Hekpoort Fm
unconformity
Black Reef
Abel Erasmus Fm
Pretoria Group
Chuniespoort Group
Wolkberg Group
TRANSVAAL SUPERGROUP
Scale 1000 m
Ngwanedzi Fm
Sabasa Fm
Soutpansberg Group
WATERBERG SUPERGROUP

other localities, the Ventersdorp Supergroup uncomforably underlies the Transvaal Supergroup.

A series of minor north-northeast trending normal faults are present in the eastern Transvaal depositional basin and appear to be gravity faults (Hunter, 1981). In general, the Transvaal Supergroup is described as being deposited on a stable craton undergoing thermal subsidence but relatively unaffected by faulting (Button, 1973; Hunter, 1981; Clendenin et al., 1988).

The Transvaal Supergroup is subdivided into three groups separated by unconformities which are, from oldest to youngest, the Wolkberg Group, Chuniespoort Group and Pretoria Group (Fig. 7b).

Wolkberg Group

The Wolkberg Group is up to 2000 m thick and occurs along the northeastern margin of the Transvaal basin. Basal coarse grained sediment consisting of subgraywacke, arkose and local conglomerates of fluvial origin and minor shales are overlain by the Abel Erasmus Formation which in turn, is overlain by a similar package of sediments. The Abel Erasumus Formation consists of basaltic rocks which are commonly massive, with minor amygdules (especially near flow tops) and rare pillows. Stromatolitic carbonates are found between flows (Button, 1973).

The next three younger formations of the Wolkberg Group are comprised of felspathic quartzite, subgraywacke and shale, occasionally in coarsening upward cycles (Hunter, 1981) reminisent of deltaic progradations.

Black Reef Formation

The Black Reef Formation is part of neither the underlying Wolkberg Group nor the overlying Chuniespoort Group (SACS, 1980). In consists of a basal conglomerate grading upwards into texturally mature quartzites, wackes and shales. The Black Reef Formation is widespread and rests conformably on underlying Wolkberg and Buffalo Springs Group in their basins proper but unconformable on Archean granite-greenstone basement, Witwatersrand sediments and Ventersdorp volcanics towards the basin margins.

Chuniespoort Group

The unconformably overlying Chuniespoort Group (up to 3500 m) is comprised of predominantly chemical sediments which grade upward from clastic sediments of the Black Reef Formation. These chemical sediments pass upwards from a thick sequence of basal cherts and carbonates into a thick sequence of iron formation, followed by carbonates, shales and minor conglomerates. Such thick sequences of chert, carbonate and iron formation are suggestive of a tectonically stable platform.

Pretoria Group

A marked regional angular unconformity separates the Chuniespoort and Pretoria Groups. This unconformity cuts progressively lower Chuniespoort units from north to south. The Pretoria Group comprises a 7-km-thick sequence (Rooiberg Felsite excluded) of shales, quartzites, minor carbonates and arkoses which repeat cyclicly throughout. Within this thick sedimentary package are three volcanic units: the Hekpoort Formation, the Machadodorp Member of the Silverton Formation and the Dullstroom Formation (Fig. 7b).

The Hekpoort Formation contains aphanitic to microcrystalline lavas and interbedded pyroclastics and rare shales. The lavas are typically greenish-gray, massive and blocky, becoming amygdaloidal and brecciated near flow tops. Pillows are reported from only one location in Hekpoort lavas (Button, 1973) and instances of lahar deposits are noteworthy (Eriksson and Twist, 1986).

The Machadodorp Member is comprised of laminated, ripple-marked tuffs which grade into coarser-grained lapilli tuffs, followed by fine-grained to aphanitic pillow basalts interbedded with lenses of tuff and shale and stromatolitic chert layers. Small quartz- and chlorite-filled amygdules of less than 1 cm are common. Green-gray to greenish black lavas of the Dullstroom Formation contain amygdules of up to 10 cm in size. Flows vary in thickness from 8 to 60 m (Tankard, 1982) and flow-top breccias are common.

In thin section, the Transvaal lavas have crystallized to a greenschist metamorphic assemblage of chiefly plagioclase (relict), tremolite-actiolite, chlorite, epidote and carbonate with minor amounts of quartz, sphene, leucoxene and magnetite. In some areas the Dullstroom lavas represent the floor of the Bushveld Complex and as a result, have undergone contact metamorphism to pyroxene hornfels facies (Button, 1973). In this instance, the metamorphic mineral assemblage is represented by plagioclase, augite and magnetite with minor amounts of amphibole, biotite and quartz.

Soutpansberg Group

Of all the units examined in this study, the Soutpansberg Group is the only one not deposited on the Kaapvaal craton. Instead, it was deposited in an elongate east-west basin on the Limpopo Mobile Belt in the northern Transvaal Province, South Africa (Fig. 7a). The basin developed in a zone of weakness between the south marginal and central zone of the Limpopo Belt (Jensen, 1975) and represents a single cycle of volcanics and sediments (no unconformities). The Soutpansberg Group is part of the Waterberg Supergroup and is comprised of a 7 km thick sequence of subaerial volcanics and sediments (fluvial sandstones and minor shales)(Fig. 7b). Sediments vary from litharenites and lithic graywackes to quartz arenites higher in the section. Volcanic rocks are typically subaerial basalts with some andesite and dacite differentiates, suggested by Barker (1979) to have erupted along linear vent systems. Normal faulting and some regional tilting are common along the basin margins.

Evaluation of the mantle source and tectonic setting of the Soutpansberg Group may prove invaluable in understanding the evolution of the Limpopo Belt and adjacent Kaapvaal and Zimbabwe cratons. Despite an apparent continental rift tectonic setting for the

Soutpansberg Group, the relationship of the rift to the underlying basement (Limpopo Belt), as an aulacogen (Jensen, 1975) or intracratonic rift (Barker, 1979) is still disputed. The mantle source has yet to be evaluated.

Rb-Sr isochron dates have been reported by Barton (1979). Results give an age of 1769 $\pm$ 34 Ma on a lava flow near the base of the Sabasa Formation and 1749 $\pm$ 104 Ma on a diabase sill further up in the section. The underlying granitic basement (Limpopo Belt) yields a date of 2692 $\pm$ 107 Ma. A garnet-cordierite gniess within this basement gives a 1790 $\pm$ 98 Ma date which Barton (1979) attributes to either a metamorphic event or uplift and erosion which ceased at approximately 1800 Ma.

In thin section the basaltic rocks of the Soutpansberg Group contain a relict mineral assemblage of pyroxene and plagioclase, and a metamorphic assemblage of pumpellyite, chlorite, epidote, quartz and sericite, plus minor amounts of calcite, leucoxene and actinolite. Albitization of feldspars is not observed. Also, X-Ray diffraction analyses by Wronkiewicz (1988) has demonstrated the presence of prehnite in the sediments of the Soutpansberg Group. Temperature estimates of 200^{0}C (representing burial to 8 km by remaining Soutpansberg rocks and Karoo volcanics; Barker, 1979) and the lack of any recorded regional metamorphic events since 2000 Ma suggest the Soutpansberg Group lies just within the prehnite-pumpellyite metamorphic facies. The presence of actinolite, however, suggests that the temperature has approached 300^{0}C. This would place the Soutpansberg in the upper prehnite-pumpellyite metamorphic facies.

The Soutpansberg Group is subdivided into four formations (Barker, 1979) which are, from oldest to youngest, the Sabasa, Musekwa, Ngwanedzi and Nzhelele Formations (Fig. 7b).

Sabasa Formation

The Sabasa Formation rests unconformably on Limpopo Belt rocks and decreases in thickness from east to west. Lavas consist of massive, fine-grained to porphyritic basalts with numerous intercalated basic to felsic pyroclastic horizons (both agglomeritic and ash flow deposits) associated with tops of flows. Lava flows vary from 30 cm to 2 m in thickness. Amygdules, both dispersed throughout flows in some areas and concentrated in flow tops in others, are up to 10 cm in diameter (Barker, 1979) and filled with quartz, calcite, zeolites and jasper. Porphyritic lavas contain megascopic and relict pyroxene (up to 1 cm) and plagioclase. Intimately associated with basaltic lavas are small quantities of acid lavas interpreted as immiscible liquids (Barker, 1979). Sediments in the Sabasa Formation are lithic graywackes to sublitharenites intercalated with lenses of shale and mudstone.

Musekwa Formation

The Musekwa Formation conformably overlies the Sabasa Formation. Sediments of the Musekwa consist of basal, thinly bedded argillites, litharenites and lithic graywackes which grade upwards into quartz arenites and conglomerates. Intercalated with these fluvial sediments are thin basalt flows.

Ngwanedzi Formation

The Ngwanedzi Formation conformably overlies the Musekwa Formation and consists of massive, porphyritic basalt flows, becoming more amyduloidal upwards. Lenses of clastic sediments and pyroclastics are common. The unit is topped by a thin (10-15 cm) ash flow tuff which is transitional with pyroclastics of the basal Nzhelele Formation.

Nzhelele Formation

The base of the Nzhelele Formation comprises a thin dacitic tuff which is transitional and conformable with the underlying Ngwanedzi Formation. This passes upward into a thick sequence of volcanoclastic rocks intercalated with thinly-bedded argillaceous sediments followed by lithic wackes and litharenites which become more mature towards the top of the unit.

RESULTS

Major Elements and Rock Classification

A complete tabulation of major element analyses is given in Appendix C, including averages for each formation or rock type, and normative compositions.

Nsuze Group

A common problem with metamorphosed volcanics is classification of the igneous protolith. Unfortunately, most classification schemes are based on SiO_2 and alkalies which are often mobile during metamorphism. On a Jensen cation plot (Jensen, 1976)(Fig. 8) the Nsuze volcanics plot as a continuous suite of rocks from basalt to rhyolite. According to this figure, the majority of the Nsuze samples used in this study are basaltic in composition but more important, rocks of intermediate composition (andesites) are also represented. This is confirmed by a SiO_2-Zr/TiO_2 diagram of Floyd and Winchester (1978) on which a continuous range in composition from basalt to rhyolite is represented (Fig. 9), although the Nsuze volcanics are represented by a greater proportion of rocks of andesitic composition. Because of the

Figure 8. Jensen cation plot showing the distribution of the Nsuze volcanics. Fields after Jensen (1976).

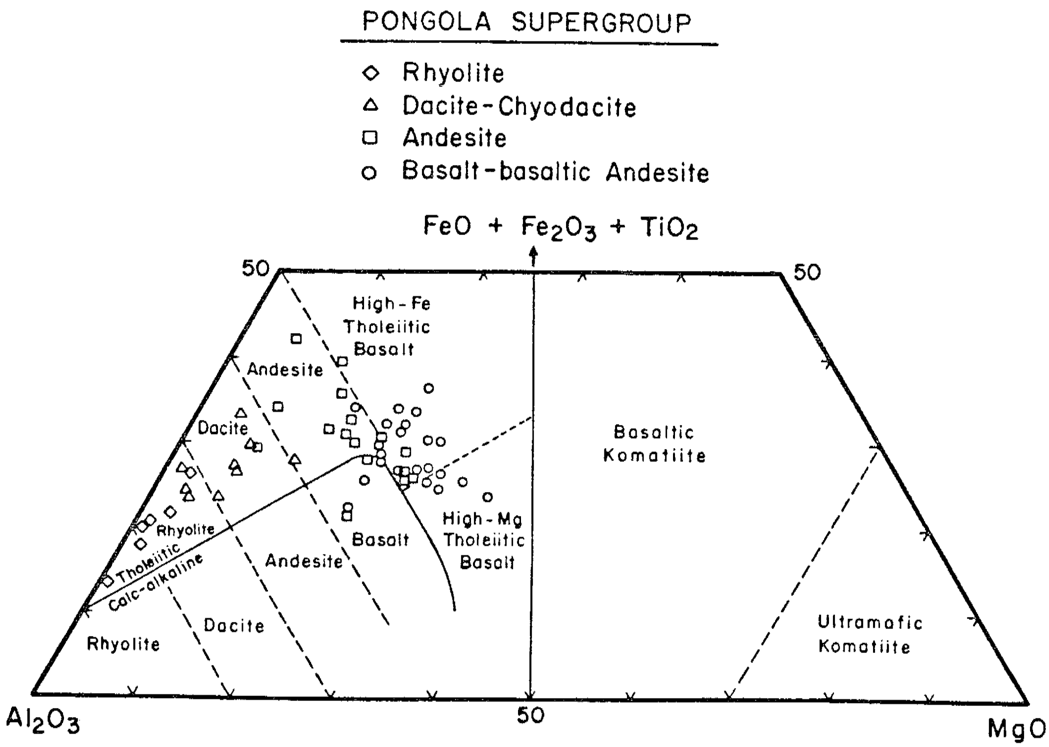
PONGOLA SUPERGROUP
◇ Rhyolite
△ Dacite-Chyodacite
□ Andesite
o Basalt-basaltic Andesite
FeO + Fe2O3 + TiO2
50
50
High-Fe
Tholeiitic
Basalt
Andesite
Dacite
Rhyolite
Tholeiitic
Calc-alkaline
Andesite
Basalt
High-Mg
Tholeiitic
Basalt
Dacite
Rhyolite
Basaltic
Komatiite
Ultramafic
Komatiite
Al2O3
50
MgO

Figure 9. Classification of the Nsuze volcanics on the SiO_2-Zr/TiO_2 diagram of Floyd and Winchester (1978). Symbols given in figure 8.

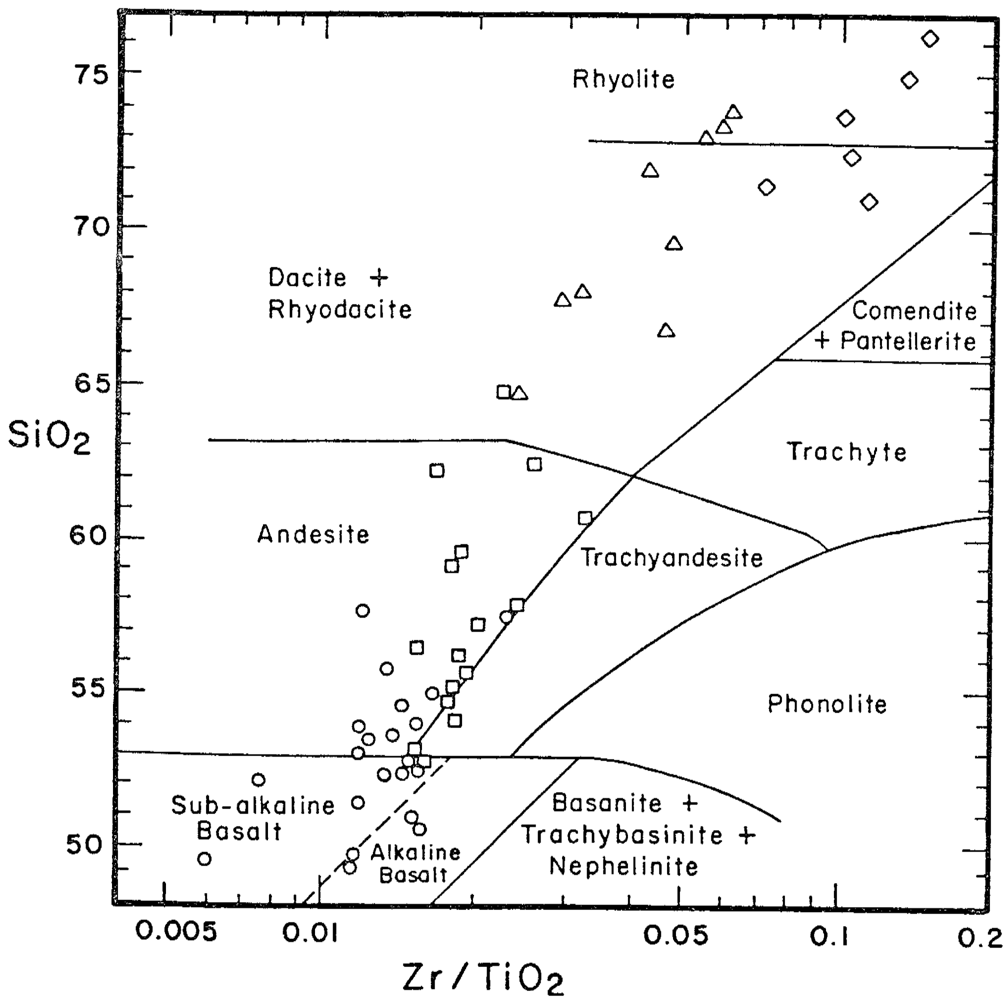

Rhyolite
Dacite + Rhyodacite
Comendite + Pantellerite
Trachyte
Andesite
Trachyandesite
Phonolite
Sub-alkaline Basalt
Alkaline Basalt
Basanite + Trachybasinite + Nephelinite
75
70
65
60
55
50
SiO2
0.005
0.01
0.05
0.1
0.2
Zr / TiO2

possible mobilization of SiO_2 during metamorphism, less importance is placed on the SiO_2-Zr/TiO_2 diagram for rock classification.

The Nsuze compositional groups from which the averages in Appendix C are calculated are based primarily on relatively immobile trace element distributions and ratios, the Jensen cation plot, and to a lesser extent, the concentration of SiO_2. The Nsuze volcanics are subdivided into four groups: 1) basalt-basaltic andesite, 2) andesite, 3) dacite-rhyodacite and 4) rhyolite. It should be noted that the classification of the Nsuze volcanics by Armstrong et al. (1986), based on the differentiation index of Thorton and Tuttle (1960), also subdivides the suite into a continuous spectrum of volcanics, from basalt to rhyolite. The presence of andesite thus appears to be real, and not an artifact of the classification scheme used.

Nsuze volcanics are tholeiitic, both in terms of iron-enrichment as seen on the AFM diagram of Irvine and Baragar (1971)(Fig. 10) and the consistent presence of normative quartz. The Jensen cation plot (Fig. 8) also demonstrates that these samples are almost exclusively tholeiitic in nature. The variation of FeO-T/MgO ratio relative to SiO_2 (Miyashiro, 1974), however, suggests a mixture of volcanics with calc-

Figure 10. AFM diagram showing the distribution of the Nsuze volcanics. Field after Irvine and Baragar (1971). Symbols given in figure 8.

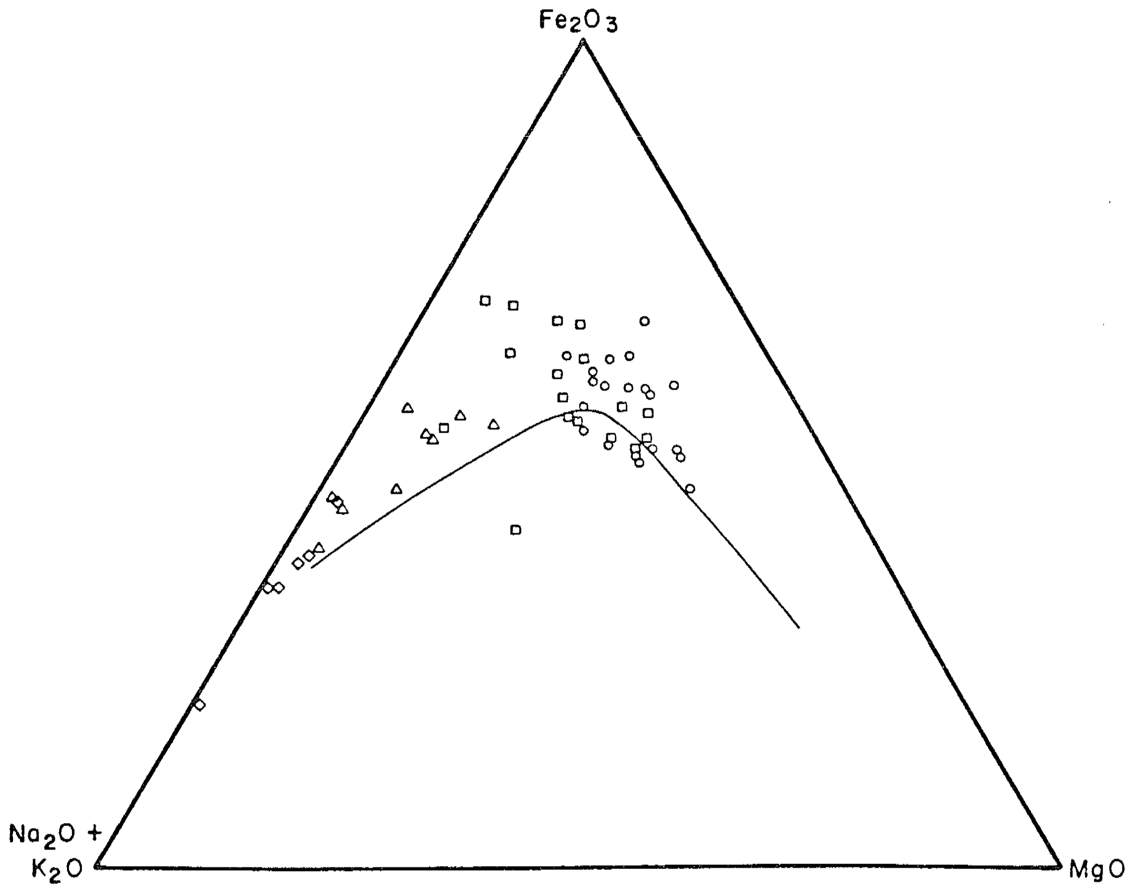

Fe2O3
Na2O +
K2O
MgO

alkaline and tholeiitic affinities with the calc-alkaline character found primarily in the mafic volcanics. Some mobilization of the major elements, primarily CaO, are noted for approximately 30% of the samples studied (regardless of composition) on geochemical alteration screens (Beswick and Soucie, 1978), and these same samples possess normative corundum (c = 0.01 to 5.1). In all, 17 samples have normative corundum, most of which are dacites and rhyolites. The amount of normative corundum does not vary systematically with either major or trace elements in dacites and rhyolites, but basalts (3 total) and andesites (4 total) show a positive correlation with Al_2O_3 and LOI. Alteration or metamorphism resulting in a depletion in CaO seems the most likely cause for the normative corundum, although fractional crystallization and crustal contamination may also be viable mechanisms (Cawthorn et al. 1976).

When considered in terms of the clinopyroxene-olivine-silica-plagioclase pseudo-liquidus phase diagram of Elthon (1983), most Nsuze basalts and basaltic andesites plot on or near the 1 atm pseudo-cotectic, suggesting that secondary processes have not greatly changed the relative proportions of major elements (the three basalt-basaltic andesite samples with normative corundum excluded). In addition, when all four projections in this system are taken into consideration, fractional crystallization appears to have occurred at a relatively shallow depth with plagioclase and olivine as the primary liquidus phases.

Rhenosterhoek Formation

Systematic compositional differences between or within the three Rhenosterhoek cores are not apparent from the data. Samples range from 49% to 62% SiO_2 and have Mg numbers (Mg number= $Mg/Mg+Fe^{+2}$; in moles; 0.793 X $Fe_2O_3T= Fe^{+2}$) of 38-65. Relatively low Al_2O_3 contents, a common feature in most Archean basalts and andesites, is also characteristic of these rocks. LOI values are generally <3% with some samples reaching 4.5%. Using major element-based classification schemes of Irvine and Baragar (1971) and Peccerillo and Taylor (1976), Rhenosterhoek samples classify as basalt, basaltic andesite or andesite. Similarly, on a Jensen cation plot (Fig. 11) most Rhenosterhoek samples plot as basalts with a few andesites. The one Syferfontein sample analyzed plots as a rhyolite. Employing the ratios of relatively immobile trace elements such as Zr/TiO_2 and Nb/Y (Floyd and Winchester, 1978) to classify volcanic rocks, most samples are andesites with a few basaltic andesites and no basalts (Fig. 12).

Figure 11. Jensen cation plot showing the distribution of the Rhenosterhoek volcanics. Fields after Jensen (1976).

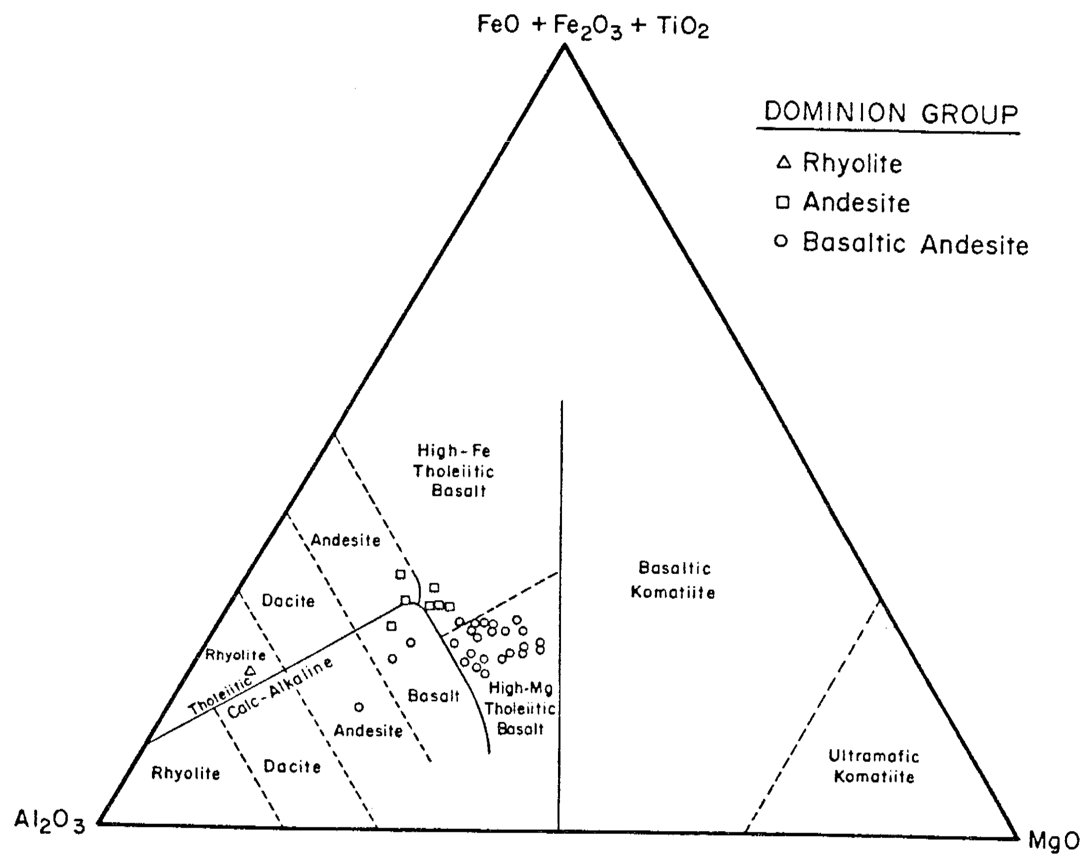
FeO + Fe2O3 + TiO2
DOMINION GROUP
Rhyolite
Andesite
Basaltic Andesite
High-Fe Tholeiitic Basalt
Andesite
Dacite
Rhyolite
Tholeiitic
Calc-Alkaline
Basalt
Andesite
High-Mg Tholeiitic Basalt
Basaltic Komatiite
Rhyolite
Dacite
Ultramafic Komatiite
Al2O3
MgO

Figure 12. Classification of volcanic rocks from the Rhenosterhoek Formation based on the Zr/TiO_2-Nb/Y diagram. Fields after Floyd and Winchester (1978). X= BTF core, O= BSF core and solid triangles= BBS core.

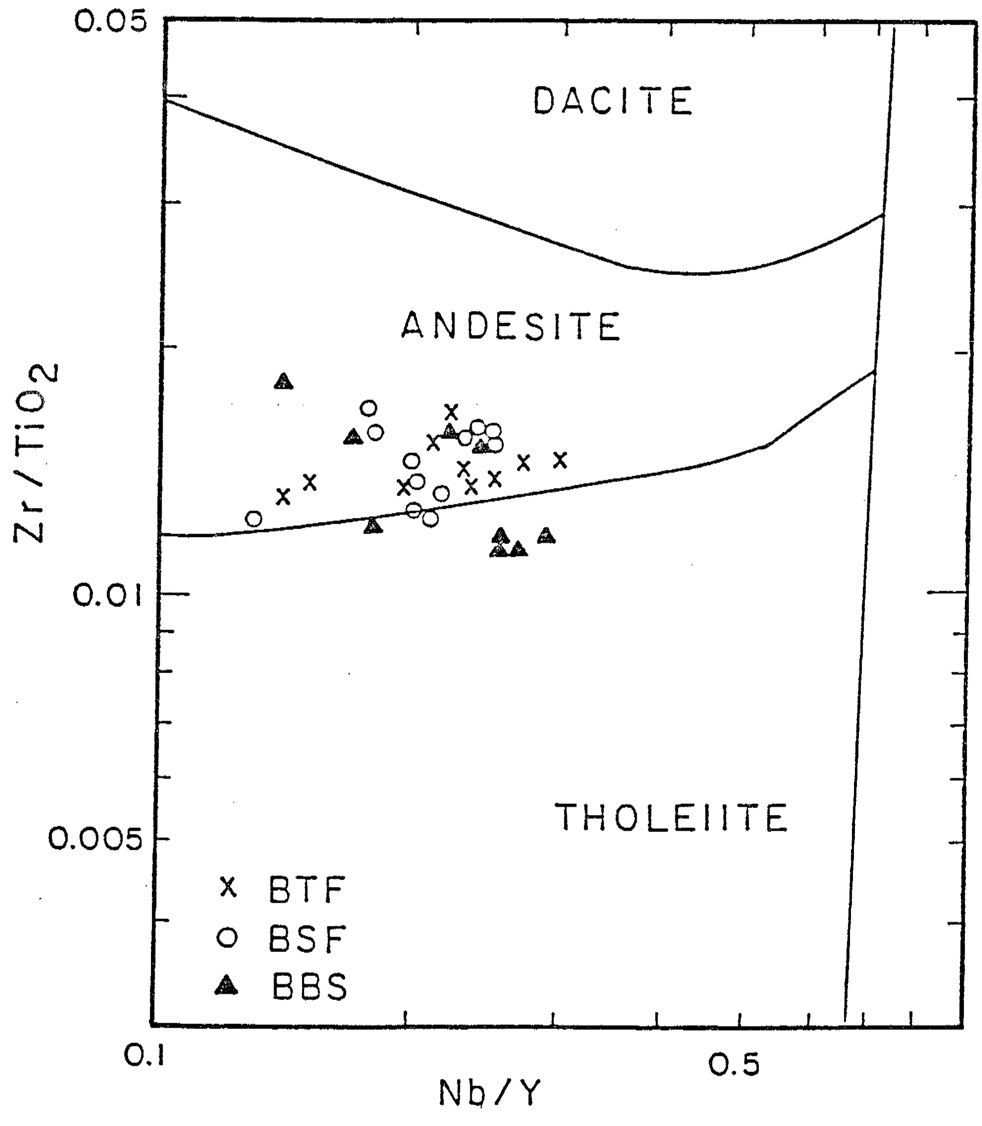
0.05
0.01
0.005
Zr / TiO2
DACITE
ANDESITE
THOLEIITE
x BTF
o BSF
▲ BBS
0.1
0.5
Nb / Y

On a SiO_2-Zr/TiO_2 plot (not shown) most samples are split into a roughly equal number of basalts and andesites. Based primarily on these incompatible trace element ratios in conjunction with consistent groupings on numerous trace element plots, the Rhenosterhoek volcanics are classified as basaltic andesites and andesites (Appendix C).

On an AFM diagram, the samples show only mild iron enrichment with most samples plotting in the calc-alkaline field. Similarily, on a SiO_2-FeO-T/MgO diagram, most samples fall in the calc-alkaline field with only a few showing significant iron-enrichment.

In all, 8 samples contain normative corundum. Of these, three are andesites, one is rhyolite (sample D-4; Syferfontain Formation), and the remaining samples are basaltic andesites. All of the corundum normative samples have lost CaO relative to the remaining major elements as seen in the alteration screens of Beswick and Soucie (1978). It is the loss of CaO and the relative enrichment in Al_2O_3 that probably produces normative corundum in these samples.

When these relatively unaltered samples are plotted in the system Ol-Di-Hy-Q, they define a broad band falling between shallow and deep crustal cotectics (Fig. 13). Such results are consistent with these volcanics fractionating in magma reservoirs at

Figure 13. Distribution of the least altered Rhenosterhoek volcanics in the Ol-Di-Hy-Q system. Cotectics from Thompson (1982) and Thompson et al., (1983). X= BTF core, O= BSF core and solid triangles= BBS core.

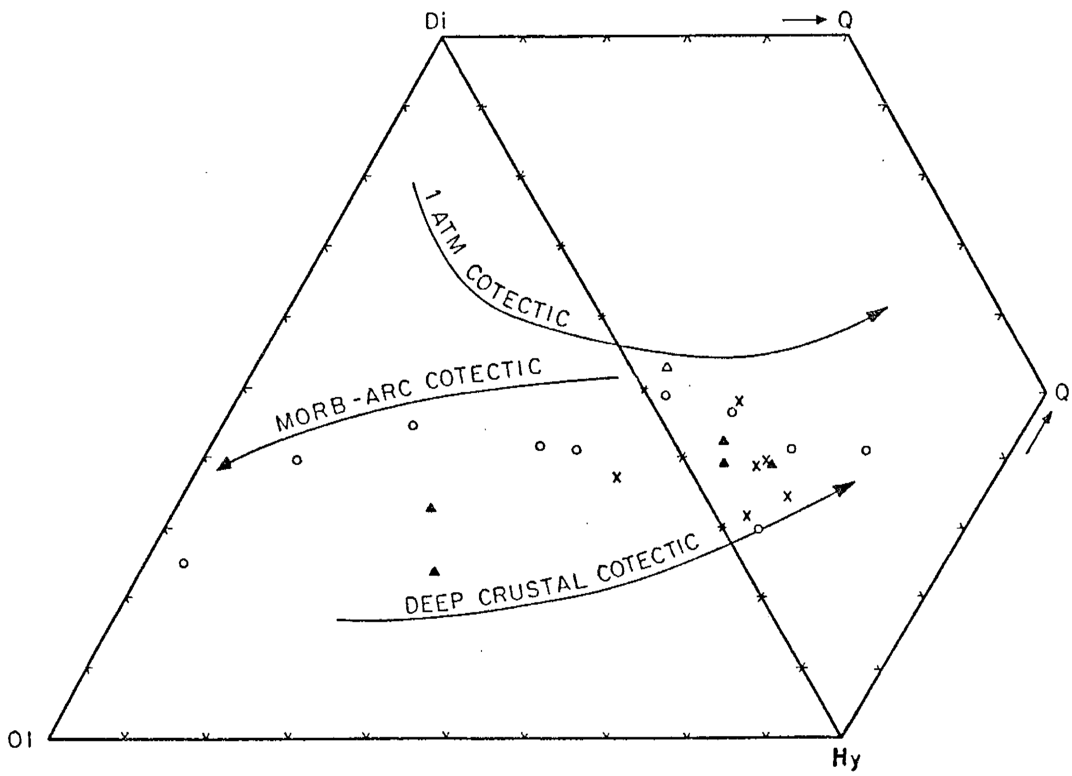
Di
Q
1 ATM COTECTIC
MORB-ARC COTECTIC
DEEP CRUSTAL COTECTIC
Q
Ol
Hy

intermediate crustal depths. In this respect, they are unlike most MORB and arc volcanics which fractionate at shallow crustal depths, but they are similar to many continental flood basalts (Thompson et al., 1983).

Ventersdorp Supergroup

Most of the Ventersdorp volcanics are quartz normative, and with increasing stratigraphic height samples with normative corundum (c = 0.3 to 4.4) become more prevalent. In total, 9 samples have normative corundum and these also have high Al_2O_3 (15-18%), highly variable SiO_2 and high TiO_2 and P_2O_5 (with one exception). The amount of normative corundum does not vary systematically with major or trace elements and corundum normative samples fall in altered fields on the alteration screens of Beswick and Soucie (1978). Thus, normative corundum appears to reflect alteration. The relatively high TiO_2 and P_2O_5 in the corundum normative samples is puzzling and may be caused by losses of other major elements relative to Ti and P which occur in refractory phases (ilmenite and apatite). The 9 corundum-normative samples are not plotted on figure 16 nor are they considered in petrogenetic studies.

As mentioned previously, a common problem with metamorphosed volcanic rocks is identification of the protolith. Previous authors have described the Ventersdorp volcanics as bimodal, alkali-rich, tholeiitic basaltic andesites, andesites and rhyolites with a slight calc-alkaline affinity (Schweitzer and Kroner, 1985) and as a weakly bimodal tholeiitic basic-acid volcanic suite of subalkaline, tholeiitic character (Bowen et al., 1986). Bowen et al. (1986) classify the Klipriviersberg Group and the majority of the Platberg Group as basalts. They consider the Allanridge Formation to be comprised chiefly of tholeiitic andesites and the Makwassie Formation of volcanics largely dacitic in composition. In comparison, Schweitzer and Kroner (1985) describe the average composition of the Ventersdorp lavas as basaltic-andesite and andesite. Bowen et al. (1986) also have shown that volcanic rocks in the Ventersdorp and Dominion successions in South Africa can be subdivided into several distinct populations based on Zr/P - P/Ti ratios.

On a Jensen cation plot, Ventersdorp samples show mixed tholeiitic and calc-alkaline affinities (Fig. 14). Mafic volcanics plot predominantly as tholeiites with about one fourth of the samples falling in or close to the calc-alkaline field. On a SiO_2-FeO-T/MgO diagram, most mafic samples fall in the calc-alkaline

Figure 14. Jensen cation diagram showing the distribution of Ventersdorp volcanics. Fields after Jensen (1976).

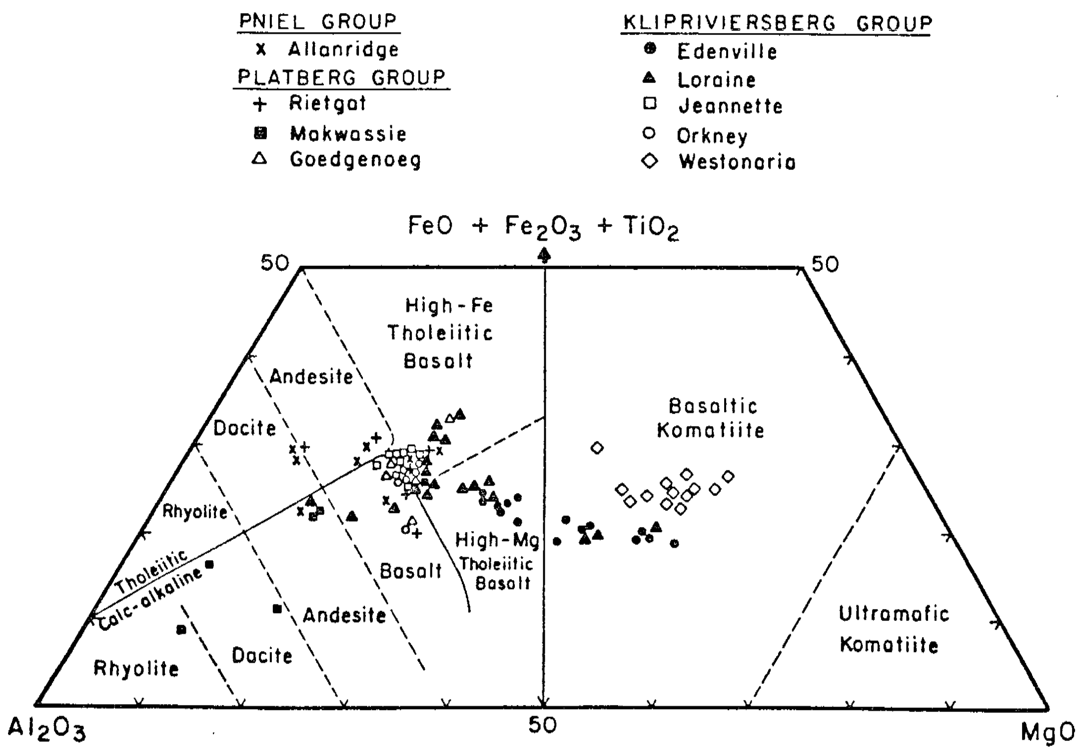
PNIEL GROUP
x Allanridge
PLATBERG GROUP
+ Rietgat
Makwassie
Goedgenoeg
KLIPRIVIERSBERG GROUP
Edenville
Loraine
Jeannette
Orkney
Westonaria
FeO + Fe2O3 + TiO2
50
50
High-Fe Tholeiitic Basalt
Andesite
Dacite
Rhyolite
Basaltic Komatiite
Tholeiitic
Calc-alkaline
Basalt
High-Mg Tholeiitic Basalt
Andesite
Dacite
Rhyolite
Ultramafic Komatiite
Al2O3
50
MgO

field. It is worth noting that most samples from the Edenville and Loraine Formations plot in calc-alkaline fields while samples from more evolved units commonly plot in tholeiite fields (mostly Platberg and Pniel Group lavas). These relationships are also apparent on an AFM diagram. According to the Jensen diagram (Fig. 14), the majority of the Klipriviersberg volcanics are tholeiitic basalts with subordinate calc-alkaline basalts. Samples from the Westonaria Formation plot as basaltic komatiites, as do some of the Edenville and Loraine volcanics. The Edenville and Loraine volcanics, however, do not exhibit spinfex textures. Samples from the Makwassie and Allanridge Formations classify as andesites and dacites. On a Zr/TiO_2-Nb/Y diagram, Klipriviersberg lavas are chiefly basalts with some andesites (Fig. 15). Samples from the Rietgat and Goedgenoeg Formations are andesites and dacites, those from the Makwassie Formation predominantly rhyodacites-dacites, and those from the Allanridge Formation are predominantly andesite with one sample plotting as a dacite and two samples as basalts.

Based mainly on relatively immobile element distributions and the Jensen cation plot, Klipriviersberg volcanics are predominantly basalts and basaltic andesites with subordinate basaltic komatiites at the top and bottom of the unit (Edenville, Loraine

Figure 15. Classification of volcanic rocks from the Ventersdorp Supergroup based on Zr/TiO_2-Nb/Y diagram of Floyd and Winchester (1978). Symbols given in figure 14.

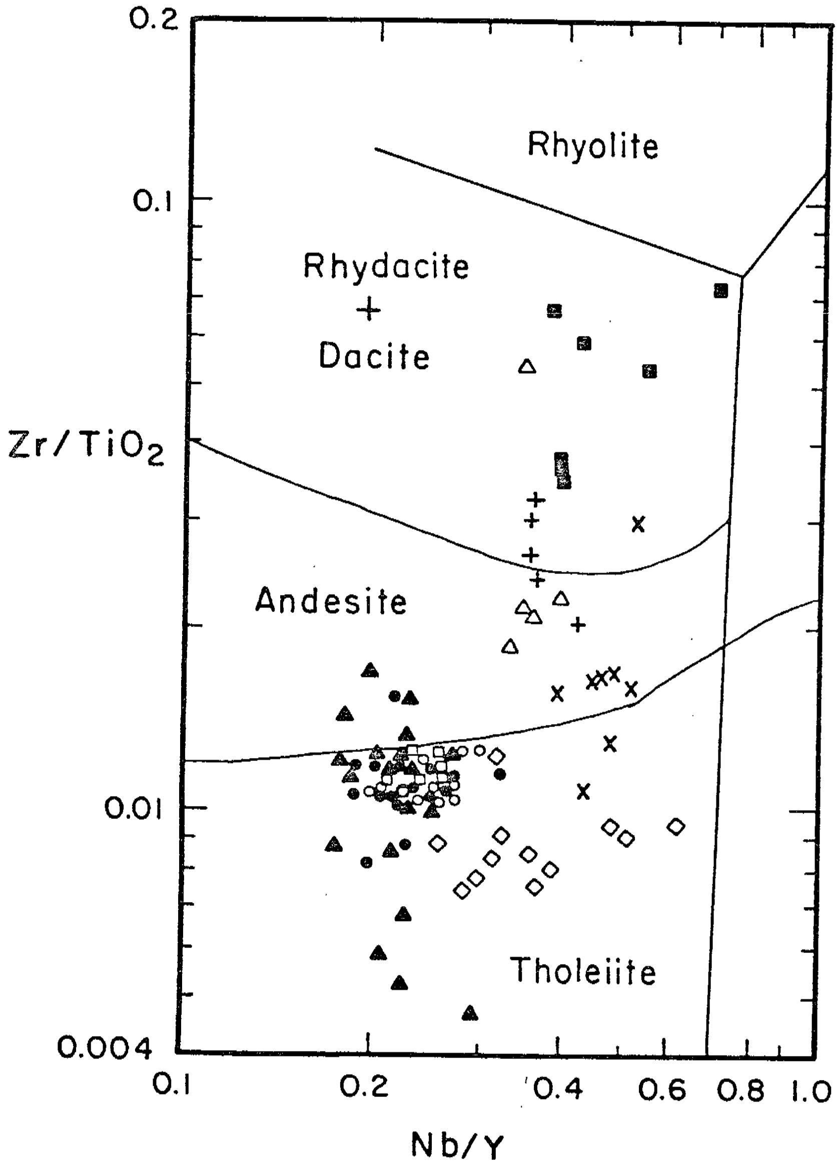

Rhyolite
Rhydacite
+
Dacite
Andesite
Tholeiite
Zr/TiO2
0.2
0.1
0.01
0.004
0.1
0.2
0.4
0.6
0.8
1.0
Nb/Y

and Westonaria Formations). The Platberg Group consists mostly of basaltic andesites with the Makwassie Formation containing rocks that vary in composition from andesite to rhyolite. The Allanridge Formation is composed primarily of andesites and basaltic andesites. Ventersdorp volcanics are chiefly tholeiitic with a mild calc-alkaline character, especially in the more mafic samples.

Except for the Westonaria Formation, major element data exhibit stratigraphic compositional changes in the mafic lavas of the Klipriviersberg Group (Figs. 14, 16; Appendix C), an attribute first noted by Bowen et al. (1986). Mg numbers increase from an average of 50 to an average of 69 with increasing stratigraphic height and average Al_2O_3/TiO_2 ratios decrease from 25 to 14 over the same stratigraphic interval. In addition, SiO_2, TiO_2, Al_2O_3 and Na_2O abundances decrease while CaO and MgO increase. The overlying mafic to felsic volcanics of the Platberg and Pniel Groups are more variable in major element composition and do not show progressive changes with stratigraphic level.

Normative compositions of Ventersdorp volcanics are plotted on two projections of the clinopyroxene-olivine-silica-plagioclase pseudo-liquidus phase diagram following the method of Elthon (1983) in Figure 16. Most Ventersdorp samples plot as an array on or

Figure 16. Distribution of Ventersdorp volcanics in the olivine-clinopyroxene-plagioclase-silica system. Cotectics and normative definitions from Elthon (1983) and Elthon and Scarfe (1984). Cotectics: A= 1 atm., B= 5 kb, C= 10 kb. a, plagioclase projection; b, clinopyroxene projection. Symbols given in figure 14.

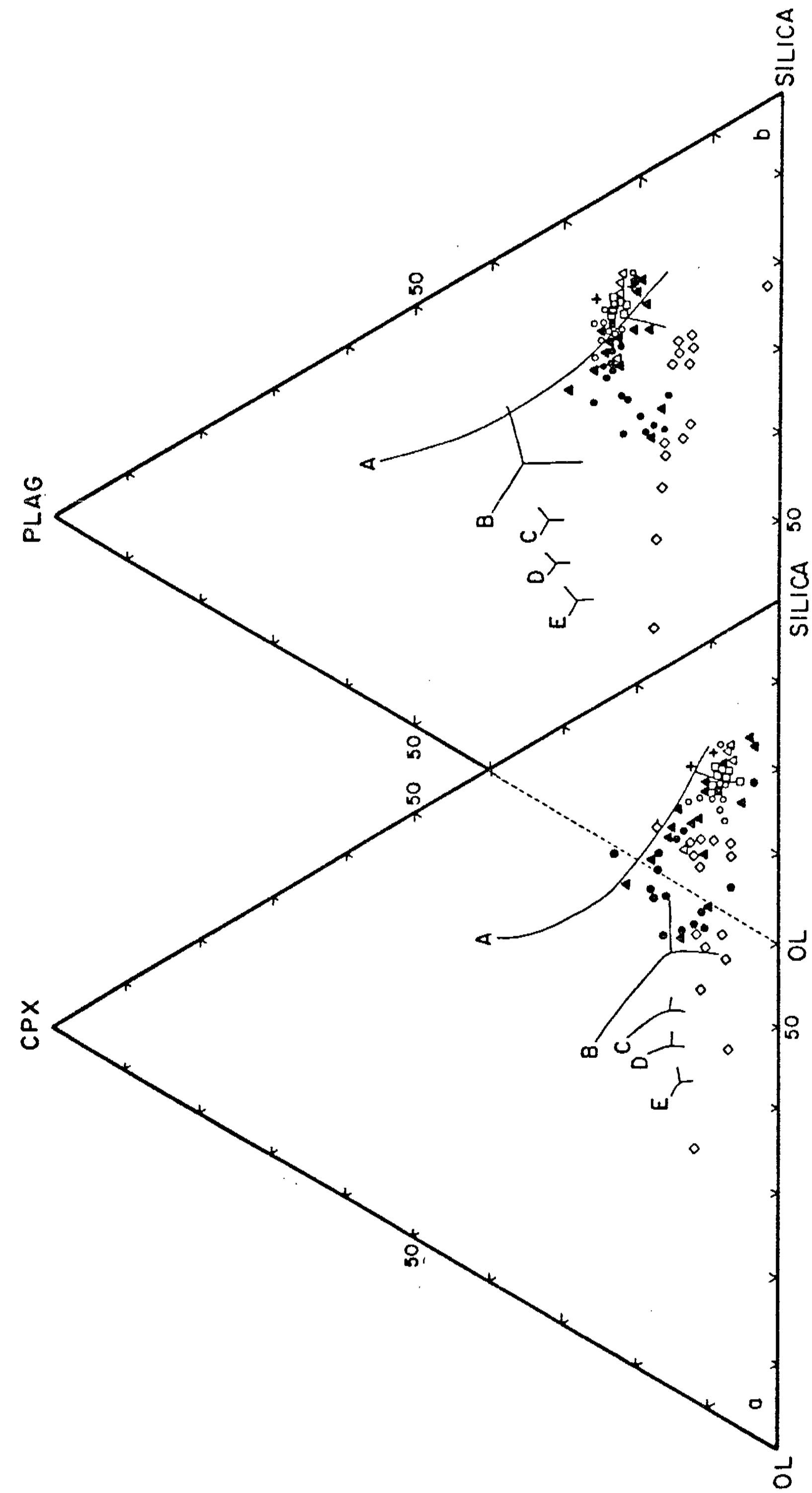
CPX
PLAG
SILICA
OL
SILICA
OL
a
b
A
B
C
D
E
A
B
C
D
E
50
50
50
50
50
50

near the 1 atm pseudo-cotectic. This fact suggests that secondary processes have not greatly changed the relative proportions of major elements. Exceptions are the samples rich in normative olivine which define a sublinear trend in the olivine phase volume. When all four projections in this system are considered, it appears that olivine and plagioclase are the primary liquidus phases and that fractional crystallization occurred at relatively shallow depths (<15km). Samples rich in olivine tend to fall near olivine control lines at shallow depths suggesting they have lost less olivine by crystal fractionation than other samples. Klipriviersberg samples have progressively less normative silica and more normative olivine with increasing stratigraphic height, consistent with previously cited major element trends.

Transvaal Supergroup

Most Transvaal samples are quartz normative, with two hypersthene normative samples and three corundum normative samples. Of the 3 samples containing normative corundum, one is rhyolitic in composition and another obviously altered. The third sample shows no obvious alteration but does possess relatively enriched LREE, and all three samples fall in altered fields on alteration screens (Beswick and Soucie, 1978).

Mg numbers range from 47 to 64 (excluding the one basaltic komatiite [picrite] sample [CDV-7] in the Hekpoort Formation [Mg #= 74, Ni= 308]) and are generally in the 50s, suggesting fractional crystallization of 10 to 40%. The Dullstroom volcanics are typically the most evolved with Mg numbers averaging 51 while more primitive Hekpoort and Machadodorp lavas have Mg numbers averaging 61 and 57, respectively.

The authors who have published papers on the Transvaal volcanics all rely on petrography and, to a lesser degree, major element geochemistry (SiO_2 in particular) to classify the protolith (Button, 1973; Tyler, 1979). SiO_2 and alkalies, as mentioned previously, may be mobile during metamorphism. To remedy this problem, Transvaal volcanics are plotted on several diagrams which utilize some of the less mobile major and trace elements for rock classification.

On a Jensen cation plot (Fig. 17), Transvaal volcanics plot predominantly as tholeiites, with a few samples showing calc-alkaline affinities. On a AFM diagram samples show mixed tholeiite and calc-alkaline affinities while on a SiO_2-FeO-T/MgO diagram the majority plot in the calc-alkaline field.

The Jensen diagram suggests the majority of the

Figure 17. Jensen cation diagram showing the distribution of Transvaal and Soutpansberg volcanics. Fields after Jensen (1976).

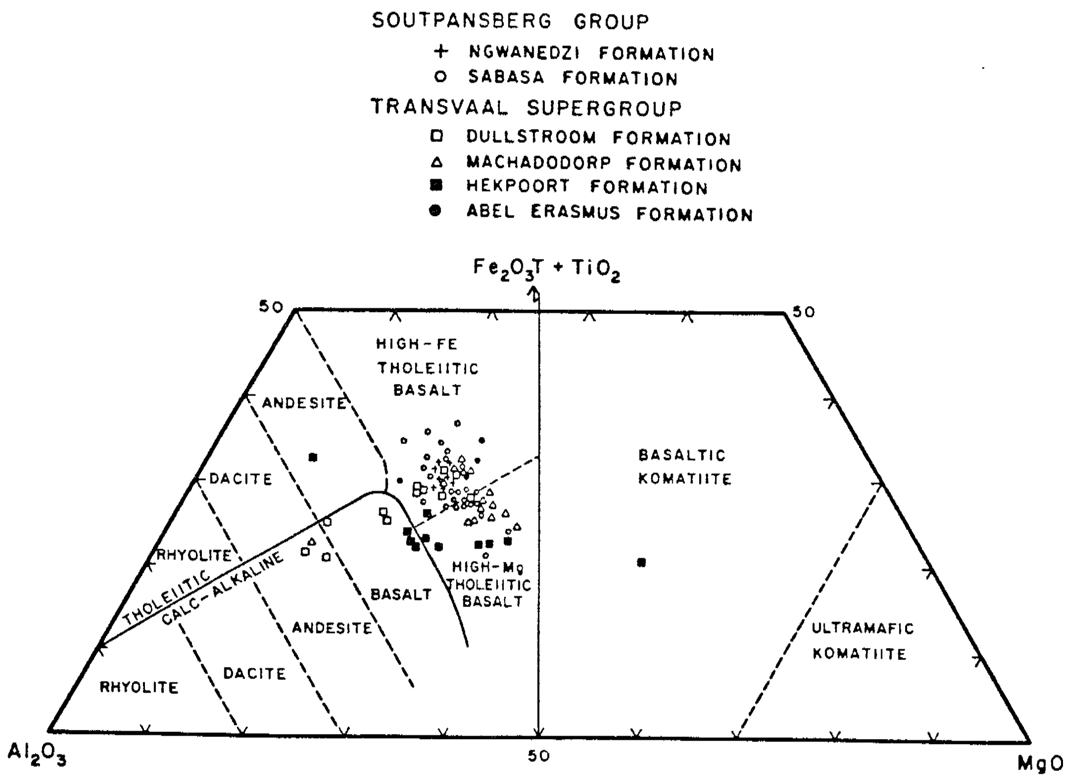
SOUTPANSBERG GROUP
+ NGWANEDZI FORMATION
O SABASA FORMATION
TRANSVAAL SUPERGROUP
□ DULLSTROOM FORMATION
△ MACHADODORP FORMATION
■ HEKPOORT FORMATION
● ABEL ERASMUS FORMATION
Fe2O3T + TiO2
50
50
HIGH-FE THOLEIITIC BASALT
ANDESITE
DACITE
RHYOLITE
THOLEIITIC
CALC-ALKALINE
BASALT
ANDESITE
DACITE
RHYOLITE
HIGH-Mg THOLEIITIC BASALT
BASALTIC KOMATIITE
ULTRAMAFIC KOMATIITE
Al2O3
50
MgO

Transvaal lavas are tholeiitic basalts, with only four andesites and one basaltic komatiite (CDV-7). On a SiO_2 -Zr/TiO_2 diagram the Machadodorp and Abel Erasmus volcanics are almost entirely composed of basalts while the Hekpoort and Dullstroom Formations are predominantly andesites. Exceptions are two Dullstroom samples which plot as dacites, and one Hekpoort sample which plots as rhyodacite. On a Zr/TiO_2-Nb/Y diagram (Fig. 18) the Abel Erasmus volcanics plot as both basalts and andesites and the Hekpoort volcanics as andesites and one rhyodacite. Samples from the Machadodorp are basalts and those of the Dullstroom range from basalt to dacite.

Based primarily on immobile element distributions and consistent groupings on numerous plots, the Abel Erasmus and Machadodorp volcanics are basalts while the Hekpoort and Dullstroom volcanics consist predominantly of basaltic andesites and andesites with some local differentiates to dacite and rhyolite. The Transvaal lavas appear to be tholeiitic with a mild calc-alkaline character, especially in the Hekpoort and Dullstroom samples.

Soutpansberg Group

Mg numbers in the Soutpansberg lavas range from 40

Figure 18. Classification of volcanic rocks from the Transvaal Supergroup and Soutpansberg Group based on Zr/TiO2-Nb/Y diagram of Floyd and Winchester (1978). Symbols given in figure 17.

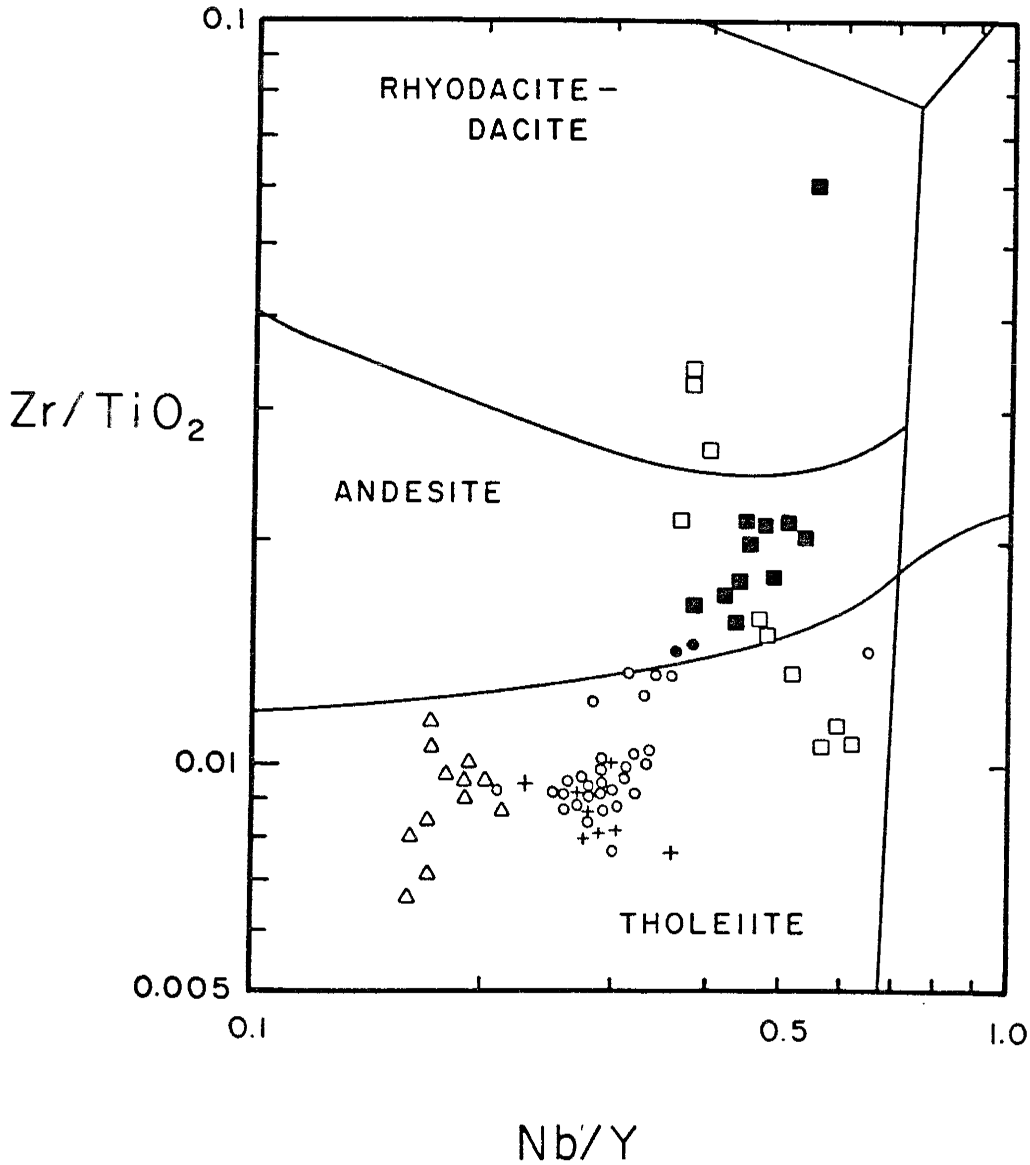
0.1
RHYODACITE-
DACITE
Zr/TiO2
ANDESITE
0.01
THOLEIITE
0.005
0.1
0.5
1.0
Nb/Y

to 66, generally falling in the mid-50s, suggesting these lavas are not primary mantle melts and from 20 to 40% fractional crystallization has occurred. Most Soutpansberg volcanics are quartz normative, with only four samples containing normative olivine and no samples with normative corundum.

The Ngwanedzi and Sabasa volcanics plot entirely in the tholeiitic portion of the Jensen diagram (Fig. 17). The same is true for SiO_2-FeO-T/MgO and AFM diagrams. The Ngwanedzi and Sabasa volcanics classify as basalts on the Jensen plot (Fig. 17) as well as the SiO_2-Zr/TiO_2 and Zr/TiO_2-Nb/Y diagrams (Fig. 18).

Trace Element Distributions

Nsuze Group

REE patterns in Nsuze volcanics are generally LREE enriched (20 to 120 X chondrites) with negative Eu anomalies increasing in size from basalt (Eu/Eu^* average 0.9) to rhyolite (Eu/Eu^* average 0.5)(Fig. 19). One basalt sample (P-16) has a flat REE pattern similar to MORB (~15 X chondrites). La/Yb ratios increase from basalt (average 7) to dacite-rhyodacite (average 15) and then decrease in the rhyolites (average 11), suggesting that accessary phases have influenced rhyolite production. Such moderate La/Yb ratios in the Nsuze basalts are intermediate between those found in modern rift (7-9) and calc-alkaline basalts (3-7) while those of Nsuze andesites (average = 10) are more like those of continental margin arcs (5-15).

Changes in REE abundances relative to stratigraphic level are apparent within the basalt-basaltic andesite compositional group. Basaltic rocks in the lower portion of the volcanic section are less enriched in total REE than those higher in the section. Variation diagrams using REE and other trace elements suggest the basaltic rocks of the lower and upper portions of the section are genetically related, with

Figure 19. Chondrite-normalized REE abundances in volcanic rocks from the Nsuze Group. Plotted are mean values from Appendix C. Basalt mean excludes one sample (P-16) with a relatively flat REE pattern.

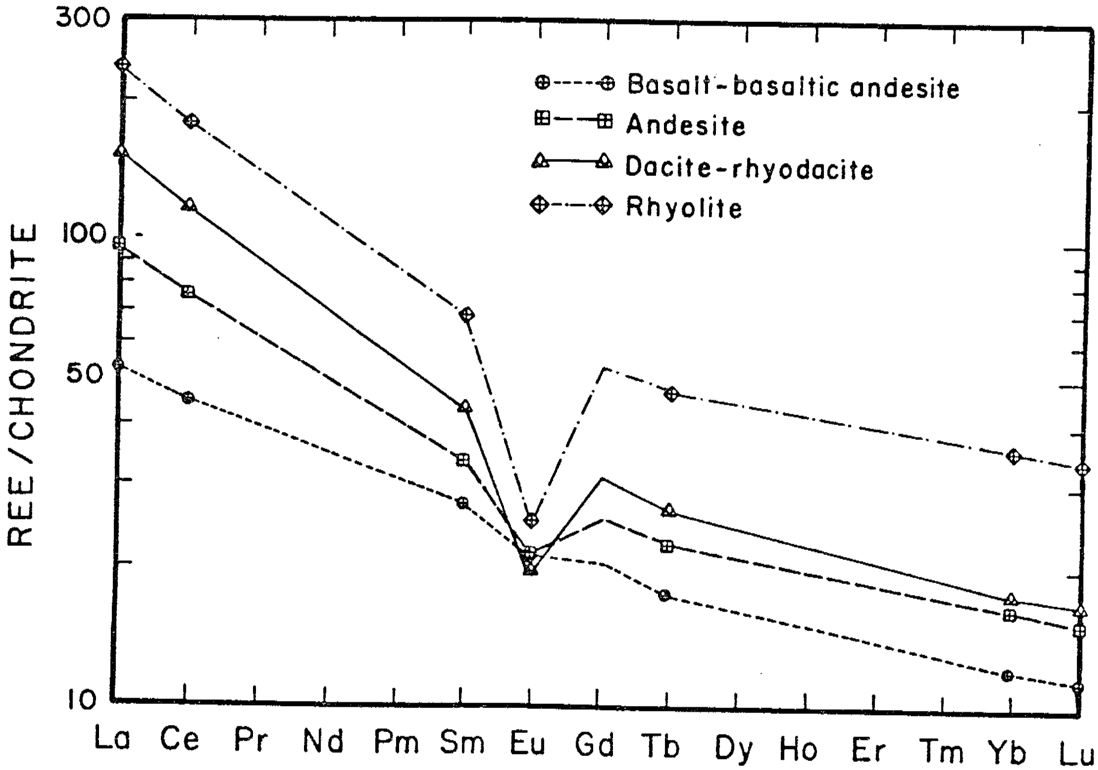

300
100
50
10
REE / CHONDRITE
La Ce Pr Nd Pm Sm Eu Gd Tb Dy Ho Er Tm Yb Lu
Basalt-basaltic andesite
Andesite
Dacite-rhyodacite
Rhyolite

the upper Nsuze volcanics being more fractionated (lower Mg numbers) than those in the lower portion of the pile. Armstrong et al. (1986) also note these trends.

The NMORB-normalized incompatible element distributions in Nsuze volcanics are similar regardless of bulk composition and show progressive enrichment from Yb to Th (Fig. 20). Negative Sr and Ba anomalies occur in most samples and are particularly prominent in andesites and felsic volcanics. Negative Ti and P anomalies also become increasingly important in the more felsic lavas. Prominent negative Ta-Nb anomalies (Th/Ta=4.4; Ce/Nb=6.1 in Nsuze basalts), are similar to those found in convergent plate volcanics (Th/Ta=3.7; Ce/Nb=4.1 in tholeiitic volcanic arc basalts [data from Pearce, 1982]), are also present. Other incompatible trace element distributions show similarities to continental-margin arcs. For example, on the Zr/Y-Zr plot (Fig. 21) of Pearce (1983) the basaltic rocks of the Nsuze Group plot predominantly in the continental arc-OIB fields (note two samples in MORB field; P-16, MS-37) to the exclusion of the oceanic arc field where Zr/Y ratios are typically less than 3. Similar results are observed on a Th/Yb-Ta/Yb plot (Fig. 22) with most samples falling in the continental arc field. Again, two exceptions which show a close affinity to MORB are

Figure 20. NMORB-normalized incompatible element distributions in Nsuze volcanics. Plotted are mean values from Appendix C. Normalizing values from Pearce (1983). Basalt mean excludes one sample (P-16) with a relatively flat REE pattern.

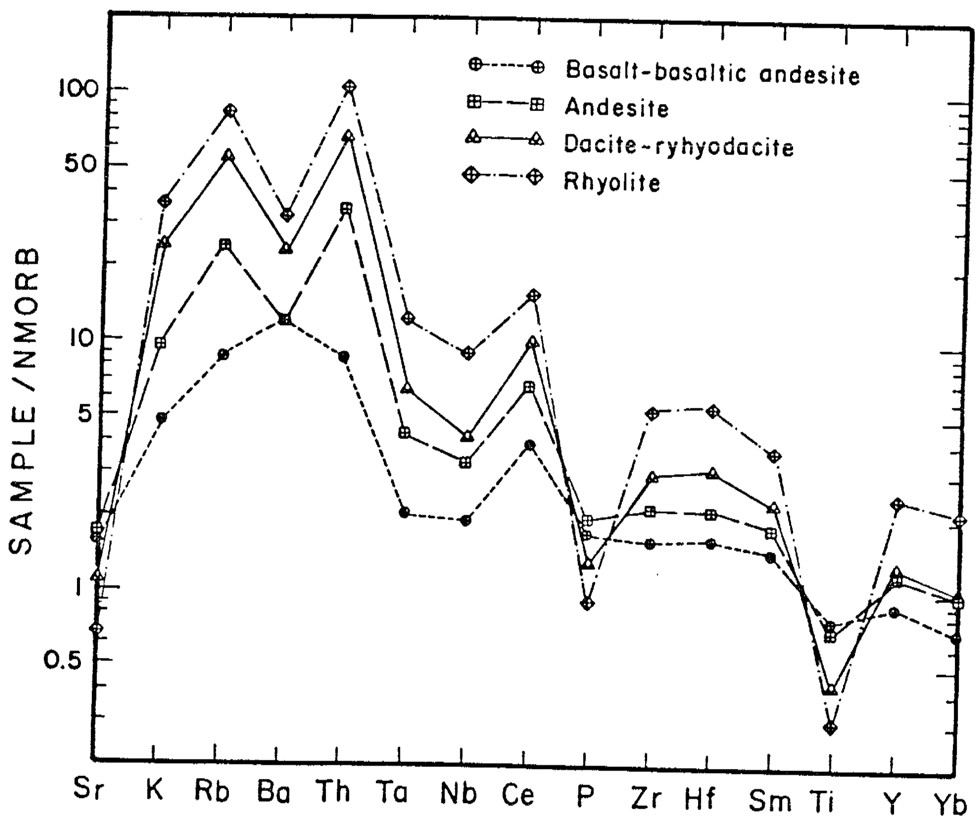
Basalt-basaltic andesite
Andesite
Dacite-ryhyodacite
Rhyolite
SAMPLE / NMORB
100
50
10
5
1
0.5
Sr K Rb Ba Th Ta Nb Ce P Zr Hf Sm Ti Y Yb

Figure 21. Distribution of the Nsuze volcanics on a Zr/Y-Zr diagram. Fields after Pearce (1983). Circles= basalt-basaltic andesites. Also shown is an error bar representing coefficient of variation (CV) of U.S.G.S. standard BCR-1 (see Appendix B).

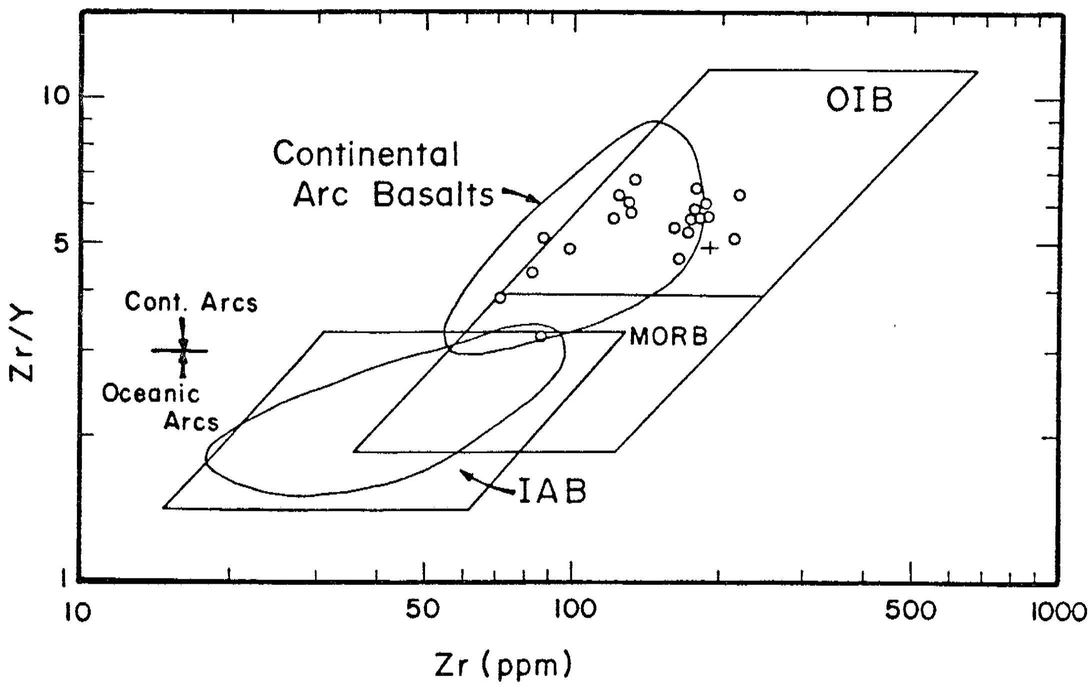
OIB
Continental
Arc Basalts
Cont. Arcs
Oceanic
Arcs
MORB
IAB
Zr/Y
10
5
1
10
50
100
500
1000
Zr (ppm)

Figure 22. Th/Yb-Ta/Yb diagram of Pearce (1983) showing the position of the Nsuze volcanics. Circles= basalt-basaltic andesites, squares= andesites, triangles= dacite-rhyodacites and diamonds= rhyolite. Error bar represent CV of standard BCR-1 (see appendix B).

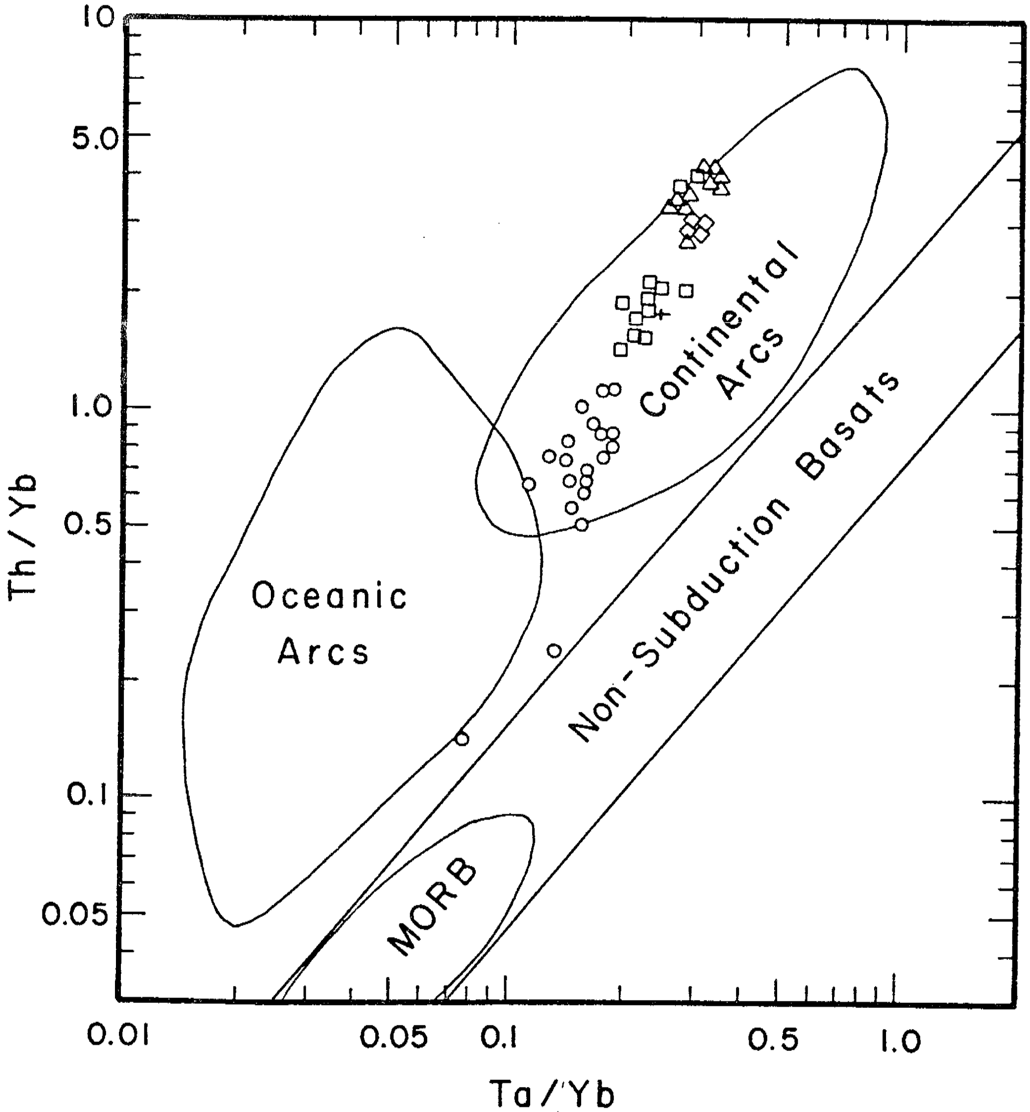
10
5.0
1.0
0.5
0.1
0.05
Th / Yb
0.01
0.05
0.1
0.5
1.0
Ta / Yb
Continental
Arcs
Oceanic
Arcs
Non-Subduction Basats
MORB

observed (P-16, WR-2). The Nsuze volcanics are also plotted on the Th-Hf-Ta diagram of Wood (1980)(Fig. 23) and, as in the previous two figures, most samples plot in the convergent plate field, with two samples (P-16, WR-2) plotting in or near the MORB field.

A summary of the tectonic classification of Nsuze basalts and basaltic andesites on various tectonic discrimination diagrams (some of which are presented above) is given in Table 2. On the whole, the Nsuze basaltic rocks are similar to basalts from modern arc systems. Not supporting this interpretation are the Ti-Zr diagram of Pearce and Cann (1973) in which roughly half the Nsuze basalts plot in the within-plate field, and one sample which resembles MORB on both the REE diagram and NMORB-normalized spidergram. It should be mentioned that the classification of Archean volcanics on these tectonic discrimination diagrams is not without ambiguity and caution should be used. These diagrams serve a more useful purpose as indicators of similar processes and sources rather than as true indicators of tectonic setting (Arculus, 1987), and it is with this purpose in mind that they are presented.

Rhenosterhoek Formation

Trace element distributions in the Rhenosterhoek volcanics are like those found in modern basaltic

Figure 23. Nsuze volcanics plotted on the Th-Hf-Ta diagram of Wood (1980). Symbols given in figure 22.

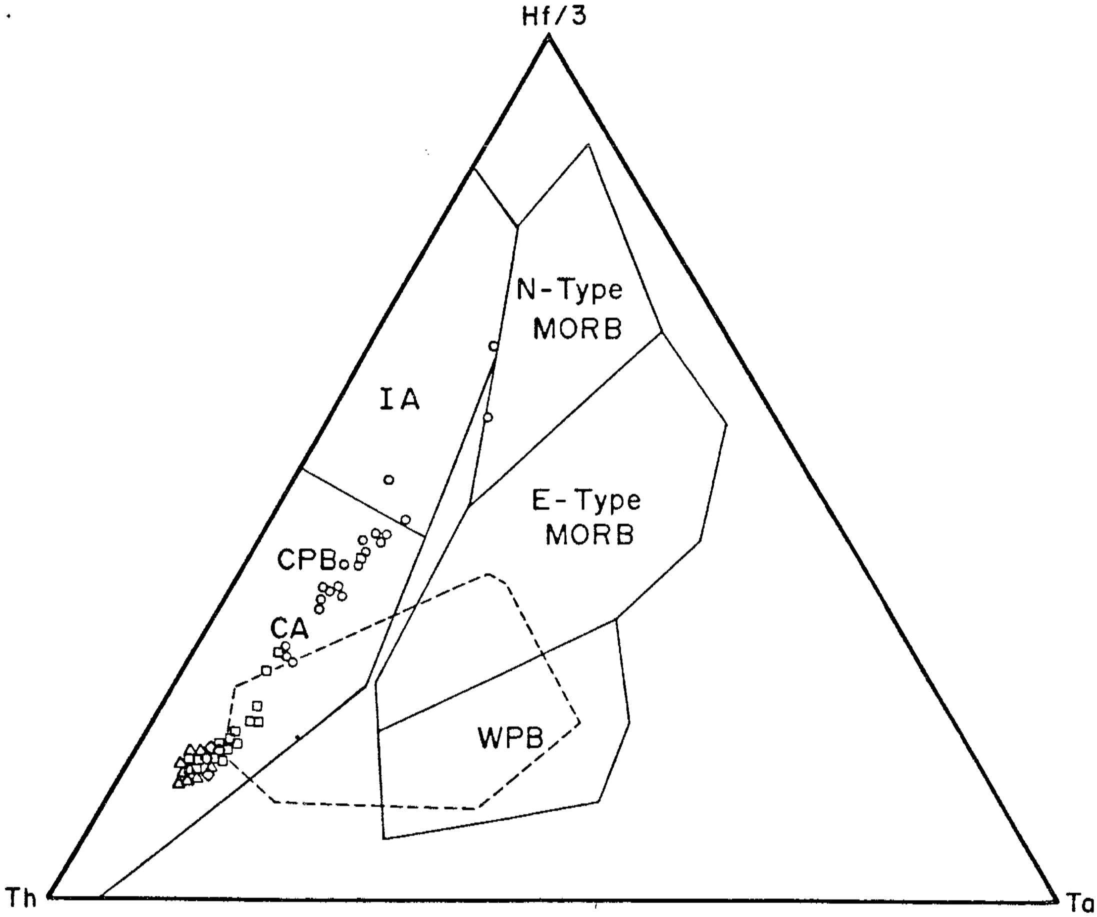
Hf/3
N-Type
MORB
IA
E-Type
MORB
CPB
CA
WPB
Th
Ta

Table 2. Summary of Tectonic Setting Classification of Nsuze Basalts and Basaltic Andesites.

Diagram	Reference	Tectonic Affinity
Ti-Zr	1	A,W
Ti-Zr-Y	2	A
Zr/Y-Zr	3	C
Th/Yb-Ta/Yb	3	C
Ta-Th-Hf	4	A
REE		C,(M)*
NMORB-normalized spidergram	3	C,(M)*

Symbols: A, arc undifferentiated; C, continental arc; W, within-plate (including rifts and back-arc basins in or near continental crust); M, ocean ridge. 1, Pharaoh and Pearce (1984); 2, Pearce and Cann (1973); 3, Pearce (1983); 4, Wood (1980).
*one sample has affinities to MORB.

andesites and andesites. For instance, the moderate La/Yb and Th/Yb ratios are similar to these ratios in andesites and basaltic andesites from evolved island arcs and continental margin arcs (Fig. 24). Similar results are apparent in terms of Ti/Zr and Ti/V distributions. It should be noted that none of the samples has low incompatible element ratios typical of primitive arcs nor very high ratios characteristic of Andean arcs (Fig. 24). On a Th-Hf-Ta diagram (Fig. 25), Rhenosterhoek basaltic andesites fall primarily in the convergent plate basalt field. On other tectonic discrimination diagrams including the Ti-Zr-Y (Pearce and Cann, 1973) and a Zr/Y-Zr (Fig. 26) diagrams, the Rhenosterhoek basaltic rocks also plot primarily with arc volcanics.

The basaltic andesites and andesites of the Rhenosterhoek Formation define two groups in terms of REE distributions. Both groups are LREE enriched with andesites having LREE contents of 60-90 x chondrites and basaltic andesites of about 20-30 x chondrites. Both groups also exhibit variable negative Eu anomalies probably reflecting variable amounts of plagioclase fractionation. The same two populations are also apparent on NMORB-normalized incompatible element diagrams (Fig. 27). For elements in the range of Ta to Yb, basaltic andesites are less enriched than

Figure 24. Distribution of Rhenosterhoek volcanics on a La/Yb-Th/Yb diagram compared to the fields of modern arc-related andesites and basaltic andesites. Fields are defined from approximately 250 published analyses of modern andesites. X= BTF core O= BSF and solid triangles= BBS core.

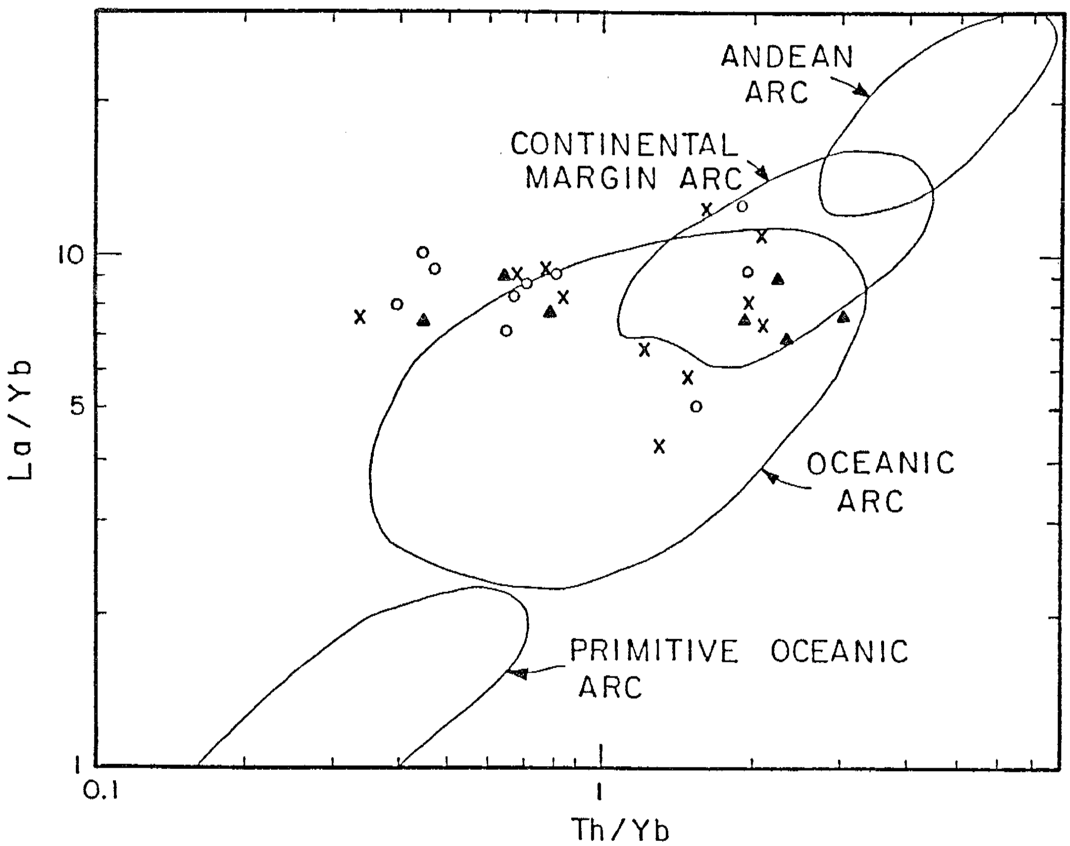
ANDEAN
ARC
CONTINENTAL
MARGIN ARC
OCEANIC
ARC
PRIMITIVE OCEANIC
ARC
10
5
1
La/Yb
0.1
1
Th/Yb

Figure 25. Position of the Rhenosterhoek volcanics on the Th-Hf-Ta diagram of Pearce (1983). open circles= Rhenosterhoek basaltic andesites.

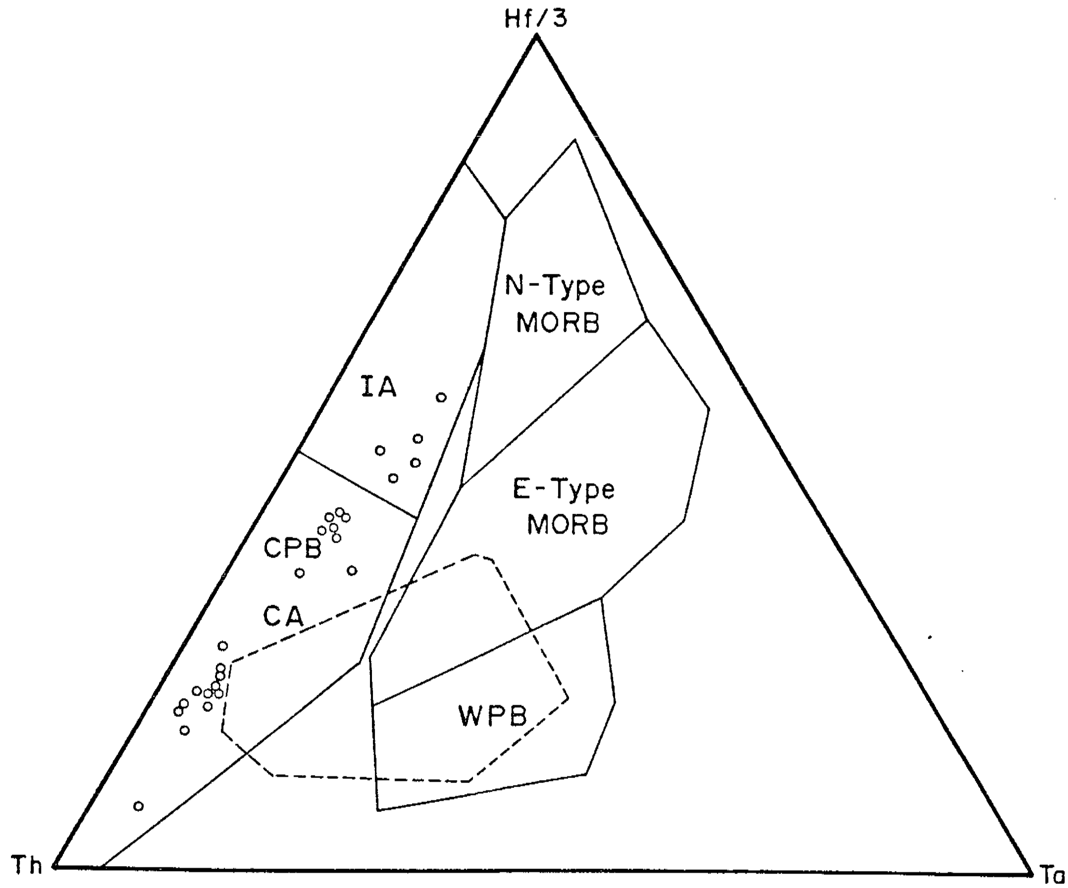
Hf/3
N-Type
MORB
IA
E-Type
MORB
CPB
CA
WPB
Th
Ta

Figure 26. Zr/Y-Zr diagram of Pearce (1983) showing the position of Rhenosterhoek basaltic andesites (circles). Error bar represents CV of standard BCR-1 (see Appendix B).

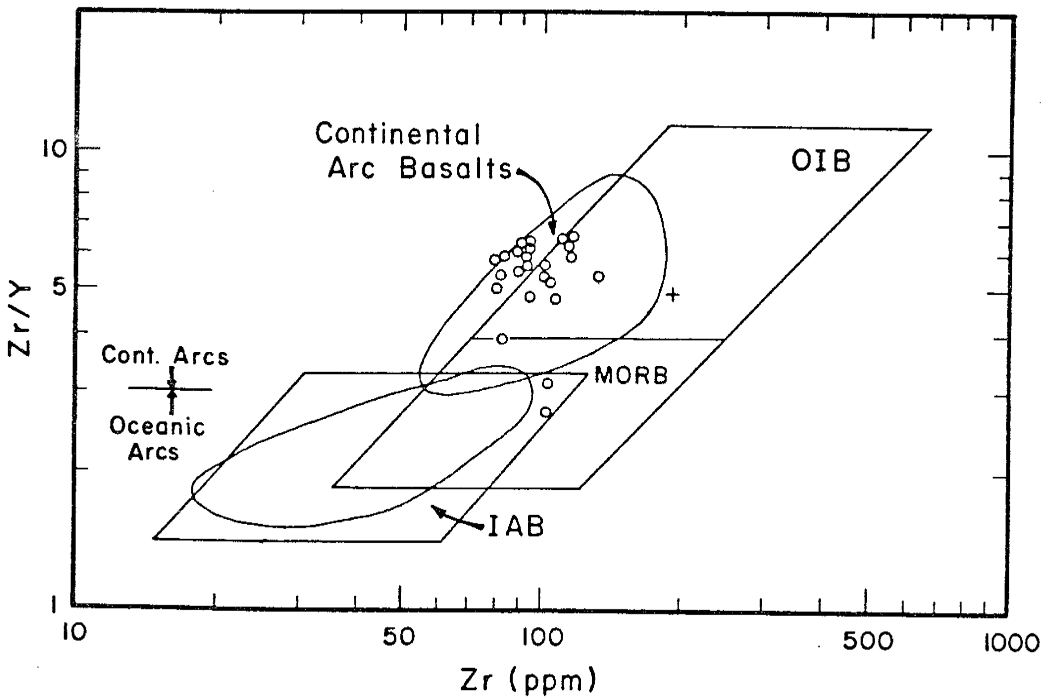

Continental
Arc Basalts
OIB
MORB
IAB
Cont. Arcs
Oceanic
Arcs
Zr/Y
10
5
1
10
50
100
500
1000
Zr (ppm)

Figure 27. NMORB-normalized incompatible element distributions in volcanic rocks from the Rhenosterhoek Formation (a) compared to basaltic andesites and andesites from modern continental-margin (b) and oceanic arcs (c). Normalization values from Pearce (1983) and modern data from Gorton (1977), Hole et al. (1984), Whitford et al. (1979), and Atherton et al. (1985). Shown are envelopes of variation for each group.

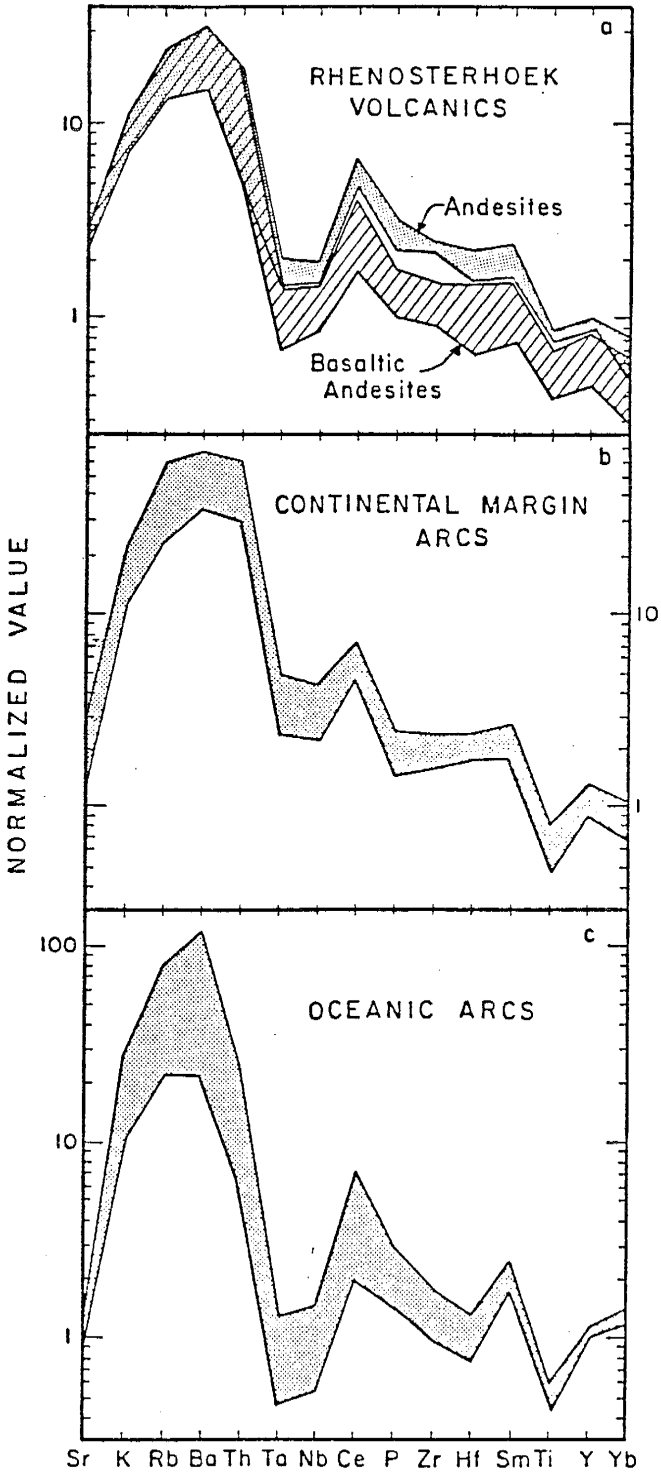
a
RHENOSTERHOEK VOLCANICS
Andesites
Basaltic Andesites
b
CONTINENTAL MARGIN ARCS
c
OCEANIC ARCS
NORMALIZED VALUE
100
10
1
Sr K Rb Ba Th Ta Nb Ce P Zr Hf Sm Ti Y Yb

andesites. LILE (Sr to Th) show comparable amounts of enrichment in both populations and may reflect some remobilization during alteration and/or low-grade metamorphism. The overall element distribution patterns, however, including LILE enrichment and negative Ta-Nb anomalies, are similar to those of modern basaltic andesites and andesites from oceanic and continental-margin arcs (Fig. 27b,c).

Three of the samples analyzed from the Rhenosterhoek Formation are probable paleosol horizons (Fig. 5). In addition to exhibiting strong depletions in CaO, Na_2O, Fe_2O_3 and MgO (and consequently strong enrichments in Al_2O_3), a feature common in Archean paleosols (Grandstaff et al., 1986), these rocks exhibit apparent enrichments in K_2O, Rb, Cs, Ba, Th, REE and high HSFE, as well as high La/Yb ratios (Appendix C, sample BTF-12 and 14).

Ventersdorp Supergroup

REE patterns in the Ventersdorp volcanics are LREE enriched with minor to negligible negative Eu anomalies (Fig. 28). Exceptions occur in some basaltic komatiites from the Westonaria Formation (Meredale Member) where slight LREE depletion is observed. In general, total REE contents are greater in volcanics from the Platberg

Figure 28. Chondrite-normalized REE abundances in volcanic rocks from the Ventersdorp Supergroup. Plotted are mean values from Appendix C. X= Allanridge Formation (Fm), += Rietgat Fm, solid square= Makwassie Fm, open triangle= Goedgenoeg Fm, solid circle= Edenville Fm, solid triangle= Loraine Fm, open square= Jeannette Fm, open circle= Okney Fm and open diamond= Westonaria Fm.

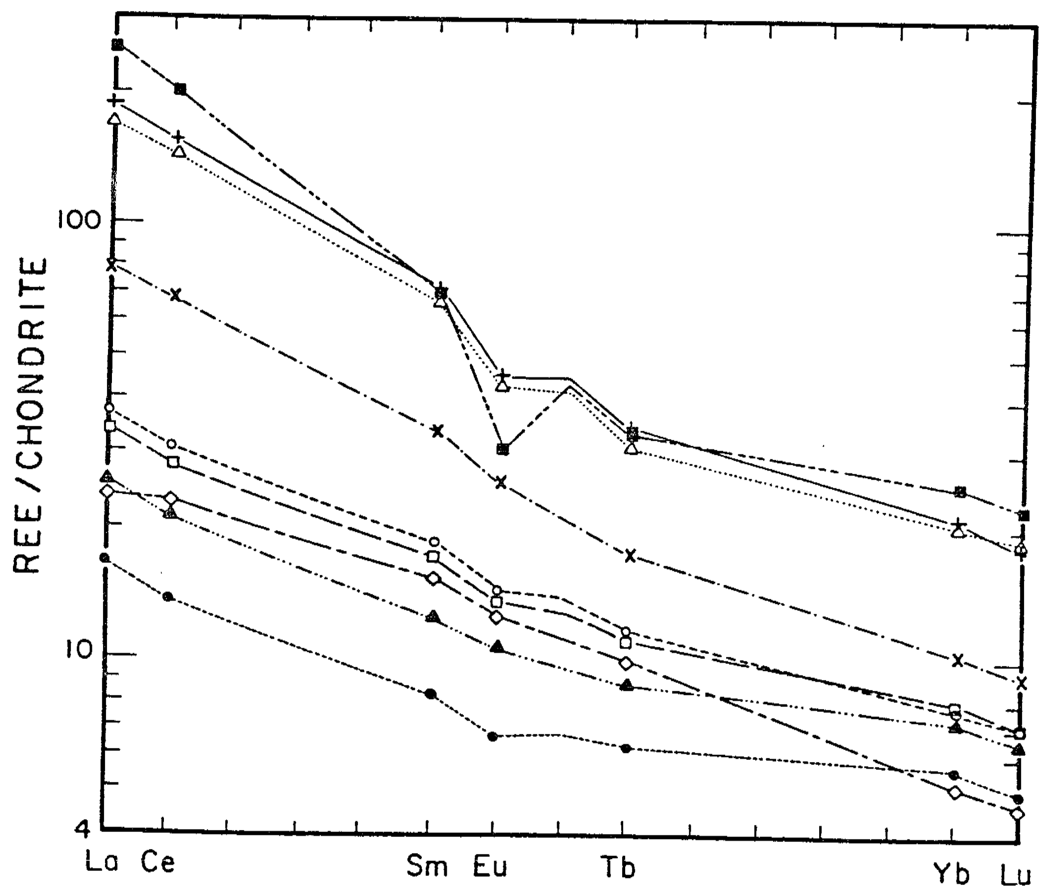
REE / CHONDRITE
100
10
4
La
Ce
Sm
Eu
Tb
Yb
Lu

and Pniel Groups than in Klipriviersberg volcanics. With exception of Westonaria samples, both the total REE contents and the La/Yb ratios decrease stratigraphically upwards in the Klipriviersberg Group consistent with major element changes suggesting less fractionated magmas at higher stratigraphic levels. This same trend is apparent on a NMORB-normalized incompatible element diagram (Fig. 29). All Ventersdorp volcanics show a similar increase in slope towards Ba with prominent negative Ta-Nb anomalies. The negative P and Ti anomalies on this diagram, especially apparent in the felsic volcanics of the Makwassie Formation, probably reflect removal of apatite and magnetite during fractional crystallization. Also consistent with secular major element changes in Klipriviersberg volcanics are decreasing contents of LILE and HFSE and increasing transition metals (especially Cr and Ni) with increasing stratigraphic level from the Orkney to the Edenville Formations.

In terms of tectonic setting, the NMORB-normalized incompatible element patterns are very similar to patterns of modern arc-related volcanics. The negative Ta-Nb anomalies are characteristic of a subduction zone component in the source and the shape of the element patterns is like that from volcanics from continental

Figure 29. NMORB-normalized incompatible distributions of Ventersdorp volcanics. Averages from Appendix C. Nb abundances of Meredale Member of the Formation are interpolated. Normalizing values from Pearce (1983). Symbols given in figure 28.

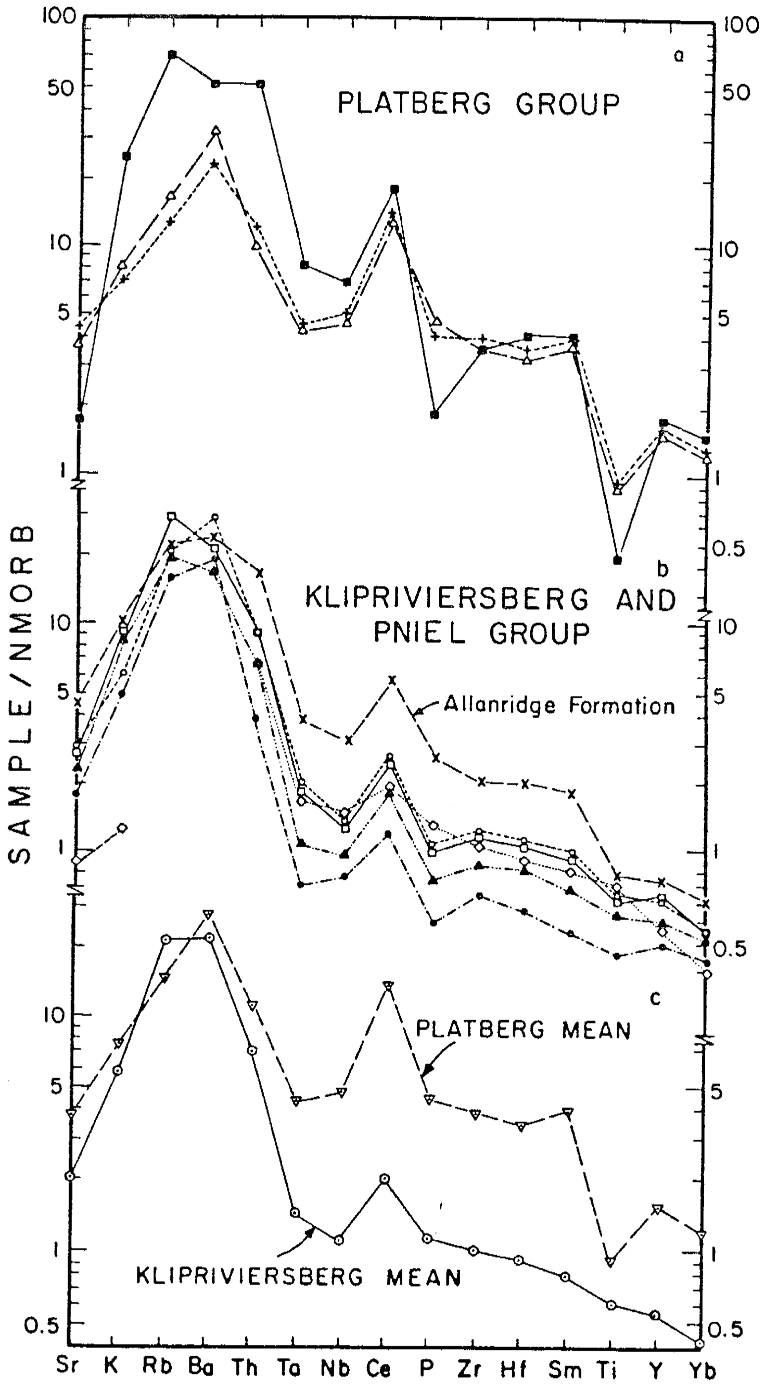
PLATBERG GROUP
a
KLIPRIVIERSBERG AND PNIEL GROUP
b
Allanridge Formation
c
PLATBERG MEAN
KLIPRIVIERSBERG MEAN
SAMPLE / NMORB
100
50
10
5
1
0.5
Sr K Rb Ba Th Ta Nb Ce P Zr Hf Sm Ti Y Yb

margin arcs and their associated back-arc basins (Pearce, 1983; Condie, 1986). Continental arc type geochemical characteristics of Ventersdorp volcanics are also apparent on Th/Yb-Ta/Yb and Th-Hf-Ta diagrams (Figs. 30 and 31). Again, stratigraphic trends are apparent in the Klipriviersberg data where both Th/Yb and Ta/Yb ratios decrease in volcanics from the Orkney Formation upwards to the Edenville Formation. On both diagrams, volcanics of the Platberg Group define a different trajectory which is characterized by relative Th depletion. With exception of the Westonaria basaltic komatiites, the Klipriviersberg volcanics plot in a remarkably tight cluster in the evolved arc field on the Th-Hf-Ta diagram (Fig. 31).

Transvaal Supergroup

REE patterns in the Dullstroom and Hekpoort Formations are LREE enriched (60 to 90 X chondrite) and mild negative Eu anomalies are common (average Eu/Eu^* = 0.8)(Fig. 32). In contrast, the Machadodorp volcanics exhibit flat to LREE depleted patterns (similar to NMORB) to only slightly LREE enriched (25 X chondrite) and possess minor Eu anomalies (Eu/Eu^* = 0.9). The Abel Erasmus volcanics have erratic REE patterns. Randomly distributed LREE (from 30 to 90 X chondrite)

Figure 30. Distribution of the Ventersdorp volcanics on a Th/Yb-Ta/Yb diagram. Fields after Pearce (1983). Symbols given in figure 28. Error bar represents CV of BCR-1 (see Appendix B).

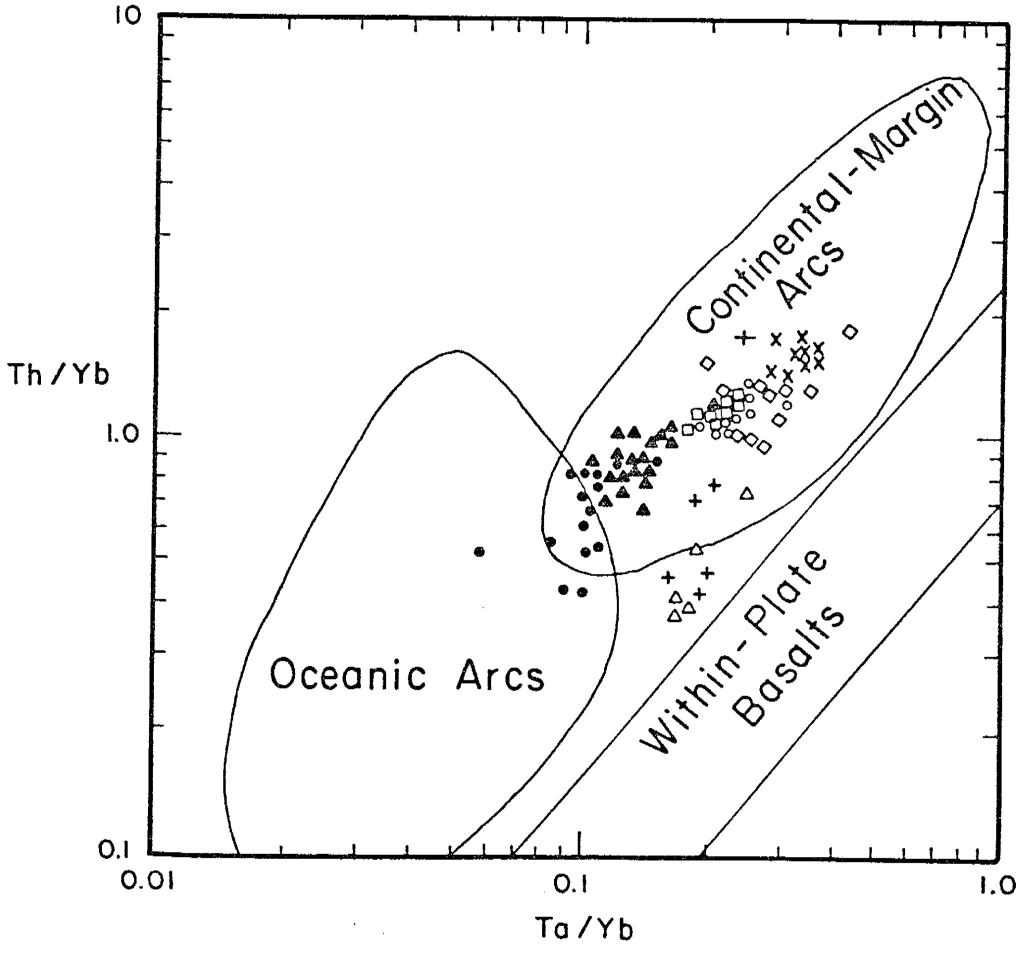
10
1.0
0.1
Th / Yb
0.01
0.1
1.0
Ta / Yb
Continental-Margin Arcs
Oceanic Arcs
Within-Plate Basalts

Figure 31. Th-Ta-Hf diagram after Wood (1980) showing the position of the Ventersdorp lavas. Symbols given in figure 28.

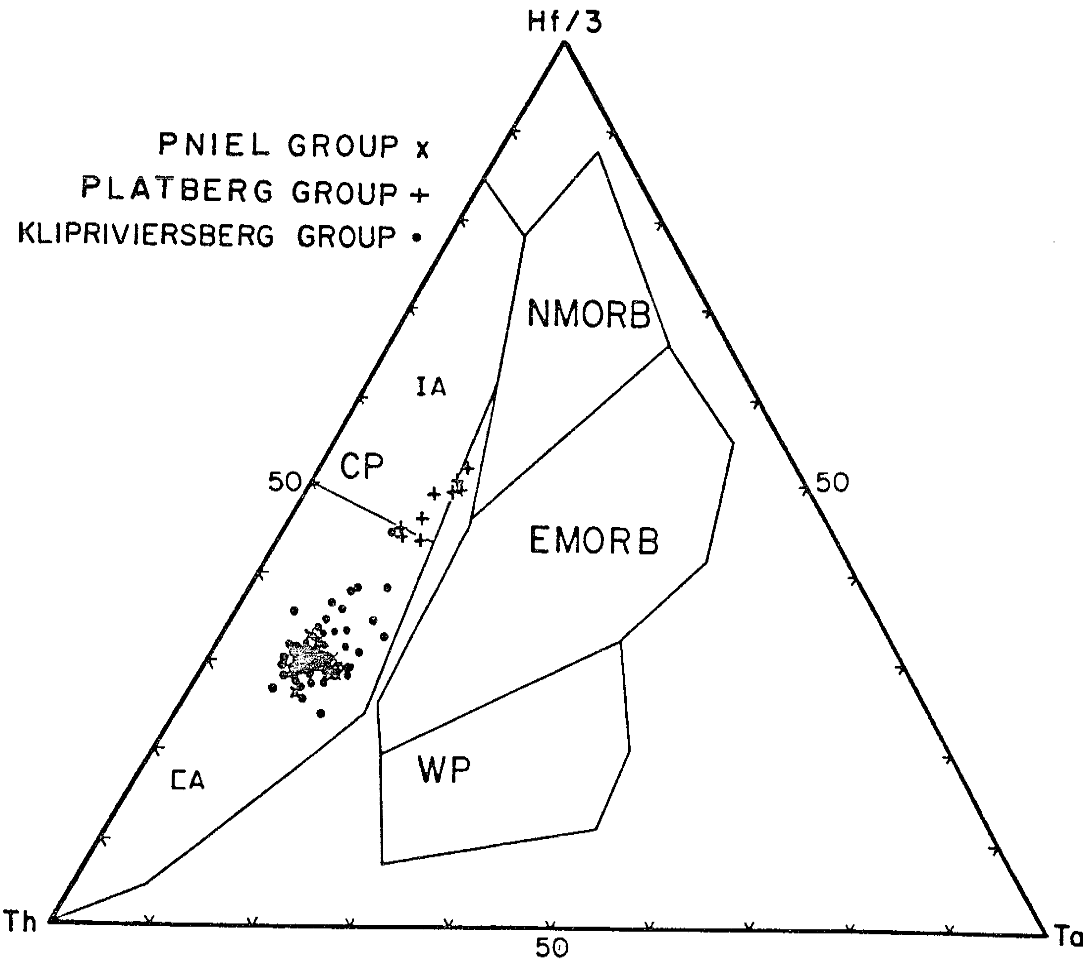
Hf/3
PNIEL GROUP x
PLATBERG GROUP +
KLIPRIVIERSBERG GROUP •
NMORB
IA
CP
50
50
EMORB
WP
CA
Th
50
Ta

Figure 32. Chondrite-normalized REE abundances in volcanic rocks from the Transvaal Supergroup and Soutpansberg Group. Plotted are averages from Appendix C. += Ngwanedzi Formation (Fm), open circle= Sabasa Fm, open square= Dullstroom Fm, open triangle= Machadodorp Fm, solid square= Hekpoort Fm and solid circle= Abel Erasmus Fm.

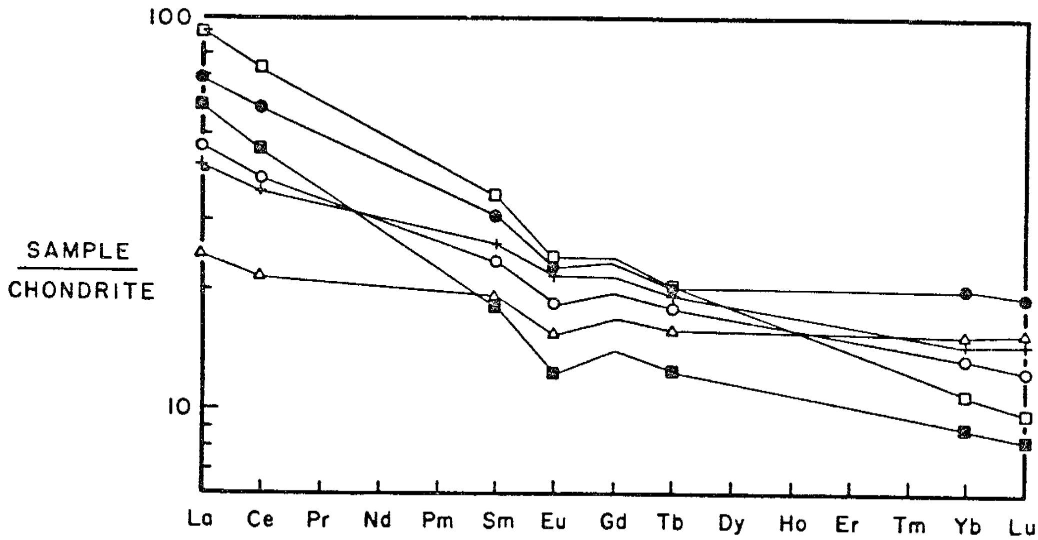
100
10
SAMPLE
CHONDRITE
La
Ce
Pr
Nd
Pm
Sm
Eu
Gd
Tb
Dy
Ho
Er
Tm
Yb
Lu

and one sample with low HREE concentrations are particularly noticeable.

On NMORB-normalized diagrams the Dullstroom and Hekpoort volcanics show similar patterns which consist of enriched LILE (Sr-Th) and LREE, and negative Ta-Nb, Ti and P anomalies (Fig. 33). The Machadodorp volcanics show flat HFSE and REE similar to NMORB and a moderate enrichment in LILE. The average NMORB-normalized patterns of the Abel Erasmus volcanic average are like that of the Machadodorp samples but patterns of individual samples are often widely dispersed. One sample in particular (D-38) shows decoupling of Ta-Nb, Zr-Hf and Y-Yb and may indicate alteration.

Tectonic setting interpretation of the NMORB-normalized diagram suggests the Machadodorp volcanics most resemble NMORB but have LILE enrichment. The Abel Erasmus volcanics appear to be intermediate between NMORB and arc volcanics. Random trace element distributions hinder any further comparison. In contrast, the Dullstroom and Hekpoort volcanics are very much like modern arc-related volcanics. The obvious subduction zone component (negative Ta-Nb anomaly) strongly suggests a subduction related source. The overall elemental pattern resembles those of modern continental arcs and associated back-arc basins

Figure 33. NMORB-normalized incompatible element distributions of Transvaal and Soutpansberg volcanics. Averages from Appendix C. Normalizing values from Pearce (1983). Symbols given in figure 32

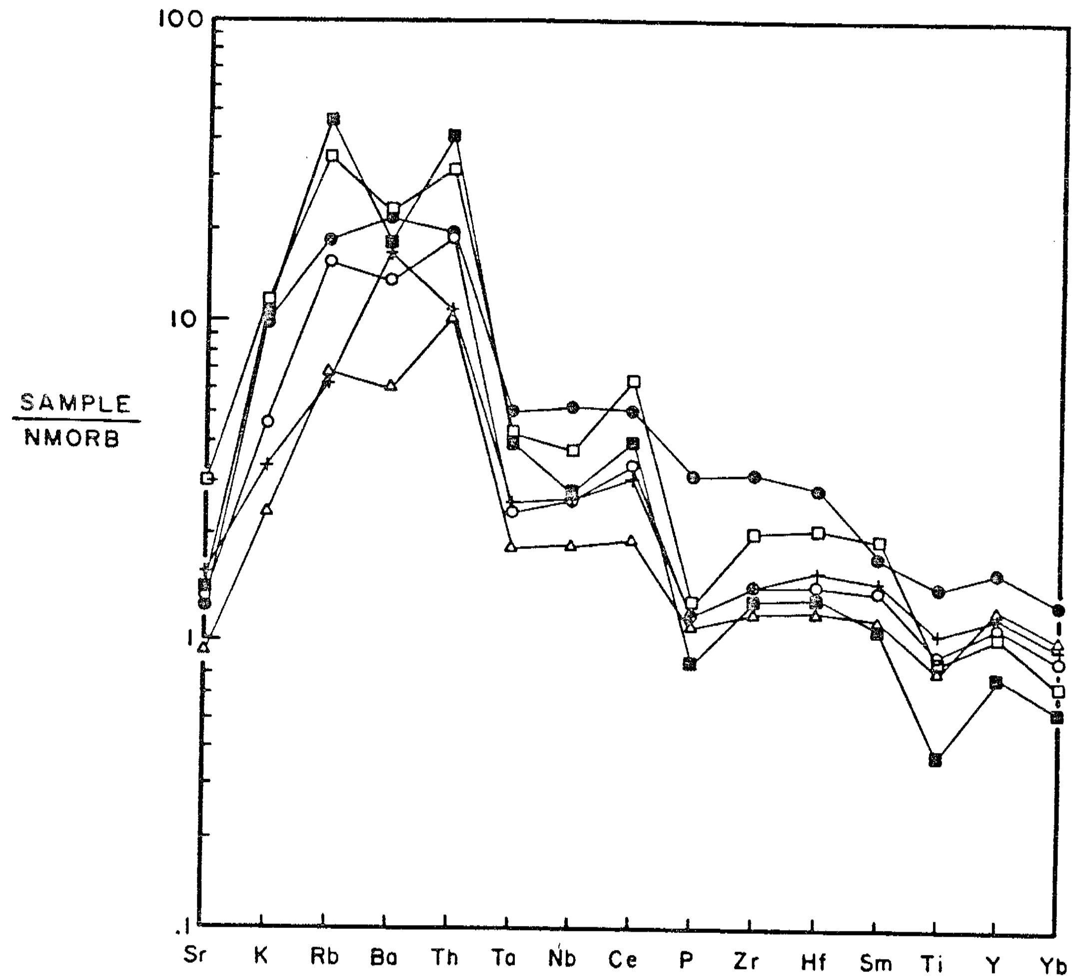
100
10
1
.1
SAMPLE
NMORB
Sr
K
Rb
Ba
Th
Ta
Nb
Ce
P
Zr
Hf
Sm
Ti
Y
Yb

(Pearce, 1983; Condie, 1986). The Abel Erasmus, Dullstroom and Hekpoort volcanics geochemical similarity to modern continental arcs is also observed on Th-Hf-Ta and Th/Yb-Ta/Yb diagrams. In comparison, the Machadodorp volcanics also plot in continental arc fields, although two samples (C26 and C61) are displaced toward NMORB. The Machadodorp volcanics similarity to NMORB is apparent on a Zr/Y-Zr diagram (Fig. 34) where all samples of this formation plot within the MORB field and possess Zr/Y ratios less than 3 (similar to oceanic arcs). Overlap of the Machadodorp volcanics into the IAB field is noted. In contrast, the Dullstroom, Hekpoort and Abel Erasmus volcanics have Zr/Y ratios greater than 3 (similar to continental arcs) and plot within the continental arc field, trending into ocean island basalts (OIB). The most primitive samples within each formation, in this case those with the lowest Zr and Zr/Y, are considered most diagnostic. Thus the trend into the OIB field in the latter example is a result of intraformational differentiation and not a sampling of two tectonic settings.

Soutpansberg Group

The Ngwanedzi and Sabasa volcanics are

Figure 34. Distribution of the Transvaal and Soutpansberg volcanics on a Zr/Y-Zr diagram. Fields after Pearce (1983). Symbols given in figure 32.

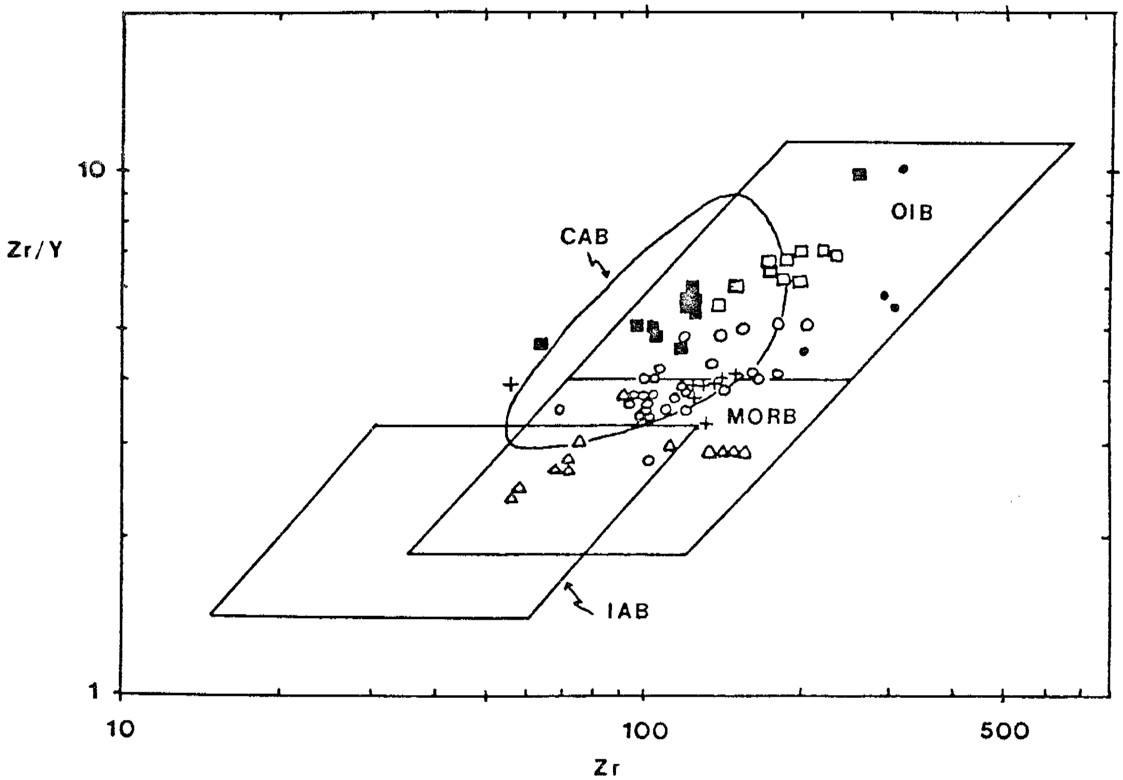
10
Zr/Y
1
10
100
500
Zr
CAB
OIB
MORB
IAB

GEOCHEMICAL MODELS

Introduction

To evaluate mechanisms of magma production and to characterize sources, well established melting and crystallization relations are employed using major and trace element distributions (Wright and Doherty, 1970, O'Hara, 1977; Allegre and Minster, 1978; DePaolo, 1981; DePaolo, 1985). Models are tested using computer programs of Knoper (1988). A more detailed description of modeling techniques is given in Appendix E. Distribution coefficients are compiled from numerous sources and given in Appendix F.

Crustal Contamination

A subduction-zone component (i.e. LILE and LREE enrichment without Ta-Nb enrichment on NMORB-normalized diagrams) is acquired by arc magmas as they travel from above a descending plate through a mantle wedge (Gill, 1981). Such enrichment may also be acquired as magmas pass through continental crust. The problem of distinguishing between these two processes has been discussed by several investigators (Pearce, 1983; Weaver and Tarney, 1983; Hawkesworth et al., 1984;

geochemically very similar. On a chondrite-normalized REE plot (Fig. 32), nearly identical patterns are observed for these formations with slightly enriched LREE (35 X chondrite) and minor Eu anomalies (average $Eu/Eu^{*} = 0.9$). Again, nearly identical patterns are observed on NMORB-normalized incompatible element distributions (Fig. 33). Deviations occur with lower Rb and Th abundances in the Ngwanedzi volcanics. Negative P and Ti anomalies and minor negative Ta-Nb anomalies are common. Enrichment in LILE, along with the negative Ta-Nb anomalies mentioned above, are similar to those observed in modern arc-related volcanics. This similarity to modern arc volcanics is also observed on Th-Hf-Ta and Th/Yb-Ta/Yb diagrams. On the Th/Yb-Ta/Yb plot, two samples (C137 and C143) plot in the oceanic arc field, one sample each from the Ngwanedzi and Sabasa Formations, representing the most primitive samples from each formation.

Similar characteristics are seen on a Zr/Y-Zr diagram where most Soutpansberg samples plot in the continental arc field (Fig. 34). Despite the apparent trend of many samples into oceanic island basalt and MORB fields, all Soutpansberg volcanics have Zr/Y ratios greater than 3, typical of continental arcs and OIB.

Arculus, 1987). Although it is generally not possible to distinguish between the processes without Nd-Sr-Pb isotopic data, incompatible element distributions can provide useful insight into the relative importance of the two processes (Weaver and Tarney, 1983).

Nsuze Group

Trace element models suggest that crustal contamination has affected the mafic to intermediate volcanics of the Nsuze Group. The possibility of crustal contamination in the Nsuze volcanics is supported by their initial epsilon Nd values of -2.6 (Hegner et al., 1984) which allows, but does not demand crustal contamination. Only a few Nsuze samples appear altered on the alteration screens of Beswick and Soucie (1978). This lack of major element decoupling (CaO/K_2O, Al_2O_3/K_2O and SiO_2/K_2O) also limits the amount of crustal contamination that could have occurred (i.e. crustal contamination would increase SiO_2, K_2O and decrease CaO). A trace element model evaluating the extent and type of crustal contamination is given in the Magma Production Section.

Rhenosterhoek Formation

Trace element models for crustal contamination with and without fractional crystallization have been tested for the Rhenosterhoek volcanics. Model AFC compositions using the equations of DePaolo (1981) are unrealistic. Because of uncertainties in the composition of the contaminant and the relatively large spread in incompatible element ratios in the volcanics, results are ambiguous. However, in the basaltic andesites and andesites, data allow up to 10% contamination with average Archean upper continental crust using the composition given by Taylor and McLennan (1985).

The relatively low Th/Yb ratios in some of the Rhenosterhoek volcanics (Fig. 24) may reflect contamination with lower crustal granulites in which Th is depleted. The fact that these rocks do not show similar depletions in Rb, Cs, and U, which are also depleted in granulites showing Th depletion (Condie and Allen, 1984), may reflect introduction of the latter three elements into the volcanics during secondary processes. Th is generally thought to be less mobile, and therefore may not be introduced, or at least not introduced to pre-mobilization levels.

Ventersdorp Supergroup

Geochemical results are plotted on a variety of element concentration and ratio diagrams for elements concentrated in the continental crust (chiefly REE and

LILE). Examples of such plots are the Th-Ba and Th-Hf diagrams (Fig. 35a and 35b). Also shown on these plots are estimates of average compositions of Archean and modern upper and lower continental crust. The Ventersdorp data define trajectories on both diagrams showing increasing Ba and Hf with Th. The Platberg lavas form a distinct low-Th population on the Th-Hf plot. The Ventersdorp trends do not lie on or near mixing lines between continental crust and the most primitive Ventersdorp basalts (those from the Edenville Formation). This suggests, at least in terms of Th and Ba, which are two elements strongly concentrated in the continental crust, that bulk upper crustal contamination of Ventersdorp lavas is minimal. Th-Hf distributions furthermore suggest that the Klipriviersberg-Allanridge and Platberg lavas belong to different magmatic suites. Similar results are obtained from other element and element ratio diagrams using both upper and lower continental crustal averages as end members. Although incompatible element distributions do not favor significant contamination of Ventersdorp magmas with continental crust, negative epsilon-Nd values (-4 to -6) reported from Ventersdorp

Figure 35. Th-Ba and Th-Hf diagrams showing distribution of Ventersdorp lavas. Also shown are average compositions of upper (AUC) and lower (ALC) Archean continental crust and upper (UC) and lower (LC) Modern continental crust from Taylor and McClennan (1985) and Weaver and Tarney (1984). X= Allanridge Fm, += Rietgat Fm, solid squares= Makwassie Fm, open triangles= Goedgenoeg Fm, solid circles= Edenville Fm, solid triangles= Loraine Fm, open squares= Jeannette Fm, open circles= Orkney Fm and open diamonds= Westonaria Fm. Error bars represent CV of BCR-1 (see Appendix B).

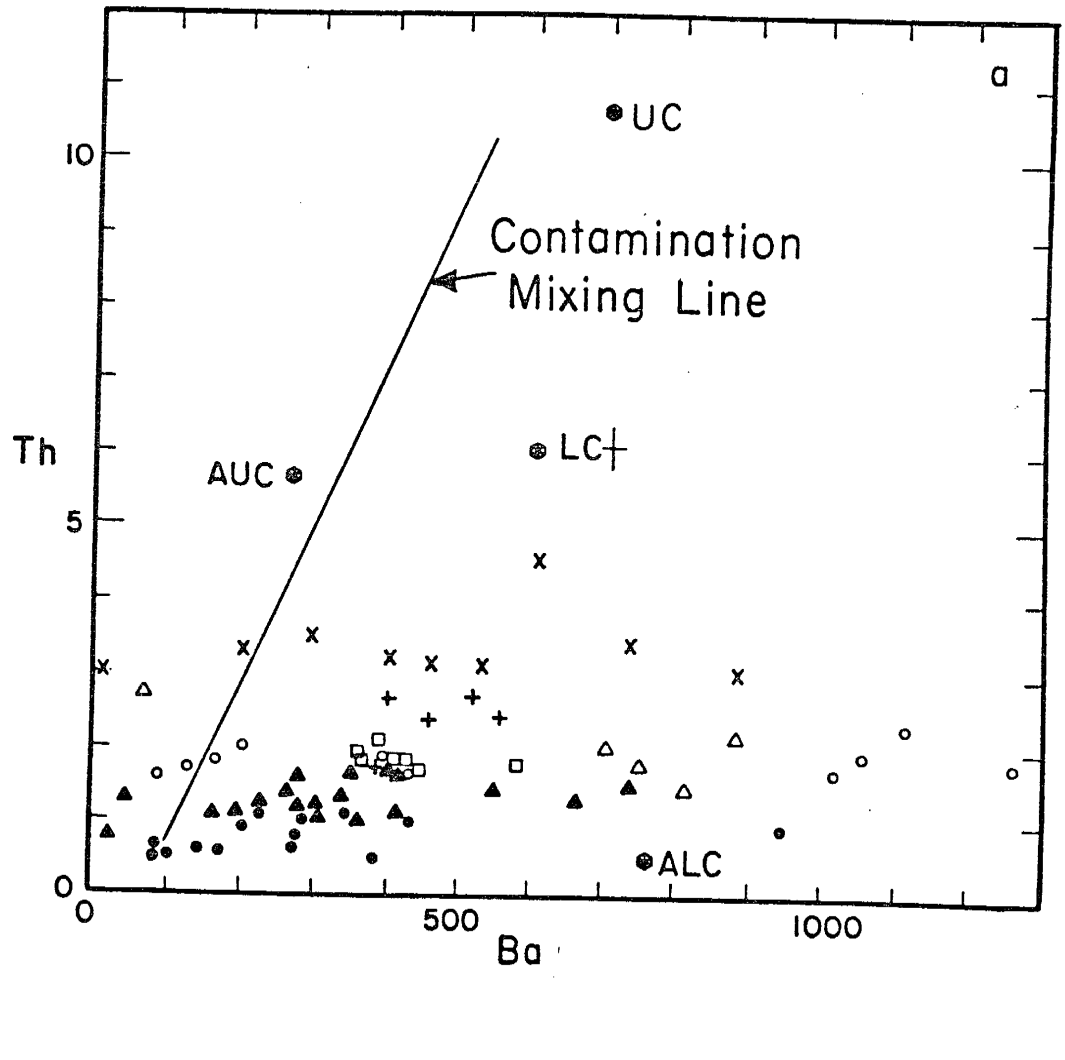
a
UC
Contamination
Mixing Line
LC
AUC
ALC
Th
Ba
0
5
10
0
500
1000

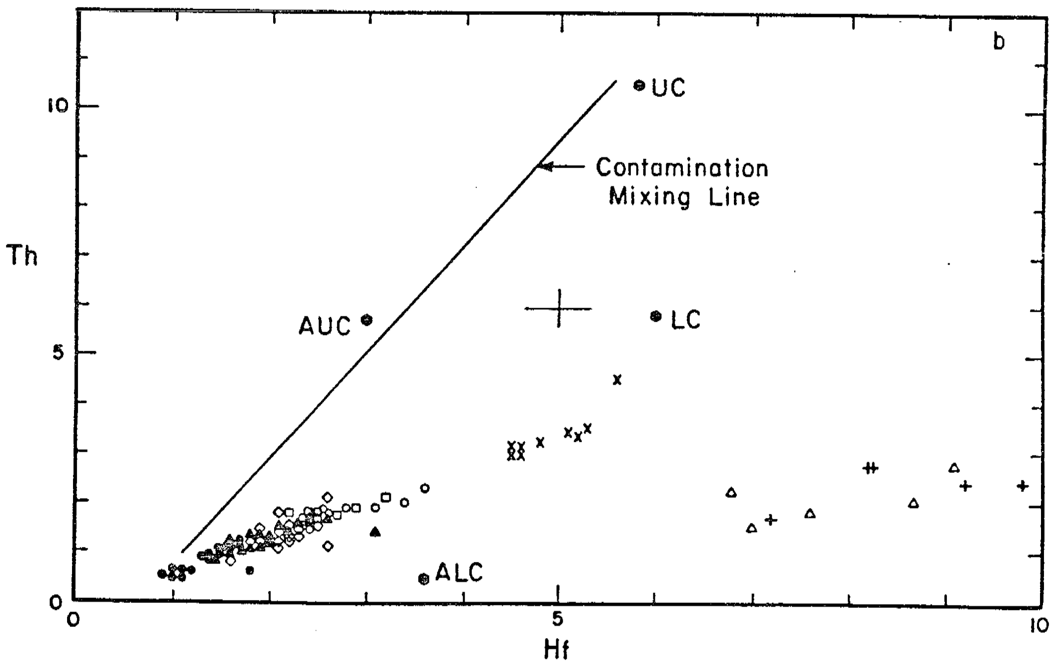

b
UC
Contamination
Mixing Line
Th
AUC
LC
ALC
0
5
10
Hf

basalt samples (A. Kroner, 1986, personal communication to K.C. Condie) allow some crustal contamination. Overall, results suggest that incompatible element distributions in Ventersdorp volcanics reflect magmatic processes and mantle source compositions.

Transvaal Supergroup and Soutpansberg Group

Evaluation of incompatible trace element diagrams involving the Transvaal volcanics suggests that there is little obvious geochemical correlation with average compositions of upper and lower crust, both Archean and modern, to that of the Transvaal volcanics. Exceptions are trends toward modern upper crust with respect to K_2O, Th and Ba in most Dullstroom volcanics, and Rb, La and Th in many of the Hekpoort volcanics. The remaining sample trajectories appear to be simple igneous differentiation trends. Large amounts of crustal contamination would change the major element concentration in these volcanics. Such changes (increased K_2O, SiO_2 and Na_2O and decreased CaO) should cause the Transvaal samples to appear altered on the SiO_2/K_2O-Al_2O_3/K_2O and CaO/K_2O-Al_2O_3/K_2O alteration screens of Beswick and Soucie (1978). This is not the case because few Transvaal samples plot in the altered fields of the above diagrams. Crustal contamination is considered to be minimal but may be responsible for scatter in the more incompatible elements (LILE and LREE).

For the Soutpansberg Group volcanics, no alteration is apparent on the alteration screens of Beswick and Soucie (1978). Thus, like the Transvaal volcanics, crustal contamination is of an amount insufficient to alter the ratios of SiO_2/K_2O, CaO/K_2O and Al_2O_3/K_2O, nor (as mentioned previously) produce normative corundum in the Soutpansberg Group samples used in this study. It should be noted that Barton (1979) reports that some Soutpansberg volcanics contain normative corundum. In addition, Barton (1979) describes Rb-Sr whole rock isochrons for Soutpansberg volcanics which give anomalously high initial 87Sr/86Sr ratios (>0.745). He attributes these high initial ratios to 1) a mantle source enriched in Rb and depleted in Sr or 2) Soutpansberg magma modification by assimilation of older continental crust. The latter is preferred by Barton (1979).

On a plot of Th-Hf (Fig. 36), possible mixing lines between the more primitive Transvaal and Soutpansberg volcanics and average compositions of modern lower crust, Archean lower crust and Archean upper crust are not apparent. However, there does seem to be a correlation with modern upper crust for some

Figure 36. Th-Hf diagram showing distribution of Transvaal and Soutpansberg volcanics. Also shown is an average composition of upper crust (UC) from Taylor and McClennan (1985). += Ngwanedzi Fm, O= Sabasa Fm, open squares= Dullstroom Fm, open triangle= Machadodorp Fm, solid squares= Hekpoort Fm and solid circles= Abel Erasmus Fm. Error bar represents CV of BCR-1 (see appendix B).

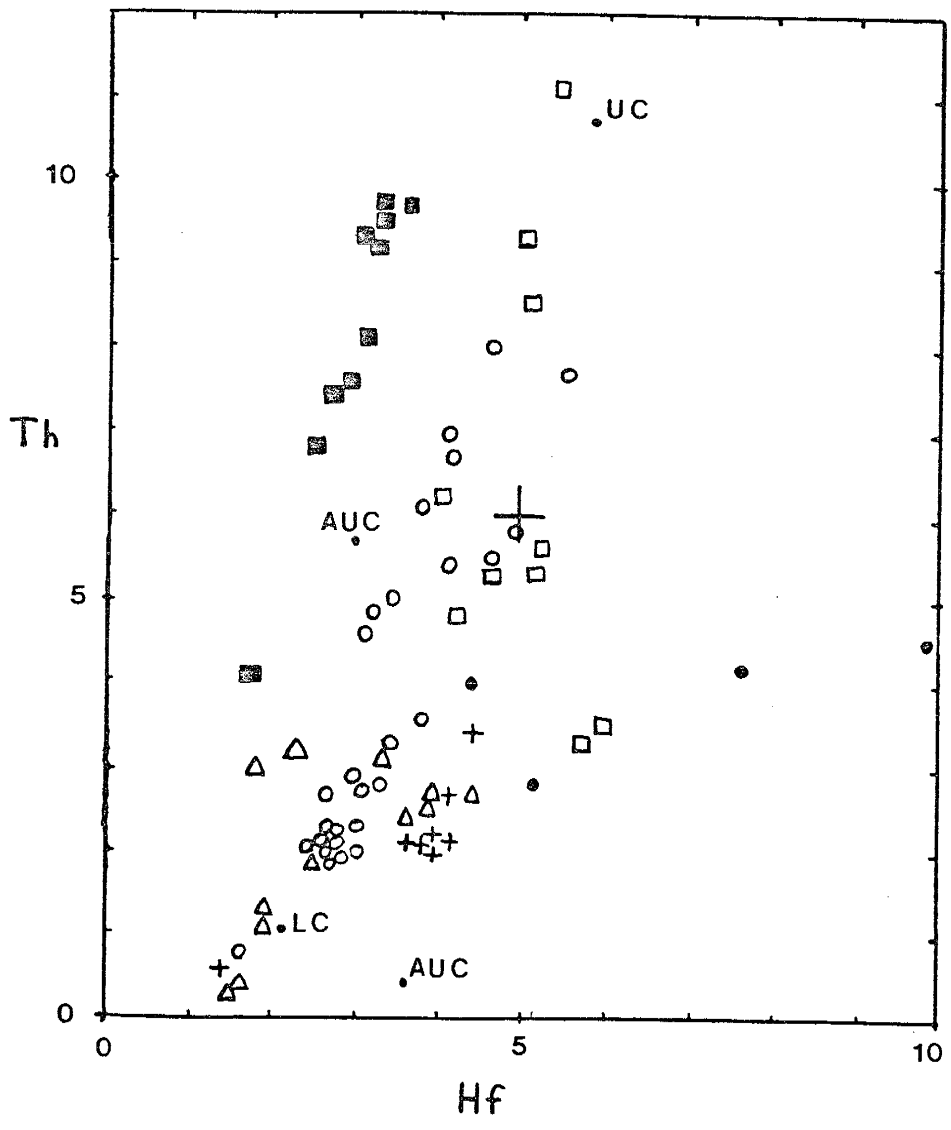

UC
10
Th
AUC
5
LC
AUC
0
0
5
10
Hf

volcanics in the Dullstroom, Hekpoort and Sabasa Formations. For approximately eleven Sabasa samples, and most Hekpoort and Dullstroom samples, enrichment in Th is greater than expected for normal igneous differentiation. Mixing trends between least evolved samples and upper crust (Fig. 36) are apparent. The same is true for K_2O, Rb, Ba, and La/Yb as well. It should be noted that some samples in figure 36 have Th and Hf abundances similar to that of upper crust. If this is taken literally, close to 100% mixing is implied, which, as previously discussed, cannot be the case. Instead, mixing with a trace element enriched crust or component is inferred, but not necessarily equivalent to upper crust. Crustal contamination may be from 5 to 10% in these samples with a crustal composition of approximately 50 ppm La, 100 ppm Ce, 20 ppm Th and variable amounts of K_2O, Rb, Sr and Ba.

Magma Production

Nsuze Group

Partial melting of a garnet lherzolite (~10%) satisfactorily produces the most primitive Nsuze basalt (this study; Armstrong et al., 1986). In addition, more than 30% fractional crystallization is required to explain the average Mg number for Nsuze basalts and basaltic andesites of approximately 50.

Partial melting models for the remaining Nsuze volcanics seem unrealistic for two reasons. First, the dramatic decrease in transition metals (Cr, Ni) from basalt to rhyolite is inconsistent with partial melting. For example, if partial melting were involved, the trajectory of the Nsuze volcanics in figure 37 would be much steeper than observed because of the minimal effect of partial melting on Ni (Cocherie, 1986); i.e., the trajectory is more like that of fractional crystallization. Similar inconsistencies are noted on numerous other incompatible-compatible trace element plots. Second, the apparent consanguinity of the suite, observed as consistent, gradual trace element enrichments from basalt to rhyolite are best explained by fractional crystallization. Figures 19 and 20 best demonstrate this genetic relationship.

In addition, open-system fractional crystallization models are not favored because incompatible element ratios are low relative to Ni and FeO-T/MgO abundances. Incompatible trace elements would be enriched relative to compatible and transition elements during crystallization in an open system magma chamber. Thus, Zr/Zr_0 and La/La_0 ratios (Kay et al.,

Figure 37. Zr-Ni diagram showing distribution of Nsuze volcanics and magma model trajectories. Tick marks represent 10% fractional crystallization (FXL). MP, average Mpuluzi granite; Avg, average values. Mineral modes: basalt to andesite, ol 30%, cpx 15%, plag 50% and mgt 5%; andesite to dacite, opx 22%, cpx 22%, plag 50% and mgt 6%; dacite to rhyolite, opx 26%, plag 59%, mgt 5%, zir 0.02%, alln 0.02% and apat 0.1%. ol= olivine, cpx= clinopyroxene, plag= plagioclase, opx= orthopyroxene, mgt= magnetite, apat= apatite, zir= zircon and alln= allanite. Distribution coefficients given in Appendix F. Error bar represents CV of BCR-1 (see Appendix B).

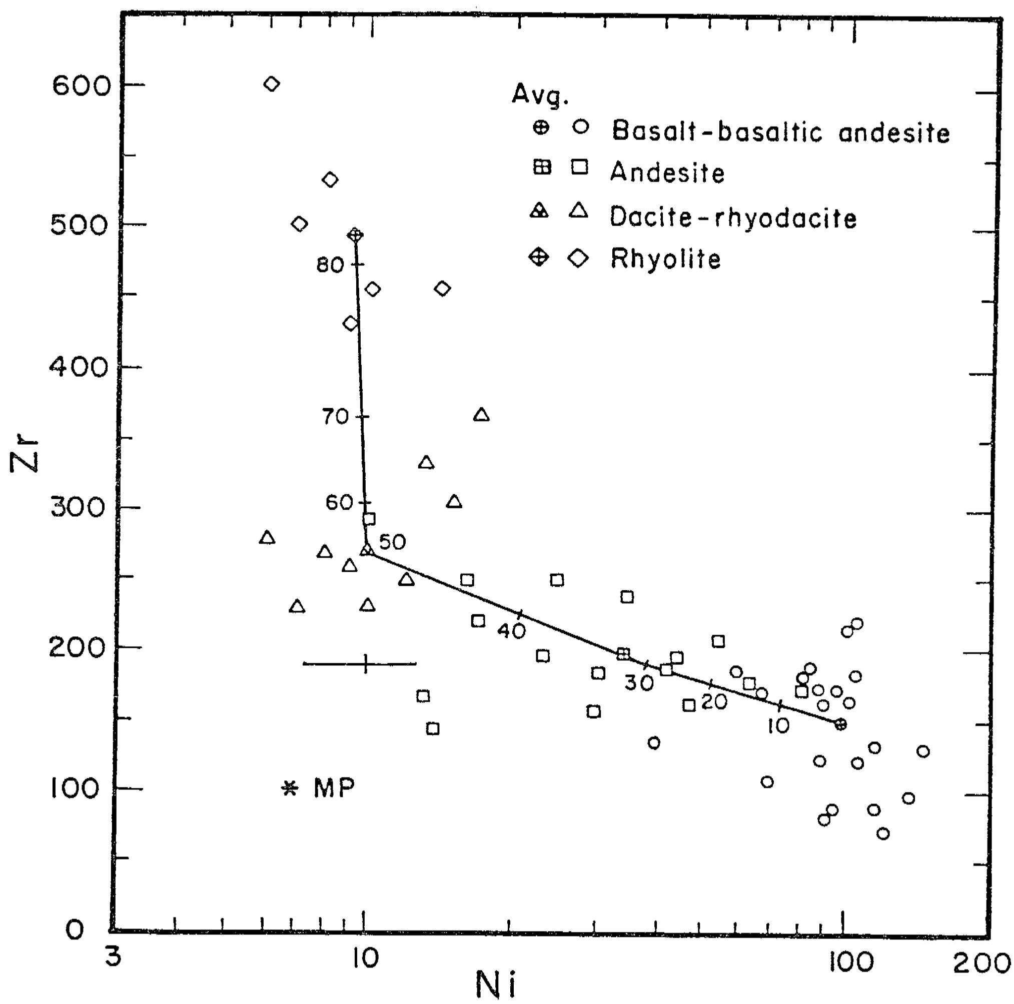

Avg.
Basalt-basaltic andesite
Andesite
Dacite-rhyodacite
Rhyolite
* MP
Zr
Ni
600
500
400
300
200
100
0
3
10
100
200
80
70
60
50
40
30
20
10

1982) should increase dramatically during this process while compatible and transition elements would increase only slightly. Instead, what is observed in the Nsuze volcanics is a gradual increase in these ratios with increasing differentiation, a trend more like that of closed-system fractional cryatallization. In keeping with these features, a closed-system fractional crystallization model is preferred to explain the Nsuze volcanic suite.

The continuum from basalt to rhyolite can be explained by closed-system fractional crystallization. Fractional crystallization models are taken in steps, starting with an average Nsuze basalt which undergoes fractional crystallization to produce an andesite. An average Nsuze andesite is then modeled to produce a dacite, and finally an Nsuze dacite to produce a rhyolite. A total of 82% fractional crystallization is required to produce rhyolite from a Nsuze basalt (Fig. 37). As discussed previously, (see Crustal Contamination section) crustal contamination involving LILE and LREE also may have occurred.

In comparison, Armstrong et al. (1986) call upon an equivalent amount of fractional crystallization (80%) and a large proportion of plagioclase in the fractionating mineral mode as in the present model. The remainder of the mineral mode, however, differs in that Armstrong et al. (1986) rely heavily on orthopyroxene in mafic models and olivine in intermediate models while the present model uses the reverse. To this author's knowledge, orthopyroxene is unlikely to be a primary fractionating phase in basalt undergoing low-pressure fractional crystallization (Grove and Baker, 1984; Grove and Kinzler, 1986), as is suggested by the distribution of Nsuze volcanics in the olivine-clinopyroxene-plagioclase-silica pseudo-liquidus system (Elthon, 1983; Elthon and Scarfe, 1984) which demonstrates olivine and plagioclase are the dominant liquidus phases during fractional crystallization. Also, contrary to the apparent tholeiitic nature of the Nsuze volcanics, the presence of olivine in the fractionating phases of intermediate magmas is more like that of a calc alkaline suite. It is therefore questionable whether olivine would be a fractionating phase in the production of andesite/dacite from a basaltic andesite as suggested by Armstrong et al. (1986), even at high pressure. Instead, the fractionating mode at 1 atm should include pigeonite and/or augite, along with plagioclase and orthopyroxene (Grove and Baker, 1984). If olivine is involved in the intermediate steps of a fractional crystallization model, then it should be used in the initial mafic steps as well.

A deficiency in LILE (K, Rb, Ba, Th) and LREE (La, Ce) in the closed system fractional crystallization models for basalt-andesite and andesite-dacite steps presents a problem. A similar deficiency in LREE was also noted by Armstrong et al. (1986). One way to enrich these elements in the derived liquid is by crustal contamination. Thompson et al. (1982) suggest that contamination of basalts from the Isle of Skye by Archean crust increases the abundance of Ba, Rb, Th, K, Sr and LREE while leaving the abundances of Nb, Ta, P, Zr, Hf, Ti, Y and middle to HREE relatively unaffected. In a similar way, the deficiency in LILE and LREE in the Nsuze closed system fractional crystallization basalt-andesite and andesite-dacite models can be solved when an average composition of the Mpuluzi pluton (Lochiel granite; Condie and Hunter, 1976) is used as a contaminant (10%)(Fig. 38). The equations for assimilation-fractional crystallization of DePaolo (1981; 1985) are used in this model. The derivation of the Nsuze rhyolite is best explained by closed system fractional crystallization of an average Nsuze dacite.

Although the calculated composition of the contaminant is very similar to the composition of the Mpuluzi pluton, the geographical distribution leaves the viability of the Mpuluzi pluton as a contaminant in question. Like other "Hood" granites in the region,

Figure 38. La/Yb-Zr diagram showing distribution of Nsuze volcanic rocks and magma model trajectories. Tick marks represent 10% fractional crystallization (10-80%) and accompaning granite contamination (2-10%). Model parameters and symbols given in Fig. 37. Mpuluzi granite contaminant: K_2O= 4.5%, Rb= 196 ppm, Ba= 682 ppm, Th= 20 ppm, La= 70 ppm, Ce= 131 ppm, Zr= 100 ppm and La/Yb=28. Error bar represents CV of BCR-1 (see Appendix B).

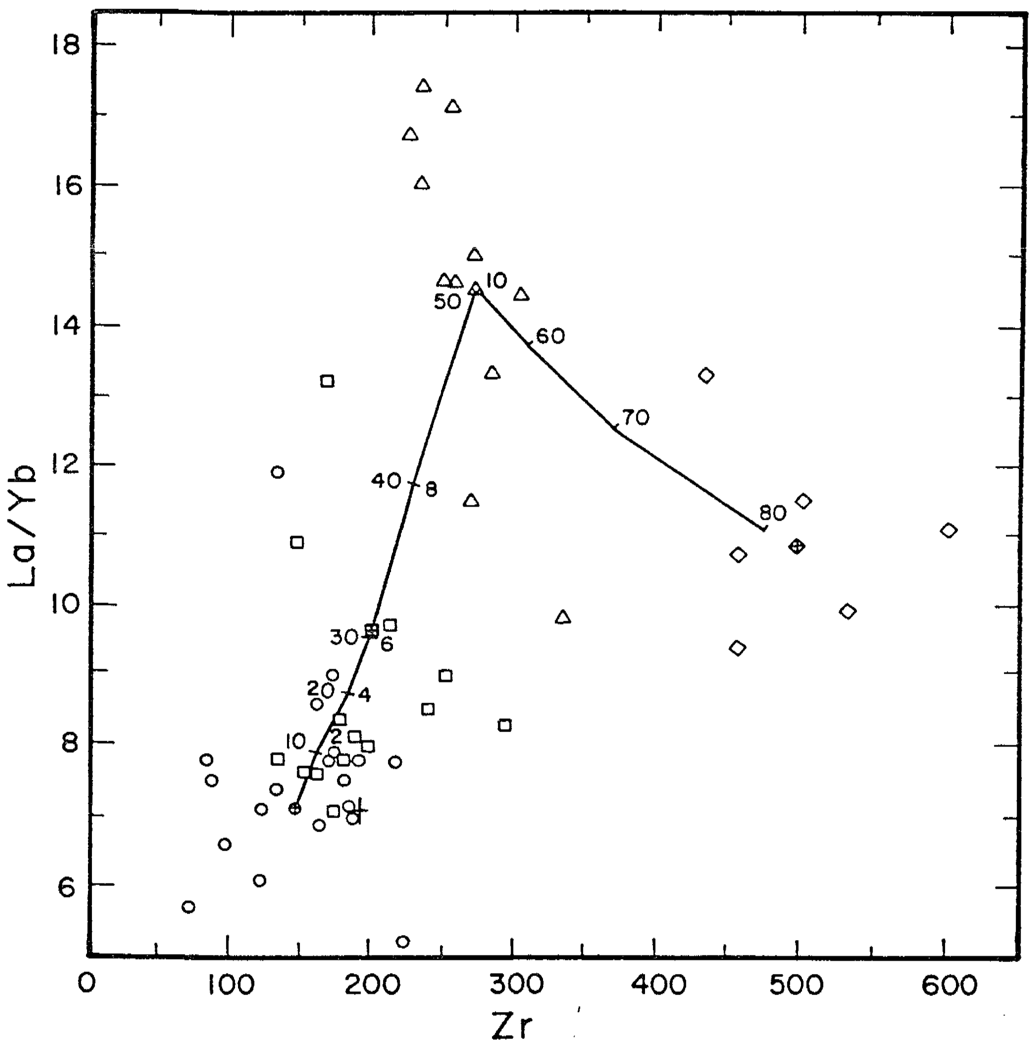
La/Yb
Zr
18
16
14
12
10
8
6
0
100
200
300
400
500
600
10
50
60
70
80
40
8
30
6
20
4
10
2

the Mpuluzi pluton is thought to form a relatively thin shield in the vicinity of its feeder dike(s), and rests on older granites (Ancient Gniess Complex [AGC]). This proposed limited vertical thickness is not appropriate for the scale of contamination required by the Nsuze volcanics, if contamination is indeed the mechanism of LILE and LREE enrichment. In addition, the Mpuluzi pluton occupies the area to the west of the Pongola basin but may underlie it in some areas.

Some authors (Hegner et al., 1984; Armstrong et al., 1986) consider the AGC a more appropriate contaminant because it directly underlies the Nsuze Group and appears to represent a much thicker plutonic suite. Because of low trace element abundances in the AGC, modeling calculations suggest nearly twice the amount of assimilation (approximately 18%) of AGC is needed to produce the required LILE and LREE abundances, compared to a Mpuluzi-type contaminant. Similarly, Hegner et al. (1984) calculate 25% crustal contamination in the Nsuze volcanics by AGC to explain the REE. Such large amounts of contamination, however, are inconsistent with major element constraints (e.g., lack of accompanying Fe_2O_3 and TiO_2 depletion, and the lack of decoupling of CaO/K_2O, Al_2O_3/K_2O and SiO_2/K_2O).

The amount of crustal contamination can be greatly reduced if the contaminants were partial melts

(Thompson et al., 1982) of the AGC or Mpuluzi pluton. These partial melts (as opposed to whole rock assimilation) should be selectively enriched in incompatible elements (K, Rb, Ba, Th, La, Ce) and thus would not modify the majority of Nsuze trace element ratios. Unfortunately, the effects of contamination by partial melts can only be described in general terms while whole rock assimilation (as used here) can be quantified.

Rhenosterhoek Formation

Although geochemical models allow Rhenosterhoek magmas to be produced by 2-8% batch melting of a garnet lherzolite with primordial elemental abundances, there are several problems with such a model. The andesite compositions are not similar to experimental liquids produced by the partial melting of lherzolites (Gill, 1981). Also, thermodynamic considerations argue against andesites, in general, representing partial melts of the mantle (Gill, 1981; Grove and Kinzler, 1986). Finally, the low Mg numbers and low Ni contents (Appendix C) demand considerable amounts of fractional crystallization of a mafic parent, which, in the case of the Rhenosterhoek andesites, is best matched by the Rhenosterhoek basaltic andesites.

Both major and compatible trace element distributions in the Rhenosterhoek volcanics indicate extensive fractional crystallization. The basaltic andesites and andesites can be produced from a calculated tholeiitic parent magma with liquidus phases, olivine, clinopyroxene and plagioclase. Employing the major-element crystallization program of Nielson (1985), olivine and clinopyroxene are the major liquidus phases until 25% fractional crystallization, after which plagioclase also becomes important. These phases are consistent with those expected to crystallize at intermediate crustal depths as indicated by the distribution of data on the Ol-Di-Hy-Q diagram (Fig. 13). For closed-system fractional crystallization, the Rhenosterhoek basaltic andesites can be produced by 10-20% crystallization of the most primitive basaltic andesite (BSF-3) by removal of olivine and clinopyroxene and a small amount of plagioclase in the ratios of 3:6:1, respectively (Fig. 39). The andesites can be produced from the most evolved basaltic andesite by up to 50% fractional crystallization of the same three minerals in the ratios of 1:2:2. In addition, open-system fractional crystallization models (O'Hara, 1977) are successful in accounting for the relatively rapid increases in incompatible element contents between the basaltic

Figure 39. Fractional crystallization models for the Rhenosterhoek volcanics shown on a Zr/Zr0-Ni diagram. Zr0 is the lowest observed Zr abundance in volcanic rocks from three drillcores (82 ppm). Sample BSF-3 is the assumed parent in all models. Closed-system fractional crystallization, models 1 and 2; open-system fractional crystallization, models 3 and 4. Mineral modes: Model 1, ol= 20%; plg= 41%; cpx= 39%; Models 2, 3 and 4 ol= 28%; plg= 39%; cpx= 33%; models 3 and 4 have leakages of 10% and 5%, respectively. Tick marks indicates degrees of fractional crystallization in percent. Distribution coefficients are given in Appendix F. X= BTF core, O= BSF core and solid triangle= BBS core.

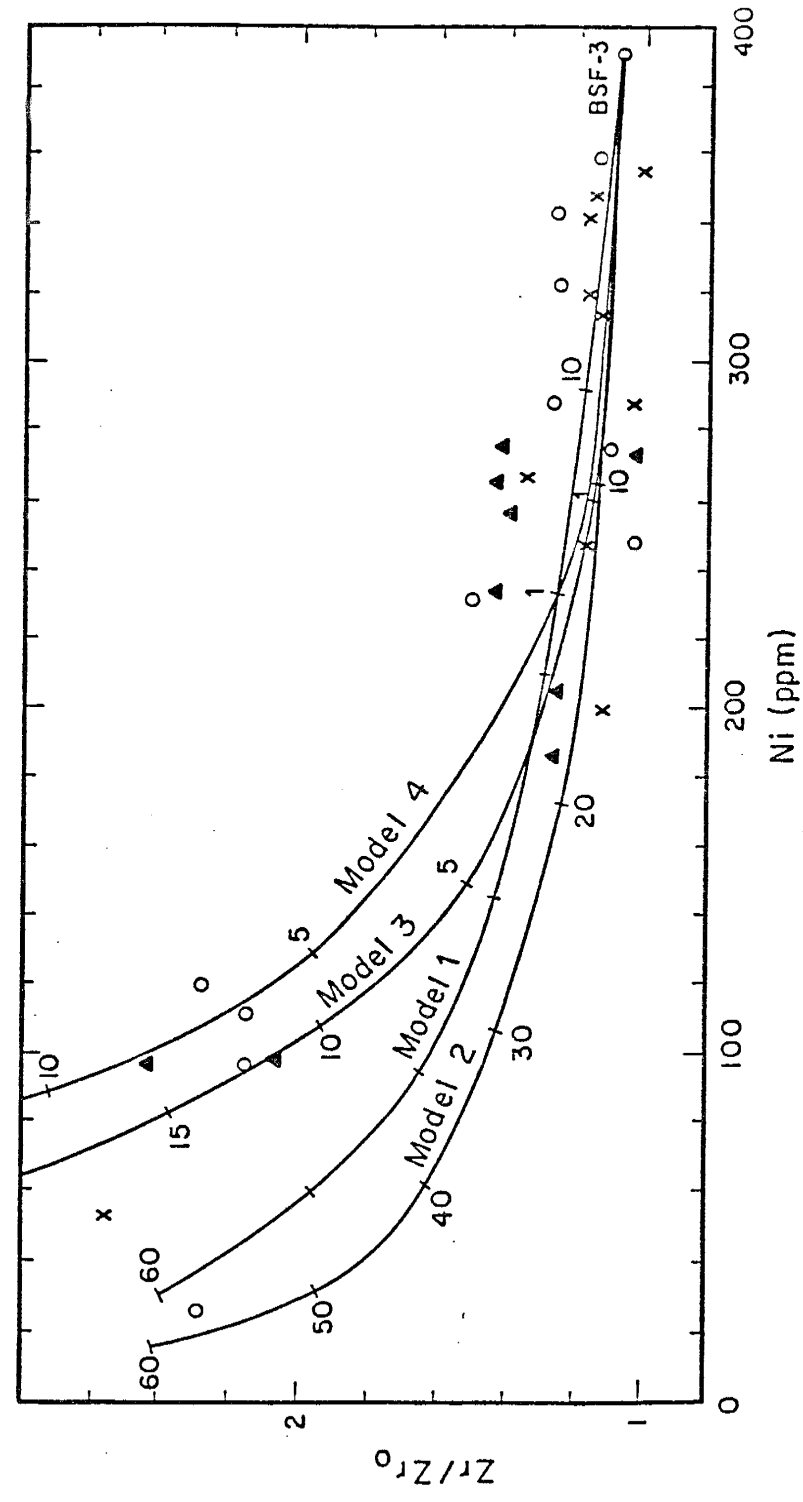

Model 4
Model 3
Model 1
Model 2
BSF-3
Ni (ppm)
Zr/Zr$_o$
0
100
200
300
400
1
2

andesites and the andesites. For instance, the rapid increase in Zr with decreasing Ni content in the volcanics, as measured by the Zr/Zr_o ratio, is more consistent with open- than with closed-system fractional crystallization (Fig. 39).

With exception of one surface sample (D-4, Appendix C), the felsic volcanic rocks of the Syferfontein Formation were not analyzed in this investigation, nor have they been extensively analyzed in other studies. Available data from felsic volcanic rocks in other areas indicate they are chiefly rhyolites and rhyodacites (Bowen et al., 1986). They have relatively small contents of Y (and because of a similar geochemical behavior, also probably of heavy REE) and Nb (Bowen, 1984; Bowen et al., 1986), and are similar in this respect to modern arc-related felsic volcanics. The low contents of HFSE are not characteristic of felsic volcanics from continental rifts. Incompatible element distributions are like those found in felsic volcanics from continental-margin arc systems. Geochemical modeling, using the data from Bowen et al. (1986) and from the one surface sample analyzed in this study, indicates these rocks can be produced by fractional crystallization of andesite, although not necessarily the same andesites found in the Rhenosterhoek Formation.

Ventersdorp Supergroup

Klipriviersberg Group

Fractional crystallization models for Klipriviersberg volcanics are faced with two major problems. First, the secular changes in magma composition from more evolved to less evolved with increasing stratigraphic height are opposite to those expected for progressive fractional crystallization. Second, the increases in incompatible element contents between Edenville and Orkney basalts require in excess of 65% fractional crystallization while major and compatible trace element constraints, including differences in Mg number, allow a maximum of 40% fractional crystallization. Although it is possible to accommodate incompatible element enrichments with up to 30% open-system fractional crystallization if leakage is small (<10%), differences in many incompatible element ratios (such as Zr/Y, La/Sm, Ti/Zr) cannot be explained even with an open system model.

The stratigraphic changes in composition of Klipriviersberg lavas are those expected from progressive melting of an ultramafic source. With exception of the Westonaria Formation, Klipriviersberg basalts can be produced by incremental batch melting of garnet lherzolite, followed in most cases by up to 30% fractional crystallization. In terms of Zr-Ni relationships, a primitive mantle composition (Source 1) progressively melted from 10 to 20% at approximately 1300^{0}C provides an acceptable source (Fig. 40). Less fractional crystallization is required for units at successively younger stratigraphic levels. The appproximately isothermal melting could occur in an adiabatically rising mantle plume. The basaltic komatiites of the Westonaria Formation can be derived from the same source although at higher temperatures of melting (1400 - 1500^{0}C) and followed by <20% fractional crystallization of olivine (Fig. 40).

Allanridge Lavas, Pniel Group

Of the numerous models tested for the basaltic andesites and andesites of the Allanridge Formation, shallow fractional crystallization of Westonaria-type basaltic komatiites results in the best overall geochemical agreement for major and trace elements. Such a model requires 50 to 60% shallow fractional crystallization of basaltic komatiite to produce most Allanridge lavas (Fig. 40).

Figure 40. Zr-Ni diagram showing distribution of Ventersdorp volcanics and magma model trajectories. Tick marks represent 10% batch melting or fractional crystallization (FXL). Makwassie fractional crystallization mineral mode: opx 20%, cpx 15%, plag 60%, mgt 4%, apatite 1.3% and zircon 0.09%. All remaining FXL mineral modes consist of ol 40%, plag 50% and cpx 10%. Batch melting mineral modes consist of ol, opx, cpx and garnet in the ratios 6:1.5:1.5:1. Melt proportions: ol 5%, opx 5%, cpx 45% and gnt 45%. X= Allanridge Fm, += Rietgat Fm, solid squares= Makwassie Fm, open triangles= Goedgenoeg Fm, solid circles= Edenville Fm, solid triangles= Loraine Fm, open squares= Jeannette Fm, open circles= Orkney Fm and open diamonds= Westonaria Fm. Error bar for Ni in figure a is that of BEN; error bar for Ni in b if for BCR-1; Zr= BCR-1 (see Appendix B).

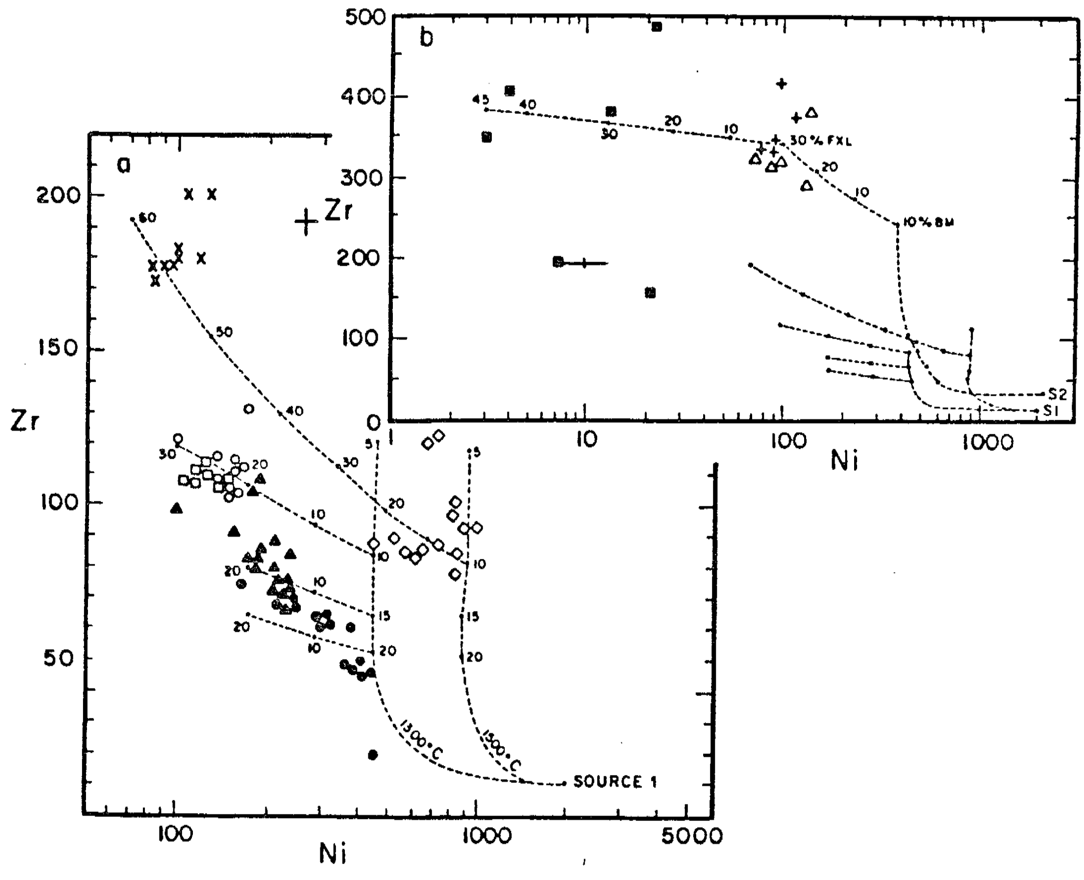
a
b
Zr
Ni
Zr
Ni
SOURCE 1
1300°C
1500°C
30% FXL
10% BM
S2
S1

Platberg Group

Compared to volcanics from the Klipriviersberg and Pniel Groups, Platberg volcanics are strongly enriched in REE and HFSE (Appendix C; Figs. 28 and 29). These enrichments cannot readily be explained by either fractional crystallization (open or closed system) of Klipriviersberg-type basalts or by incremental batch melting of a mantle source similar to the Klipriviersberg and Allanridge sources. Clearly an enriched mantle source is required for the Platberg magmas. The basaltic andesites of the Goedgenoeg and Rietgat Formations can be produced by about 10% batch melting of an enriched garnet lherzolite source (S2) followed by up to 30% fractional crystallization in which plagioclase is a dominant liquidus phase (Fig. 40). Felsic volcanics of the Makwassie Formation, in turn, can be related to the Goedgenoeg-Rietgat basaltic andesites by 25-45% fractional crystallization involving removal of plagioclase, pyroxenes and minor amounts of magnetite, zircon and apatite. Two Makwassie samples that fall below the calculated fractional crystallization trajectory (Fig. 40) may reflect more zircon fractionation. A summary of the magmatic processes relating volcanics from the two sources is given in figure 41.

Figure 41. Summary of proposed magma generation models of Ventersdorp lavas. Vertical trajectories= batch melting (BM); horizontal trajectories= fractional crystallization (FXL).

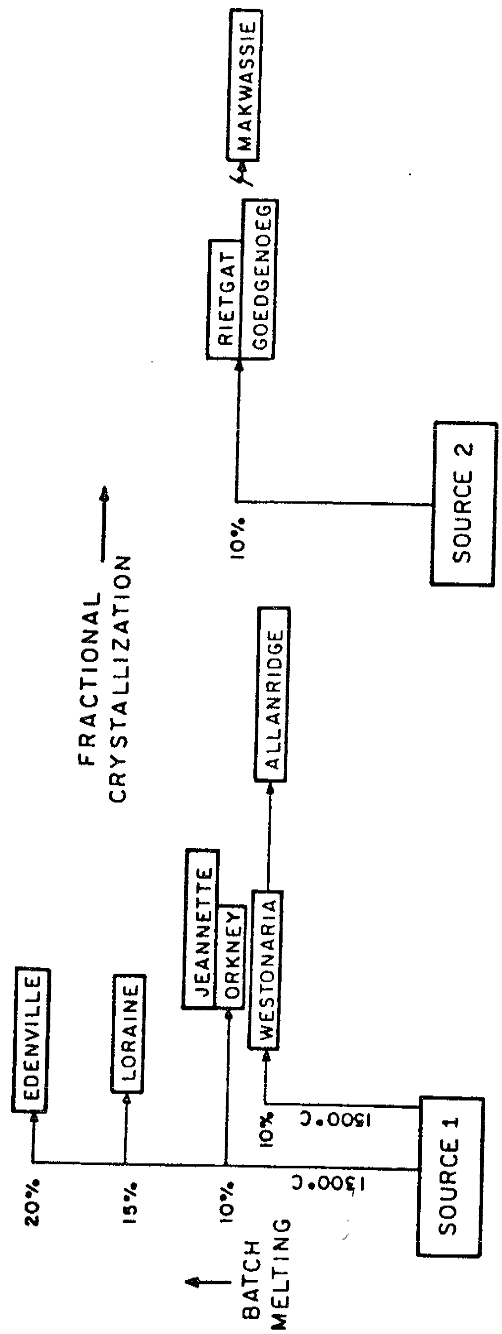
FRACTIONAL CRYSTALLIZATION
BATCH MELTING
SOURCE 1
SOURCE 2
20%
15%
10%
10%
10%
1300°C
1500°C
EDENVILLE
LORAINE
JEANNETTE
ORKNEY
WESTONARIA
ALLANRIDGE
RIETGAT
GOEDGENOEG
MAKWASSIE

Transvaal Supergroup

Open-system fractional crystallization is not favored to explain the genesis of Transvaal volcanics. Incompatible element abundances do not increase rapidly (as described previously) with FeO-T/MgO or Ni content (Kay et al., 1982). Also, in the case of the Dullstroom and Hekpoort volcanics, calculated open-system liquid trajectories do not follow observed trends. In the Machadodorp volcanics, steep trajectories similar to those expected for open-system fractional crystallization are observed (Fig. 42) but low La/Yb and Zr/Y ratios suggest some other process has occurred.

Hekpoort Formation

The most primitive Hekpoort basalt (CDV-7; Mg number= 74; Ni= 308) can be produced by 15 to 20% batch melting of a garnet lherzolite enriched in LILE and LREE relative to primordial mantle (Fig. 42). The remaining basaltic andesites and andesites in the Hekpoort Formation can be related by up to 50% closed-system fractional crystallization of CDV-7.

Figure 42. Zr-Ni diagram showing distribution of Transvaal and Soutpansberg volcanics and magma model trajectories. Tick marks on subvertical trajectory represent 20, 15, 8 and 5% batch melting. Tick marks on subhorizontal trajectories represent 10% fractional crystallization (FXL). Batch melting mineral mode: ol 60%, opx 18%, cpx 15% and gnt 7%. FXL mineral modes: Hekpoort model, ol 40%, cpx 50%, plag 8% and mgt 2%; all other models, ol 40%, cpx 10% and plag 50%. += Ngwanedzi Fm, O= Sabasa Fm, open squares= Dullstroom Fm, open triangle= Machadodorp Fm, solid squares= Hekpoort Fm and solid circles= Abel Erasmus Fm. Error bar for Ni is that of BEN (267 ppm); Zr= BCR-1 (see Appendix B).

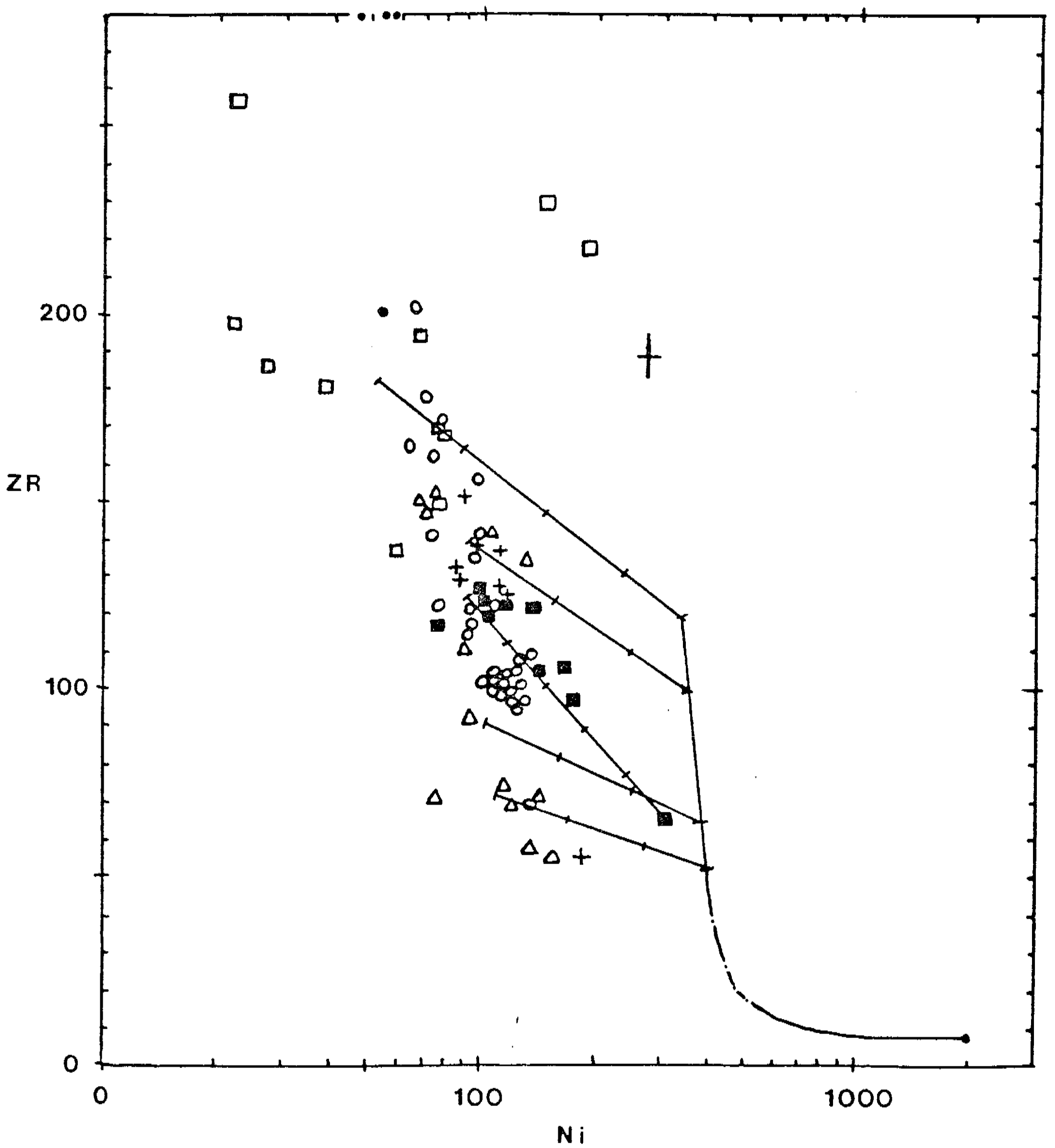
200
100
0
ZR
0
100
1000
Ni

Dullstroom Formation

The Dullstroom volcanics are geochemically very similar to those of the Hekpoort Formation, often lying along the same elemental concentration trajectory (Fig. 42) but enriched in incompatible elements and depleted in Ni and Cr. Model liquid trajectories (along with similar chondrite-normalized patterns [Fig. 32] and incompatible element ratios) confirm this similarity and suggest that the Dullstroom volcanics can be related to the most primitive Hekpoort volcanics by up to 60% closed system fractional crystallization. On a NMORB-normalized diagram (Fig. 33), however, the Hekpoort volcanics are typically enriched in Th relative to Dullstroom samples. Also, average Mg numbers of the two units differ by only 10. These facts limit the fractional crystallization which could relate the Hekpoort to the Dullstroom to less than 10-20% and strongly suggests source differences are involved. Alternatively, Dullstroom volcanics may be derived by an 5-8% batch melt of a garnet lherzolite followed by 50% fractional crystallization (Fig. 42).

Machadodorp Member

Unlike the previous units, the Machododorp volcanics possess geochemically distinct incompatible trace element ratios and normalized abundances (Fig. 32, 33 and 34). In figure 42, the Machadodorp samples define a steeper trend than previously described units. This trend or trajectory is best modeled by variable degrees of batch melting (from 8 to 20%) followed by up to 35% fractional crystallization.

Abel Erasmus Formation

A statistically viable evaluation of the Abel Erasumus volcanics petrogenesis was not obtained. With only four analyzed samples and numerous signs of alteration, all attempts were discontinued.

Soutpansberg Group

Geochemical modeling of the Soutpansberg volcanics are made using various systems. The relative rapid enrichment in Zr relative to Ni (Fig. 42) may be caused by 2 mechanisms, 1) open-system fractional crystallization or 2) variable degrees of partial melting. Open-system fractional crystallization has been ruled out as a possible mechanism because incompatible element abundances do not increase rapidly (as described previously) with FeO-T/MgO or Ni content (Kay et al., 1982).

Like the Machadodorp volcanics of the Transvaal Supergroup, the Ngwanedzi and Sabasa volcanics of the Soutpansberg Group may to be derived by variable degrees of batch melting (8 to 20%) followed by 10 to 40% fractional crystallization (Fig. 42).

Mantle Sources

Geochemical modeling suggests that the compositional continuum from basalt to rhyolite in Nsuze volcanics is a result of fractional crystallization which, in turn, implies a genetic link between units. Thus the Nsuze volcanics appear to be derived from a single source. Incompatible trace element ratios and normalized distributions substantiate this genetic relationship as well as demonstrate the similarity of the Nsuze mantle source to that of modern arc related volcanics.

Like the Pongola volcanics, the Rhenosterhoek volcanics can be related to intraformational fractional crystallization and thus related to a single source. The geochemical similarity of this source to that of modern arc volcanics also is noted.

The necessity of two mantle sources for

Ventersdorp magmas can be seen by comparing incompatible element distributions (Fig. 29). REE and HFSE are enriched in Platberg lavas compared to Klipriviersberg and Allanridge lavas. Allanridge magmas can be related to Westonaria basaltic komatiite magmas by fractional crystallization as previously described, but Platberg magmas must have been derived from a different source. The enrichment in HFSE and REE as well as LILE in Platberg lavas reflects an enriched within-plate mantle source, whereas preferential enrichment of LILE and LREE in the Klipriviersberg and Allanridge lavas reflects a strong subduction zone component (SZC). The fact that the Platberg lavas also have a negative Ta-Nb anomaly (Fig. 29), however, suggests that these lavas carry both subduction-zone and within-plate geochemical signatures. It is possible that the Platberg source is an enriched within-plate source, perhaps a trace element enriched mantle lithosphere, to which a subduction zone component (LILE and LREE) was later added.

Two mantle sources are necessary to explain the Transvaal volcanics. The geochemically similar Dullstroom and Hekpoort Formations are most like modern arc volcanics, possessing a prominent subduction zone component (enriched LILE and LREE) (Fig. 33) and ratios similar to modern arc-related volcanics. The Dullstroom volcanics are enriched in HFSE and REE relative to the Hekpoort volcanics such that the mantle sources can only be termed similar, not identical. The Machadodorp volcanics contain LREE depletions and low Zr/Y ratios like those of NMORB and OIB. They also possess relatively flat REE and HFSE patterns on a NMORB-normalized diagram (Fig. 33), further supporting a MORB-type source. The depletion of REE and HFSE in the Machadodorp volcanics may reflect a depleted asthenospheric source like that of NMORB. The LILE enrichment in most of these samples could reflect contamination with SZC or continental crust.

The geochemical similarity between the Ngwanedzi and Sabasa volcanics suggests they are from a similar source. Based on incompatible trace element ratios and normalized HFSE and HREE abundances, the Soutpansberg volcanics are remarkably similar to the Dullstroom and Hekpoort volcanics of the Transvaal Supergroup (see Discussion, below).

DISCUSSION

Mantle Sources and Tectonic Setting

Nsuze Group

The Nsuze group constitutes one of the oldest, least deformed volcanic suites on earth. Structural and sedimentological data suggest the Nsuze Group and overlying Mozaan Group formed in a rift basin (Burke et al. 1985). Recent geochemical and petrographic evidence on the sediments of the Mozaan Group presented by Wronkiewicz and Condie (1988) suggests that the Pongola Supergroup was deposited in a cratonic basin or continental rift. However, the Nsuze volcanics do not comprise a bimodal suite nor do they contain alkali basalts, both of which are commonly found in present-day continental rift environments (Armstrong et al., 1986). A subduction-related model for the formation of the Pongola basin and Nsuze volcanics is also rejected by Armstrong et al. (1986), primarily on the basis of the postulated shallow-level fractional crystallization. The persistent subduction zone component (SZC) exhibited in Nsuze volcanics thus requires further evaluation.

Three sources for the SZC component are possible,

1) actual subduction during Nsuze volcanic formation, 2) crustal contamination and 3) an inherited source from earlier subduction during greenstone belt formation.

Contemporaneous subduction during Nsuze volcanic formation faces several difficulties. The main problem is locating the surface artifacts of subduction, primarily remnants of the arc. Also, conditions at the continental margin to the east are not known, and subduction from the north prior to Kaapvaal-Zimbabwe craton collision may be too distant to be a source for the SZC.

A SZC could be enhanced, and according to Arculus (1987), even produced by selective interaction of mantle melts with fluids and silicic melts derived from the continental crust. The fractionation of LILE from REE (by fluids) and of LILE and REE from HFSE (by silicic melts) produced by this contamination process could mask the true identity of the original liquid and mimic the elemental decoupling in subduction-related lavas such that the trace element ratios correspond to those observed in a subduction zone suite. In the case of the Nsuze volcanics, however, the amount of crustal contamination appears to be minimal. Incompatible trace elements that could be enriched by crustal contamination (K, Rb, Ba, La, Ce), and according to the present model (Fig. 38) have been enriched by crustal contamination, still show positive correlations with unaffected incompatible trace elements (Zr, Y, Hf, Yb). As mentioned previously, the same lack of decoupling applies to major elements. Attempts to mix the most primitive Nsuze volcanics with various crustal compositions have failed, further supporting the hypothesis that the crustal contamination was minimal and selective. Thus, the LILE and LREE enrichments in the Nsuze volcanics thought to be produced by crustal contamination may enhance the SZC, but do not appear to be entirely responsible for its production. The 10% crustal contamination used in the present model (Fig. 38) is for whole rock assimilation. If the model involved partial melts of the crust following the suggestion of Thompson et al. (1982) and Arculus (1987) the proportion of crustal assimilation should be much lower, probably less than 5%.

These trace element enrichments need not be entirely from the continental crust, but a characteristic of the subcontinental lithosphere beneath old cratonic regions (Hawkesworth et al., 1984). The SZC may be derived from the subcontinental lithosphere (mantle source) as a result of prior interaction of the subcontinental lithosphere with a subducted slab. These processes have been proposed as two means of explaining the SZC in the Karoo basalts of southern Africa (Duncan, 1987; Marsh, 1987). The effect of either process will be essentially the same, with a fluid phase or siliceous melt transporting LILE and LREE into the subcontinental lithosphere. The actual location of subduction is not known. The most likely location, primarily on the basis of close proximity, is the Barberton region located just north of the Pongola basin. Greenstone belts like the Swaziland succession (3.3-3.4 Ga) may have formed by a process similar to present-day convergent plate-boundary zones (Lamb, 1987) and are suggested to have formed over a subduction-like regime (Condie, 1986). The SZC would thus appear to be inherited from the mantle source that was enriched by earlier subduction, possibly during greenstone belt formation.

Rhenosterhoek Formation

The tectonic setting of the Dominion Group is a major unresolved problem. Possible models include a continental rift, a continental-margin arc system, and a foreland basin. Any model must accommodate the Dominion Group lithologic package which includes conglomerates, feldspathic quartzites, and compositionally bimodal volcanics with the mafic end member represented mainly by basaltic andesites rather than basalts. Also, there is a paucity of volcanic sediments in the succession and the occurrence of paleosols indicate stable periods during which extensive weathering occurred. The apparent limited geographic distribution of the Dominion Group near the center of the Kaapvaal Craton is another important constraint on the origin. The fact that these rocks were deposited or erupted primarily, if not exclusively, in a subaerial environment onto older continental basement is also significant. Finally, from the results of this geochemical study and those of Bowen et al. (1986), it is clear that the Dominion volcanics have a geochemical signature similar to that of modern continental-margin or evolved island-arc volcanics.

Some investigators have pointed to the immature sediments, bimodal volcanics, and underlying Archean basement to favor a continental rift model for the Dominion Group (Pretorius, 1976; Tankard et al., 1982). However, the fact that andesites are important and that the volcanic rocks exhibit a strong subduction-zone geochemical component with only a minor within-plate component seems inconsistent with a rift model. Like the Pongola model, one solution to this problem is for the subduction-zone component to be inherited from older mantle lithosphere that retained such a component from an earlier subduction regime. Later rifting and partial melting of this lithosphere could give rise to within-plate magmas carrying an arc geochemical signature. It is interesting in this respect that some "young" within-plate basalts from the Keewenawan (1 Ga), Karoo (200 Ma), and northern Rio Grande rift (5 Ma) exhibit negative Ta-Nb anomalies on NMORB-normalized plots, a feature once thought to be characteristic only of arc-related basalts (data from Basaltic Volcanism on the Terrestrial Planets, 1981; Hawkesworth et al., 1984; Dungan et al., 1986). Hawkesworth et al. (1984) and Erlank et al. (1984) report, however, that the Karoo basalts show low Sr/Nb and Sr/Ce ratios, as do other within-plate basalts. In the Dominion volcanics, these ratios are quite variable (Sr/Nb= 10-130; Sr/Ce=3-20), probably reflecting Sr mobility during alteration or metamorphism, and hence cannot be used to further evaluate the existence of an inherited subduction-zone component.

Burke et al. (1986) have recently suggested that the Dominion Group formed in an Andean-type arc system. This suggestion is based partly on the assumption that the Dominion succession has a large proportion of pyroclastic rocks and a sparsity of mafic volcanics, neither of which is supported by existing data. On the contrary, the Dominion Group is composed dominantly of flows (Bowen, 1984) and contains a large proportion of basaltic andesites and andesites. Also, the Dominion volcanics are compositionally bimodal, another feature atypical of Andean arcs. The relatively restricted geographic distribution of the Dominion Group in the center of the Kaapvaal Craton (Fig. 4) also remains unexplained if this succession represents part of a linear arc parallel to the northern margin of the craton as proposed by Burke et al. (1986).

Burke et al. (1986) suggest that the Witwatersrand Supergroup that overlies the Dominion Group was deposited in a foreland basin developed adjacent to a continental-margin arc system to the north. Geochemical studies of shales from the Witwatersrand Supergroup are consistent with such an interpretation (Wronkiewicz and Condie, 1987). Volcanics of the Dominion Group may have formed during the incipient stages of development of such a foreland basin. In this scenario, the immature sediments at the base of the Dominion Group are deposited during initial rifting and basaltic magmas are derived from the subcontinental lithosphere (mantle wedge?) which is enriched in LILE due to interaction with fluids and partial melts derived from devolatilization of a decending plate. These magmas undergo fractional crystallization in the crust to produce basaltic andesites and andesites. The chiefly subaerial character of the sediments and volcanics reflects a relatively short-lived rifting event in which continental crust is thinned but not eliminated beneath the rift basin. The sparsity of volcaniclastic sediments may reflect volcanism keeping pace with basin subsidence such that the basin is always full of volcanic rocks. Paleosols may have formed during local periods of volcanic quiescence.

Ventersdorp Supergroup

Any model for the tectonic evolution of the Kaapvaal craton must accommodate the geochemical constraints from the Ventersdorp volcanics. Geological data favor a rift basin in which Ventersdorp volcanics are erupted into a system of northeast-trending grabens and half grabens (Burke et al., 1986; Stanistreet et al., 1986). Major extensional faulting is responsible for the main Ventersdorp depositional basin that lies along the western margin of the Witwatersrand basin. Schweitzer and Kroner (1985) consider the rifting to have occurred in response to a within-plate ascending mantle plume, whereas Burke et al. (1986) and Winter (1986) consider it to be a foreland basin related to the collision between the Zimbabwe and Kaapvaal cratons at about 2800 Ma.

The consistent subduction zone component (SZC) shown by Ventersdorp volcanics clearly favors some relationship to a convergent plate margin (unless it was inherited). The model suggested here involves a descending slab beneath the Kaapvaal craton, presumably part of the Zimbabwe plate to the north. The two mantle sources required by the geochemical data are, 1) a mildly LILE-LREE enriched subcontinental lithosphere (Source 1), which serves as a source for Klipriviersberg and Allanridge mafic and komatiitic lavas and, 2) a ubiquitous trace element enriched subcontinental lithosphere (source 2) which is the source of Platberg mafic magmas (Fig. 41). Source 1 acquires a SZC (i.e., enriched LILE and LREE compared to Nb and Ta) from devolatilization of the descending Zimbabwe slab. The Ventersdorp basin is produced by collision with the Zimbabwe craton as suggested by Burke et al. (1986) and the Westonaria basaltic komatiite magmas are derived from the subcontinental lithosphere at depths at which the temperature is on the order of 1400 to 1500^{0}C, possibly just above the descending slab. These magmas carry a weak SZC imparted to the subcontinental lithosphere by upward escaping volatiles. Continued partial melting of the subcontinental lithosphere gives rise to a plume which ascends adiabatically. During ascent, the plume undergoes progressively larger degrees of melting. Magmas are tapped successively forming the Klipriviersberg lavas with the youngest Edenville lavas (most primitive) repesenting the most highly melted portions of the plume. As the plume loses its magmatic component, volcanism wanes and sediments (the Kameeldoorns Formation) are deposited in the Ventersdorp basin. Heating of the trace element-enriched lithosphere (Source 2) by the plume causes partial melting giving rise to Platberg basaltic andesite magmas. These undergo fractional crystallization to produce felsic components of the Makwassie Formation. Allanridge magmas may be produced by fractional crystallization of a second generation of Westonaria-type basaltic komatiite produced in the subcontinental lithosphere. The enriched within-plate geochemical component (WPC) in the trace element-enriched lithosphere (Source 2) may have been acquired earlier by CO_2-rich fluids rising from the asthenosphere. A WPC (Fig. 29) may have been superimposed on the SZC in the lithospheric source by volatiles lost from the ascending plume.

Transvaal Supergroup and Soutpansberg Group

The geochemical data herein reported can lend important insight into the mantle source and tectonic setting of the Transvaal and Soutpansberg volcanics despite their development in separate basins on separate crustal blocks. Faulting in the Transvaal basin is most often described as of minor importance. The sedimentary packages of the Transvaal Supergroup, consisting predominantly of shallow water sediments deposited on a stable cratonic platform, supports the conclusion that faulting is minor. Yet, faulting must have occurred to facilitate magma ascent to the surface. In addition, a ubiquitous subduction zone component (SZC) in all the Transvaal basalts (except the Machadodorp) requires a mantle source which carries a SZC, although the SZC in that mantle source may be inherited.

In the Soutpansberg basin, major normal faulting is well documented and lithologic associations such as lithic graywackes and litharenites are in agreement with an intracratonic rift setting. However, the Soutpansberg basalts also possess a SZC which, again, may be inherited.

Despite crustal contamination affecting LILE and LREE abundances of most of the Dullstroom volcanics, some of the Hekpoort and Sabasa volcanics, it has not masked the striking similarity between units. Mantle source evaluation using incompatible trace element ratios and normalized abundances (Figs. 32 and 33) has revealed that the mafic end members of the Dullstroom and Hekpoort volcanics require some source differences because the Dullstroom basaltic andesites are slightly enriched in HREE and HFSE and depleted in LILE relative to those of the Hekpoort Formation. Differences in the mantle sources between basins (the Transvaal volcanics with residual garnet, the Soutpansberg volcanics without) is the result of either minor changes in composition or degree of partial melting. Considering the thinner subcontinental lithosphere (140 km) and higher heat flow (65 mWm^{-2})(Ballard and Pollack, 1988) of the Limpopo Belt compared to that of the Kaapvaal craton (150-200 km thick and heat flow averaging 40 mWm^{-2}), it may be possible to relate the compositional and/or partial melting differences to depth and heat flow, respectively. Unfortunately, it is not possible to determine which mechanism is more applicable.

Any tectonic model for the Transvaal and Soutpansberg basins must accommodate the ubiquitous SZC in all units but the Machadodorp volcanics. Clearly, at least two mantle sources are required. One possible model involves subduction of an oceanic slab beneath the Kaapvaal craton, possibly related to the Orange River mobile belt to the west. One mantle source would be the subcontinental lithosphere which obtained a SZC from devolatilization of the decending slab. The Soutpansberg, Dullstroom and Hekpoort volcanics are derived from this mantle source. A second source consisting of an asthenospheric diapir would explain the MORB-like Machadodorp volcanics. Alternatively, the second source may represent a depleted portion of a heterogeneous subcontinental lithosphere. The depletion of this source is the result of previous partial melting.

The cause of faulting in the Transvaal basin is not fully understood. Major tectonic episodes had ceased by Transvaal time and, as mentioned earlier, the sedimentary record suggests the Transvaal basin formed on a stable platform. In the Soutpansberg basin, thermal subsidence following the accretion of the Limpopo Belt to the Kaapvaal craton was responsible for faulting (Barker, 1979; Clendenin et al., 1988). Thermal subsidence may be the cause of faulting in the Transvaal basin as well.

Mantle Sources With Time

The geographical relationship between the volcanic sequences of the Kaapvaal craton is presented in figure 1. The basins in which the Dominion, Ventersdorp and

Transvaal volcanics formed are located near the center of the Kaapvaal craton while those of the Pongola and Soutpansberg are on the periphery. This geographical distribution is also apparent in the geochemical data.

In an attempt to explain the geochemical-geographical relationship, a geochemical comparison of mantle sources is made for mafic volcanic units of comparable Mg number and Ni abundance, thus eliminating any inherent problem due to large differences in degree of partial melting or fractional crystallization. Formations such as the Rietgat and Goedgenoeg of the Platberg Group (Ventersdorp Supergroup) and the Machadodorp Formation of the Pretoria Group (Transvaal Supergroup) were shown to be genetically unrelated to other units of this study and will not be included. The units chosen for this comparison are basalts and basaltic andesites of the Pongola Supergroup, Dominion Group, Orkney Formation (Klipriviersberg Group), Hekpoort Formation (Pretoria Group) and Sabasa Formation (Soutpansberg Group). The total number of basaltic samples used is 94.

The Edenville, Loraine and Jeannette Formations of the Klipriviersberg Group are genetically related to the Orkney Formation of that same Group (see Ventersdorp section). Similarly, the Ngwanedzi Formation of the Soutpansberg Group is genetically related to the Sabasa Formation. The total number of samples used in this comparison is 143.

On a primordial mantle-normalized diagram (Fig. 43) all units show the same basic shape from La to Yb. Wide variations in LILE (Rb, Ba, Th, K, and Sr) are apparent, especially in the Orkney and Hekpoort Formations. Ta and Nb vary from 5 to 15 times primordial mantle. On the whole, REE and HFSE show a restricted range. Major deviations occur in the HREE and Y where the oldest and youngest units of this study (Pongola and Sabasa) are enriched relative to the remaining units. The same enrichment in HREE is also apparent on a chondrite-normalized diagram (Fig. 44). On this diagram, the LREE are also enriched in the Pongola and Sabasa volcanics. LREE enrichment in the Hekpoort volcanics (which, according to the modeling of this study, may be due to crustal contamination) is also notable.

There appear to be two genetically distinct populations, one enriched in HREE (Pongola-Soutpansberg volcanics) relative to the other (Dominion-Ventersdorp-Transvaal volcanics). However, with the aid of geochemical modeling there are two ways of relating these seemingly different groups: 1)derivation from a constant mantle source composition with different degrees of partial melting and 2) derivation by a

Figure 43. a= Primordial mantle normalized diagram showing the distribution of basaltic volcanics in the Pongola (solid circle), Dominion (+), Orkney (*), Hekpoort (solid square) and Sabasa (x) units. Normalizing values after Wood (1980); stipple pattern= CV of BCR-1 (see Appendix B).

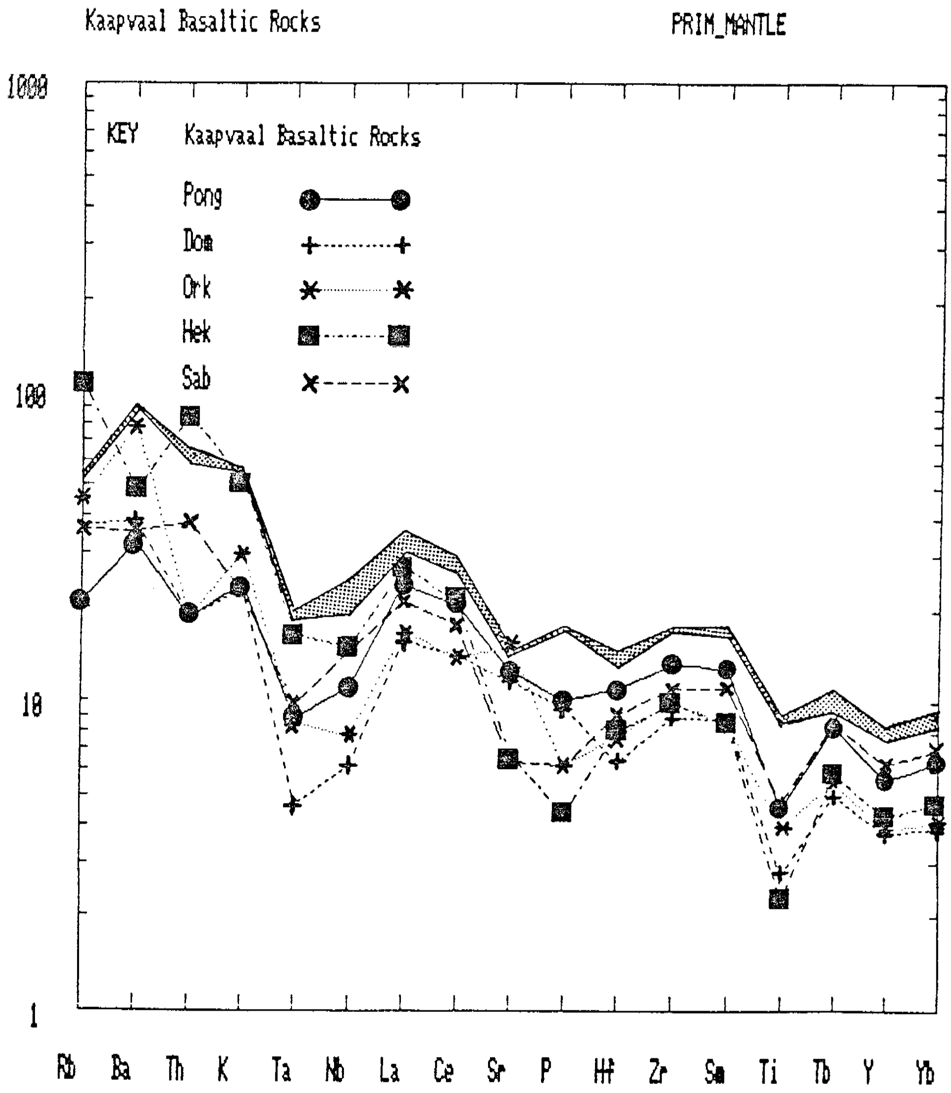

Kaapvaal Basaltic Rocks
PRIM_MANTLE
1000
100
10
1
KEY Kaapvaal Basaltic Rocks
Pong
Dom
Ork
Hek
Sab
Rb Ba Th K Ta Nb La Ce Sr P Hf Zr Sm Ti Tb Y Yb

Figure 44. a= Chondrite normalized REE distributions of the Pongola (solid circle), Dominion (+), Orkney (*), Hekpoort (solid square) and Sabasa (x) basaltic volcanics; stipple pattern= CV of BCR-1 (see Appendix B).

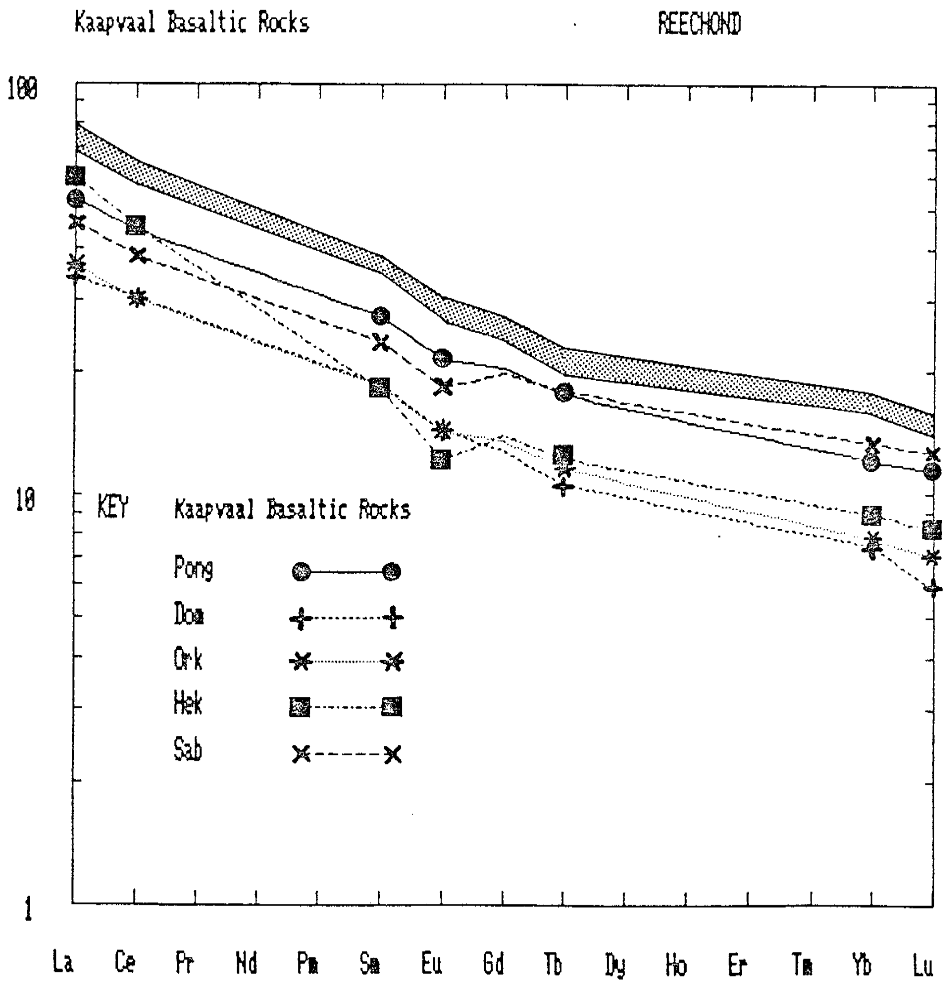
Kaapvaal Basaltic Rocks
REECHOND
100
10
1
KEY Kaapvaal Basaltic Rocks
Pong
Dom
Ork
Hek
Sab
La
Ce
Pr
Nd
Pm
Sm
Eu
Gd
Tb
Dy
Ho
Er
Tm
Yb
Lu

constant amount of partial melting with a variable mantle source composition. Geochemical modeling suggests that in either case garnet is not a residual phase in the Pongola-Sabasa mantle source while the Dominion-Orkney-Hekpoort mantle source retains a >2% garnet residuum. This is demonstrated in figure 45 where the degree of partial melting is kept constant at 11% while the mantle source composition varies from ol 0.6, opx 0.2, cpx 0.15 and gnt 0.05 in the Pongola and Sabasa models to ol 0.6, opx 0.18, cpx 0.15 and gnt 0.07 in the Dominion, Orkney and Hekpoort models (melt fractions= ol 0.05, opx 0.05, cpx 0.45 and gnt 0.45). The only other step required is fractional crystallization of 20 to 30% such that each unit contains comparable and primary Mg numbers.

The results (Fig. 45) suggest that the mantle sources are similar with most HFSE and HREE concentrations at about 1 X primordial mantle. LREE (La, Ce) are enriched slightly at approximately 2 X primordial mantle. The LILE show variable concentrations, and a wide range (0.8 to 2 X primordial mantle) is apparent in Ta-Nb. On the whole, however, the units are remarkably similar.

The same is apparent on a REE diagram (Fig. 46). Calculated source compositions are 2 X chondrite for HREE with increasing relative abundances towards the

Figure 45. Calculated mantle source compositions (Co) on a primordial mantle normalized diagram. Pongola (solid circle), Dominion (+), Orkney (*), Hekpoort (solid square) and Sabasa (x) basaltic volcanics. All units are produced by 11% batch melting of garnet lherzolite. Mineral mode: Pongola and Sabasa models= ol 60%, opx 20%, cpx 15% and gnt 5%; Dominion, Orkney and Hekpoort models= ol 60%, opx 18%, cpx 15% and gnt 7%. Melt fractions= ol 5%, opx 5%, cpx 45% and gnt 45%. Distribution coefficients given in Appendix F.

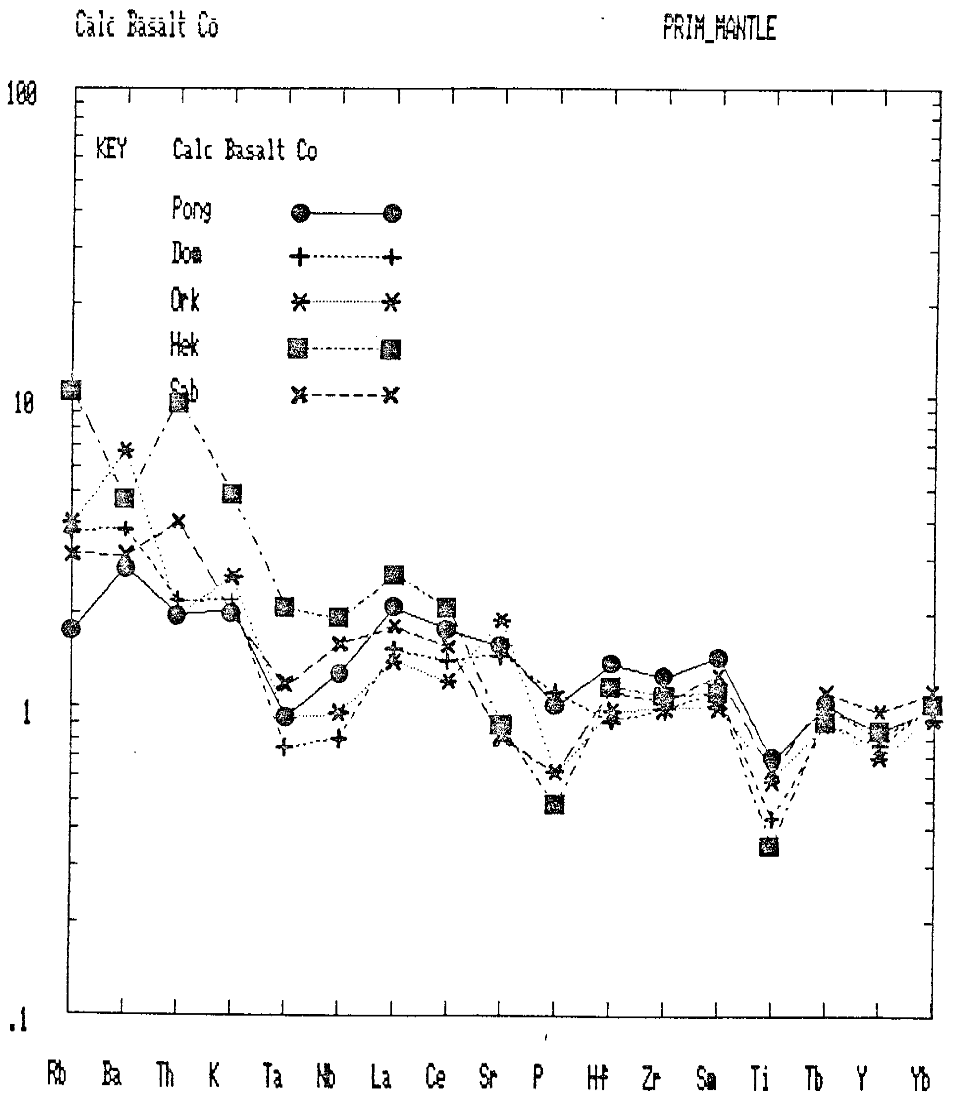
Calc Basalt Co
PRIM_MANTLE
100
10
1
.1
KEY
Calc Basalt Co
Pong
Dom
Ork
Hek
Sab
Rb
Ba
Th
K
Ta
Nb
La
Ce
Sr
P
Hf
Zr
Sm
Ti
Tb
Y
Yb

Figure 46. Calculated mantle source compositions (Co) on a chondrite normalized REE diagram. Model parameters and symbols given in figure 45.

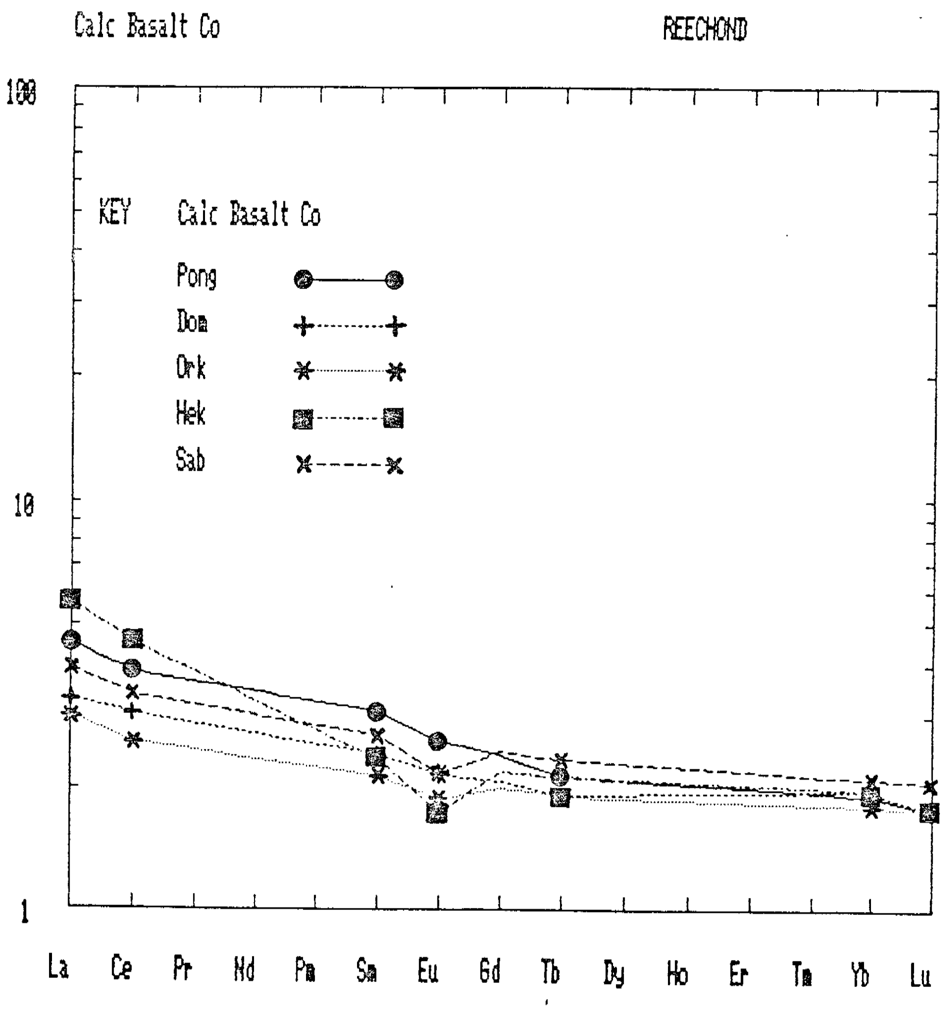

Calc Basalt Co
REECHOND
100
10
1
KEY
Calc Basalt Co
Pong
Dom
Ork
Hek
Sab
La
Ce
Pr
Nd
Pm
Sm
Eu
Gd
Tb
Dy
Ho
Er
Tm
Yb
Lu

LREE which range from 3 to 6 X chondrite. As discussed in a previous section, the Pongola, Hekpoort and Sabasa volcanics are probably contaminated with continental crust and it may be this contamination which is responsible for their enriched LREE (La, Ce, Sm) contents.

The differences in mantle sources, either as slight changes in mineralogy or in the degree of melting of each source, can be related to thickness of the mantle root or heat flow, respectively. If a change in mineralogy is the cause (as assumed in the above model; Fig. 45 and 46), volcanics at the center of the craton can be ultimately derived from a source deeper in the garnet stability field which in turn could allow for a greater percentage of garnet in the mantle source. Alternatively, a higher heat flow near the edge of the craton may allow or produce larger degrees of partial melting which, with a fixed composition, would result in little or no garnet left in the mantle residue in the Pongola-Soutpansberg mantle source.

Mantle Xenoliths

Data from mantle-derived kimberlites and associated diamonds can provide important insight into the mantle source and processes which affect the geochemistry of basalts derived from this source. Model Sm-Nd ages of inclusion-bearing diamonds from kimberlite pipes of the Kaapvaal craton range from 3.2 to 3.4 Ga (Richardson et al., 1984; Boyd and Gurney, 1986). Estimates of crystallization temperatures based on peridotitic inclusion pairs (olivine-garnet and clinopyroxene-garnet) range from 900 to 1200^{0}C (and up to 1400^{0}C in some instances) with an estimated pressure stability field for diamond of 150 to 200 km depth. These temperature and pressure ranges for Kaapvaal diamonds, along with Archean ages, indicate a deep subcontinental lithosphere root has existed beneath the Kaapvaal craton since the Archean. This root is thought to contain large amounts of depleted, low-Ca garnet peridotite (Boyd and Gurney, 1986) which at its base (200 km), defines the subcontinental lithosphere-asthenosphere boundary. The base of the continental lithosphere in the surrounding mobile belts is estimated to be 140 km. The source of kimberlites (and associated diamond) is this depleted garnet peridotite. Depletion may result from by previous basaltic (Groves et al., 1987) or komatiitic (Richardson et al., 1984; Boyd, 1987) melt extraction during greenstone belt formation. Prior to diamond formation, fluids or melts derived from either the asthenosphere (Richardson et al., 1984) or a subducted oceanic slab may have caused secondary mantle enrichment of alkalies, LREE and CO_2. It is interesting to note that diamondiferous kimberlites and low-Ca garnets are only found within the boundaries of the Kaapvaal craton suggesting dispersion beyond the craton boundaries by mantle flow did not occur (Boyd and Gurney, 1986). Thus the root of the Kaapvaal craton has been stable since the Archean and remained relatively cool (900-1200^{0}C), similar to present day geotherms (Boyd and Gurney, 1986; Burke and Kidd, 1978).

A deep mantle root beneath the Kaapvaal craton is substantiated by recent studies on eclogite xenoliths in kimberlites. Eclogite nodules from near the edge of the craton (Bellsbank kimberlite for example) are estimated to have formed at 100 to 135 km depth at 800-850^{0}C (Shervais et al., 1988). The 2.1 $\pm$ 0.1 Ga dates of these nodules coincides with the stabilization of the Orange River mobile belt. Delta 18 oxygen values of these eclogites of 1-3 per mil below a primitive mantle value (5.5 per mil) are in the range of altered MORB, and negative correlations between delta 18 oxygen and 87Sr/86Sr ratios resemble that observed in oceanic crust. In is suggested by Shervais et al. (1988) that the eclogites represent metamorphosed oceanic crust. Near the center of the craton, eclogites from Roberts

Victor kimberlite, Orange Free State are derived from a deeper source (165-190 km). Dates of 2.47 Ga are obtained on the least altered samples while Sm-Nd whole rock ages range up to 2.7 Ga (MacGregor and Manton, 1986). Like the peripheral eclogites, low delta 18 oxygen and negative oxygen-strontium isotopic correlations resemble altered oceanic crust, as do the major and trace element compositions (Ti excluded). MacGregor and Manton (1986) describe the Roberts Victor eclogites as subducted oceanic basalts and gabbros and suggest that diamonds originate from subducted carbon.

Heat Flow

Heat flow data is another means of evaluating the subcontinental lithosphere root of the Kaapvaal craton and, possibly, plate tectonic schemes. Ballard and Pollack (1987) report modern heat flow in the center of the Kaapvaal craton to be 40 mWm^{-2}, an amount typical of Archean cratons and remarkably similar to corresponding geothermal gradients for the same depths today. On the edge of the craton and in the surrounding mobile belts, however, the heat flow averages 65 mWm^{-2} (Ballard and Pollack, 1987). The preferred model to explain these heat flow differences is a deep subcontinental lithosphere root beneath the

Kaapvaal craton (as suggested by diamond data) which diverts mantle heat into the surrounding mobile belts. In the Archean, these mobile belts had not yet accreted (Ballard and Pollack, 1987) and in their place was oceanic crust. However, the 2-3 times greater total heat production and a 200^0 hotter mantle in the Archean compared to today is not supported by diamond thermobarometry data that suggests the root of the Kaapvaal craton was relatively cool in the Archean (Ballard and Pollack, 1988). Ballard and Pollack (1988) suggest the Kaapvaal craton root was larger in the Archean, thus reducing the conductive heat transfer from the surrounding mantle and aiding in additional heat diversion away from the craton. Inherent in this model is the reduction in size of the root with time. As pointed out by these authors, Archean volcanism and mobile belt accretion of the Kaapvaal craton attest to thermal perturbations which may be responsible for reduction of the root.

A recent article by Wilks (1988) involving possible Archean tectonic models in relation to heat flow expounds the attributes of thicker oceanic plates. Whether thicker oceanic plates, faster spreading rates (Hargraves, 1986) or other possible models might be more applicable will not be debated here. More important, however, is the proposition that some form of plate tectonics (collisions in the case of Wilks, 1988) is possible and that heat flow data substantiates a deep Kaapvaal craton root.

A Tectonic Model

How can a predominantly rift-related suite of rocks that span over a billion years and are derived from a similar mantle source be related to both an inherited and actively produced SZC? Exceptions to the rifting environment are the Transvaal basin where evidence for rifting is lacking, and the Pongola basin where, except in the White-Mfolozi inlier, all contacts with older units have been masked by younger intrusions.

As mentioned previously, a deep subcontinental lithosphere root probably developed beneath the proto-Kaapvaal craton beginning about 3.7-3.5 Ga coincident with the development of greenstone belts. Extraction of greenstone belt volcanic assemblages from this root resulted in a depleted garnet peridotite residuum but enrichments by fluids from a devolatilizing subducted oceanic crust kept pace with the depletion events and imparted a SZC to a large portion of the root. Asthenospheric mantle plumes could aid in producing heat and possibly mix with the continental lithosphere contributing to the mild within-plate signature observed in some units. The SZC in Pongola volcanics is largely inherited from enrichment events during previous arc accretions, possibly related to greenstone belt formation. The SZC of the Dominion and Ventersdorp volcanics may be the result of contemporaneous subduction of oceanic crust underneath the Kaapvaal craton as the Kaapvaal and Zimbabwe cratons approached each other. Evidence of the Kaapvaal-Zimbabwe craton collision (the Limpopo Mobile Belt) at 2.7 Ga enhances this model but an inherited SZC for the Dominion-Ventersdorp volcanics can not be ruled out. Like the Pongola volcanics, the Transvaal and Soutpansberg volcanics inherited their SZC. It is noteworthy that a SZC is a characteristic of continental lithosphere from old cratons (Dupuy et al., 1988).

Thus the mantle source for the volcanics of the Kaapvaal craton may be a relatively homogeneous subcontinental lithosphere which has been enriched by devolatilization associated with subduction, either contemporaneous with the production of the volcanics, or inherited by previous subduction episodes. Anomalous units such as the Rietgat, Goedgenoeg and Machadodorp are the result of tapping different mantle sources or a different portion of the subcontinental lithosphere, both enriched and depleted relative to the majority of the Kaapvaal volcanics. Geochemical differences between units can be related to either depth of origin or degree of partial melting of the mantle source.

CONCLUSIONS

1) Kaapvaal volcanics are tholeiitic in character with some mild calc-alkaline affinities.

2) Most Kaapvaal volcanics plot in arc related fields on tectonic discrimination diagrams. Exceptions are the Machadodorp volcanics which commonly plot in MORB fields.

3) Chondrite-normalized REE distributions and NMORB-normalized incompatible element distributions are consistent with a subduction related mantle source. Exceptions are the Machadodorp volcanics which commonly display flat to depleted patterns similar to MORB.

4) Fractionating phases are typically olivine and plagioclase except for the Rhenosterhoek, Dullstroom and Hekpoort Formations where olivine and clinopyroxene dominate.

5) Crustal contamination has affected most of the volcanics of the Kaapvaal craton, but not to the

extent of masking the mantle source trace element signature.

6) The Kaapvaal craton possesses a deep subcontinental lithosphere root which is the source of most, if not all, Kaapvaal volcanics.

7) The subcontinental lithosphere root of the Kaapvaal craton possesses a SZC and other attributes of CPB which is imparted to volcanics derived for that source.

8) Differences in mantle source (excluding the Platberg Group and Makwassie Formation) can be related to the position of the basins on the craton: Dominion-Ventersdorp-Transvaal volcanics have approximately 2% garnet in the mantle residuum and are located in the center of the Kaapvaal craton; Pongola-Soutpansberg volcanics have approximately 0% garnet in the mantle residuum and are located on the edge of the Kaapvaal craton. These relationships appear to be a function of either depth of origin or degree of partial melting.

9) Trace elements alone cannot distinguish between cratonic (Transvaal Supergroup) and rift (Soutspansberg Group and Ventersdorp Supergroup) tectonic environments.

10) A change in the geochemistry at 2.5 Ga (the Archean-Proterozoic boundary) is not observed in the

volcanics of the Kaapvaal craton.

Overview

Previous studies all suggest that a change in the geochemistry at the Archean-Proterozoic boundary (2.5 Ga) is a common occurrence and results from fundamental changes in mantle sources (Condie, 1985; Taylor and McClennan, 1985) reflected by enrichments in some trace element concentrations. The results of this study indicate that there is no discernable change in the geochemistry of volcanic rocks at 2.5 Ga in the Kaapvaal craton of South Africa. A likely reason for these differing conclusions is that the previous studies compared Archean greenstone belt successions with Proterozoic supracrustal successions whereas the present study examines only supracrustal successions. Thus, the geochemical change at 2.5 Ga in other localities may be related to a gross change from greenstone belts to supracrustal successions and not a fundamental change in mantle sources alone.

The implied homogeneous subcontinental lithosphere mantle source beneath South Africa is also controversial. The derivation of basalts from this mantle source for over a billion years may prove to be an oversimplification of a subtly complex geologic environment. Future work on isotopes and mantle xenoliths should provide further insights into this problem, particularly the extent of crustal contamination. Extensive crustal contamination of mantle-derived basalt could potentially mask mantle source major and trace element differences, even to the extent of making MORB look like a convergent-plate basalt. Within the limits of the data presented in this dissertation, however, the volcanics of the Kaapvaal craton appear to be only mildly and selectively contaminated with continental crust.

APPENDIX A

Sample Locations and Technique

Almost all Dominion Group and Ventersdorp Supergroup samples analyzed for this study are from drillcore. Also, a few Transvaal Supergroup samples (CDV and WBK cores) are from drillcore. Samples were collected in the drillcore at appropriate intervals so that adaquate coverage of the exposed stratigraphic thickness was obtained. Core sampling consists of wetting the core to enhance visual examination and constructing a stratigraphic column to aid sample collection and for future reference. Removal of from 4 to 8 inches of core (depending on diameter) was accomplished with a rock hammer. Samples are labeled with tape and the depth from the surface noted. Obvious alteration, fractures and amygdules are avoided.

The remaining samples from the Pongola Supergroup, Transvaal Supergroup and Soutpansberg Group are from surface outcrop. Outcrop sampling consists of, first, the removal of all weathered surfaces (weathered rind) from the sample to be collected. The sample is then labeled, recorded in a field notebook and the position noted on the appropriate topo sheet. As with the core samples, amygdules, fractures and altered samples are avoided.

Pongola Supergroup

All Pongola samples (except samples with P prefix) are provided by Armstrong et al. (1986) and sample locations are shown on their figure 1.

P-1 and P-2: Richards Bay topo; Vutshini tributary of Nsuze River; road from Kranskop to Dlolwana (see Figure 47); side road off highway, 17 km north of highways intersection with Tugela River; $31^{0}0'$ east, $29^{0}50'$ south.

P-16 - P-24: Richards Bay topo; 70 km southeast of Vryheid where Highway 34 crosses the White-Mfolozi River (near Ulundi)(see Figure 48); outcrops are from the highway to the east approximately 3 km along the river; $31^{0}10'$ east, $30^{0}15'$ south.

Dominion Group

BTF-core: 15 km south of Ventersdorp (see figure 4).

BSF- and BBS-core: 10 km north of Klerksdorp (see figure 4).

Ventersdorp Supergroup

J-core: 7 km southwest of Orkney (see figure 6).

Figure 47. Road map of Zululand and northern Natal Province showing location of cities and rivers referred to in Appendix A.

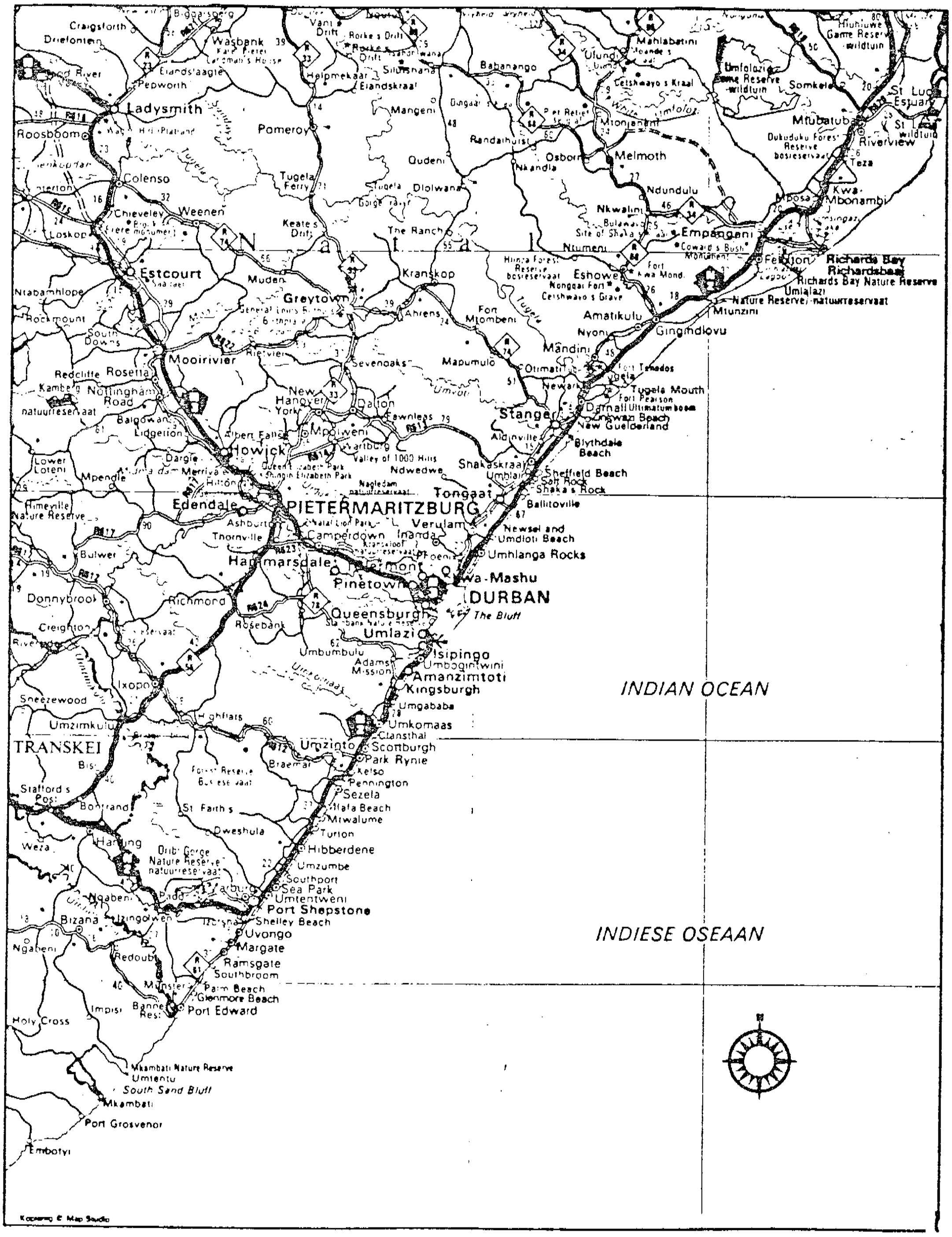
Craigsforth
Driefontein
Wasbank
Elandslaagte
Pepworth
Ladysmith
Roosboom
Pomeroy
Helpmekaar
Elandskraal
Mangeni
Babanango
Ulundi
Mahlabatini
Hluhluwe Game Reserve wildtuin
Umfolozi Game Reserve wildtuin
Somkele
St Lucia Estuary
Mtubatuba
Riverview
Teza
Dukuduku Forest Reserve bosreserwaat
Melmoth
Ndundulu
Nkwalini
Empangeni
Kwa-Mbonambi
Mposa
Felixton
Richards Bay
Richardsbaai
Richards Bay Nature Reserve
Umlalazi Nature Reserve/natuurreservaat
Mtunzini
Gingindlovu
Amatikulu
Nyoni
Mandini
Eshowe
Kwa Mondi
Coward's Bush
Ntumeni
Nkandla
Qudeni
Dlolwana
Randalhurst
Osborn
Colenso
Chieveley
Weenen
Tugela Ferry
Keate's Drift
The Ranch
Kranskop
Loskop
Estcourt
Muden
Greytown
Ntabamhlope
Rockmount
Mooirivier
Rosetta
Nottingham Road
Kamberg
Balgowan
Lidgetton
Redcliffe
Sevenoaks
Mapumulo
New Hanover
York
Dalton
Fawnleas
Mpolweni
Wartburg
Valley of 1000 Hills
Ndwedwe
Stanger
Darnall
Zinkwazi Beach
New Guelderland
Blythdale Beach
Tugela Mouth
Fort Pearson
Fort Tenedos
Ahrens
Fort Mtombeni
Albert Falls
Howick
Dargle
Lower Loteni
Mpendle
Merrivale
Hilton
Edendale
PIETERMARITZBURG
Ashburton
Thornville
Camperdown
Inanda
Verulam
Tongaat
Shakaskraal
Umhlali
Sheffield Beach
Salt Rock
Shaka's Rock
Ballitoville
Newsel and Umdloti Beach
Umhlanga Rocks
Kwa-Mashu
DURBAN
The Bluff
Hammarsdale
Pinetown
Queensburgh
Umlazi
Isipingo
Umbogintwini
Amanzimtoti
Kingsburgh
Umgababa
Umkomaas
Clansthal
Scottburgh
Park Rynie
Kelso
Pennington
Sezela
Ifafa Beach
Mtwalume
Turton
Hibberdene
Umzumbe
Southport
Sea Park
Umtentweni
Port Shepstone
Shelley Beach
Uvongo
Margate
Ramsgate
Southbroom
Palm Beach
Glenmore Beach
Port Edward
Mkambati Nature Reserve
Umtentu
South Sand Bluff
Mkambati
Port Grosvenor
Embotyi
Himeville Nature Reserve
Bulwer
Donnybrook
Creighton
Richmond
Rosebank
Ixopo
Sneezewood
Umzimkulu
TRANSKEI
Highflats
Umzinto
Braemar
St Faith's
Dweshula
Harding
Oribi Gorge Nature Reserve natuurreservaat
Stafford's Post
Weza
Ngabeni
Bizana
Izingolweni
Redoubt
Munster
Impisi
Holy Cross
INDIAN OCEAN
INDIESE OSEAAN
Kopiereg © Map Studio

Figure 48. Road map of Swaziland and southeastern Transvaal Province showing location of cities and rivers referred to in Appendix A.

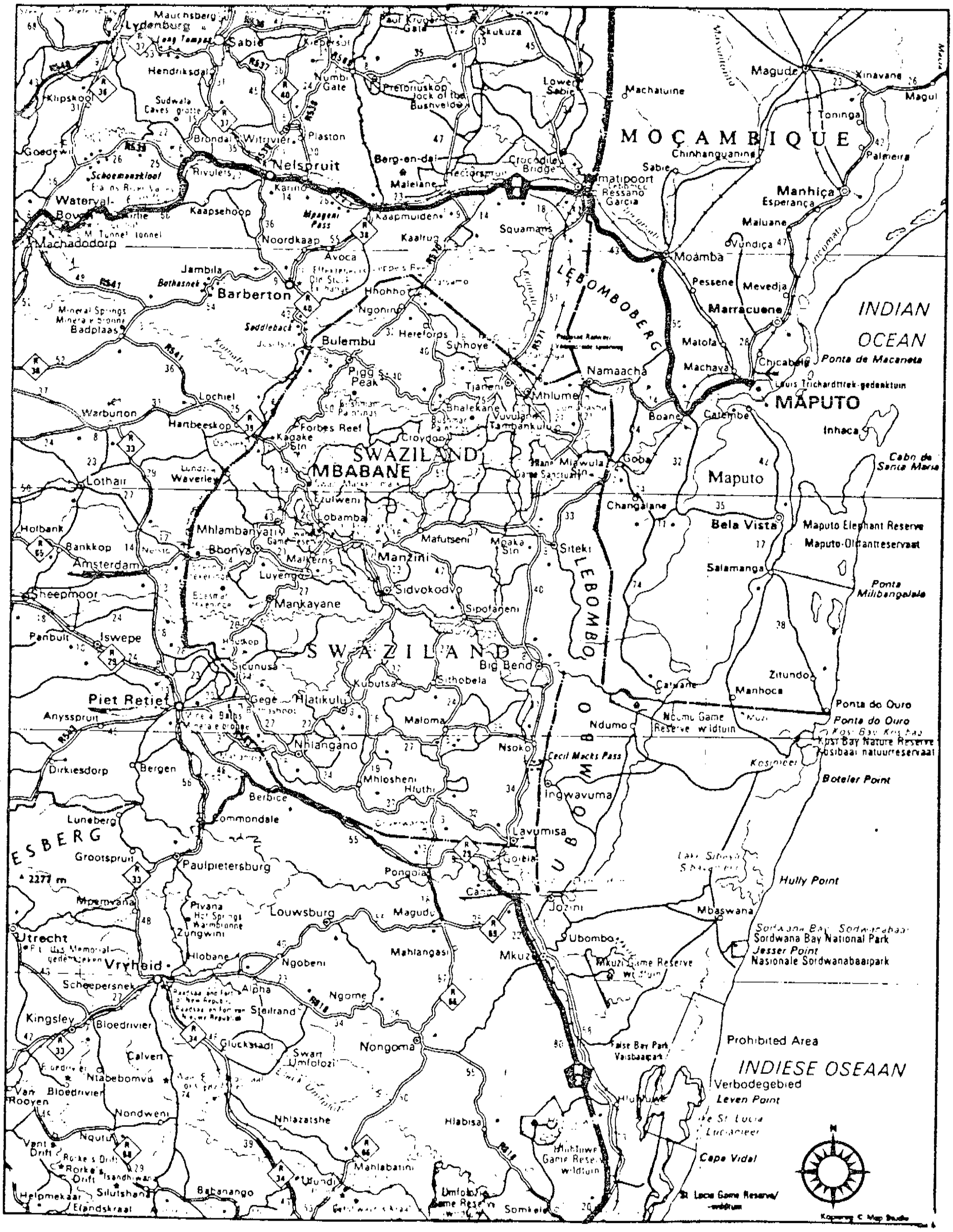
MOÇAMBIQUE
INDIAN OCEAN
INDIESE OSEAAN
SWAZILAND
MBABANE
MAPUTO
Maputo
LEBOMBOBERG
LEBOMBO
UBOMBO
Lydenburg
Sabie
Nelspruit
Barberton
Komatipoort
Machadodorp
Badplaas
Bulembu
Pigg's Peak
Manzini
Big Bend
Piet Retief
Amsterdam
Lothair
Warburton
Vryheid
Paulpietersburg
Louwsburg
Nongoma
Pongola
Jozini
Mkuze
Ubombo
Ingwavuma
Magude
Manhiça
Moamba
Marracuene
Namaacha
Boane
Bela Vista
Salamanga
Ponta do Ouro
Kingsley
Utrecht
Prohibited Area
Verbodegebied

S-core: 9 km southwest of Virgina (see figure 6).

Westonaria Formation samples: 10 km south of Johannesburg, Klipriviersberg Hills garbage dump.

C1M, C2M and C3L: side road east of highway between Klerksdorp and Ventersdorp, 15 km north of Klerksdorp and 6 km northeast of Dominion BBS-core (see figure 4).

C5A: on road from Hartbeesfontein to Ottosdal, 6 km west of Hartbeesfontein on roadside.

D6M: outcrop within Klerksdorp city limits; southwest part of town; south side of Highway 29.

Transvaal Supergroup

WBK-core: 35 km southwest of Johannesburg.

CDV-core: same as WBK-core.

C-23: Barberton topo; 2 km northwest of Lydenburg on road to Burgersfort (see Figure 49 and 50); $30^{0}27'$ east, $25^{0}5'$ south.

C-24: same as C-23.

C-25: Barberton topo; 4.5 km northwest of Lydenburg on the road to Burgersfort; $30^{0}26'$ east, $25^{0}3'$ south.

C-26: same as C-25.

C-31: Pilgrams Rest topo; 4 km southwest of Ohrigstad on Highway 36 (see Figure 50); $30^{0}32'$ east, $24^{0}45'$ south.

Figure 49. Road map of Transvaal and Limpopo Provinces showing location of cities and rivers referred to in Appendix A.

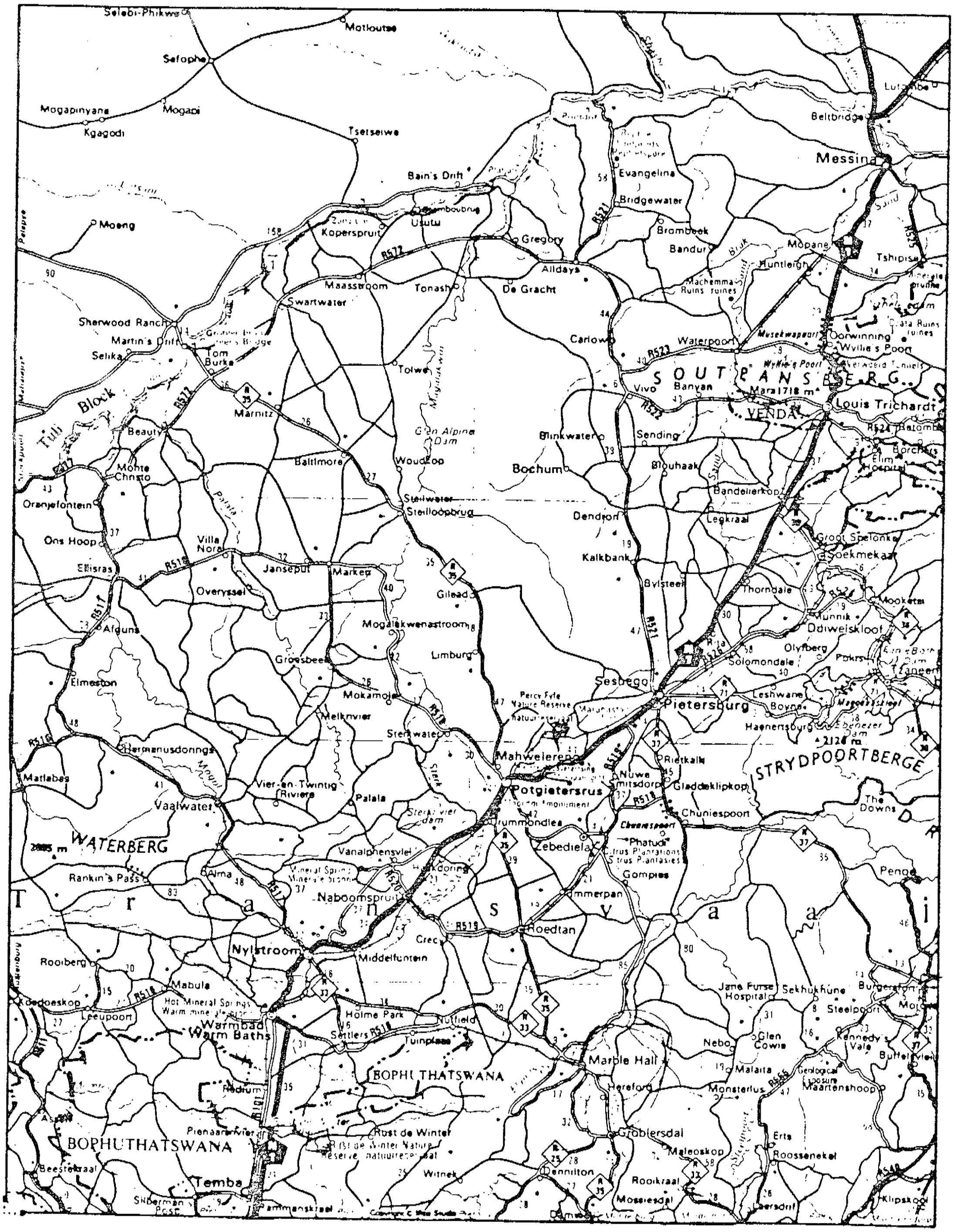
Selebi-Phikwe
Motloutse
Sefophe
Mogapinyana
Mogapi
Kgagodi
Tsetsebwe
Bain's Drift
Moeng
Kopersprui
Usutu
Gregory
Alldays
Maasstroom
Tonash
De Gracht
Swartwater
Sherwood Ranch
Selika
Tom Burke
Carlow
Waterpoort
Tolwe
Marnitz
Tuli Block
Beauty
Monte Christo
Oranjefontein
Ons Hoop
Ellisras
Villa Nora
Janseput
Markep
Overyssel
Baltimore
Woudkop
Steilwater
Steilloopbrug
Glen Alpine Dam
Blinkwater
Bochum
Dendron
Kalkbank
Gilead
Mogalakwenastroom
Limburg
Groesbeek
Mokamole
Melkrivier
Sterkwater
Afguns
Elmeston
Hermanusdorings
Matlabas
Vaalwater
WATERBERG
Rankin's Pass
Alma
Naboomspruit
Vanalphensvlei
Palala
Mahwelereng
Potgietersrus
Zebediela
Gompies
Roedtan
Nylstroom
Middelfontein
Rooiberg
Mabula
Leeupoort
Warmbad
Warm Baths
Holme Park
Settlers
Nutfield
Tuinplaas
BOPHUTHATSWANA
Radium
Pienaarsrivier
Rust de Winter
Temba
Witnek
Dennilton
Groblersdal
Marble Hall
Hereford
Moosesdal
Rooikraal
Laersdrif
Maleoskop
Roossenekal
Monsterlus
Malaita
Nebo
Glen Cowie
Jane Furse Hospital
Sekhukhune
Steelpoort
Burgersfort
Kennedy's Vale
Maartenshoop
Klipskool
Penge
The Downs
Chuniespoort
Gladdeklipkop
STRYDPOORTBERGE
Rietkalk
Pietersburg
Sesbego
Haenertsburg
Boyne
Leshwane
Solomondale
Olyfberg
Duiwelskloof
Mooketsi
Thorndale
Bylsteel
Soekmekaar
Groot Spelonke
Legkraal
Bandelierkop
Louis Trichardt
VENDA
SOUTPANSBERG
Vivo
Banyan
Sending
Elim Hospital
Wyllie's Poort
Messina
Beitbridge
Evangelina
Bridgewater
Brombeek
Bandur
Mopane
Huntleigh
Tshipise
Machemma Ruins
T r a n s v a a l

Figure 50. Road map of Transvaal and Limpopo Provinces showing location of cities and rivers referred to in Appendix A.

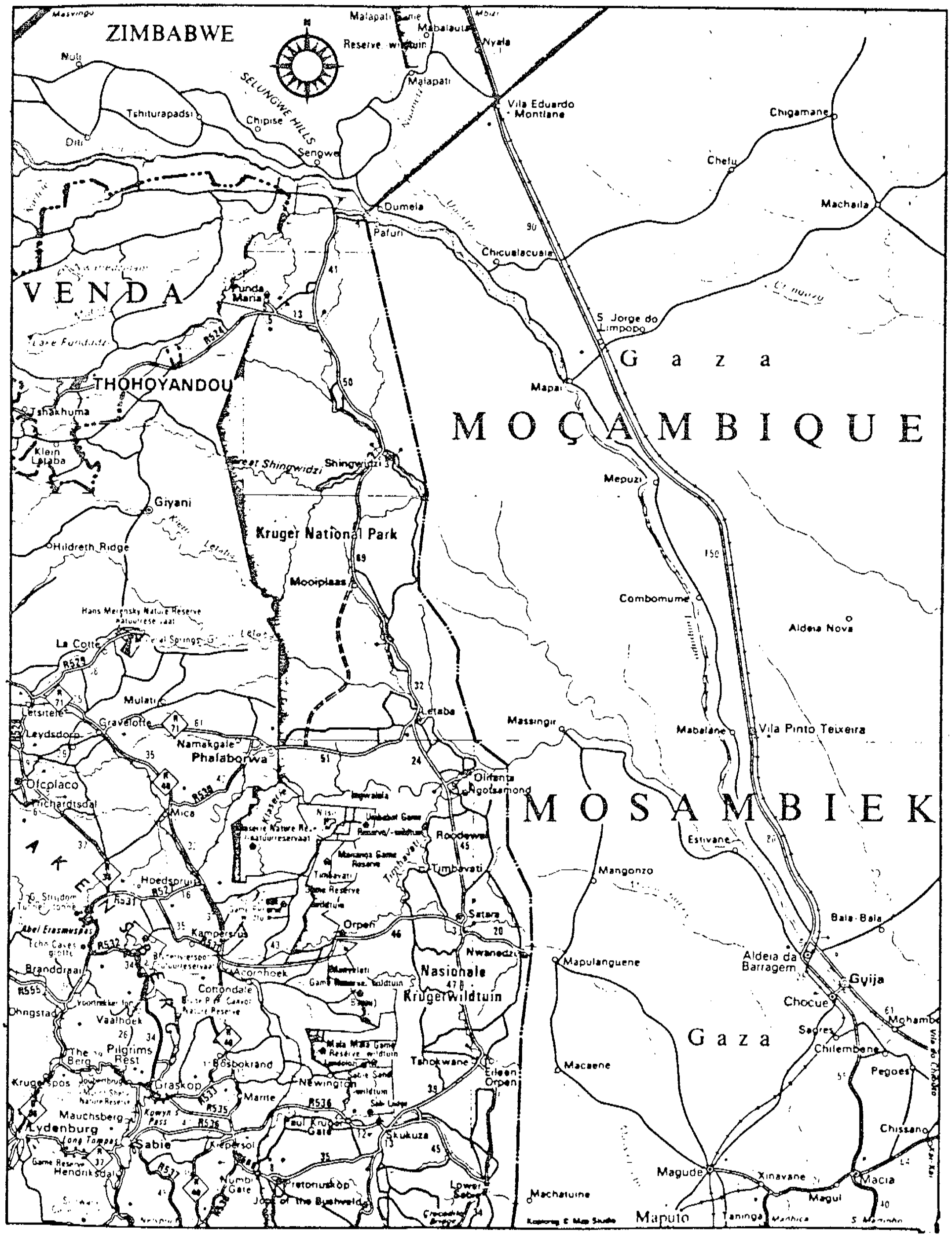
ZIMBABWE
VENDA
THOHOYANDOU
MOÇAMBIQUE
MOSAMBIEK
Gaza
Gaza
Kruger National Park
Nasionale Krugerwildtuin
SELUNGWE HILLS
Malapati
Vila Eduardo Montlane
Chigamane
Chefu
Machaila
Dumela
Pafuri
Chicualacuala
Punda Maria
S. Jorge do Limpopo
Mapai
Tshakhuma
Giyani
Shingwidzi
Mepuzi
Hildreth Ridge
Mooiplaas
Combomume
Aldeia Nova
La Cotte
Mulati
Letaba
Massingir
Mabalane
Vila Pinto Teixeira
Gravelotte
Leydsdorp
Namakgale
Phalaborwa
Olifants
Ofcplaco
Mica
Estivane
Hoedspruit
Roodewal
Timbavati
Mangonzo
Satara
Orpen
Nwanedzi
Mapulanguene
Aldeia da Barragem
Gyija
Chocue
Acornhoek
Sagres
Chilembene
Pegoes
Pilgrims Rest
Tshokwane
Macaene
Graskop
Bosbokrand
Newington
Eileen Orpen
Lydenburg
Sabie
Skukuza
Paul Kruger Gate
Pretoriuskop
Numbi Gate
Lower Sabie
Magude
Xinavane
Chissano
Macia
Magul
Machatuine
Maputo
Taninga

C-57: Barberton topo; 2 km northeast of Machadodorp on Highway 539 (see Figure 48); 30°16′ east, 25°39′ south.

C-60: Barberton topo 5 km northeast of Machadodorp on Highway 539; 30°17′ east, 25°39′ south.

C-61: Barberton topo; 17 km south of Machadodorp (see Figure 48); 30°15′ east, 25°52′ south.

C-66: same as C-61.

C-208: Pilgrams Rest topo; Highway 37 from Pietersburg to Ohrigstad; sideroad east to Penge, 95 km from Pietersburg (see Figure 49).

C-209: Pilgrams Rest topo; 18 km west of Penge.

C-211: Pilgrams Rest topo; 9 km west of Penge (see Figure 49).

C-212: same as C-211.

D-37 - D-40: Pilgrams Rest topo; road cut just northeast of Strijdom Tunnel at junction of Highway 36 and Olifants River (Abel Erasmus Pass) (see Figure 50); 30°37′ east, 24°27′ south.

D-105: Barberton topo; 25 km east of Machadodorp (see Figure 48); 30°27′ east, 25°37′ south.

Soutpansberg Group

D-10: Pieterburg topo; 5 km west of Louis Trichardt on Highway 522 and 0.5 km south on side road; 29°48′

east, $23^0 2'$ south (see Figure 49).

D-12: Pieterburg topo; 2.5 km west of Louis Trichardt on Highway 522; $29^0 52'$ east, $23^0 2'$ south.

C-108 - C-116: Pieterburg topo; 30 km west of Louis Trichardt at junction of Highway 522 and Sand River; samples collected along 1.5 km tranverse north along Sand River (see Figure 49); $29^0 37'$ east, $23^0 3'$ south.

C-118: same as C-108 - C-116 except 1 km south of Highway 522.

C-125 - C-126: 1 km west of Louis Trichardt on Highway 522; quarry on north side of highway; $29^0 55'$ east, $23^0 2.5'$ south.

C-127: 1.5 km north of Louis Trichardt on Highway N1.

C-132: 28 km west of Sabasa, 22 km northeast of Louis Trichardt and 1 km south of Nzhelele River; $30^0 12'$ east, $22^0 56'$ south.

C-137: 7 km northeast of Louis Trichardt (9 km by road) and 28 km west of Sabasa; $30^0 30'$ east, $22^0 57'$ south.

C-138: Tzaneen topo; 1 km north of Highway 524 on sideroad commencing 19 km east of Louis Trichardt; $30^0 4'$ east, $23^0 3'$ south (see Figure 49).

C-140: Tzaneen topo; on same sideroad as C-138; 9 km form Highway 524; $30^0 7.5'$ east, $23^0 2'$ south.

C-141: Tzaneen topo; on same sideroad as C-138; 12 km form Highway 524; $30^{0}11'$ east, $23^{0}2'$.

C-143: Tzaneen topo; 44 km east of Louis Trichardt on highway 524; $30^{0}17'$ east, $23^{0}5'$ south.

C-145: 7 km west of Sabasa and 3 km northwest of Luvuvhu River; $30^{0}17'$ east, $22^{0}58'$ south.

C-146: 9 km west of Sabasa and 5.5 km northwest of Luvuvhu River; $30^{0}16'$ east, $22^{0}57'$ south.

C-147: 2 km west of Sabasa; $30^{0}26'$ east, $22^{0}57'$ south.

C-148: 5 km northeast of Sabasa; $30^{0}30'$ east $22^{0}55'$ south.

C-149: 12 km northeast of Sabasa; $30^{0}34'$ east, $22^{0}53'$ south.

C-150: 15 km northeast of Sabasa; $30^{0}35'$ east, $22^{0}52'$ south.

C-151: 10 km northeast of Sabasa; $30^{0}33'$ east, $22^{0}54'$ south.

C-153 - C-154: 22 km northeast of Sabasa and on Luvuvhu River; $30^{0}41'$ east, $22^{0}55'$ south.

C-155: 23 km northeast of Sabasa and on Luvuvhu River; $30^{0}41.5'$ east, $22^{0}56'$ south.

C-156: 40 km northeast of Sabasa on road to Pafuri and 17 km from Kruger National Park; $30^{0}52'$ east, $22^{0}49'$ south.

C-189 - C-194: roadcut 18-19 km south of Limpopo River and 9 km west of Luvuvhu River; just north of Tshamavhudzi fault; $30^{0}52.5'$ east, $22^{0}34'$ south.

C-195: 24 km south of Limpopo River; 30°40′ east, 22°33′ south.

APPENDIX B

Analytical Methods

For most samples, major and some trace elements (Rb, Sr, Ba, Nb, Y, Zr, Ni, V, and Pb) were determined by X-Ray fluoresence using an automated Rigaku 3064 XRF spectrometer with an on-line DEC computer. Calibration curves were made using international rock standards. Sample preparation for major element analyses involved melting approximately 0.5 mg rock powder in about 2.7 gm of Spectroflux 105 (lithium tetraborate-lanthanum oxide flux) and a few grains of ammonium nitrate (to insure oxidation of iron) in a platinum (+5% Au) crucible. The mixture is fused over a propane burner for 15 minutes. Once molten, the mixture is poured into an aluminum mold held at 450^0C and then cooled to room temperature.

Trace element sample preparation involved the compression (to 20 tons) of from 5 to 8 gm rock powder and 1-2 gm of boric acid powder (plus 5 to 8 drops of polyvinyl binder) in a hydraulic press to form a press pellet with a boric acid backing. For the remaining samples (all Pongola samples except those with P prefix; all 16 of the Meredale Member, Westonaria Formation samples), major elements and some trace elements (Zr, Ni, [Nb], Rb [Ba], Sr and Y) were provided by N.V. Armstrong (Pongola) and R.G. Cawthorn (Westonaria) of the University of Natal, Pietermaritzburg, South Africa and the University of Witwatersrand, South Africa, respectively.

XRF Analytical methods similar to those described by Norrish and Hutton (1969) and Norrish and Chappel (1977) were followed. Instrumental parameters are summarized in Table B-1. Background counts are typically for 40 seconds. Energies are first-order K-alpha peaks whenever possible. XRF trace element analysis uses the factor method of background correction. For runs involving Pb, Th, Rb, U, Sr, Y, Zr, Nb, and Ni, mass absordtion coefficients are calculated using the rhodium compton K-alpha peak for Rhodium (Rh). Rh was also counted in order to subtract interferences for Ni. Mass absorbtion coefficients correct for enhancement and absorbtion.

Other trace elements (Cs, Th, U, Sc, Cr, Co, Hf, Ta, La, Ce, Sm, Eu, Tb, Yb, and Lu) were determined by instrumental neutron activation analysis (INAA). Sealed polyethylene vials containing approximately 300 mg rock powder were irradiated in the Annular Core Research Reactor at Sandia National Laboratory, Albuquerque, New Mexico. The vials are subjected to a

Table. B1
XRF Instrumental Parameters

	Crystal	Angle(2θ)	Time(sec)
SiO_2	PET	109.1	40
TiO_2	LIF3	86.1	20
Al_2O_3	Pet	144.7	80
Fe_2O_3	LIF3	57.5	40
MgO	TAP	45.4	100
CaO	LIF3	113.1	20
Na_2O	TAP	55.2	200
K_2O	LIF3	136.7	20
MnO	LIF3	63.0	20
P_2O_5	Ge	140.9	40
Cr	LIF3	69.3	100
V	LIF3	77.0	100
Ba	LIF3	87.2	100
Pb	LIF1	28.2	200
Th	LIF1	27.5	200
Rb	LIF1	26.6	100
U	LIF1	26.1	200
Sr	LIF1	25.1	100
Y	LIF1	23.8	100
Zr	LIF1	22.5	100
Nb	LIF1	21.4	200
Ni	LIF1	48.5	100

Ge= germanium, LIF1= scintillation counter, LIF3= lithium fluoride, PET= pentaerythritol crystal.

Table. B2
INAA Interferences

	Peak (KeV) 7 day	Peak (KeV) 40 day
Sc	1120.6	-
Cs	564.2	-
La	396.3	-
Sm	531.3	-
Eu	411.6	810.8
	564.2	-
Tb	197.9	765.9
	1115.5	-
Yb	145.4	-
Lu	320.0	-
Ta	228.0	1112.0
	1120.6	1120.6
	-	263.9
Pa	97.5	298.5
Np	103.2	-
	208.3	-

Table. B3
INAA Peaks

	Peak (KeV) 7 day	Peak (KeV) 40 day
Cs	604.6	*795.9
Th	*311.7	*311.8
U	228.0	-
	*277.6	-
Sc	*889.2	*889.2
	*1120.6	*1120.6
Cr	320.0	*320.0
Co	1173.2	*1173.3
	1332.5	*1332.5
Hf	482.2	*482.2
Ta	1189.2	1189.2
	1221.6	*1221.6
	1231.1	*1231.0
La	*328.7	-
	815.7	-
	*1596.0	-
Ce	145.4	*145.4
Sm	*103.2	-
Eu	244.6	*244.6
	-	344.2
	779.1	779.1
	1408.4	1408.1
Tb	*298.6	298.6
	879.4	879.4
	1177.5	1177.5
Yb	177.1	177.1
	-	197.9
	*282.5	-
	396.3	-
Lu	*208.3	-
Ni	-	*810.8

*= preferred peak; if more than one star shown, an average is used: dash= peak not available or not used.

neutron flux estimated at 2.7 X 10^{13} n/cm^2/s for 2.78 hours. Analytical methods are similar to those proposed by Jacobs et al. (1977) and Lindstrom and Korotev (1982). Calibration was based on NBS Fly Ash standard 1633a. Counts are taken on each sample at intervals of 7 and 40 days after irradiation using a Nuclear Data 6600 gamma-ray spectrometer in conjunction with two Ge detectors. Interfering gamma-ray peaks for Sc, Cs, La, Sm, Eu, Tb, Yb, Lu, Ta, Pa and Np are removed by TEABAGS, a data reduction program by Lindstrom and Korotev (1982). The interfering peaks vary with each run. An example is given in Table B-2 Also, contributions to the abundances of LREE by the fission of uranium are automatically removed. Final data reduction involves determining which peaks or combinations of peaks gives the value closest to the known value for NBS 1633a (Gladney, 1980)(run as an unknown) and these are used to obtain the final results. Table B-3 gives the peaks (energies) examined in each INAA run.

Presented in Table B-4 is a compilation of numerous XRF and INAA analyses for BCR-1 (Basalt Columbia River) in an attempt to evaluate precision and accuracy for all the analyses of this study. Individual analyses are given in Table B-5. Data are from M. Knoper, D. Wronkiewicz, M. Boryta and the author. Given is the mean (X) and one standard deviation of that mean (S) for 21 major element runs, a minimum of 6 XRF trace element runs and approximately 10 INAA runs. Actual BCR-1 values are from Govindaraju (1984). Because the concentration of Ni in BCR-1 (10 ppm) is near the detection limit, a triplicate of BEN, a French basalt standard (Govindaraju, 1980; 1984)(by INAA) is also shown. Also shown is the coefficient of variation (C.V.) which is the relative standard deviation in percent and a measure of precision (Levin and Rubin, 1980). Precision is a measure of the scatter or dispersion of a series of test results. The C.V. is used to construct the error bars shown on the figures of this dissertation. Accuracy (ACC), a measure of the difference between the average result and the true result (relative error), is also shown. The true value is the value of the standard as given by Gorvindaraju (1984).

Table. B4
BCR-1 Statistics

	Actual	X	S	C.V.	ACC	N
SiO2	54.53	54.59	0.11	0.2%	0.11	21
TiO2	2.26	2.23	0.03	1.4	1.33	21
Al2O3	13.72	13.66	0.13	1.0	0.44	21
Fe2O3T	13.41	13.08	0.35	2.7	2.5	21
MgO	3.48	3.69	0.31	8.4	6.0	21
CaO	6.97	7.00	0.07	1.0	0.43	21
Na2O	3.3	3.66	0.14	3.8	10.9	21
K2O	1.7	1.70	0.03	1.8	0	21
MnO	0.18	0.18	0.02	11.1	0	21
P2O5	0.36	0.36	0.01	2.8	0	21
Rb	47	51.3	0.8	1.6	9.2	14
Ba	680	686	17	2.5	0.9	11
*Cs	0.96	0.95	0.06	6.3	1.0	10
Sr	330	334	4.5	1.4	1.2	14
Pb	13.6	17.3	2.3	13.3	27.2	14
*Th	6.04	5.8	0.3	5.2	4.0	10
*U	1.72	1.7	0.1	5.9	1.2	10
*Sc	33	32	2.0	6.3	3.0	10
V	420	432	6.4	1.5	2.9	6
*Cr	15	14	1.0	7.1	6.7	10
*Co	37	37	2.1	5.7	0	10
Ni	10	11	3.0	27.3	10.0	6
*Ni	267	272	13.1	4.8	7.6	3
Y	39	38	2.0	5.3	2.6	14
Zr	191	190	5.2	2.7	0.5	13
Nb	14	13.4	1.8	13.4	4.3	14
*Hf	5	5	0.3	6.0	0	8
*Ta	0.83	0.78	0.03	3.9	6.0	8
*La	24	24.5	1.8	7.4	2.1	10
*Ce	53.5	53.2	3.3	6.2	0.6	10
*Sm	6.6	6.79	0.32	4.7	2.9	10
*Eu	1.96	1.89	0.12	6.4	3.6	10
*Tb	1.0	1.07	0.09	8.4	7.0	10
*Yb	3.38	3.36	0.20	6.0	0.6	10
*Lu	0.51	0.52	0.03	5.8	2.0	10

X= mean; S= one standard deviation of the mean; N= number of samples; C.V.= coefficient of variation= S/X x 100; ACC= accuracy= X - actual value/actual value x

Table B-5
Individual BCR-1 Analyses

	1	2	3	4	5	6	7
SiO2	54.37	54.58	54.48	54.49	54.65	54.70	54.78
TiO2	2.18	2.18	2.20	2.26	2.21	2.22	2.21
Al2O3	13.75	13.60	13.71	13.54	13.75	13.75	13.86
Fe2O3T	12.64	12.64	12.65	13.38	12.59	12.63	12.64
MgO	3.81	3.77	3.74	3.32	3.72	3.78	3.73
CaO	6.92	6.91	6.91	7.05	6.90	6.89	6.93
Na2O	3.66	3.66	3.62	3.62	3.88	3.84	3.69
K2O	1.66	1.63	1.70	1.71	1.66	1.67	1.66
MnO	0.17	0.16	0.17	0.19	0.15	0.14	0.14
P2O5	0.37	0.36	0.36	0.37	0.36	0.36	0.36
Rb	52	52	50	51	52	53	51
Ba	717	681	687	649	680	703	684
Cs	0.99	0.92	0.89	1.04	1.00	0.99	0.98
Sr	332	330	328	332	330	331	339
Pb	19.6	20.5	18.0	18.0	14.6	18.0	13.9
Th	8.8	8.9	5.8	5.9	9.0	9.0	-
*Th	5.7	5.8	5.0	5.8	5.8	5.8	5.7
U	2.8	3.8	2.6	2.4	3.9	2.7	3.8
*U	1.8	1.3	1.7	1.8	1.6	1.7	1.7
Sc	32	32	26	32	32	32	32
V	420	436	429	433	435	437	-
*Cr	13.0	13.9	12.2	15.4	14.6	13.3	14.6
*Co	37.2	36.3	31.2	38.0	38.0	37.2	36.7
Ni	16	11	12	12	6.8	10	-
*Ni	13	13	9	9	8	-	-
Y	37.6	37.8	37.6	37.0	40.7	39.4	39.8
Zr	187	189	188	189	182.4	181.2	191.2
Nb	12.5	13.0	13.6	14.0	13.3	13.2	11.0
*Hf	5.3	5.0	4.4	5.2	5.1	5.0	5.0
*Ta	0.77	0.82	0.78	0.81	0.79	0.80	0.75
*La	24	25.1	20	25	25	24	24.4
*Ce	54.9	53.0	44.2	54.0	55.0	54.9	54.9
*Sm	6.81	6.96	6.00	7.10	7.10	6.87	6.75
*Eu	1.93	1.91	1.60	1.94	1.93	2.02	1.96
*Tb	1.07	1.07	0.93	1.20	1.20	1.05	1.01
*Yb	3.14	3.55	3.05	3.61	3.61	3.15	3.33
*Lu	0.52	0.52	0.43	0.54	0.53	0.53	0.52

Table B-5 Continued
Individual BCR-1 Analyses

	1	2	3	4	5	6	7
SiO2	54.67	54.76	54.48	54.58	54.72	54.69	54.51
TiO2	2.24	2.20	2.20	2.21	2.24	2.24	2.23
Al2O3	13.42	13.81	13.78	13.81	13.52	13.38	13.61
Fe2O3T	13.37	13.46	13.48	13.50	12.85	12.94	12.91
MgO	3.30	4.22	4.28	4.42	3.72	3.63	3.74
CaO	6.96	6.95	6.99	6.99	7.08	7.07	7.05
Na2O	3.69	3.41	3.23	3.45	3.77	3.76	3.72
K2O	1.71	1.68	1.70	1.69	1.73	1.73	1.72
MnO	0.19	0.17	0.17	0.17	0.20	0.19	0.19
P2O5	0.36	0.33	0.33	0.33	0.37	0.36	0.36
Rb	52	51	50	51	52	52	51
Ba	692	682	690	684	-	-	-
Cs	0.88	0.98	0.85	-	-	-	-
Sr	344	331	338	337	338	336	332
Pb	16	18	14	14	19	20	18
Th	-	-	-	-	-	-	-
*Th	5.7	6.4	5.8	-	-	-	-
U	3.9	-	-	-	-	-	-
*U	1.6	1.7	1.6	-	-	-	-
*Sc	32	33	33	-	-	-	-
V	-	-	-	-	-	-	-
*Cr	15.1	12.9	13.0	-	-	-	-
*Co	37.0	36.9	39.0	-	-	-	-
Ni	-	-	-	-	-	-	-
*Ni	-	-	-	-	-	-	-
Y	37	38.8	40.5	39.9	35	34	37
Zr	193	189.4	192.6	191.8	197	200	-
Nb	15	12.9	10.9	11.1	16	17	14
*Hf	5.3	-	-	-	-	-	-
*Ta	0.75	-	-	-	-	-	-
*La	26.9	25.9	25	-	-	-	-
*Ce	53.1	52.8	55	-	-	-	-
*Sm	6.60	6.69	7.00	-	-	-	-
*Eu	1.84	1.95	1.80	-	-	-	-
*Tb	0.99	1.12	1.10	-	-	-	-
*Yb	3.28	3.43	3.40	-	-	-	-
*Lu	0.52	0.50	0.54	-	-	-	-

Table B-5 Continued
Individual BCR-1 Analyses

	1	2	3	4	5	6	7
SiO2	54.46	54.63	64.64	54.53	54.63	54.55	54.49
TiO2	2.28	2.26	2.27	2.26	2.28	2.26	2.26
Al2O3	13.67	13.61	13.65	13.64	13.61	13.67	13.61
Fe2O3T	13.36	12.90	13.34	13.33	13.36	13.37	13.35
MgO	3.45	3.72	3.47	3.42	3.41	3.51	3.42
CaO	7.05	7.08	7.03	7.03	7.05	7.03	7.07
Na2O	3.68	3.69	3.70	3.70	3.71	3.64	3.73
K2O	1.72	1.73	1.71	1.71	1.72	1.72	1.71
MnO	0.2	0.2	0.2	0.19	0.2	0.19	0.19
P2O5	0.37	0.36	0.37	0.37	0.37	0.37	0.37

Appendix C

Analytical Results

In this appendix is a compilation of all analytical results from this investigation. Results are arranged in order of decreasing age, from the Pongola Supergroup to the Soutpansberg Group. Some units such as the Nsuze Group, Pongola Supergroup and Rhenosterhoek Formation, Dominion Group have variable composition. In these instances, units are arranged according to rock-type (basalt, andesite etc.) and an average is given for each rock-type. In other units where volcanic compositions are relatively constant, averages are given for each formation.

In the Rhenosterhoek andesite average, sample D-4 (a rhyolite) and samples BTF-12 and BTF-14 (possible paleosols) are excluded. P_2O_5 values in four Loraine samples (J26L, J29L, J30L and J33L) are excluded from the formation average because alteration is thought to have artifically increased their value. Two averages and standard deviations are given for the Dullstroom Formation: one with and one without samples C-40 and C-50. Similarly, the Hekpoort Formation data have two averages and standard deviations, one with and one without sample D-105.

CIPW Norms are calculated with a computer program

(PETCAL 2) available in the Precambrian Research Laboratory at New Mexico Tech.

Major elements are in weight percent; trace elements are in parts per million (ppm). No entry indicates either not determined or below detectability limit. Also, Fe_2O_3-T is total iron as Fe_2O_3.

Basaltic Andesites, Nsuze Gp, Pongola Supergroup

SAMPLE	P-1	P-2	P-16	P-17	P-18
SiO2	55.0	50.5	49.5	51.4	49.3
TiO2	1.04	1.08	1.46	1.52	1.65
Al2O3	14.4	14.7	14.0	13.5	13.6
Fe2O3-T	10.9	11.3	13.3	16.4	14.3
MgO	5.26	4.75	6.36	5.34	5.07
CaO	7.84	12.03	10.6	3.94	6.63
Na2O	3.09	2.04	2.04	2.43	2.94
K2O	1.12	0.86	0.28	0.04	0.07
MnO	0.16	0.17	0.2	0.19	0.18
P2O5	0.21	0.21	0.14	0.26	0.31
LOI	1.55	2.52	2.1	4.96	6.86
TOTAL	100.6	100.2	100.0	100.0	100.8
Rb	22.3	14.0	9.1	5.4	4.7
Ba	481	379	289	141	75
Cs	0.3	0.1	0.3	0.3	0.1
Sr	391	463	232	111	102
Pb	9.1	10.9	13.3	10.1	9.8
Th	2.3	2.2	0.4	2.4	2.3
U					
Sc	25.0	25.8	38.3	24.7	22.4
V	192	206	295	189	184
Cr	178	194	195	46	196
Co	49	50	54	84	57
Ni	96	87	95	105	84
Y	29.5	26.9	27.3	32.7	31.5
Zr	173.9	174.2	86.9	183.3	189.9
Nb	6.9	6.9	3.7	10.5	10.0
Hf	4.1	4.1	2.3	8.3	5.3
Ta	0.41	0.38	0.22	0.54	0.52
La	22.8	20.6	5.7	22.1	22.1
Ce	51.4	45.6	14.0	51.9	49.5
Sm	5.56	5.22	3.00	7.36	6.76
Eu	1.63	1.64	1.07	1.79	1.92
Tb	0.87	0.92	0.70	1.22	1.11
Yb	2.53	2.61	2.85	3.10	2.83
Lu	0.38	0.39	0.47	0.47	0.47
Mg Number	52.0	48.5	51.8	42.2	44.4
K2O/Na2O	0.36	0.42	0.14	0.02	0.02
Na2O+K2O	4.21	2.90	2.32	2.47	3.01
Al2O3/TiO2	13.8	13.6	9.6	8.9	8.2

Basaltic Andesites, Nsuze Gp, Pongola Supergroup

SAMPLE	P-1	P-2	P-16	P-17	P-18
CaO/TiO2	7.5	11.1	7.3	2.6	4.0
Zr/TiO2	0.017	0.016	0.006	0.012	0.012
K/Rb	416.9	511.0	254.8	61.6	123.6
Ba/Sr	1.23	0.82	1.25	1.27	0.74
Rb/Sr	0.057	0.030	0.039	0.049	0.046
La/Yb	9.0	7.9	2.0	7.1	7.8
La/Sm	4.1	3.9	1.9	3.0	3.3
Sm/Eu	3.4	3.2	2.8	4.1	3.5
Ti/Zr	35.9	37.2	100.8	49.8	52.1
Zr/Nb	25.2	25.2	23.5	17.5	19.0
Nb/Y	0.23	0.26	0.14	0.32	0.32
Zr/Y	5.9	6.5	3.2	5.6	6.0
Nb/Ta	16.8	18.2	16.8	19.4	19.2
Nb/La	0.30	0.33	0.65	0.48	0.45
La/Ta	55.6	54.2	25.9	40.9	42.5
La/Th	9.9	9.4	13.9	9.2	9.6
Y/Tb	33.9	29.3	39.0	26.8	28.4
Th/Yb	0.91	0.84	0.14	0.77	0.81
Ta/Yb	0.162	0.146	0.077	0.174	0.184
Hf/Th	1.78	1.86	5.61	3.46	2.30
Ti/V	32.5	31.5	29.7	48.2	53.8
U/Pb	0.00	0.00	0.00	0.00	0.00
Ce/Nb	7.45	6.61	3.78	4.94	4.95
Th/Ta	5.61	5.79	1.86	4.44	4.42
Th/Sc	0.09	0.09	0.01	0.10	0.10
Th/Nb	0.33	0.32	0.11	0.23	0.23
Sc/Ni	0.26	0.30	0.40	0.24	0.27
Hf/Ta	10.00	10.79	10.45	15.37	10.19
FeO-T/MgO	1.86	2.15	1.88	2.77	2.53
Sm/Yb	2.20	2.00	1.05	2.37	2.39
Eu/Eu*	0.89	0.92	0.97	0.73	0.85
g(x)	5.06	5.09	4.82	4.88	4.88
Score 1	1.14	1.30	0.65	-0.10	-0.19
Score 2	-0.20	-0.25	-0.06	-0.48	-0.57

Fe2O3-T ==> Total Fe as Fe2O3
NO ENTRY ==> No determination OR below detectability limi
MAJOR ELEMENTS ==> In weight percent
TRACE ELEMENTS ==> In parts per million

Basaltic Andesites, Nsuze Gp, Pongola Supergroup

SAMPLE	P-19	P-20	P-22	P-23	P-24
SiO2	49.7	57.7	52.8	52.6	55.9
TiO2	1.55	1.84	0.88	0.82	0.92
Al2O3	13.9	12.7	13.5	14.3	14.2
Fe2O3-T	13.0	12.4	10.8	10.9	11.3
MgO	4.61	4.15	6.06	6.31	5.76
CaO	6.74	3.39	8.24	8.02	2.94
Na2O	3.63	3.13	2.82	3.33	3.09
K2O	0.23	0.44	0.95	0.58	0.26
MnO	0.16	0.16	0.16	0.17	0.15
P2O5	0.26	0.32	0.16	0.15	0.15
LOI	6.64	3.68	3.36	2.67	5.28
TOTAL	100.5	99.8	99.7	99.9	99.9
Rb	7.6	10.8	12.9	10.8	10.4
Ba	166	189	599	320	233
Cs	0.5	1.1	0.2	0.2	0.4
Sr	140	90	248	274	56
Pb	9.1	11.6	9.9	13.3	9.2
Th	2.5	2.3	1.2	1.0	2.3
U	0.5				
Sc	22.9	25.5	26.3	25.8	23.3
V	181	196	197	183	188
Cr	74	207	257	243	95
Co	49	55	52	54	53
Ni	82	107	116	108	89
Y	32.1	35.5	23.0	21.2	19.6
Zr	181.5	221.9	132.4	121.3	124.0
Nb	10.2	13.7	5.1	4.7	5.8
Hf	4.9	6.1	3.3	3.1	3.1
Ta	0.53	0.60	0.32	0.31	0.36
La	21.3	19.7	16.0	14.0	12.5
Ce	49.2	45.6	34.9	31.8	24.4
Sm	6.86	6.38	4.17	3.88	3.23
Eu	1.79	1.76	1.26	1.23	0.83
Tb	1.03	1.13	0.63	0.64	0.53
Yb	2.84	3.77	2.16	1.97	2.04
Lu	0.48	0.58	0.33	0.31	0.33
Mg Number	44.3	43.0	55.7	56.5	53.3
K2O/Na2O	0.06	0.14	0.34	0.17	0.08
Na2O+K2O	3.86	3.57	3.77	3.91	3.35
Al2O3/TiO2	9.0	6.9	15.3	17.5	15.4

Basaltic Andesites, Nsuze Gp, Pongola Supergroup

SAMPLE	P-19	P-20	P-22	P-23	P-24
CaO/TiO2	4.3	1.8	9.4	9.8	3.2
Zr/TiO2	0.012	0.012	0.015	0.015	0.013
K/Rb	249.9	337.5	611.2	445.3	207.5
Ba/Sr	1.18	2.09	2.42	1.17	4.20
Rb/Sr	0.054	0.120	0.052	0.039	0.187
La/Yb	7.5	5.2	7.4	7.1	6.1
La/Sm	3.1	3.1	3.8	3.6	3.9
Sm/Eu	3.8	3.6	3.3	3.2	3.9
Ti/Zr	51.2	49.8	39.9	40.6	44.5
Zr/Nb	17.8	16.2	26.0	25.8	21.4
Nb/Y	0.32	0.39	0.22	0.22	0.30
Zr/Y	5.7	6.3	5.8	5.7	6.3
Nb/Ta	19.2	22.8	15.9	15.2	16.1
Nb/La	0.48	0.70	0.32	0.34	0.46
La/Ta	40.2	32.8	50.0	45.2	34.7
La/Th	8.5	8.6	13.3	14.0	5.4
Y/Tb	31.2	31.4	36.4	33.1	37.0
Th/Yb	0.88	0.61	0.56	0.51	1.13
Ta/Yb	0.187	0.159	0.148	0.157	0.176
Hf/Th	1.96	2.65	2.75	3.10	1.35
Ti/V	51.3	56.5	26.8	26.9	29.4
U/Pb	0.05	0.00	0.00	0.00	0.00
Ce/Nb	4.82	3.33	6.84	6.77	4.21
Th/Ta	4.72	3.83	3.75	3.23	6.39
Th/Sc	0.11	0.09	0.05	0.04	0.10
Th/Nb	0.25	0.17	0.24	0.21	0.40
Sc/Ni	0.28	0.24	0.23	0.24	0.26
Hf/Ta	9.25	10.17	10.31	10.00	8.61
FeO-T/MgO	2.54	2.68	1.61	1.55	1.77
Sm/Yb	2.42	1.69	1.93	1.97	1.58
Eu/Eu*	0.80	0.81	0.92	0.95	0.77
g(x)	4.94	4.95	4.78	4.74	4.36
Score 1	0.10	-0.39	0.94	1.08	-0.26
Score 2	-0.46	-0.62	-0.25	-0.22	-0.58

Fe2O3-T ==> Total Fe as Fe2O3
NO ENTRY ==> No determination OR below detectability limi
MAJOR ELEMENTS ==> In weight percent
TRACE ELEMENTS ==> In parts per million

Basaltic Andesites, Nsuze Gp, Pongola Supergroup

SAMPLE	MS-34	WR-1	MS-32	HKS-28	MS-37
SiO2	51.0	52.2	52.4	52.6	53.1
TiO2	1.41	1.09	1.24	0.63	0.59
Al2O3	14.7	15.3	14.8	13.9	14.0
Fe2O3-T	13.8	13.2	14.0	11.7	11.2
MgO	6.2	4.8	4.6	7.4	8.7
CaO	9	9.3	9.2	10.2	8.3
Na2O	1.7	3	2.9	2.2	2.6
K2O	1.5	0.79	0.42	0.97	1
MnO	0.39	0.26	0.22	0.23	0.39
P2O5	0.29	0.09	0.24	0.11	0.11
LOI	2.1	1.6	4.1	2.1	1.8
TOTAL	100.0	100.0	100.0	99.9	100.0
Rb	28.0	25.0	8.0	22.0	20.0
Ba	298	132	123	200	132
Cs	0.6	1.2	0.3	0.2	0.2
Sr	343	403	602	293	172
Pb					
Th	2.0	1.6	2.0	1.3	1.1
U		0.4			
Sc	24.6	25.7	29.3	31.6	30.5
V	196	182	172	226	214
Cr	158	144	83	650	672
Co	60	62	70	60	58
Ni	101	93	67	137	122
Y	42.0	19.0	32.0	20.0	18.0
Zr	215.0	83.0	171.0	98.0	71.0
Nb	10.0	3.6	8.7	3.9	2.7
Hf	5.2	2.2	4.9	2.5	2.1
Ta	0.43	0.24	0.46	0.22	0.19
La	23.1	12.2	22.4	11.3	9.6
Ce	53.2	26.2	52.0	26.3	21.0
Sm	6.80	3.00	6.40	3.00	2.60
Eu	2.14	1.19	2.12	0.92	0.80
Tb	1.22	0.48	1.00	0.50	0.46
Yb	2.97	1.57	2.87	1.72	1.69
Lu	0.48	0.26	0.45	0.27	0.28
Mg Number	50.2	45.0	42.5	58.7	63.6
K2O/Na2O	0.88	0.26	0.14	0.44	0.38
Na2O+K2O	3.20	3.79	3.32	3.17	3.60
Al2O3/TiO2	10.4	14.0	11.9	22.1	23.7

Basaltic Andesites, Nsuze Gp, Pongola Supergroup

SAMPLE	MS-34	WR-1	MS-32	HKS-28	MS-37
CaO/TiO2	6.4	8.5	7.4	16.2	14.1
Zr/TiO2	0.015	0.008	0.014	0.016	0.012
K/Rb	444.6	262.3	435.8	366.0	415.0
Ba/Sr	0.87	0.33	0.20	0.68	0.77
Rb/Sr	0.082	0.062	0.013	0.075	0.116
La/Yb	7.8	7.8	7.8	6.6	5.7
La/Sm	3.4	4.1	3.5	3.8	3.7
Sm/Eu	3.2	2.5	3.0	3.3	3.3
Ti/Zr	39.3	78.8	43.5	38.6	49.9
Zr/Nb	21.5	23.1	19.7	25.1	26.3
Nb/Y	0.24	0.19	0.27	0.20	0.15
Zr/Y	5.1	4.4	5.3	4.9	3.9
Nb/Ta	23.3	15.0	18.9	17.7	14.2
Nb/La	0.43	0.30	0.39	0.35	0.28
La/Ta	53.7	50.8	48.7	51.4	50.5
La/Th	11.6	7.6	11.2	8.7	8.7
Y/Tb	34.4	39.6	32.0	40.0	39.1
Th/Yb	0.67	1.02	0.70	0.76	0.65
Ta/Yb	0.145	0.153	0.160	0.128	0.112
Hf/Th	2.60	1.38	2.45	1.92	1.91
Ti/V	43.2	35.9	43.3	16.7	16.5
U/Pb	ERR	ERR	ERR	ERR	ERR
Ce/Nb	5.32	7.28	5.98	6.74	7.78
Th/Ta	4.65	6.67	4.35	5.91	5.79
Th/Sc	0.08	0.06	0.07	0.04	0.04
Th/Nb	0.20	0.44	0.23	0.33	0.41
Sc/Ni	0.24	0.28	0.44	0.23	0.25
Hf/Ta	12.09	9.17	10.65	11.36	11.05
FeO-T/MgO	2.00	2.48	2.74	1.42	1.16
Sm/Yb	2.29	1.91	2.23	1.74	1.54
Eu/Eu*	0.92	1.19	1.00	0.91	0.90
g(x)	5.25	4.79	5.23	4.63	4.37
Score 1	0.76	1.37	1.40	1.28	0.92
Score 2	-0.18	-0.12	-0.12	-0.04	.00

Fe2O3-T ==> Total Fe as Fe2O3
NO ENTRY ==> No determination OR below detectability limi
MAJOR ELEMENTS ==> In weight percent
TRACE ELEMENTS ==> In parts per million

Basaltic Andesites, Nsuze Gp, Pongola Supergroup

SAMPLE	WR-9	WR-2	MS-33	WR-7	WR-6
SiO2	53.7	54.0	53.6	54.0	54.5
TiO2	0.63	1.09	1.28	1.06	1.31
Al2O3	15.2	16.4	15.2	14.6	14.8
Fe2O3-T	11.6	11.1	11.9	13.8	14.3
MgO	7.3	4.9	4.9	5.1	3.7
CaO	8	9.3	7.8	5.9	6.6
Na2O	2.7	2.4	4.2	2.8	2.5
K2O	0.46	0.17	0.61	2.2	1.7
MnO	0.28	0.37	0.29	0.29	0.41
P2O5	0.14	0.35	0.23	0.2	0.27
LOI	2.2	6.6	1.9	4.5	2.7
TOTAL	100.0	100.1	100.0	100.0	100.1
Rb	9.0	3.3	8.0	90.0	30.0
Ba	94	35	160	405	446
Cs	0.3	0.4	0.9	16.1	1.5
Sr	250	824	276	238	263
Pb					
Th	1.2	0.4	2.3	3.0	1.7
U	0.4	0.2		0.9	0.4
Sc	30.1	20.9	21.6	26.9	21.9
V	213	236	171	197	205
Cr	558	84	133	197	119
Co	58	46	47	57	66
Ni	116	149	90	101	59
Y	17.0	22.0	30.0	36.0	33.0
Zr	88.0	131.0	162.0	164.0	188.0
Nb	4.1	3.9	9.0	9.0	8.0
Hf	2.7	3.3	4.6	4.0	4.6
Ta	0.23	0.22	0.46	0.48	0.41
La	12.3	19.8	22.2	18.2	18.0
Ce	27.2	48.8	51.0	39.7	40.2
Sm	3.06	6.10	6.60	4.65	5.03
Eu	0.96	1.72	1.84	1.60	1.49
Tb	0.57	0.74	1.00	0.96	0.83
Yb	1.63	1.67	2.59	2.64	2.57
Lu	0.27	0.25	0.41	0.42	0.40
Mg Number	58.6	49.8	48.1	45.4	36.8
K2O/Na2O	0.17	0.07	0.15	0.79	0.68
Na2O+K2O	3.16	2.57	4.81	5.00	4.20
Al2O3/TiO2	24.1	15.0	11.9	13.8	11.3

Basaltic Andesites, Nsuze Gp, Pongola Supergroup

SAMPLE	WR-9	WR-2	MS-33	WR-7	WR-6
CaO/TiO2	12.7	8.5	6.1	5.6	5.0
Zr/TiO2	0.014	0.012	0.013	0.015	0.014
K/Rb	424.2	427.6	632.9	202.9	470.3
Ba/Sr	0.38	0.04	0.58	1.70	1.70
Rb/Sr	0.036	0.004	0.029	0.378	0.114
La/Yb	7.5	11.9	8.6	6.9	7.0
La/Sm	4.0	3.2	3.4	3.9	3.6
Sm/Eu	3.2	3.5	3.6	2.9	3.4
Ti/Zr	43.0	49.9	47.4	38.8	41.8
Zr/Nb	21.5	33.6	18.0	18.2	23.5
Nb/Y	0.24	0.18	0.30	0.25	0.24
Zr/Y	5.2	6.0	5.4	4.6	5.7
Nb/Ta	17.8	17.7	19.6	18.8	19.5
Nb/La	0.33	0.20	0.41	0.49	0.44
La/Ta	53.5	90.0	48.3	37.9	43.9
La/Th	10.3	49.5	9.7	6.1	10.6
Y/Tb	29.8	29.7	30.0	37.5	39.8
Th/Yb	0.74	0.24	0.89	1.14	0.66
Ta/Yb	0.141	0.132	0.178	0.182	0.160
Hf/Th	2.25	8.25	2.00	1.33	2.71
Ti/V	17.7	27.7	44.9	32.3	38.3
U/Pb	ERR	ERR	ERR	ERR	ERR
Ce/Nb	6.63	12.51	5.67	4.41	5.03
Th/Ta	5.22	1.82	5.00	6.25	4.15
Th/Sc	0.04	0.02	0.11	0.11	0.08
Th/Nb	0.29	0.10	0.26	0.33	0.21
Sc/Ni	0.26	0.14	0.24	0.27	0.37
Hf/Ta	11.74	15.00	10.00	8.33	11.22
FeO-T/MgO	1.43	2.04	2.19	2.44	3.48
Sm/Yb	1.88	3.65	2.55	1.76	1.96
Eu/Eu*	0.91	0.90	0.85	0.97	0.88
g(x)	4.52	5.12	5.01	4.98	5.07
Score 1	1.21	1.88	0.77	0.64	0.67
Score 2	-0.13	-0.15	-0.27	-0.10	-0.30

Fe2O3-T ==> Total Fe as Fe2O3
NO ENTRY ==> No determination OR below detectability limi
MAJOR ELEMENTS ==> In weight percent
TRACE ELEMENTS ==> In parts per million

Basaltic Andesites, Nsuze Gp, Pongola Supergroup

SAMPLE	HKS-30	Avg	Std
SiO2	57.6	52.8	2.1
TiO2	0.57	1.15	0.34
Al2O3	15.6	14.4	0.8
Fe2O3-T	9.0	12.6	1.5
MgO	4.4	5.56	1.19
CaO	9.1	7.70	2.29
Na2O	2.7	2.78	0.57
K2O	0.72	0.73	0.56
MnO	0.24	0.24	0.09
P2O5	0.13	0.21	0.07
LOI	6.1	3.46	1.73
TOTAL	100.1	100.1	0.3
Rb	21.0	17.57	18.35
Ba	95	245	149
Cs		1.26	3.42
Sr	368	289	180
Pb		10.62	1.54
Th		1.78	0.70
U		0.5	0.2
Sc		26.16	4.05
V	142	201	27
Cr	137	224	179
Co		57	9
Ni	39	100	21
Y	20.0	27.41	6.91
Zr	136.0	148.01	44.62
Nb	4.9	7.02	2.97
Hf		4.04	1.49
Ta		0.38	0.12
La	13.0	17.30	5.08
Ce	42.5	39.20	12.10
Sm	3.84	4.98	1.58
Eu	1.15	1.49	0.41
Tb		0.83	0.25
Yb	1.67	2.43	0.58
Lu		0.39	0.09
Mg Number	52.3	49.52	6.63
K2O/Na2O	0.27	0.29	0.25
Na2O+K2O	3.42	3.51	0.70
Al2O3/TiO2	27.4	13.82	4.81

Basaltic Andesites, Nsuze Gp, Pongola Supergroup

SAMPLE	HKS-30	Avg	Std
CaO/TiO2	16.0	7.58	3.74
Zr/TiO2	0.024	0.01	.00
K/Rb	284.6	365.04	147.19
Ba/Sr	0.26	1.18	0.92
Rb/Sr	0.057	0.08	0.08
La/Yb	7.8	7.23	1.79
La/Sm	3.4	3.51	0.50
Sm/Eu	3.3	3.33	0.37
Ti/Zr	25.1	48.63	14.99
Zr/Nb	27.8	22.40	4.09
Nb/Y	0.25	0.25	0.06
Zr/Y	6.8	5.37	0.81
Nb/Ta	ERR	18.11	2.28
Nb/La	0.38	0.41	0.12
La/Ta	ERR	47.54	12.47
La/Th	ERR	11.79	8.93
Y/Tb	ERR	33.92	4.21
Th/Yb	0.00	0.73	0.25
Ta/Yb	0.000	0.15	0.03
Hf/Th	ERR	2.68	1.58
Ti/V	24.1	35.16	11.71
U/Pb	ERR	ERR	ERR
Ce/Nb	8.67	6.05	1.93
Th/Ta	ERR	4.69	1.32
Th/Sc	ERR	0.07	0.03
Th/Nb	0.00	0.26	0.09
Sc/Ni	0.00	0.27	0.06
Hf/Ta	ERR	10.79	1.74
FeO-T/MgO	1.84	2.14	0.56
Sm/Yb	2.30	2.06	0.51
Eu/Eu*	1.18	0.90	0.10
g(x)	4.74	4.87	0.25
Score 1	1.48	0.76	0.62
Score 2	-0.15	-0.25	0.18

Fe2O3-T ==> Total Fe as Fe2O3
NO ENTRY ==> No determination OR below detectability limi
MAJOR ELEMENTS ==> In weight percent
TRACE ELEMENTS ==> In parts per million

Andesites, Nsuze Gp, Pongola Supergroup

SAMPLE	AS-25	OS-44	WR-15	KB-48	AS-24
SiO2	52.9	55.8	53.3	54.1	54.9
TiO2	1.00	0.91	1.18	1.31	0.97
Al2O3	15.3	14.5	16.3	16.7	14.7
Fe2O3-T	11.1	11.1	16.7	15.0	10.8
MgO	6.00	5.50	3.30	4.00	6.00
CaO	9.80	9.30	4.10	3.30	8.50
Na2O	2.40	2.30	2.90	3.60	2.60
K2O	1.00	0.58	1.50	1.50	1.10
MnO	0.26	0.10	0.39	0.29	0.22
P2O5	0.20	0.20	0.39	0.24	0.21
LOI	2.70	2.10	4.80	4.30	1.90
ORIGINAL TOTAL	100.0	100.3	100.1	100.0	100.0
Rb	34.0	22.0	48.0	35.0	43.0
Ba	229	129	251	257	239
Cs	0.4	0.4	1.8	0.4	0.4
Sr	186	197	99	51	198
Pb					
Th	5.3	5.8	6.3	8.7	5.2
U	1.8	1.4	1.7	2.0	0.9
Sc	28.5	26.2	30.1	30.0	35.1
V	203	195	328	249	204
Cr	56	48	21	8	44
Co	44	45	67	48	55
Ni	47	81	30	34	63
Y	33	35	36	44	37
Zr	160	177	182	238	175
Nb	10	10	11	18	10
Hf	4.7	4.2	5.0	6.4	5.1
Ta	0.74	0.61	0.77	1.20	0.72
La	25.6	25.7	28.4	36.3	28.0
Ce	53.6	54.4	56.4	76.7	60.4
Sm	5.55	5.30	5.60	7.62	5.59
Eu	1.30	1.33	1.44	1.60	1.47
Tb	1.10	0.92	1.01	1.25	1.09
Yb	3.35	3.06	3.66	4.28	3.65
Lu	0.51	0.48	0.58	0.69	0.60
Mg Number	54.8	52.7	30.8	37.5	55.5
K2O/Na2O	0.42	0.25	0.52	0.42	0.42
Na2O+K2O	3.40	2.88	4.40	5.10	3.70
Al2O3/TiO2	15.3	15.9	13.8	12.7	15.2

Andesites, Nsuze Gp, Pongola Supergroup

SAMPLE	AS-25	OS-44	WR-15	KB-48	AS-24
CaO/TiO2	9.8	10.2	3.5	2.5	8.8
Zr/TiO2	0.016	0.019	0.015	0.018	0.018
K/Rb	244.1	218.8	259.4	355.7	212.3
Ba/Sr	1.23	0.65	2.54	5.04	1.21
Rb/Sr	0.183	0.112	0.485	0.686	0.217
La/Yb	7.6	8.4	7.8	8.5	7.7
La/Sm	4.6	4.8	5.1	4.8	5.0
Sm/Eu	4.3	4.0	3.9	4.8	3.8
Ti/Zr	37.5	30.8	38.9	33.0	33.3
Zr/Nb	16.0	17.7	16.5	13.2	17.5
Nb/Y	0.30	0.29	0.31	0.41	0.27
Zr/Y	4.8	5.1	5.1	5.4	4.7
Nb/Ta	13.5	16.4	14.3	15.0	13.9
Nb/La	0.39	0.39	0.39	0.50	0.36
La/Ta	34.6	42.1	36.9	30.3	38.9
La/Th	4.8	4.4	4.5	4.2	5.4
Y/Tb	30.0	38.0	35.6	35.2	33.9
Th/Yb	1.58	1.90	1.72	2.03	1.42
Ta/Yb	0.221	0.199	0.210	0.280	0.197
Hf/Th	0.89	0.72	0.79	0.74	0.98
Ti/V	29.6	28.0	21.6	31.6	28.5
U/Pb	ERR	ERR	ERR	ERR	ERR
Ce/Nb	5.36	5.44	5.13	4.26	6.04
Th/Ta	7.16	9.51	8.18	7.25	7.22
Th/Sc	0.19	0.22	0.21	0.29	0.15
Th/Nb	0.53	0.58	0.57	0.48	0.52
Sc/Ni	0.61	0.32	1.00	0.88	0.56
Hf/Ta	6.35	6.89	6.49	5.33	7.08
FeO-T/MgO	1.67	1.82	4.56	3.38	1.62
Sm/Yb	1.66	1.73	1.53	1.78	1.53
Eu/Eu*	0.67	0.74	0.75	0.63	0.75
g(x)	4.88	4.91	4.81	4.79	4.93
Score 1	0.49	0.54	-0.14	-0.83	0.50
Score 2	-0.17	-0.14	-0.34	-0.48	-0.12

Fe2O3-T ==> Total Fe as Fe2O3
NO ENTRY ==> No determinion; belowelow detectability limi
MAJOR ELEMENTS ==> In weight percent
TRACE ELEMENTS ==> In parts per million

Andesites, Nsuze Gp, Pongola Supergroup

SAMPLE	AS-23	WR-5	WR-14	WR-12	AS-22
SiO2	55.1	56.2	56.5	57.3	57.9
TiO2	1.04	1.11	0.99	0.70	1.03
Al2O3	14.0	13.9	14.6	16.6	14.1
Fe2O3-T	12.0	11.9	12.2	14.2	11.4
MgO	5.10	4.20	3.50	3.40	3.60
CaO	8.60	7.50	8.50	3.80	7.40
Na2O	2.20	3.50	3.20	2.40	2.90
K2O	1.30	1.20	0.18	1.00	1.30
MnO	0.43	0.15	0.22	0.36	0.20
P2O5	0.21	0.23	0.21	0.16	0.19
LOI	1.70	1.40	7.30	4.20	1.30
ORIGINAL TOTAL	100.0	99.9	100.1	99.9	100.0
Rb	35.0	20.0	7.0	22.0	49.0
Ba	292	294	37	232	177
Cs	1.2	1.4	0.3	0.6	1.5
Sr	155	330	266	296	121
Pb					
Th	6.9	2.0	4.6	2.4	11.2
U	1.7	0.4	1.2	0.5	2.4
Sc	27.9	23.2	31.3	26.7	28.9
V	200	198	227	207	194
Cr	9	156	21	35	12
Co	46	45	53	63	44
Ni	42	54	29	14	25
Y	41	35	28	24	52
Zr	187	208	156	143	250
Nb	11	7	8	6	19
Hf	5.3	4.8	4.1	3.3	7.1
Ta	0.86	0.47	0.62	0.33	1.18
La	30.7	24.1	22.2	18.1	46.1
Ce	64.1	51.7	47.3	39.0	97.3
Sm	6.49	5.93	4.80	4.03	8.00
Eu	1.38	1.82	1.24	1.35	1.65
Tb	1.23	0.91	0.85	0.62	1.47
Yb	3.79	2.49	2.93	1.66	5.12
Lu	0.60	0.42	0.48	0.27	0.78
Mg Number	48.9	44.2	39.2	35.0	41.5
K2O/Na2O	0.59	0.34	0.06	0.42	0.45
Na2O+K2O	3.50	4.70	3.38	3.40	4.20
Al2O3/TiO2	13.5	12.5	14.7	23.7	13.7

Andesites, Nsuze Gp, Pongola Supergroup

SAMPLE	AS-23	WR-5	WR-14	WR-12	AS-22
CaO/TiO2	8.3	6.8	8.6	5.4	7.2
Zr/TiO2	0.018	0.019	0.016	0.020	0.024
K/Rb	308.3	498.0	213.4	377.3	220.2
Ba/Sr	1.88	0.89	0.14	0.78	1.46
Rb/Sr	0.226	0.061	0.026	0.074	0.405
La/Yb	8.1	9.7	7.6	10.9	9.0
La/Sm	4.7	4.1	4.6	4.5	5.8
Sm/Eu	4.7	3.3	3.9	3.0	4.8
Ti/Zr	33.4	32.0	38.1	29.4	24.7
Zr/Nb	17.0	31.5	19.5	23.8	13.2
Nb/Y	0.27	0.19	0.29	0.25	0.37
Zr/Y	4.6	5.9	5.6	6.0	4.8
Nb/Ta	12.8	14.0	12.9	18.2	16.1
Nb/La	0.36	0.27	0.36	0.33	0.41
La/Ta	35.7	51.3	35.8	54.8	39.1
La/Th	4.4	12.1	4.8	7.5	4.1
Y/Tb	33.3	38.5	32.9	38.7	35.4
Th/Yb	1.82	0.80	1.57	1.45	2.19
Ta/Yb	0.227	0.189	0.212	0.199	0.230
Hf/Th	0.77	2.40	0.89	1.38	0.63
Ti/V	31.2	33.6	26.2	20.3	31.9
U/Pb	ERR	ERR	ERR	ERR	ERR
Ce/Nb	5.83	7.83	5.91	6.50	5.12
Th/Ta	8.02	4.26	7.42	7.27	9.49
Th/Sc	0.25	0.09	0.15	0.09	0.39
Th/Nb	0.63	0.30	0.58	0.40	0.59
Sc/Ni	0.66	0.43	1.08	1.91	1.16
Hf/Ta	6.16	10.21	6.61	10.00	6.02
FeO-T/MgO	2.12	2.55	3.14	3.76	2.85
Sm/Yb	1.71	2.38	1.64	2.43	1.56
Eu/Eu*	0.61	0.93	0.76	1.02	0.60
g(x)	4.93	5.13	4.91	4.79	5.00
Score 1	0.23	0.89	0.86	1.15	-0.09
Score 2	-0.14	-0.22	-0.22	-0.15	-0.16

Fe2O3-T ==> Total Fe as Fe2O3
NO ENTRY ==> No determination OR below detectability limi
MAJOR ELEMENTS ==> In weight percent
TRACE ELEMENTS ==> In parts per million

Andesites, Nsuze Gp, Pongola Supergroup

SAMPLE	OS-42	WR-17	D-38	HKS-31	NS-47
SiO2	59.1	59.6	60.8	62.2	62.5
TiO2	1.62	1.06	0.59	1.00	0.96
Al2O3	12.6	14.3	14.2	14.0	12.3
Fe2O3-T	14.2	10.9	7.7	11.7	14.5
MgO	2.30	4.20	4.00	1.40	1.00
CaO	4.00	5.20	5.80	5.10	2.70
Na2O	3.10	4.10	4.30	2.10	1.60
K2O	2.40	0.21	1.90	1.80	3.30
MnO	0.42	0.19	0.24	0.41	0.27
P2O5	0.36	0.21	0.35	0.26	0.21
LOI	3.10	5.20	0.70	5.20	3.90
ORIGINAL TOTAL	100.1	100.0	99.9	100.0	99.3
Rb	97.0	46.0	42.0	53.0	129.0
Ba	310		356	275	379
Cs	6.8	0.4	0.8	1.7	3.6
Sr	109	75	414	247	103
Pb					
Th	9.7	9.1	3.9	8.3	10.2
U	2.3	2.2	0.4	2.1	1.7
Sc	24.5	24.3	14.8	18.1	15.5
V	229	206	100	148	146
Cr	2	13	147	40	14
Co	38	38	26	28	28
Ni	10	23	43	13	16
Y	49	42	24	28	37
Zr	292	194	189	166	249
Nb	20	15	9	9	12
Hf	7.1	5.8	4.7	4.8	6.3
Ta	1.14	1.09	0.71	0.74	0.78
La	42.2	35.3	31.0	35.4	43.7
Ce	89.6	75.3	62.8	70.3	87.9
Sm	8.70	6.70	5.14	5.69	6.50
Eu	1.85	1.25	1.35	1.31	1.35
Tb	1.59	1.16	0.78	0.86	0.94
Yb	5.10	4.39	2.02	2.58	2.55
Lu	0.81	0.63	0.31	0.39	0.37
Mg Number	26.7	46.4	53.9	21.2	13.4
K2O/Na2O	0.77	0.05	0.44	0.86	2.06
Na2O+K2O	5.50	4.31	6.20	3.90	4.90
Al2O3/TiO2	7.8	13.5	24.1	14.0	12.8

Andesites, Nsuze Gp, Pongola Supergroup

SAMPLE	OS-42	WR-17	D-38	HKS-31	NS-47
CaO/TiO2	2.5	4.9	9.8	5.1	2.8
Zr/TiO2	0.018	0.018	0.032	0.017	0.026
K/Rb	205.4	37.9	375.5	281.9	212.3
Ba/Sr	2.84	0.00	0.86	1.11	3.68
Rb/Sr	0.890	0.613	0.101	0.215	1.252
La/Yb	8.3	8.0	15.3	13.7	17.1
La/Sm	4.9	5.3	6.0	6.2	6.7
Sm/Eu	4.7	5.4	3.8	4.3	4.8
Ti/Zr	33.3	32.8	18.7	36.1	23.1
Zr/Nb	14.6	12.9	21.0	18.4	20.8
Nb/Y	0.41	0.36	0.38	0.32	0.32
Zr/Y	6.0	4.6	7.9	5.9	6.7
Nb/Ta	17.5	13.8	12.7	12.2	15.4
Nb/La	0.47	0.42	0.29	0.25	0.27
La/Ta	37.0	32.4	43.7	47.8	56.0
La/Th	4.4	3.9	7.9	4.3	4.3
Y/Tb	30.8	36.2	30.8	32.6	39.4
Th/Yb	1.90	2.07	1.93	3.22	4.00
Ta/Yb	0.224	0.248	0.351	0.287	0.306
Hf/Th	0.73	0.64	1.21	0.58	0.62
Ti/V	42.4	30.9	35.4	40.5	39.5
U/Pb	ERR	ERR	ERR	ERR	ERR
Ce/Nb	4.48	5.02	6.98	7.81	7.33
Th/Ta	8.51	8.35	5.49	11.22	13.08
Th/Sc	0.40	0.37	0.26	0.46	0.66
Th/Nb	0.49	0.61	0.43	0.92	0.85
Sc/Ni	2.45	1.06	0.34	1.39	0.97
Hf/Ta	6.23	5.32	6.62	6.49	8.08
FeO-T/MgO	5.56	2.34	1.73	7.52	13.05
Sm/Yb	1.71	1.53	2.54	2.21	2.55
Eu/Eu*	0.62	0.55	0.80	0.70	0.64
g(x)	5.11	4.77	4.91	4.91	4.86
Score 1	-0.33	-0.40	1.47	0.79	-0.06
Score 2	-0.46	-0.27	-0.20	-0.27	-0.42

Fe2O3-T ==> Total Fe as Fe2O3
NO ENTRY ==> No determination OR below detectability limi
MAJOR ELEMENTS ==> In weight percent
TRACE ELEMENTS ==> In parts per million

Andesites, Nsuze Gp, Pongola Supergroup

SAMPLE	NS-46	Avg	Std
SiO2	64.9	57.7	3.4
TiO2	0.94	1.03	0.22
Al2O3	13.9	14.5	1.2
Fe2O3-T	9.2	12.2	2.2
MgO	1.40	3.68	1.51
CaO	3.30	6.06	2.35
Na2O	2.90	2.88	0.71
K2O	3.10	1.46	0.86
MnO	0.10	0.27	0.11
P2O5	0.22	0.24	0.06
LOI	2.90	3.29	1.74
ORIGINAL			
TOTAL	100.0	100.0	0.2
Rb	85.0	47.94	30.39
Ba	420	258	93
Cs	4.1	1.61	1.73
Sr	265	195	99
Pb			
Th	10.0	6.85	2.77
U	1.9	1.5	0.7
Sc	16.3	25.09	5.89
V	152	199	49
Cr	24	41	45
Co	30	44	12
Ni	17	34	19
Y	31	36	8
Zr	220	199	40
Nb	12	12	4
Hf	6.2	5.3	1.1
Ta	0.76	0.80	0.24
La	45.3	32.4	8.4
Ce	90.0	67.3	16.8
Sm	7.10	6.17	1.19
Eu	1.52	1.45	0.18
Tb	0.97	1.05	0.24
Yb	2.72	3.33	0.99
Lu	0.44	0.52	0.15
Mg Number	25.5	39.19	12.52
K2O/Na2O	1.07	0.57	0.46
Na2O+K2O	6.00	4.34	0.96
Al2O3/TiO2	14.8	14.88	3.84

Andesites, Nsuze Gp, Pongola Supergroup

SAMPLE	NS-46	Avg	Std
CaO/TiO2	3.5	6.23	2.71
Zr/TiO2	0.023	0.02	.00
K/Rb	302.7	270.20	99.51
Ba/Sr	1.58	1.62	1.29
Rb/Sr	0.321	0.37	0.33
La/Yb	16.7	10.27	3.31
La/Sm	6.4	5.22	0.75
Sm/Eu	4.7	4.25	0.62
Ti/Zr	25.6	31.30	5.52
Zr/Nb	18.3	18.25	4.51
Nb/Y	0.39	0.32	0.06
Zr/Y	7.1	5.63	0.93
Nb/Ta	15.8	14.65	1.73
Nb/La	0.26	0.36	0.07
La/Ta	59.6	42.25	8.75
La/Th	4.5	5.35	2.07
Y/Tb	32.0	34.58	2.93
Th/Yb	3.68	2.08	0.82
Ta/Yb	0.279	0.24	0.05
Hf/Th	0.62	0.91	0.44
Ti/V	37.1	31.76	6.09
U/Pb	ERR	ERR	ERR
Ce/Nb	7.50	6.03	1.13
Th/Ta	13.16	8.47	2.33
Th/Sc	0.61	0.30	0.17
Th/Nb	0.83	0.58	0.16
Sc/Ni	0.96	0.99	0.55
Hf/Ta	8.16	7.00	1.39
FeO-T/MgO	5.91	3.97	2.88
Sm/Yb	2.61	1.94	0.41
Eu/Eu*	0.67	0.71	0.12
g(x)	5.01	4.92	0.10
Score 1	0.81	0.37	0.61
Score 2	-0.32	-0.25	0.11

Fe2O3-T ==> Total Fe as Fe2O3
NO ENTRY ==> No determination OR below detectability limi
MAJOR ELEMENTS ==> In weight percent
TRACE ELEMENTS ==> In parts per million

Dacites-Rhyodacites, Nsuze Gp, Pongola Supergroup

SAMPLE	OS-39	WR-4	PKB-18	HKS-27	WR-3
SiO2	64.8	69.5	67.9	68.2	72.0
TiO2	0.96	0.63	0.84	0.72	0.59
Al2O3	13.7	11.6	12.6	12.0	12.1
Fe2O3-T	7.6	7.8	8.4	9.2	5.9
MgO	1.2	1.9	1.2	0.66	0.92
CaO	6.2	3.9	2.9	3	2.8
Na2O	2.1	0.92	2.8	2.3	2.9
K2O	2.5	3.3	3	3.7	2.6
MnO	0.60	0.15	0.21	0.10	0.15
P2O5	0.25	0.21	0.18	0.22	0.15
LOI	5.8	4.1	2.2	2.7	2.8
ORIGINAL TOTAL	99.9	99.9	100.0	100.1	100.1
Rb	86.0	124.0	112.0	102.0	108.0
Ba	408	505	309	358	538
Cs	2.8	2.6	1.9	0.5	4.4
Sr	157	50	221	69	182
Pb					
Th	10.2	13.9	12.6	12.2	12.0
U	1.9	3.3	3.2	3.0	3.3
Sc	15.2	9.0	19.7	12.2	10.2
V	136	8	105	31	11
Cr	10	8	10	21	8
Co	22	7	27	13	6
Ni	7	6	12	10	9
Y	31	41	38	32	40
Zr	230	278	247	229	256
Nb	11	14	14	12	14
Hf	6.5	7.8	7.8	6.5	6.6
Ta	0.86	1.13	1.00	0.92	1.11
La	45.8	51.9	55.1	47.6	46.6
Ce	93.0	104.9	112.1	98.2	93.7
Sm	7.10	8.19	8.07	7.40	7.30
Eu	1.43	1.41	1.50	1.43	1.35
Tb	1.02	1.35	1.21	1.07	1.10
Yb	2.99	3.91	3.78	2.97	3.19
Lu	0.45	0.58	0.59	0.45	0.51
Mg Number	26.2	35.4	24.3	13.9	25.9
K2O/Na2O	1.19	3.59	1.07	1.61	0.90
Na2O+K2O	4.60	4.22	5.80	6.00	5.50
Al2O3/TiO2	14.3	18.4	15.0	16.7	20.5

Dacites-Rhyodacites, Nsuze Gp, Pongola Supergroup

SAMPLE	OS-39	WR-4	PKB-18	HKS-27	WR-3
CaO/TiO2	6.5	6.2	3.5	4.2	4.7
Zr/TiO2	0.024	0.044	0.029	0.032	0.043
K/Rb	241.3	220.9	222.3	301.1	199.8
Ba/Sr	2.60	10.10	1.40	5.19	2.96
Rb/Sr	0.548	2.480	0.507	1.478	0.593
La/Yb	15.3	13.3	14.6	16.0	14.6
La/Sm	6.5	6.3	6.8	6.4	6.4
Sm/Eu	5.0	5.8	5.4	5.2	5.4
Ti/Zr	25.0	13.6	20.4	18.9	13.8
Zr/Nb	20.9	19.9	17.6	19.1	18.3
Nb/Y	0.35	0.34	0.37	0.38	0.35
Zr/Y	7.4	6.8	6.5	7.2	6.4
Nb/Ta	12.8	12.4	14.0	13.0	12.6
Nb/La	0.24	0.27	0.25	0.25	0.30
La/Ta	53.3	45.9	55.1	51.7	42.0
La/Th	4.5	3.7	4.4	3.9	3.9
Y/Tb	30.4	30.4	31.4	29.9	36.4
Th/Yb	3.41	3.55	3.33	4.11	3.76
Ta/Yb	0.288	0.289	0.265	0.310	0.348
Hf/Th	0.64	0.56	0.62	0.53	0.55
Ti/V	42.4	472.5	48.0	139.4	321.8
U/Pb	ERR	ERR	ERR	ERR	ERR
Ce/Nb	8.45	7.49	8.01	8.18	6.69
Th/Ta	11.86	12.30	12.60	13.26	10.81
Th/Sc	0.67	1.54	0.64	1.00	1.18
Th/Nb	0.93	0.99	0.90	1.02	0.86
Sc/Ni	2.17	1.50	1.64	1.22	1.13
Hf/Ta	7.56	6.90	7.80	7.07	5.95
FeO-T/MgO	5.70	3.70	6.30	12.55	5.77
Sm/Yb	2.37	2.09	2.13	2.49	2.29
Eu/Eu*	0.62	0.51	0.57	0.59	0.56
g(x)	4.90	4.62	5.02	4.63	4.90
Score 1	0.37	-0.56	0.62	-0.23	0.56
Score 2	-0.44	-0.37	-0.23	-0.44	-0.12

Fe2O3-T ==> Total Fe as Fe2O3
NO ENTRY ==> No determination OR below detectability limi
MAJOR ELEMENTS ==> In weight percent
TRACE ELEMENTS ==> In parts per million

Dacites-Rhyodacites, Nsuze Gp, Pongola Supergroup

SAMPLE	WR-11	MS-35	WR-10	WR-13	Avg
SiO2	73.1	73.5	74.2	66.9	70.0
TiO2	0.49	0.45	0.49	0.7	0.65
Al2O3	11.5	11.3	11.4	13.6	12.2
Fe2O3-T	6.2	5.4	5.5	8.0	7.1
MgO	0.19	0.41	0.38	1.1	0.88
CaO	1.5	1.3	1.9	3.8	3.03
Na2O	2.3	2.2	1.8	1.6	2.10
K2O	4.4	5.1	4.3	3.9	3.64
MnO	0.09	0.00	0.00	0.10	0.16
P2O5	0.11	0.09	0.09	0.15	0.16
LOI	0.7	1.2	0.7	2.2	2.49
ORIGINAL TOTAL	99.9	99.8	100.1	99.9	100.0
Rb	131.0	109.0	90.0	131.0	110.33
Ba	455	558	687	404	469
Cs	12.6	0.5	1.3	3.0	3.29
Sr	93	97	181	147	133
Pb					
Th	15.1	14.6	14.2	16.4	13.47
U	3.7	3.6	3.7	3.8	3.3
Sc	7.5	7.3	6.9	13.2	11.24
V	7	10	7	109	47
Cr	8	10	3	8	10
Co	6	4	7	20	13
Ni	8	10	15	13	10
Y	37	36	43	53	39
Zr	268	267	301	332	268
Nb	13	16	18	21	15
Hf	8.0	8.0	7.2	10.2	7.62
Ta	1.20	1.21	1.18	1.73	1.15
La	54.4	42.3	50.8	59.4	50.43
Ce	111.6	94.5	99.9	119.5	103.04
Sm	8.06	7.04	7.58	9.88	7.85
Eu	1.36	0.94	1.23	1.48	1.35
Tb	1.24	1.22	1.28	1.77	1.25
Yb	3.65	3.69	3.53	6.07	3.46
Lu	0.58	0.53	0.52	0.92	0.57
Mg Number	6.4	14.6	13.4	23.6	20.42
K2O/Na2O	1.91	2.32	2.39	2.44	1.93
Na2O+K2O	6.70	7.30	6.10	5.50	5.75
Al2O3/TiO2	23.5	25.1	23.3	19.4	19.57

Dacites-Rhyodacites, Nsuze Gp, Pongola Supergroup

SAMPLE	WR-11	MS-35	WR-10	WR-13	Avg
CaO/TiO2	3.1	2.9	3.9	5.4	4.47
Zr/TiO2	0.055	0.059	0.061	0.047	0.04
K/Rb	278.8	388.3	396.6	247.1	277.35
Ba/Sr	4.89	5.75	3.80	2.75	4.38
Rb/Sr	1.409	1.124	0.497	0.891	1.06
La/Yb	14.9	11.5	14.4	9.8	13.82
La/Sm	6.7	6.0	6.7	6.0	6.43
Sm/Eu	5.9	7.5	6.2	6.7	5.89
Ti/Zr	11.0	10.1	9.8	12.7	15.03
Zr/Nb	20.6	16.7	16.7	15.8	18.40
Nb/Y	0.35	0.44	0.42	0.40	0.38
Zr/Y	7.2	7.4	7.0	6.3	6.91
Nb/Ta	10.8	13.2	15.3	12.1	12.92
Nb/La	0.24	0.38	0.35	0.35	0.29
La/Ta	45.3	35.0	43.1	34.3	45.08
La/Th	3.6	2.9	3.6	3.6	3.79
Y/Tb	29.8	29.5	33.6	29.9	31.26
Th/Yb	4.14	3.96	4.02	2.70	3.67
Ta/Yb	0.329	0.328	0.334	0.285	0.31
Hf/Th	0.53	0.55	0.51	0.62	0.57
Ti/V	420.0	270.0	420.0	38.5	241.40
U/Pb	ERR	ERR	ERR	ERR	ERR
Ce/Nb	8.58	5.91	5.55	5.69	7.17
Th/Ta	12.58	12.07	12.03	9.48	11.89
Th/Sc	2.01	2.00	2.06	1.24	1.37
Th/Nb	1.16	0.91	0.79	0.78	0.93
Sc/Ni	0.94	0.73	0.46	1.02	1.20
Hf/Ta	6.67	6.61	6.10	5.90	6.73
FeO-T/MgO	29.37	11.85	13.03	6.55	10.54
Sm/Yb	2.21	1.91	2.15	1.63	2.14
Eu/Eu*	0.51	0.39	0.48	0.44	0.52
g(x)	4.68	4.66	4.91	5.03	4.82
Score 1	0.10	0.17	0.59	0.19	0.20
Score 2	-0.25	-0.23	-0.09	-0.15	-0.26

Fe2O3-T ==> Total Fe as Fe2O3
NO ENTRY ==> No determination OR below detectability limi
MAJOR ELEMENTS ==> In weight percent
TRACE ELEMENTS ==> In parts per million

Dacites-Rhyodacites, Nsuze Gp, Pongola Supergroup

SAMPLE	Std
SiO2	3.1
TiO2	0.16
Al2O3	0.9
Fe2O3-T	1.3
MgO	0.50
CaO	1.42
Na2O	0.57
K2O	0.82
MnO	0.17
P2O5	0.05
LOI	1.56
ORIGINAL TOTAL	0.1
Rb	15.37
Ba	109
Cs	3.50
Sr	55
Pb	
Th	1.78
U	0.5
Sc	4.03
V	50
Cr	5
Co	8
Ni	3
Y	6
Zr	31
Nb	3
Hf	1.09
Ta	0.24
La	5.06
Ce	8.97
Sm	0.82
Eu	0.16
Tb	0.21
Yb	0.34
Lu	0.13
Mg Number	8.39
K2O/Na2O	0.80
Na2O+K2O	0.90
Al2O3/TiO2	3.64

Dacites-Rhyodacites, Nsuze Gp, Pongola Supergroup

SAMPLE	Std
CaO/TiO2	1.24
Zr/TiO2	0.01
K/Rb	67.94
Ba/Sr	2.42
Rb/Sr	0.62
La/Yb	1.88
La/Sm	0.28
Sm/Eu	0.75
Ti/Zr	4.96
Zr/Nb	1.73
Nb/Y	0.03
Zr/Y	0.42
Nb/Ta	1.16
Nb/La	0.05
La/Ta	7.02
La/Th	0.44
Y/Tb	2.15
Th/Yb	0.44
Ta/Yb	0.03
Hf/Th	0.04
Ti/V	167.69
U/Pb	ERR
Ce/Nb	1.16
Th/Ta	1.06
Th/Sc	0.53
Th/Nb	0.11
Sc/Ni	0.48
Hf/Ta	0.64
FeO-T/MgO	7.40
Sm/Yb	0.24
Eu/Eu*	0.07
g(x)	0.16
Score 1	0.37
Score 2	0.12

Fe2O3-T ==> Total Fe as Fe2O3
NO ENTRY ==> No determination OR below detectability limi
MAJOR ELEMENTS ==> In weight percent
TRACE ELEMENTS ==> In parts per million
==========

Rhyolite, Nsuze Gp, Pongola Supergroup

SAMPLE	OS-40	WR-16	C-19	OS-41	OS-43
SiO2	71.1	71.7	72.4	73.9	75.2
TiO2	0.52	0.6	0.48	0.45	0.39
Al2O3	13.4	12.1	12.7	12.2	12.9
Fe2O3-T	5.6	6.4	4.5	4.5	4.1
MgO	0.4	0.29	0.08	0.19	0.22
CaO	0.92	1.5	1.6	0.66	0.86
Na2O	2.3	2.9	2.7	3.3	0.93
K2O	5.7	4.1	5.2	4.5	5.2
MnO	0.21	0.14	0.12	0.17	0.09
P2O5	0.12	0.19	0.12	0.09	0.05
LOI	1.7	1.6	1.4	0.8	1.9
ORIGINAL TOTAL	100.3	99.9	99.9	100.0	99.9
Rb	213.0	132.0	164.0	137.0	196.0
Ba	584	606	545	390	938
Cs	3.3		24.0	5.3	
Sr	68	159	69	48	80
Pb					
Th	21.1		22.4	23.9	
U	5.1		5.4	5.8	
Sc	5.1		5.1	4.1	
V	18	20	16	16	2
Cr	14	7	11	11	
Co	5		5	4	
Ni	6	9	7	10	8
Y	86	59	72	76	86
Zr	599	430	501	455	532
Nb	37	26	31	32	34
Hf	13.7		14.1	12.9	
Ta	2.09		2.19	2.47	
La	80.7	64.0	85.4	84.8	88.0
Ce	163.1	116.8	172.4	172.6	180.0
Sm	12.80	9.10	13.20	13.00	14.90
Eu	1.78	1.42	1.55	1.44	2.43
Tb	2.12		2.31	2.35	
Yb	7.25	4.82	7.40	7.89	8.90
Lu	1.13		1.16	1.21	
Mg Number	13.8	9.2	3.8	8.7	10.8
K2O/Na2O	2.48	1.41	1.93	1.36	5.59
Na2O+K2O	8.00	7.00	7.90	7.80	6.13
Al2O3/TiO2	25.8	20.2	26.5	27.1	33.1

Rhyolite, Nsuze Gp, Pongola Supergroup

SAMPLE	OS-40	WR-16	C-19	OS-41	OS-43
CaO/TiO2	1.8	2.5	3.3	1.5	2.2
Zr/TiO2	0.115	0.072	0.104	0.101	0.136
K/Rb	222.1	257.8	263.2	272.6	220.2
Ba/Sr	8.59	3.81	7.90	8.13	11.73
Rb/Sr	3.132	0.830	2.377	2.854	2.450
La/Yb	11.1	13.3	11.5	10.7	9.9
La/Sm	6.3	7.0	6.5	6.5	5.9
Sm/Eu	7.2	6.4	8.5	9.0	6.1
Ti/Zr	5.2	8.4	5.7	5.9	4.4
Zr/Nb	16.2	16.5	16.2	14.2	15.6
Nb/Y	0.43	0.44	0.43	0.42	0.40
Zr/Y	7.0	7.3	7.0	6.0	6.2
Nb/Ta	17.7	ERR	14.2	13.0	ERR
Nb/La	0.46	0.41	0.36	0.38	0.39
La/Ta	38.6	ERR	39.0	34.3	ERR
La/Th	3.8	ERR	3.8	3.5	ERR
Y/Tb	40.6	ERR	31.2	32.3	ERR
Th/Yb	2.91	0.00	3.03	3.03	0.00
Ta/Yb	0.288	0.000	0.296	0.313	0.000
Hf/Th	0.65	ERR	0.63	0.54	ERR
Ti/V	173.3	180.0	180.0	168.8	1170.0
U/Pb	ERR	ERR	ERR	ERR	ERR
Ce/Nb	4.41	4.49	5.56	5.39	5.29
Th/Ta	10.10	ERR	10.23	9.68	ERR
Th/Sc	4.14	ERR	4.39	5.83	ERR
Th/Nb	0.57	0.00	0.72	0.75	0.00
Sc/Ni	0.85	0.00	0.73	0.41	0.00
Hf/Ta	6.56	ERR	6.44	5.22	ERR
FeO-T/MgO	12.60	19.86	50.63	21.32	16.77
Sm/Yb	1.77	1.89	1.78	1.65	1.67
Eu/Eu*	0.41	0.61	0.35	0.32	0.64
g(x)	5.03	5.10	4.92	4.81	4.97
Score 1	-0.58	0.25	-0.45	-0.75	-0.33
Score 2	-0.14	-0.15	-0.14	-0.09	0.05

Fe2O3-T ==> Total Fe as Fe2O3
NO ENTRY ==> No determination OR below detectability limi
MAJOR ELEMENTS ==> In weight percent
TRACE ELEMENTS ==> In parts per million

Rhyolite, Nsuze Gp, Pongola Supergroup

SAMPLE	AS-21	Avg	Std
SiO2	76.7	73.5	2.0
TiO2	0.31	0.46	0.09
Al2O3	11.3	12.4	0.7
Fe2O3-T	2.4	4.6	1.2
MgO	0.04	0.20	0.12
CaO	0.44	1.00	0.42
Na2O	1.4	2.26	0.84
K2O	7.3	5.33	1.02
MnO	0.03	0.13	0.06
P2O5	0.06	0.11	0.05
LOI	0.7	1.35	0.45
ORIGINAL			
TOTAL	100.0	100.0	0.1
Rb	171.0	168.83	29.12
Ba	732	633	170
Cs	3.5	9.03	8.68
Sr	64	81	36
Pb			
Th	20.2	21.90	1.39
U	5.8	5.5	0.3
Sc	3.3	4.40	0.75
V	3	13	7
Cr	10	11	2
Co	1	4	2
Ni	14	9	3
Y	69	75	10
Zr	456	496	57
Nb	28	31	4
Hf	12.9	13.40	0.52
Ta	2.17	2.23	0.14
La	67.6	78.42	9.23
Ce	139.4	157.38	22.25
Sm	11.60	12.43	1.78
Eu	1.89	1.75	0.35
Tb	2.19	2.24	0.09
Yb	7.22	7.25	1.23
Lu	1.09	1.15	0.04
Mg Number	3.6	8.33	3.64
K2O/Na2O	5.21	3.00	1.74
Na2O+K2O	8.70	7.59	0.82
Al2O3/TiO2	36.5	28.17	5.27

Rhyolite, Nsuze Gp, Pongola Supergroup

SAMPLE	AS-21	Avg	Std
CaO/TiO2	1.4	2.12	0.67
Zr/TiO2	0.147	0.11	0.02
K/Rb	354.3	265.04	44.61
Ba/Sr	11.44	8.60	2.63
Rb/Sr	2.672	2.39	0.74
La/Yb	9.4	10.99	1.26
La/Sm	5.8	6.34	0.40
Sm/Eu	6.1	7.24	1.15
Ti/Zr	4.1	5.62	1.40
Zr/Nb	16.3	15.84	0.77
Nb/Y	0.41	0.42	0.02
Zr/Y	6.6	6.67	0.46
Nb/Ta	12.9	ERR	ERR
Nb/La	0.41	0.40	0.03
La/Ta	31.2	ERR	ERR
La/Th	3.3	ERR	ERR
Y/Tb	31.5	ERR	ERR
Th/Yb	2.80	1.96	1.39
Ta/Yb	0.301	0.20	0.14
Hf/Th	0.64	ERR	ERR
Ti/V	620.0	415.35	374.51
U/Pb	ERR	ERR	ERR
Ce/Nb	4.98	5.02	0.44
Th/Ta	9.31	ERR	ERR
Th/Sc	6.12	ERR	ERR
Th/Nb	0.72	0.46	0.33
Sc/Ni	0.24	0.37	0.33
Hf/Ta	5.94	ERR	ERR
FeO-T/MgO	54.01	29.20	16.60
Sm/Yb	1.61	1.73	0.10
Eu/Eu*	0.47	0.47	0.12
g(x)	4.76	4.93	0.12
Score 1	-0.33	-0.36	0.31
Score 2	0.01	-0.08	0.08

Fe2O3-T ==> Total Fe as Fe2O3
NO ENTRY ==> No determination OR below detectability limi
MAJOR ELEMENTS ==> In weight percent
TRACE ELEMENTS ==> In parts per million

Dominion Group basaltic andesites

SAMPLE	BTF-3	BTF-4	BTF-5	BTF-6	BTF-8
SiO2	51.5	50.2	52.1	52.1	56.6
TiO2	0.57	0.64	0.64	0.59	0.61
Al2O3	13.9	17.3	14.1	14.2	13.8
Fe2O3-T	9.9	13.2	10.5	9.6	12.2
MgO	7.94	8.20	8.18	7.14	7.17
CaO	8.17	1.42	7.45	8.92	1.81
Na2O	2.85	4.98	3.07	2.47	3.23
K2O	1.09	0.10	0.67	0.93	0.17
MnO	0.15	0.14	0.16	0.14	0.12
P2O5	0.12	0.20	0.16	0.15	0.28
LOI	4.13	4.53	3.24	3.35	4.25
TOTAL	100.3	100.9	100.3	99.6	100.2
Rb	36	1	19	34	3
Ba	482	34	372	304	57
Cs	2.0	1.2	2.0	2.5	1.1
Sr	379	69	324	360	88
Pb	11	8	12	9	8
Th	0.8	2.0	1.0	0.9	1.9
U	2.7	1.8	2.2	0.5	0.7
Sc	21	26	30	25	22
V	185	200	193	169	183
Cr	588	528	815	532	575
Co	42	30	64	52	52
Ni	356	250	342	289	288
Y	14	16	15	16	16
Zr	80	94	94	90	81
Nb	3.1	4.2	4.5	3.5	3.3
Hf	1.5	2.3	2.3	2.3	1.9
Ta	0.11	0.12	0.15	0.15	0.14
La	7.9	15.7	13.3	12.3	7.7
Ce	17.7	30.2	31.8	28.5	19.4
Sm	2.5	2.7	3.5	3.2	2.5
Eu	0.69	0.71	1.02	1.11	0.52
Tb	0.36	0.39	0.45	0.45	0.39
Yb	1.00	1.25	1.43	1.36	1.30
Lu	0.14	0.20	0.23	0.21	0.21
Mg Number	64.22	58.24	63.54	62.51	56.95
K2O/Na2O	0.38	0.02	0.22	0.38	0.05
Na2O+K2O	3.94	5.08	3.74	3.40	3.40
Al2O3/TiO2	24.32	27.03	22.14	24.12	22.71

Dominion Group basaltic andesites

SAMPLE	BTF-3	BTF-4	BTF-5	BTF-6	BTF-8
CaO/TiO2	14.33	2.22	11.71	15.11	2.98
Zr/TiO2	0.01	0.01	0.01	0.02	0.01
K/Rb	251	1297	293	226	404
Ba/Sr	1.27	0.50	1.15	0.84	0.65
Rb/Sr	0.09	0.01	0.06	0.09	0.04
La/Yb	7.90	12.53	9.30	9.01	5.91
La/Sm	3.16	5.74	3.76	3.78	3.08
Sm/Eu	3.62	3.85	3.47	2.92	4.79
Ti/Zr	42.75	40.83	40.62	39.17	44.96
Zr/Nb	25.81	22.39	20.88	25.82	24.55
Nb/Y	0.22	0.27	0.30	0.21	0.20
Zr/Y	5.71	6.04	6.22	5.55	5.01
Nb/Ta	28.18	35.00	30.00	23.33	23.57
Nb/La	0.39	0.27	0.34	0.29	0.43
La/Ta	71.82	130.50	88.67	81.73	54.86
La/Th	9.88	7.99	13.85	13.62	4.06
Y/Tb	38.89	39.90	33.56	36.20	41.49
Th/Yb	0.80	1.57	0.67	0.66	1.45
Ta/Yb	0.11	0.10	0.10	0.11	0.11
Hf/Th	1.88	1.19	2.40	2.59	0.99
Ti/V	18.49	19.21	19.82	20.97	19.86
U/Pb	0.25	0.22	0.18	0.06	0.09
Ce/Nb	5.71	7.19	7.07	8.14	5.88
Th/Ta	7.27	16.33	6.40	6.00	13.50
Th/Sc	0.04	0.07	0.03	0.04	0.09
Th/Nb	0.26	0.47	0.21	0.26	0.57
Sc/Ni	0.06	0.10	0.09	0.09	0.08
Hf/Ta	13.64	19.42	15.33	15.53	13.36
FeO-T/MgO	1.13	1.45	1.16	1.21	1.53
Sm/Yb	2.50	2.18	2.48	2.38	1.92
Eu/Eu*	0.9	0.8	0.9	1.1	0.6
g(x)	4.5	4.2	4.6	4.6	4.2
Score 1	1.7	0.2	1.5	1.6	0.4
Score 2	-0.1	-0.4	-0.2	-0.1	-0.3

Fe2O3-T ==> Total Fe as Fe2O3
NO ENTRY ==> No determination OR below detectability limi
MAJOR ELEMENTS ==> In weight percent
TRACE ELEMENTS ==> In parts per million

Dominion Group basaltic andesites

SAMPLE	BTF-9	BTF-10	BTF-11	BTF-15	BTF-2D
SiO2	57.7	54.3	51.5	50.6	51.7
TiO2	0.61	0.83	0.69	0.68	0.68
Al2O3	14.6	18.3	13.6	13.2	13.1
Fe2O3-T	9.8	9.9	11.0	10.9	11.0
MgO	6.87	5.25	8.60	9.20	9.10
CaO	2.25	1.59	7.87	8.99	8.74
Na2O	4.81	6.82	3.78	2.00	2.17
K2O	0.05	0.23	0.07	0.22	0.12
MnO	0.10	0.08	0.17	0.16	0.17
P2O5	0.53	0.40	0.16	0.17	0.17
LOI	3.46	3.08	2.65	2.90	2.83
TOTAL	100.7	100.8	100.2	99.0	99.7
Rb	1	7	4	17	10
Ba	8	54	29	78	52
Cs	1.5	1.5	0.4	1.4	0.6
Sr	121	119	334	338	360
Pb	12	8	9	10	11
Th	2.5	2.4	3.0	3.4	0.3
U	0.8	1.8	1.0	1.6	1.5
Sc	25	22	30	31	18
V	187	265	198	195	195
Cr	614	818	774	887	510
Co	35	34	57	66	40
Ni	199	266	317	347	318
Y	22	23	15	17	15
Zr	84	108	90	92	93
Nb	3.3	3.3	4.0	3.8	3.8
Hf	2.1	2.4	2.3	2.9	1.6
Ta	0.14	0.18	0.13	0.24	0.11
La	14.6	8.1	10.7	14.5	7.8
Ce	32.4	20.5	27.5	34.3	19.7
Sm	4.1	3.2	3.3	4.2	2.8
Eu	1.08	0.92	0.89	1.53	0.75
Tb	0.63	0.51	0.44	0.63	0.40
Yb	2.19	1.86	1.43	1.79	1.01
Lu	0.35	0.30	0.22	0.27	0.16
Mg Number	61.23	54.27	63.76	65.51	65.10
K2O/Na2O	0.01	0.03	0.02	0.11	0.06
Na2O+K2O	4.86	7.05	3.85	2.22	2.29
Al2O3/TiO2	24.14	21.88	19.72	19.45	19.34

Dominion Group basaltic andesites

SAMPLE	BTF-9	BTF-10	BTF-11	BTF-15	BTF-2D
CaO/TiO2	3.71	1.90	11.37	13.26	12.88
Zr/TiO2	0.01	0.01	0.01	0.01	0.01
K/Rb	431	282	174	110	95
Ba/Sr	0.07	0.45	0.09	0.23	0.14
Rb/Sr	0.01	0.06	0.01	0.05	0.03
La/Yb	6.68	4.35	7.50	8.12	7.70
La/Sm	3.57	2.57	3.26	3.43	2.74
Sm/Eu	3.80	3.42	3.70	2.76	3.79
Ti/Zr	43.45	46.15	46.03	44.16	43.73
Zr/Nb	25.36	32.86	22.55	24.24	24.48
Nb/Y	0.15	0.14	0.27	0.23	0.25
Zr/Y	3.85	4.71	6.04	5.55	6.13
Nb/Ta	23.57	18.33	30.77	15.83	34.55
Nb/La	0.23	0.41	0.37	0.26	0.49
La/Ta	104.43	45.00	82.46	60.54	70.73
La/Th	5.97	3.39	3.60	4.34	23.58
Y/Tb	34.46	45.18	33.95	26.33	37.95
Th/Yb	1.12	1.28	2.08	1.87	0.33
Ta/Yb	0.06	0.10	0.09	0.13	0.11
Hf/Th	0.84	1.01	0.77	0.87	4.91
Ti/V	19.45	18.87	21.00	20.86	20.87
U/Pb	0.07	0.21	0.11	0.16	0.14
Ce/Nb	9.82	6.21	6.88	9.03	5.18
Th/Ta	17.50	13.28	22.92	13.96	3.00
Th/Sc	0.10	0.11	0.10	0.11	0.02
Th/Nb	0.74	0.72	0.75	0.88	0.09
Sc/Ni	0.13	0.08	0.09	0.09	0.06
Hf/Ta	14.71	13.39	17.54	12.08	14.73
FeO-T/MgO	1.28	1.70	1.15	1.06	1.08
Sm/Yb	1.87	1.69	2.30	2.36	2.81
Eu/Eu*	0.8	0.9	0.8	1.1	0.8
g(x)	4.4	4.5	4.6	4.6	4.6
Score 1	0.5	0.4	1.5	1.4	1.5
Score 2	.0	-0.2	-0.2	-0.1	-0.2

Fe2O3-T ==> Total Fe as Fe2O3
NO ENTRY ==> No determination OR below detectability limi
MAJOR ELEMENTS ==> In weight percent
TRACE ELEMENTS ==> In parts per million

Dominion Group basaltic andesites

SAMPLE	BSF-3	BSF-5	BSF-6	BSF-8	BSF-12
SiO2	50.5	51.7	53.3	55.9	50.6
TiO2	0.66	0.84	0.60	0.63	0.83
Al2O3	13.8	16.9	15.0	14.0	13.9
Fe2O3-T	10.7	10.6	9.3	8.6	12.0
MgO	8.85	5.36	6.84	6.76	7.88
CaO	8.76	5.55	8.57	7.01	8.11
Na2O	2.27	5.81	2.82	5.15	3.63
K2O	1.77	0.16	1.22	0.26	0.94
MnO	0.20	0.13	0.13	0.15	0.17
P2O5	0.14	0.21	0.15	0.15	0.20
LOI	2.80	3.31	2.20	2.01	2.16
TOTAL	100.3	100.7	100.1	100.5	100.4
Rb	80	7	47	8	42
Ba	774	50	475	143	674
Cs	5.2	2.3	3.3	1.0	1.0
Sr	228	295	414	410	358
Pb	9	10	8	7	10
Th	1.0	0.9	0.8	0.6	0.5
U	2.2	0.1	1.9	0.5	2.2
Sc	32	29	20	28	24
V	192	222	169	181	237
Cr	933	291	308	678	675
Co	65	52	40	53	48
Ni	390	237	278	247	344
Y	18	25	15	14	20
Zr	89	133	93	84	104
Nb	3.5	4.4	3.5	3.1	4.3
Hf	2.4	3.4	2.0	2.2	2.1
Ta	0.16	0.30	0.12	0.13	0.16
La	13.3	18.8	10.3	12.9	10.9
Ce	30.2	44.2	23.6	29.3	26.5
Sm	3.4	4.9	3.0	3.4	3.6
Eu	1.01	1.72	0.93	1.03	1.01
Tb	0.54	0.67	0.46	0.50	0.50
Yb	1.57	1.97	1.07	1.44	1.35
Lu	0.24	0.31	0.16	0.23	0.22
Mg Number	65.06	53.10	62.38	63.80	59.61
K2O/Na2O	0.78	0.03	0.43	0.05	0.26
Na2O+K2O	4.04	5.97	4.04	5.42	4.57
Al2O3/TiO2	20.83	20.20	24.83	22.26	16.76

Dominion Group basaltic andesites

SAMPLE	BSF-3	BSF-5	BSF-6	BSF-8	BSF-12
CaO/TiO2	13.27	6.62	14.21	11.18	9.77
Zr/TiO2	0.01	0.02	0.02	0.01	0.01
K/Rb	185	192	215	291	186
Ba/Sr	3.40	0.17	1.15	0.35	1.88
Rb/Sr	0.35	0.02	0.11	0.02	0.12
La/Yb	8.50	9.55	9.66	8.92	8.09
La/Sm	3.97	3.85	3.51	3.76	3.06
Sm/Eu	3.33	2.84	3.17	3.32	3.53
Ti/Zr	44.35	37.72	39.05	44.64	48.12
Zr/Nb	25.51	30.33	26.47	27.19	24.07
Nb/Y	0.19	0.18	0.23	0.22	0.22
Zr/Y	4.95	5.41	6.11	5.93	5.20
Nb/Ta	21.88	14.67	29.17	23.85	26.88
Nb/La	0.26	0.23	0.34	0.24	0.39
La/Ta	83.38	62.70	86.17	98.85	68.25
La/Th	13.08	20.90	12.77	21.42	21.00
Y/Tb	33.43	36.85	32.98	28.44	39.80
Th/Yb	0.65	0.46	0.76	0.42	0.39
Ta/Yb	0.10	0.15	0.11	0.09	0.12
Hf/Th	2.37	3.77	2.41	3.62	3.94
Ti/V	20.66	22.63	21.42	20.84	21.06
U/Pb	0.24	0.01	0.24	0.08	0.22
Ce/Nb	8.63	10.05	6.74	9.45	6.16
Th/Ta	6.38	3.00	6.75	4.62	3.25
Th/Sc	0.03	0.03	0.04	0.02	0.02
Th/Nb	0.29	0.20	0.23	0.19	0.12
Sc/Ni	0.08	0.12	0.07	0.11	0.07
Hf/Ta	15.13	11.30	16.25	16.69	12.81
FeO-T/MgO	1.09	1.79	1.22	1.15	1.37
Sm/Yb	2.14	2.48	2.76	2.38	2.64
Eu/Eu*	0.9	1.1	1.0	0.9	0.9
g(x)	4.5	4.8	4.6	4.6	4.8
Score 1	1.1	1.1	1.7	1.7	1.3
Score 2	-0.1	-0.2	-0.1	-0.2	-0.1

Fe2O3-T ==> Total Fe as Fe2O3
NO ENTRY ==> No determination OR below detectability limi
MAJOR ELEMENTS ==> In weight percent
TRACE ELEMENTS ==> In parts per million

Dominion Group basaltic andesites

SAMPLE	BSF-14	BSF-15	BSF-17	BBS-2	BBS-4
SiO2	50.8	49.0	60.3	52.8	53.1
TiO2	0.84	0.80	0.86	1.00	0.99
Al2O3	13.0	13.6	14.2	14.3	14.1
Fe2O3-T	11.3	13.0	9.7	10.9	10.9
MgO	8.09	8.16	5.93	6.44	6.01
CaO	7.49	7.38	0.93	6.97	8.43
Na2O	3.56	3.96	2.91	3.74	3.70
K2O	0.98	0.51	1.36	0.96	0.86
MnO	0.17	0.19	0.13	0.14	0.15
P2O5	0.21	0.19	0.22	0.14	0.16
LOI	3.48	3.06	3.29	2.53	2.26
TOTAL	99.9	99.9	99.8	99.8	100.6
Rb	58	30	134	46	34
Ba	286	325	201	450	295
Cs	1.1	0.7	2.6	0.9	0.6
Sr	247	302	39	399	291
Pb	7	5	24	5	8
Th	0.7	0.9	3.6	1.2	4.1
U	0.8	1.1	7.9	0.8	0.1
Sc	20	25	27	17	20
V	227	231	271	189	181
Cr	653	739	719	270	295
Co	48	57	50	39	42
Ni	361	323	289	259	264
Y	20	18	34	19	18
Zr	96	102	104	115	117
Nb	3.9	3.7	4.3	4.7	5.2
Hf	1.8	2.1	2.6	2.5	2.6
Ta	0.13	0.16	0.15	0.30	0.27
La	9.2	9.8	12.5	10.2	10.4
Ce	22.5	24.4	32.8	23.4	25.7
Sm	3.4	3.5	4.9	3.1	3.1
Eu	0.78	0.87	1.66	0.93	0.96
Tb	0.46	0.51	0.72	0.50	0.46
Yb	1.18	1.38	2.48	1.13	1.37
Lu	0.18	0.21	0.39	0.18	0.22
Mg Number	61.58	58.46	57.90	57.11	55.34
K2O/Na2O	0.28	0.13	0.47	0.26	0.23
Na2O+K2O	4.54	4.47	4.27	4.70	4.56
Al2O3/TiO2	15.43	16.99	16.55	14.25	14.22

Dominion Group basaltic andesites

SAMPLE	BSF-14	BSF-15	BSF-17	BBS-2	BBS-4
CaO/TiO2	8.92	9.21	1.08	6.97	8.52
Zr/TiO2	0.01	0.01	0.01	0.01	0.01
K/Rb	140	141	84	173	210
Ba/Sr	1.16	1.08	5.18	1.13	1.01
Rb/Sr	0.23	0.10	3.45	0.12	0.12
La/Yb	7.78	7.07	5.02	9.06	7.61
La/Sm	2.71	2.83	2.55	3.29	3.36
Sm/Eu	4.35	3.97	2.94	3.34	3.23
Ti/Zr	52.39	47.35	49.47	52.17	50.77
Zr/Nb	24.67	27.43	24.26	24.47	22.50
Nb/Y	0.20	0.20	0.13	0.25	0.29
Zr/Y	4.81	5.61	3.05	6.18	6.50
Nb/Ta	30.00	23.13	28.67	15.67	19.26
Nb/La	0.42	0.38	0.35	0.46	0.50
La/Ta	70.62	60.94	83.00	34.13	38.63
La/Th	13.11	10.96	3.42	8.53	2.56
Y/Tb	43.48	35.49	47.56	37.20	39.13
Th/Yb	0.59	0.64	1.47	1.06	2.97
Ta/Yb	0.11	0.12	0.06	0.27	0.20
Hf/Th	2.56	2.38	0.71	2.06	0.64
Ti/V	22.21	20.81	19.04	31.75	32.82
U/Pb	0.11	0.23	0.32	0.16	0.01
Ce/Nb	5.77	6.59	7.63	4.98	4.94
Th/Ta	5.38	5.56	24.27	4.00	15.07
Th/Sc	0.04	0.04	0.13	0.07	0.20
Th/Nb	0.18	0.24	0.85	0.26	0.78
Sc/Ni	0.06	0.08	0.09	0.06	0.08
Hf/Ta	13.77	13.25	17.20	8.23	9.63
FeO-T/MgO	1.26	1.44	1.47	1.52	1.63
Sm/Yb	2.87	2.50	1.97	2.75	2.26
Eu/Eu*	0.7	0.8	1.0	0.9	0.9
g(x)	4.6	4.7	4.3	4.8	4.8
Score 1	1.0	1.2	-0.8	1.4	1.1
Score 2	-0.2	-0.2	-0.1	-0.3	-0.4

Fe2O3-T ==> Total Fe as Fe2O3
NO ENTRY ==> No determination OR below detectability limi
MAJOR ELEMENTS ==> In weight percent
TRACE ELEMENTS ==> In parts per million

Dominion Group basaltic andesites

SAMPLE	BBS-5	BBS-8	BBS-9	BBS-16	BBS-18
SiO_2	53.7	54.8	53.9	52.8	62.6
TiO_2	1.01	1.01	0.54	0.83	0.57
Al_2O_3	13.8	13.6	15.3	14.2	16.0
Fe_2O_3-T	11.1	11.2	9.2	11.6	5.3
MgO	6.47	6.65	7.94	7.39	3.93
CaO	6.93	6.22	5.05	5.71	0.63
Na_2O	3.72	3.84	4.99	5.00	3.87
K_2O	1.11	0.91	1.13	0.61	4.47
MnO	0.15	0.15	0.15	0.18	0.08
P_2O_5	0.15	0.15	0.13	0.20	0.11
LOI	2.34	2.29	2.43	2.34	2.05
TOTAL	100.4	100.8	100.6	100.7	99.6
Rb	47	40	50	24	185
Ba	570	442	490	362	1712
Cs	0.9	0.7	1.1	0.6	2.2
Sr	213	329	236	203	124
Pb	9	9	11	21	440
Th	4.0	3.2	2.1	0.6	11.2
U	2.2	1.1	1.9	0.5	0.3
Sc	25	19	23	23	19
V	189	183	187	247	172
Cr	366	281	556	636	409
Co	53	43	47	43	25
Ni	274	234	276	202	182
Y	20	18	15	21	38
Zr	117	115	82	103	104
Nb	5.0	5.0	3.5	3.7	5.3
Hf	3.4	2.5	1.9	2.0	2.7
Ta	0.35	0.26	0.17	0.16	0.63
La	11.5	10.8	8.3	10.2	21.1
Ce	29.4	25.4	20.0	25.9	45.7
Sm	3.5	3.2	2.6	3.5	4.6
Eu	1.18	0.92	0.58	1.02	1.06
Tb	0.64	0.53	0.37	0.52	0.63
Yb	1.71	1.38	1.08	1.33	2.34
Lu	0.27	0.22	0.17	0.20	0.37
Mg Number	56.62	57.09	66.10	58.96	62.67
K_2O/Na_2O	0.30	0.24	0.23	0.12	1.16
Na_2O+K_2O	4.83	4.75	6.12	5.61	8.34
Al_2O_3/TiO_2	13.62	13.43	28.26	17.05	28.09

Dominion Group basaltic andesites

SAMPLE	BBS-5	BBS-8	BBS-9	BBS-16	BBS-18
CaO/TiO2	6.86	6.16	9.35	6.88	1.11
Zr/TiO2	0.01	0.01	0.02	0.01	0.02
K/Rb	196	189	188	215	201
Ba/Sr	2.68	1.34	2.08	1.78	13.81
Rb/Sr	0.22	0.12	0.21	0.12	1.49
La/Yb	6.73	7.83	7.69	7.65	9.02
La/Sm	3.30	3.38	3.20	2.95	4.62
Sm/Eu	2.96	3.48	4.47	3.38	4.31
Ti/Zr	51.79	52.70	39.75	48.54	32.88
Zr/Nb	23.40	23.00	23.29	27.73	19.62
Nb/Y	0.25	0.28	0.23	0.18	0.14
Zr/Y	5.82	6.39	5.43	4.89	2.74
Nb/Ta	14.29	19.23	20.59	23.13	8.41
Nb/La	0.43	0.46	0.42	0.36	0.25
La/Ta	32.86	41.54	48.82	63.63	33.49
La/Th	2.88	3.38	4.03	17.86	1.88
Y/Tb	31.41	33.96	40.54	40.38	60.32
Th/Yb	2.34	2.32	1.91	0.43	4.80
Ta/Yb	0.20	0.19	0.16	0.12	0.27
Hf/Th	0.84	0.77	0.90	3.53	0.24
Ti/V	32.06	33.11	17.33	20.16	19.88
U/Pb	0.25	0.12	0.16	0.02	.00
Ce/Nb	5.88	5.08	5.71	7.00	8.62
Th/Ta	11.43	12.31	12.12	3.56	17.84
Th/Sc	0.16	0.17	0.09	0.02	0.59
Th/Nb	0.80	0.64	0.59	0.15	2.12
Sc/Ni	0.09	0.08	0.08	0.11	0.10
Hf/Ta	9.63	9.50	10.94	12.56	4.32
FeO-T/MgO	1.55	1.52	1.04	1.41	1.20
Sm/Yb	2.04	2.32	2.40	2.59	1.95
Eu/Eu*	1.0	0.9	0.7	0.9	0.7
g(x)	4.7	4.8	4.4	4.6	4.6
Score 1	0.8	1.2	1.3	0.8	0.3
Score 2	-0.3	-0.3	-0.1	-0.2	0.3

Fe2O3-T ==> Total Fe as Fe2O3
NO ENTRY ==> No determination OR below detectability limi
MAJOR ELEMENTS ==> In weight percent
TRACE ELEMENTS ==> In parts per million

Dominion Group basaltic andesites

SAMPLE	AVG	STD
SiO2	53.0	2.6
TiO2	0.7	0.1
Al2O3	14.4	1.3
Fe2O3-T	10.8	1.1
MgO	7.4	1.1
CaO	6.3	2.6
Na2O	3.8	1.2
K2O	0.7	0.5
MnO	0.1	.0
P2O5	0.2	0.1
LOI	3.0	0.7
TOTAL	100.3	0.5
Rb	32.4	29.4
Ba	292	218
Cs	1.5	1.1
Sr	269	110
Pb	10.1	4.2
Th	1.8	1.2
U	1.6	1.5
Sc	24.3	4.3
V	203	28
Cr	585	196
Co	48	9
Ni	290	50
Y	18.5	4.3
Zr	98.3	13.5
Nb	3.9	0.6
Hf	2.3	0.5
Ta	0.2	0.1
La	11.3	2.7
Ce	26.9	5.8
Sm	3.4	0.6
Eu	1.0	0.3
Tb	0.5	0.1
Yb	1.5	0.4
Lu	0.2	0.1
Mg Number	60.4	3.8
K2O/Na2O	0.2	0.2
Na2O+K2O	4.5	1.1
Al2O3/TiO2	20.0	4.2

Dominion Group basaltic andesites

SAMPLE	AVG	STD
CaO/TiO2	8.7	4.1
Zr/TiO2	.0	.0
K/Rb	257	232
Ba/Sr	1.2	1.2
Rb/Sr	0.2	0.7
La/Yb	7.9	1.6
La/Sm	3.4	0.6
Sm/Eu	3.5	0.5
Ti/Zr	45.4	4.5
Zr/Nb	25.1	2.6
Nb/Y	0.2	.0
Zr/Y	5.5	0.8
Nb/Ta	23.9	5.9
Nb/La	0.4	0.1
La/Ta	69.3	23.2
La/Th	10.3	6.7
Y/Tb	37.0	4.9
Th/Yb	1.2	0.7
Ta/Yb	0.1	.0
Hf/Th	2.0	1.2
Ti/V	22.3	4.7
U/Pb	0.2	0.1
Ce/Nb	6.9	1.5
Th/Ta	9.9	6.1
Th/Sc	0.1	0.1
Th/Nb	0.4	0.3
Sc/Ni	0.1	.0
Hf/Ta	13.6	2.8
FeO-T/MgO	1.3	0.2
Sm/Yb	2.4	0.3
Eu/Eu*	0.9	0.1
g(x)	4.6	0.2
Score 1	1.1	0.6
Score 2	-0.2	0.1

Fe2O3-T ==> Total Fe as Fe2O3
NO ENTRY ==> No determination OR below detectability limi
MAJOR ELEMENTS ==> In weight percent
TRACE ELEMENTS ==> In parts per million

Dominion Group andesites

SAMPLE	BTF-2	BSF-2	BSF-9	BSF-10	BSF-11
SiO_2	58.4	52.8	54.4	55.3	53.2
TiO_2	1.22	1.13	1.15	1.19	1.18
Al_2O_3	13.7	14.0	14.5	15.6	14.8
Fe_2O_3-T	12.4	12.5	11.5	12.0	11.9
MgO	4.56	3.45	4.92	4.23	5.18
CaO	2.26	5.45	6.33	3.39	5.90
Na_2O	3.69	3.93	4.34	4.96	4.23
K_2O	0.21	0.59	0.53	0.27	1.22
MnO	0.12	0.16	0.17	0.12	0.17
P_2O_5	0.30	0.26	0.36	0.37	0.37
LOI	3.59	5.26	1.93	3.18	2.13
TOTAL	100.5	99.5	100.0	100.6	100.3
Rb	7	33	17	10	48
Ba	60	198	505	99	770
Cs	0.8	1.8	1.0	2.8	1.2
Sr	90	246	570	305	503
Pb	10	13	10	11	7
Th	3.6	4.4	1.0	0.5	0.4
U	2.1	3.1	3.2	0.6	0.4
Sc	20	26	22	33	19
V	353	322	249	279	262
Cr	3	10	25	41	22
Co	36	50	44	60	39
Ni	49	24	98	110	119
Y	28	28	25	23	26
Zr	204	193	182	182	188
Nb	6.0	5.0	6.3	5.7	6.3
Hf	4.3	4.9	4.3	6.0	3.6
Ta	0.30	0.28	0.26	0.34	0.28
La	20.4	29.5	22.7	34.1	19.4
Ce	46.2	66.5	54.3	80.3	47.3
Sm	5.2	6.2	6.5	8.5	5.9
Eu	1.13	1.97	2.04	2.67	1.54
Tb	0.77	0.77	0.83	1.12	0.80
Yb	1.80	2.35	2.21	2.91	1.70
Lu	0.28	0.35	0.33	0.42	0.27
Mg Number	45.21	38.26	49.04	44.24	49.35
K_2O/Na_2O	0.06	0.15	0.12	0.05	0.29
Na_2O+K_2O	3.90	4.52	4.87	5.23	5.45
Al_2O_3/TiO_2	11.25	12.35	12.57	13.08	12.47

Dominion Group andesites

SAMPLE	BTF-2	BSF-2	BSF-9	BSF-10	BSF-11
CaO/TiO2	1.85	4.82	5.50	2.84	4.98
Zr/TiO2	0.02	0.02	0.02	0.02	0.02
K/Rb	252.61	148.39	253.38	221.95	212.72
Ba/Sr	0.67	0.80	0.89	0.33	1.53
Rb/Sr	0.08	0.13	0.03	0.03	0.09
La/Yb	11.33	12.55	10.27	11.72	11.41
La/Sm	3.93	4.74	3.48	4.03	3.31
Sm/Eu	4.59	3.16	3.20	3.17	3.81
Ti/Zr	35.88	35.13	37.82	39.23	37.66
Zr/Nb	34.00	38.60	28.96	31.99	29.92
Nb/Y	0.21	0.18	0.25	0.25	0.24
Zr/Y	7.29	6.89	7.26	8.02	7.24
Nb/Ta	20.00	17.86	24.23	16.76	22.50
Nb/La	0.29	0.17	0.28	0.17	0.32
La/Ta	68.00	105.36	87.27	100.29	69.29
La/Th	5.65	6.78	23.39	68.20	48.50
Y/Tb	36.36	36.36	30.27	20.29	32.53
Th/Yb	2.01	1.85	0.44	0.17	0.24
Ta/Yb	0.17	0.12	0.12	0.12	0.16
Hf/Th	1.20	1.13	4.41	12.06	9.08
Ti/V	20.74	21.06	27.70	25.66	27.07
U/Pb	0.21	0.24	0.31	0.06	0.06
Ce/Nb	7.70	13.30	8.62	14.09	7.51
Th/Ta	12.03	15.54	3.73	1.47	1.43
Th/Sc	0.18	0.17	0.04	0.02	0.02
Th/Nb	0.60	0.87	0.15	0.09	0.06
Sc/Ni	0.42	1.08	0.22	0.30	0.16
Hf/Ta	14.40	17.57	16.46	17.74	12.96
FeO-T/MgO	2.45	3.26	2.10	2.55	2.08
Sm/Yb	2.88	2.65	2.95	2.91	3.45
Eu/Eu*	0.7	1.0	1.0	1.0	0.8
g(x)	4.8	5.0	5.2	5.0	5.1
Score 1	-0.1	0.7	1.5	1.0	1.3
Score 2	-0.6	-0.4	-0.3	-0.5	-0.3

Fe2O3-T ==> Total Fe as Fe2O3
NO ENTRY ==> No determination OR below detectability limi
MAJOR ELEMENTS ==> In weight percent
TRACE ELEMENTS ==> In parts per million

Dominion Group andesites

SAMPLE	BBS-11	BBS-13	AVG	STD	D-4
SiO2	61.5	52.8	55.5	3.1	75.2
TiO2	1.05	1.23	1.2	0.1	0.52
Al2O3	13.3	15.0	14.4	0.7	12.1
Fe2O3-T	8.5	12.5	11.6	1.3	4.6
MgO	3.49	5.87	4.5	0.8	0.84
CaO	4.13	3.43	4.4	1.4	0.53
Na2O	3.75	3.94	4.1	0.4	5.22
K2O	0.75	1.22	0.7	0.4	0.99
MnO	0.11	0.17	0.1	.0	0.05
P2O5	0.32	0.38	0.3	.0	0.14
LOI	3.14	3.24	3.2	1.0	1.00
TOTAL	99.9	99.8	100.1	0.4	101.2
Rb	30	47	27.3	15.4	35
Ba	335	879	406.5	299.5	216
Cs	0.7	1.0	1.3	0.7	0.6
Sr	458	241	344.6	158.4	129
Pb	11	34	13.7	8.6	13
Th	0.3	0.5	1.5	1.6	8.9
U	2.1	0.4	1.7	1.1	0.1
Sc	16	26	23.2	5.4	7
V	222	264	278.7	41.5	
Cr	18	30	21.3	11.8	2
Co	27	62	45.4	11.6	5
Ni	95	94	84.1	31.9	3
Y	29	29	26.9	2.2	28
Zr	166	196	187.5	11.3	223
Nb	4.9	6.2	5.8	0.6	11.0
Hf	2.9	5.0	4.4	0.9	7.0
Ta	0.24	0.34	0.3	.0	0.84
La	16.7	29.4	24.6	6.0	29.0
Ce	39.5	66.6	57.2	13.4	58.0
Sm	5.3	7.5	6.4	1.1	4.6
Eu	1.45	2.11	1.8	0.5	0.97
Tb	0.71	0.98	0.9	0.1	0.71
Yb	1.34	2.61	2.1	0.5	2.20
Lu	0.21	0.38	0.3	0.1	0.33
Mg Number	48.10	51.26	46.5	4.0	29.10
K2O/Na2O	0.20	0.31	0.2	0.1	0.19
Na2O+K2O	4.50	5.16	4.8	0.5	6.21
Al2O3/TiO2	12.67	12.21	12.4	0.5	23.27

Dominion Group andesites

SAMPLE	BBS-11	BBS-13	AVG	STD	D-4
CaO/TiO2	3.94	2.79	3.8	1.3	1.02
Zr/TiO2	0.02	0.02	.0	.0	0.04
K/Rb	209.60	215.81	216.4	32.5	234.77
Ba/Sr	0.73	3.65	1.2	1.0	1.67
Rb/Sr	0.06	0.20	0.1	0.1	0.27
La/Yb	12.45	11.25	11.6	0.7	13.18
La/Sm	3.14	3.90	3.8	0.5	6.30
Sm/Eu	3.67	3.56	3.6	0.5	4.74
Ti/Zr	37.89	37.66	37.3	1.3	13.99
Zr/Nb	33.87	31.61	32.7	3.0	20.27
Nb/Y	0.17	0.22	0.2	.0	0.39
Zr/Y	5.64	6.83	7.0	0.7	7.96
Nb/Ta	20.42	18.24	20.0	2.5	13.10
Nb/La	0.29	0.21	0.2	0.1	0.38
La/Ta	69.50	86.35	83.7	14.2	34.52
La/Th	66.72	58.72	39.7	25.3	3.26
Y/Tb	41.41	29.30	32.4	6.3	39.44
Th/Yb	0.19	0.19	0.7	0.8	4.05
Ta/Yb	0.18	0.13	0.1	.0	0.38
Hf/Th	11.72	9.96	7.1	4.4	0.79
Ti/V	28.39	27.95	25.5	3.0	ERR
U/Pb	0.20	0.01	0.2	0.1	0.01
Ce/Nb	8.06	10.74	10.0	2.5	5.27
Th/Ta	1.04	1.47	5.2	5.5	10.60
Th/Sc	0.02	0.02	0.1	0.1	1.33
Th/Nb	0.05	0.08	0.3	0.3	0.81
Sc/Ni	0.16	0.28	0.4	0.3	2.23
Hf/Ta	12.21	14.65	15.1	2.0	8.33
FeO-T/MgO	2.18	1.92	2.4	0.4	4.93
Sm/Yb	3.97	2.88	3.1	0.4	2.09
Eu/Eu*	0.9	0.9	0.9	0.1	0.6
g(x)	5.1	5.0	5.0	0.1	4.7
Score 1	1.3	0.7	0.9	0.5	0.5
Score 2	-0.2	-0.4	-0.4	0.1	-0.3

Fe2O3-T ==> Total Fe as Fe2O3
NO ENTRY ==> No determination OR below detectability limi
MAJOR ELEMENTS ==> In weight percent
TRACE ELEMENTS ==> In parts per million

Dominion Group andesites

SAMPLE	BTF-12	BTF-14
SiO2	51.9	52.5
TiO2	0.86	0.80
Al2O3	26.0	22.9
Fe2O3-T	2.8	4.9
MgO	2.96	2.63
CaO	2.34	8.26
Na2O	0.22	1.00
K2O	8.18	3.42
MnO	0.03	0.05
P2O5	0.11	0.09
LOI	4.22	3.16
TOTAL	99.6	99.7
Rb	453	196
Ba	2268	970
Cs	25.4	14.1
Sr	124	911
Pb	15	8
Th	14.0	5.2
U	4.2	1.9
Sc	19	21
V	188	157
Cr	330	385
Co	19	23
Ni	174	162
Y	53	36
Zr	164	156
Nb	12.1	12.7
Hf	3.9	4.5
Ta	1.23	1.31
La	41.8	53.0
Ce	93.6	114.6
Sm	8.2	8.1
Eu	1.10	3.12
Tb	1.06	1.05
Yb	3.02	3.45
Lu	0.46	0.48
Mg Number	70.45	54.72
K2O/Na2O	37.18	3.42
Na2O+K2O	8.40	4.42
Al2O3/TiO2	30.19	28.68

Dominion Group andesites

SAMPLE	BTF-12	BTF-14
CaO/TiO2	2.72	10.33
Zr/TiO2	0.02	0.02
K/Rb	149.88	144.83
Ba/Sr	18.29	1.06
Rb/Sr	3.65	0.22
La/Yb	13.84	15.36
La/Sm	5.10	6.54
Sm/Eu	7.45	2.60
Ti/Zr	31.46	30.77
Zr/Nb	13.55	12.28
Nb/Y	0.23	0.35
Zr/Y	3.09	4.33
Nb/Ta	9.84	9.69
Nb/La	0.29	0.24
La/Ta	33.98	40.46
La/Th	2.99	10.19
Y/Tb	50.00	34.29
Th/Yb	4.64	1.51
Ta/Yb	0.41	0.38
Hf/Th	0.28	0.87
Ti/V	27.45	30.57
U/Pb	0.28	0.24
Ce/Nb	7.74	9.02
Th/Ta	11.38	3.97
Th/Sc	0.74	0.25
Th/Nb	1.16	0.41
Sc/Ni	0.11	0.13
Hf/Ta	3.17	3.44
FeO-T/MgO	0.85	1.67
Sm/Yb	2.72	2.35
Eu/Eu*	0.4	1.2
g(x)	4.9	5.2
Score 1	.0	1.9
Score 2	0.2	0.2

Fe2O3-T ==> Total Fe as Fe2O3
NO ENTRY ==> No determination OR below detectability limi
MAJOR ELEMENTS ==> In weight percent
TRACE ELEMENTS ==> In parts per million

Allanridge Formation, Pniel Group, Ventersdorp Supergroup

SAMPLE	J1A	J2A	J3A	J4A	J5A
SiO2	50.5	58.9	58.7	56.8	60.7
TiO2	1.52	1.13	1.11	0.65	1.12
Al2O3	14.8	13.9	13.9	14.6	13.8
Fe2O3-T	13.2	9.1	9.2	9.0	10.7
MgO	6.02	1.87	1.86	4.74	3.48
CaO	4.2	4.55	4.5	5.68	2.39
Na2O	3.74	4.88	4.92	3.35	2.86
K2O	0.3	1.62	1.63	1.49	2.45
MnO	0.17	0.09	0.09	0.11	0.11
P2O5	0.7	0.2	0.21	0.11	0.2
LOI	4.91	4.09	3.98	3.66	3.14
TOTAL	100.0	100.3	100.1	100.2	100.9
Rb	14.4	37.4	43.5	63.1	43.1
Ba	204	604	739	296	884
Cs	0.2	0.6	1.1	1.1	0.4
Sr	458	664	859	204	105
Pb	10.1	13.4	8.3	10.7	10.2
Th	3.3	4.5	3.4	3.5	3.0
U	1.1	1.1	1.0	1.0	0.8
Sc	17.3	17.1	16.2	16.1	13.4
V	196	165	155	232	173
Cr	15	12	12	11	9
Co	56	53	54	50	43
Ni	125	97	90	107	81
Y	25.2	22.7	22.5	25.2	20.8
Zr	197.3	186.8	181.6	194.0	165.8
Nb	11.9	10.2	10.0	13.0	10.2
Hf	5.2	5.6	5.1	5.3	4.5
Ta	0.72	0.75	0.67	0.78	0.64
La	27.9	29.6	29.8	22.9	23.4
Ce	65.3	65.5	63.2	56.3	53.8
Sm	6.90	6.51	6.13	6.33	5.37
Eu	1.98	2.08	1.94	2.12	1.23
Tb	1.00	0.92	0.79	0.89	0.81
Yb	2.33	2.53	2.30	2.12	1.97
Lu	0.34	0.36	0.32	0.35	0.29
Mg Number	50.7	31.5	31.3	54.1	42.2
K2O/Na2O	0.08	0.33	0.33	0.44	0.86
Na2O+K2O	4.04	6.50	6.55	4.84	5.31
Al2O3/TiO2	9.7	12.3	12.6	22.4	12.3

Allanridge Formation, Pniel Group, Ventersdorp Supergroup

SAMPLE	J1A	J2A	J3A	J4A	J5A
CaO/TiO2	2.8	4.0	4.1	8.7	2.1
Zr/TiO2	0.013	0.017	0.016	0.030	0.015
K/Rb	172.9	359.5	311.0	196.0	471.8
Ba/Sr	0.45	0.91	0.86	1.45	8.42
Rb/Sr	0.031	0.056	0.051	0.310	0.410
La/Yb	12.0	11.7	13.0	10.8	11.9
La/Sm	4.0	4.5	4.9	3.6	4.4
Sm/Eu	3.5	3.1	3.2	3.0	4.4
Ti/Zr	46.2	36.3	36.7	20.1	40.5
Zr/Nb	16.6	18.3	18.2	14.9	16.3
Nb/Y	0.47	0.45	0.44	0.52	0.49
Zr/Y	7.8	8.2	8.1	7.7	8.0
Nb/Ta	16.5	13.6	14.9	16.7	15.9
Nb/La	0.43	0.34	0.34	0.57	0.44
La/Ta	38.8	39.5	44.5	29.4	36.6
La/Th	8.5	6.6	8.8	6.5	7.8
Y/Tb	25.2	24.7	28.5	28.3	25.7
Th/Yb	1.42	1.78	1.48	1.65	1.52
Ta/Yb	0.309	0.296	0.291	0.368	0.325
Hf/Th	1.58	1.24	1.50	1.51	1.50
Ti/V	46.5	41.0	43.1	16.8	38.9
U/Pb	0.11	0.08	0.12	0.09	0.08
Ce/Nb	5.49	6.42	6.32	4.33	5.27
Th/Ta	4.58	6.00	5.07	4.49	4.69
Th/Sc	0.19	0.26	0.21	0.22	0.22
Th/Nb	0.28	0.44	0.34	0.27	0.29
Sc/Ni	0.14	0.18	0.18	0.15	0.17
Hf/Ta	7.22	7.47	7.61	6.79	7.03
FeO-T/MgO	1.97	4.39	4.44	1.71	2.76
Sm/Yb	2.96	2.57	2.67	2.99	2.73
Eu/Eu*	0.88	0.99	1.00	1.04	0.70
g(x)	5.19	5.17	5.22	4.77	4.65
Score 1	1.18	1.65	1.88	0.82	0.15
Score 2	-0.49	-0.38	-0.32	-0.32	-0.66

Fe2O3-T ==> Total Fe as Fe2O3
NO ENTRY ==> No determination OR below detectability limi
MAJOR ELEMENTS ==> In weight percent
TRACE ELEMENTS ==> In parts per million

Allanridge Formation, Pniel Group, Ventersdorp Supergroup

SAMPLE	J6A	J7A	J8A	C5A	AVG
SiO2	51.4	57.3	50.2	54.7	55.5
TiO2	1.64	1.14	1.12	1.13	1.17
Al2O3	15.4	14.0	13.7	13.2	14.1
Fe2O3-T	10.1	10.0	6.3	10.3	9.8
MgO	5.94	3.39	2.46	4.7	3.83
CaO	4.65	5.6	11.64	6.22	5.49
Na2O	4.79	4.78	0.24	4.05	3.73
K2O	0.6	1.11	3.18	1.1	1.50
MnO	0.11	0.11	0.14	0.13	0.12
P2O5	0.84	0.19	0.2	0.21	0.32
LOI	4.92	2.39	11.54	4.47	4.79
TOTAL	100.4	100.0	100.7	100.1	100.3
Rb	25.1	26.2	121.8	22.5	44.12
Ba	532	463	401	5	459
Cs	0.9	17.5	2.5	0.6	2.77
Sr	410	958	225	534	491
Pb	10.5	11.0	13.9	13.0	11.23
Th	3.1	3.1	3.2	3.0	3.34
U	0.8	0.9	0.9	0.8	0.9
Sc	13.7	14.0	13.8	15.9	15.28
V	165	150	165	180	176
Cr	9	10	9	47	15
Co	47	46	44	48	49
Ni	94	98	82	117	99
Y	21.2	21.8	26.5	21.0	22.99
Zr	175.0	189.6	173.6	180.0	182.63
Nb	9.1	10.1	10.3	10.8	10.62
Hf	4.5	4.6	4.8	4.6	4.91
Ta	0.64	0.64	0.66	0.69	0.69
La	24.4	26.2	27.2	25.2	26.29
Ce	52.8	55.2	58.7	55.6	58.49
Sm	5.85	5.89	6.02	5.61	6.07
Eu	1.61	1.73	1.68	1.62	1.78
Tb	0.77	0.78	0.82	0.75	0.84
Yb	1.85	1.88	1.92	1.85	2.08
Lu	0.30	0.29	0.30	0.29	0.32
Mg Number	56.9	43.2	46.8	50.7	45.28
K2O/Na2O	0.13	0.23	13.25	0.27	1.77
Na2O+K2O	5.39	5.89	3.42	5.15	5.23
Al2O3/TiO2	9.4	12.3	12.2	11.7	12.76

Allanridge Formation, Pniel Group, Ventersdorp Supergroup

SAMPLE	J6A	J7A	J8A	C5A	AVG
CaO/TiO2	2.8	4.9	10.4	5.5	5.04
Zr/TiO2	0.011	0.017	0.015	0.016	0.02
K/Rb	198.4	351.6	216.7	405.8	298.20
Ba/Sr	1.30	0.48	1.78	0.01	1.74
Rb/Sr	0.061	0.027	0.541	0.042	0.17
La/Yb	13.2	13.9	14.2	13.6	12.69
La/Sm	4.2	4.4	4.5	4.5	4.34
Sm/Eu	3.6	3.4	3.6	3.5	3.47
Ti/Zr	56.2	36.1	38.7	37.7	38.72
Zr/Nb	19.2	18.8	16.9	16.7	17.31
Nb/Y	0.43	0.46	0.39	0.51	0.46
Zr/Y	8.3	8.7	6.6	8.6	7.99
Nb/Ta	14.2	15.8	15.6	15.7	15.44
Nb/La	0.37	0.39	0.38	0.43	0.41
La/Ta	38.1	40.9	41.2	36.5	38.38
La/Th	7.9	8.5	8.5	8.4	7.93
Y/Tb	27.5	27.9	32.3	28.0	27.57
Th/Yb	1.68	1.65	1.67	1.62	1.61
Ta/Yb	0.346	0.340	0.344	0.373	0.33
Hf/Th	1.45	1.48	1.50	1.53	1.48
Ti/V	59.8	45.6	40.7	37.7	41.11
U/Pb	0.08	0.08	0.06	0.06	0.09
Ce/Nb	5.80	5.47	5.70	5.15	5.55
Th/Ta	4.84	4.84	4.85	4.35	4.86
Th/Sc	0.23	0.22	0.23	0.19	0.22
Th/Nb	0.34	0.31	0.31	0.28	0.32
Sc/Ni	0.15	0.14	0.17	0.14	0.16
Hf/Ta	7.03	7.19	7.27	6.67	7.14
FeO-T/MgO	1.53	2.66	2.30	1.97	2.64
Sm/Yb	3.16	3.13	3.14	3.03	2.93
Eu/Eu*	0.86	0.92	0.87	0.90	0.91
g(x)	5.11	5.26	4.92	5.09	5.04
Score 1	1.14	1.97	0.69	1.50	1.22
Score 2	-0.59	-0.36	-0.39	-0.45	-0.44

Fe2O3-T ==> Total Fe as Fe2O3
NO ENTRY ==> No determination OR below detectability limi
MAJOR ELEMENTS ==> In weight percent
TRACE ELEMENTS ==> In parts per million

Allanridge Formation, Pniel Group, Ventersdorp Supergroup

SAMPLE	STD
SiO2	3.7
TiO2	0.26
Al2O3	0.6
Fe2O3-T	1.7
MgO	1.52
CaO	2.41
Na2O	1.42
K2O	0.84
MnO	0.02
P2O5	0.25
LOI	2.51
TOTAL	0.3
Rb	30.69
Ba	255
Cs	5.25
Sr	278
Pb	1.72
Th	0.44
U	0.1
Sc	1.46
V	24
Cr	12
Co	4
Ni	14
Y	1.99
Zr	9.67
Nb	1.09
Hf	0.38
Ta	0.05
La	2.39
Ce	4.67
Sm	0.44
Eu	0.27
Tb	0.08
Yb	0.24
Lu	0.03
Mg Number	8.65
K2O/Na2O	4.06
Na2O+K2O	0.98
Al2O3/TiO2	3.59

Allanridge Formation, Pniel Group, Ventersdorp Supergroup

SAMPLE	STD
CaO/TiO2	2.65
Zr/TiO2	0.01
K/Rb	100.68
Ba/Sr	2.42
Rb/Sr	0.19
La/Yb	1.09
La/Sm	0.34
Sm/Eu	0.38
Ti/Zr	9.01
Zr/Nb	1.31
Nb/Y	0.04
Zr/Y	0.59
Nb/Ta	0.96
Nb/La	0.07
La/Ta	3.96
La/Th	0.79
Y/Tb	2.16
Th/Yb	0.11
Ta/Yb	0.03
Hf/Th	0.09
Ti/V	10.59
U/Pb	0.02
Ce/Nb	0.59
Th/Ta	0.45
Th/Sc	0.02
Th/Nb	0.05
Sc/Ni	0.02
Hf/Ta	0.28
FeO-T/MgO	1.02
Sm/Yb	0.21
Eu/Eu*	0.09
g(x)	0.20
Score 1	0.56
Score 2	0.11

Fe2O3-T ==> Total Fe as Fe2O3
NO ENTRY ==> No determination OR below detectability limi
MAJOR ELEMENTS ==> In weight percent
TRACE ELEMENTS ==> In parts per million

Rietgat Fm, Platberg Group, Ventersdorp Supergroup

SAMPLE	J13R	J14R	J15R	J16R	J17R
SiO2	53.0	50.9	50.8	54.6	54.4
TiO2	1.26	1.66	1.53	1.28	1.14
Al2O3	13.8	14.4	14.9	15.1	13.1
Fe2O3-T	7.2	10.0	12.9	12.4	10.2
MgO	2.95	4.18	6.08	3.91	4.75
CaO	8.49	6.88	4.23	3.32	6
Na2O	2.6	4.89	3.91	3.29	3.9
K2O	1.84	0.8	0.3	1.31	1.17
MnO	0.12	0.12	0.17	0.12	0.13
P2O5	0.57	0.77	0.67	0.22	0.2
LOI	8.25	6.13	4.47	4.55	5.8
TOTAL	100.0	100.8	100.0	100.0	100.8
Rb	58.0	39.6	3.6	11.6	15.3
Ba	520	401	459	557	392
Cs	1.7	1.1	0.7	0.4	2.0
Sr	283	389	985	510	418
Pb	11.7	13.0	28.3	9.2	9.9
Th	2.7	2.7	2.4	2.4	1.7
U	0.6	0.5	0.5	0.4	0.4
Sc	18.0	18.3	25.1	22.5	18.5
V	187	177	237	193	216
Cr	193	207	246	183	165
Co	27	27	43	33	29
Ni	88	79	118	96	91
Y	47.3	40.3	51.4	54.5	48.8
Zr	331.1	335.3	375.8	418.3	345.2
Nb	16.5	16.9	18.4	19.4	17.1
Hf	8.3	8.2	9.2	9.8	7.2
Ta	0.72	0.73	0.83	0.99	0.76
La	61.1	50.3	79.2	62.6	59.1
Ce	129.6	113.8	176.6	146.8	127.1
Sm	11.65	11.19	15.88	14.99	12.15
Eu	2.39	2.25	4.42	3.50	2.95
Tb	1.42	1.33	1.95	1.87	1.55
Yb	3.79	3.42	5.11	4.90	3.91
Lu	0.58	0.51	0.75	0.75	0.57
Mg Number	48.0	48.3	51.4	41.6	51.1
K2O/Na2O	0.71	0.16	0.08	0.40	0.30
Na2O+K2O	4.44	5.69	4.21	4.60	5.07
Al2O3/TiO2	10.9	8.7	9.8	11.8	11.5

Rietgat Fm, Platberg Group, Ventersdorp Supergroup

SAMPLE	J13R	J14R	J15R	J16R	J17R
CaO/TiO2	6.7	4.1	2.8	2.6	5.3
Zr/TiO2	0.026	0.020	0.025	0.033	0.030
K/Rb	263.3	167.7	691.7	937.3	634.7
Ba/Sr	1.83	1.03	0.47	1.09	0.94
Rb/Sr	0.205	0.102	0.004	0.023	0.037
La/Yb	16.1	14.7	15.5	12.8	15.1
La/Sm	5.2	4.5	5.0	4.2	4.9
Sm/Eu	4.9	5.0	3.6	4.3	4.1
Ti/Zr	22.8	29.7	24.4	18.4	19.8
Zr/Nb	20.1	19.8	20.4	21.6	20.2
Nb/Y	0.35	0.42	0.36	0.36	0.35
Zr/Y	7.0	8.3	7.3	7.7	7.1
Nb/Ta	22.9	23.2	22.2	19.6	22.5
Nb/La	0.27	0.34	0.23	0.31	0.29
La/Ta	84.9	68.9	95.4	63.2	77.8
La/Th	22.6	18.6	33.0	26.1	34.8
Y/Tb	33.3	30.3	26.4	29.1	31.5
Th/Yb	0.71	0.79	0.47	0.49	0.43
Ta/Yb	0.190	0.213	0.162	0.202	0.194
Hf/Th	3.07	3.04	3.83	4.08	4.24
Ti/V	40.4	56.2	38.8	39.8	31.6
U/Pb	0.05	0.04	0.02	0.04	0.04
Ce/Nb	7.85	6.73	9.60	7.57	7.43
Th/Ta	3.75	3.70	2.89	2.42	2.24
Th/Sc	0.15	0.15	0.10	0.11	0.09
Th/Nb	0.16	0.16	0.13	0.12	0.10
Sc/Ni	0.20	0.23	0.21	0.23	0.20
Hf/Ta	11.53	11.23	11.08	9.90	9.47
FeO-T/MgO	2.19	2.16	1.91	2.85	1.93
Sm/Yb	3.07	3.27	3.11	3.06	3.11
Eu/Eu*	0.6537	0.643828	0.885761	0.740784	0.766959
g(x)	5.3101	5.421324	5.722622	5.554667	5.400357
Score 1	0.5658	0.791320	1.494117	0.978593	0.912118
Score 2	-0.325	-0.49369	-0.20308	-0.26380	-0.23026

Fe2O3-T ==> Total Fe as Fe2O3
NO ENTRY ==> No determination OR below detectability limi
MAJOR ELEMENTS ==> In weight percent
TRACE ELEMENTS ==> In parts per million

Rietgat Fm, Platberg Group, Ventersdorp Supergroup

SAMPLE	Avg	Std
SiO2	52.8	1.6
TiO2	1.37	0.19
Al2O3	14.2	0.7
Fe2O3-T	10.5	2.0
MgO	4.37	1.03
CaO	5.78	1.85
Na2O	3.72	0.76
K2O	1.08	0.51
MnO	0.13	0.02
P2O5	0.49	0.23
LOI	5.84	1.37
TOTAL	100.3	0.4
Rb	25.62	20.16
Ba	466	65
Cs	1.18	0.60
Sr	517	245
Pb	14.42	7.07
Th	2.38	0.37
U	0.5	0.1
Sc	20.48	2.84
V	202	22
Cr	199	27
Co	32	6
Ni	94	13
Y	48.46	4.76
Zr	361.14	32.58
Nb	17.66	1.08
Hf	8.54	0.89
Ta	0.81	0.10
La	62.46	9.39
Ce	138.78	21.63
Sm	13.17	1.89
Eu	3.10	0.79
Tb	1.62	0.25
Yb	4.23	0.66
Lu	0.63	0.10
Mg Number	48.08	3.55
K2O/Na2O	0.33	0.22
Na2O+K2O	4.80	0.53
Al2O3/TiO2	10.52	1.16

Rietgat Fm, Platberg Group, Ventersdorp Supergroup

SAMPLE	Avg	Std
CaO/TiO2	4.30	1.56
Zr/TiO2	0.03	.00
K/Rb	538.94	284.61
Ba/Sr	1.07	0.44
Rb/Sr	0.07	0.07
La/Yb	14.84	1.13
La/Sm	4.75	0.38
Sm/Eu	4.37	0.51
Ti/Zr	23.03	3.97
Zr/Nb	20.42	0.60
Nb/Y	0.37	0.03
Zr/Y	7.48	0.48
Nb/Ta	22.07	1.28
Nb/La	0.29	0.04
La/Ta	78.04	11.41
La/Th	27.02	6.10
Y/Tb	30.12	2.33
Th/Yb	0.58	0.14
Ta/Yb	0.19	0.02
Hf/Th	3.65	0.50
Ti/V	41.38	8.08
U/Pb	0.04	0.01
Ce/Nb	7.84	0.95
Th/Ta	3.00	0.63
Th/Sc	0.12	0.03
Th/Nb	0.14	0.02
Sc/Ni	0.22	0.01
Hf/Ta	10.64	0.81
FeO-T/MgO	2.21	0.34
Sm/Yb	3.12	0.08
Eu/Eu*	0.74	0.09
g(x)	5.48	0.14
Score 1	0.95	0.31
Score 2	-0.30	0.10

Fe2O3-T ==> Total Fe as Fe2O3
NO ENTRY ==> No determination OR below detectability limi
MAJOR ELEMENTS ==> In weight percent
TRACE ELEMENTS ==> In parts per million

Makwassie Fm, Platberg Group, Ventersdorp Supergroup

SAMPLE	J18M	J19M	J20M	C1M	C2M
SiO2	73.7	54.4	71.2	75.4	75.3
TiO2	0.97	0.73	1.03	0.29	0.26
Al2O3	10.6	14.6	11.9	11.5	13.4
Fe2O3-T	4.7	10.6	5.6	2.5	1.8
MgO	2.13	5.89	2.44	2.21	1.12
CaO	1.54	6.84	1.52	0.97	0.51
Na2O	2.27	3.76	1.89	1.35	3.32
K2O	2.63	1.46	3.17	5.84	4.89
MnO	0.04	0.14	0.08	0.06	0.03
P2O5	0.41	0.12	0.42	0.07	0.06
LOI	1.62	2.48	1.73	1.23	0.79
TOTAL	100.7	101.1	101.0	101.4	101.5
Rb	104.5	164.2	154.4	142.5	142.1
Ba	691	785	1258	1691	470
Cs	2.6	3.6	2.6	2.4	2.6
Sr	192	265	157	222	143
Pb	29.5	15.8	25.6	10.9	10.6
Th	6.4	9.0	6.2	12.5	16.9
U	1.2	1.8	1.2	2.2	3.3
Sc	10.5	15.7	9.7	4.4	3.1
V	84	130	92	30	15
Cr	17	20	13	39	19
Co	8	14	9	6	2
Ni	3	22	13	21	7
Y	54.5	79.8	56.4	39.0	43.0
Zr	347.4	489.7	382.4	154.4	192.2
Nb	21.5	30.0	21.9	21.0	29.3
Hf	10.5	15.4	10.0	5.7	7.2
Ta	1.20	1.65	1.15	1.48	2.24
La	76.0	160.5	78.5	61.9	48.0
Ce	175.0	318.0	165.1	130.6	119.8
Sm	14.25	21.40	13.20	7.72	8.39
Eu	2.73	4.49	2.15	0.93	0.64
Tb	1.66	2.71	1.50	1.25	1.01
Yb	5.11	7.22	4.91	3.95	5.34
Lu	0.80	1.03	0.76	0.61	0.83
Mg Number	50.3	55.4	49.3	66.7	58.4
K2O/Na2O	1.16	0.39	1.68	4.33	1.47
Na2O+K2O	4.90	5.22	5.06	7.19	8.21
Al2O3/TiO2	11.0	20.0	11.5	39.7	51.6

Makwassie Fm, Platberg Group, Ventersdorp Supergroup

SAMPLE	J18M	J19M	J20M	C1M	C2M
CaO/TiO2	1.6	9.4	1.5	3.3	2.0
Zr/TiO2	0.036	0.067	0.037	0.053	0.074
K/Rb	208.9	73.8	170.4	340.2	285.6
Ba/Sr	3.60	2.97	8.01	7.62	3.29
Rb/Sr	0.545	0.621	0.983	0.642	0.994
La/Yb	14.9	22.2	16.0	15.7	9.0
La/Sm	5.3	7.5	5.9	8.0	5.7
Sm/Eu	5.2	4.8	6.1	8.3	13.1
Ti/Zr	16.8	8.9	16.2	11.3	8.1
Zr/Nb	16.2	16.3	17.5	7.4	6.6
Nb/Y	0.39	0.38	0.39	0.54	0.68
Zr/Y	6.4	6.1	6.8	4.0	4.5
Nb/Ta	17.9	18.2	19.0	14.2	13.1
Nb/La	0.28	0.19	0.28	0.34	0.61
La/Ta	63.3	97.3	68.3	41.8	21.4
La/Th	11.9	17.8	12.7	5.0	2.8
Y/Tb	32.8	29.4	37.6	31.2	42.6
Th/Yb	1.25	1.25	1.26	3.16	3.16
Ta/Yb	0.235	0.229	0.234	0.375	0.419
Hf/Th	1.64	1.71	1.61	0.46	0.43
Ti/V	69.0	33.7	67.1	57.8	106.8
U/Pb	0.04	0.11	0.05	0.20	0.31
Ce/Nb	8.14	10.60	7.54	6.22	4.09
Th/Ta	5.33	5.45	5.39	8.45	7.54
Th/Sc	0.61	0.57	0.64	2.84	5.45
Th/Nb	0.30	0.30	0.28	0.60	0.58
Sc/Ni	3.50	0.71	0.75	0.21	0.42
Hf/Ta	8.75	9.33	8.70	3.85	3.21
FeO-T/MgO	1.99	1.63	2.08	1.01	1.44
Sm/Yb	2.79	2.96	2.69	1.95	1.57
Eu/Eu*	0.62	0.66	0.53	0.36	0.24
g(x)	5.19	5.39	5.19	4.64	4.58
Score 1	0.28	0.48	0.07	1.03	0.65
Score 2	-0.22	0.02	-0.30	0.42	0.33

Fe2O3-T ==> Total Fe as Fe2O3
NO ENTRY ==> No determination OR below detectability limi
MAJOR ELEMENTS ==> In weight percent
TRACE ELEMENTS ==> In parts per million

Makwassie Fm, Platberg Group, Ventersdorp Supergroup

SAMPLE	D6M	Avg	Std
SiO2	70.7	70.1	7.2
TiO2	0.69	0.66	0.30
Al2O3	13.4	12.6	1.3
Fe2O3-T	3.7	4.8	2.9
MgO	1.26	2.51	1.59
CaO	2.17	2.26	2.11
Na2O	3.67	2.71	0.92
K2O	3.89	3.65	1.44
MnO	0.07	0.07	0.04
P2O5	0.21	0.22	0.15
LOI	1.58	1.57	0.51
TOTAL	101.4	101.2	0.3
Rb	97.5	134.20	24.73
Ba	1145	1007	406
Cs	1.3	2.52	0.67
Sr	274	209	50
Pb	19.1	18.58	7.06
Th	9.6	10.10	3.70
U	1.3	1.8	0.8
Sc	6.2	8.27	4.25
V	43	66	40
Cr	7	19	10
Co	5	7	4
Ni	4	12	8
Y	49.0	53.62	13.18
Zr	408.4	329.08	118.69
Nb	20.4	24.02	4.01
Hf	9.9	9.78	3.04
Ta	1.16	1.48	0.39
La	74.3	83.20	36.10
Ce	161.7	178.37	65.41
Sm	12.07	12.84	4.51
Eu	1.84	2.13	1.27
Tb	1.40	1.59	0.54
Yb	3.79	5.05	1.13
Lu	0.59	0.77	0.15
Mg Number	43.2	53.91	7.46
K2O/Na2O	1.06	1.68	1.25
Na2O+K2O	7.56	6.36	1.33
Al2O3/TiO2	19.5	25.54	15.03

Makwassie Fm, Platberg Group, Ventersdorp Supergroup

SAMPLE	D6M	Avg	Std
CaO/TiO2	3.1	3.48	2.73
Zr/TiO2	0.059	0.05	0.01
K/Rb	331.1	235.00	94.61
Ba/Sr	4.18	4.94	2.07
Rb/Sr	0.356	0.69	0.23
La/Yb	19.6	16.23	4.12
La/Sm	6.2	6.45	0.97
Sm/Eu	6.6	7.35	2.81
Ti/Zr	10.1	11.90	3.37
Zr/Nb	20.0	13.98	5.13
Nb/Y	0.42	0.47	0.11
Zr/Y	8.3	6.01	1.46
Nb/Ta	17.6	16.67	2.21
Nb/La	0.27	0.33	0.13
La/Ta	64.1	59.36	23.45
La/Th	7.7	9.65	5.05
Y/Tb	35.0	34.78	4.36
Th/Yb	2.53	2.10	0.88
Ta/Yb	0.306	0.30	0.07
Hf/Th	1.03	1.15	0.55
Ti/V	96.7	71.87	24.25
U/Pb	0.07	0.13	0.10
Ce/Nb	7.93	7.42	1.98
Th/Ta	8.28	6.74	1.38
Th/Sc	1.55	1.94	1.76
Th/Nb	0.47	0.42	0.13
Sc/Ni	1.55	1.19	1.11
Hf/Ta	8.53	7.06	2.52
FeO-T/MgO	2.66	1.80	0.52
Sm/Yb	3.18	2.53	0.57
Eu/Eu*	0.49	0.48	0.14
g(x)	5.21	5.04	0.31
Score 1	0.73	0.54	0.31
Score 2	-0.22	.00	0.28

Fe2O3-T ==> Total Fe as Fe2O3
NO ENTRY ==> No determination OR below detectability limi
MAJOR ELEMENTS ==> In weight percent
TRACE ELEMENTS ==> In parts per million

Goedgenoeg Fm, Platberg Gp, Ventersdorp Supergroup

SAMPLE	J21G	J22G	J23G	J24G	J25G
SiO2	54.7	47.3	54.5	52.8	53.2
TiO2	1.45	1.75	1.45	0.59	1.56
Al2O3	14.5	17.7	14.4	13.3	14.4
Fe2O3-T	9.5	12.6	9.6	10.8	10.2
MgO	4.53	6.62	4.41	7.93	4.49
CaO	7.27	3.58	7.21	8.96	5.82
Na2O	2.71	5.22	2.74	2.52	3.76
K2O	1.49	0.21	1.47	1.12	1.84
MnO	0.13	0.12	0.12	0.16	0.11
P2O5	0.65	0.78	0.65	0.08	0.68
LOI	2.91	3.86	4.09	2.57	3.16
TOTAL	99.8	99.7	100.6	100.9	99.1
Rb	59.4	3.9	26.3	33.0	41.9
Ba	885	68	705	750	816
Cs	1.0	0.3	0.8	0.8	1.5
Sr	261	365	565	494	489
Pb	11.5	12.3	10.7	11.7	10.8
Th	2.2	2.7	2.0	1.8	1.5
U	0.4	0.5	0.4	0.4	0.3
Sc	15.1	24.5	22.9	20.2	20.6
V	184	198	183	216	194
Cr	105	207	167	127	267
Co	24	42	35	31	35
Ni	71	136	90	93	137
Y	38.1	55.5	42.9	50.8	44.5
Zr	322.3	380.3	313.5	319.9	292.3
Nb	15.0	18.9	14.9	17.4	14.6
Hf	6.8	9.1	8.7	7.6	7.0
Ta	0.75	0.89	0.84	0.80	0.68
La	45.7	55.9	66.0	61.6	51.3
Ce	106.4	134.9	150.5	135.0	116.4
Sm	10.25	14.53	13.51	13.14	11.57
Eu	2.02	3.47	3.45	3.38	2.84
Tb	1.11	1.80	1.55	1.55	1.38
Yb	2.92	4.90	4.76	4.51	3.93
Lu	0.43	0.76	0.70	0.69	0.62
Mg Number	51.8	54.2	50.9	62.2	49.9
K2O/Na2O	0.55	0.04	0.54	0.44	0.49
Na2O+K2O	4.20	5.43	4.21	3.64	5.60
Al2O3/TiO2	10.0	10.1	9.9	22.6	9.2

Goedgenoeg Fm, Platberg Gp, Ventersdorp Supergroup

SAMPLE	J21G	J22G	J23G	J24G	J25G
CaO/TiO2	5.0	2.0	5.0	15.2	3.7
Zr/TiO2	0.022	0.022	0.022	0.054	0.019
K/Rb	208.2	446.9	463.9	281.7	364.5
Ba/Sr	3.39	0.19	1.25	1.52	1.67
Rb/Sr	0.228	0.011	0.047	0.067	0.086
La/Yb	15.7	11.4	13.9	13.7	13.1
La/Sm	4.5	3.8	4.9	4.7	4.4
Sm/Eu	5.1	4.2	3.9	3.9	4.1
Ti/Zr	27.0	27.6	27.8	11.1	32.0
Zr/Nb	21.5	20.1	21.0	18.4	20.0
Nb/Y	0.39	0.34	0.35	0.34	0.33
Zr/Y	8.5	6.9	7.3	6.3	6.6
Nb/Ta	20.0	21.2	17.7	21.7	21.5
Nb/La	0.33	0.34	0.23	0.28	0.28
La/Ta	60.9	62.8	78.6	77.0	75.4
La/Th	20.8	20.7	33.0	34.2	34.2
Y/Tb	34.3	30.8	27.7	32.8	32.2
Th/Yb	0.75	0.55	0.42	0.40	0.38
Ta/Yb	0.257	0.182	0.176	0.177	0.173
Hf/Th	3.09	3.37	4.35	4.22	4.67
Ti/V	47.4	53.0	47.7	16.4	48.3
U/Pb	0.04	0.04	0.04	0.03	0.03
Ce/Nb	7.09	7.14	10.10	7.76	7.97
Th/Ta	2.93	3.03	2.38	2.25	2.21
Th/Sc	2.93	3.03	2.38	2.25	2.21
Th/Nb	0.15	0.14	0.13	0.10	0.10
Sc/Ni	0.21	0.18	0.25	0.22	0.15
Hf/Ta	9.07	10.22	10.36	9.50	10.29
FeO-T/MgO	1.88	1.71	1.95	1.23	2.03
Sm/Yb	3.51	2.97	2.84	2.91	2.94
Eu/Eu*	0.64	0.76	0.82	0.82	0.79
g(x)	5.26	5.53	5.48	5.27	5.45
Score 1	0.53	0.58	1.13	1.29	0.97
Score 2	-0.53	-0.36	-0.31	0.09	-0.29

Fe2O3-T ==> Total Fe as Fe2O3
NO ENTRY ==> No determination OR below detectability limi
MAJOR ELEMENTS ==> In weight percent
TRACE ELEMENTS ==> In parts per million

Goedgenoeg Fm, Platberg Gp, Ventersdorp Supergroup

SAMPLE	Avg	Std
SiO2	52.5	2.7
TiO2	1.36	0.40
Al2O3	14.9	1.5
Fe2O3-T	10.5	1.1
MgO	5.60	1.43
CaO	6.57	1.80
Na2O	3.39	1.01
K2O	1.23	0.56
MnO	0.13	0.02
P2O5	0.57	0.25
LOI	3.32	0.57
TOTAL	100.0	0.6
Rb	32.90	18.26
Ba	645	295
Cs	0.88	0.39
Sr	435	108
Pb	11.40	0.59
Th	2.04	0.40
U	0.4	0.1
Sc	20.66	3.19
V	195	12
Cr	175	58
Co	33	6
Ni	105	26
Y	46.36	6.11
Zr	325.66	29.29
Nb	16.16	1.70
Hf	7.84	0.91
Ta	0.79	0.07
La	56.10	7.20
Ce	128.64	15.50
Sm	12.60	1.51
Eu	3.03	0.56
Tb	1.48	0.23
Yb	4.20	0.72
Lu	0.64	0.11
Mg Number	53.79	4.46
K2O/Na2O	0.41	0.19
Na2O+K2O	4.62	0.76
Al2O3/TiO2	12.36	5.12

Goedgenoeg Fm, Platberg Gp, Ventersdorp Supergroup

SAMPLE	Avg	Std
CaO/TiO2	6.19	4.63
Zr/TiO2	0.03	0.01
K/Rb	353.04	97.27
Ba/Sr	1.60	1.03
Rb/Sr	0.09	0.07
La/Yb	13.53	1.37
La/Sm	4.46	0.35
Sm/Eu	4.23	0.44
Ti/Zr	25.09	7.24
Zr/Nb	20.21	1.07
Nb/Y	0.35	0.02
Zr/Y	7.10	0.76
Nb/Ta	20.44	1.48
Nb/La	0.29	0.04
La/Ta	70.95	7.50
La/Th	28.58	6.42
Y/Tb	31.57	2.24
Th/Yb	0.50	0.14
Ta/Yb	0.19	0.03
Hf/Th	3.94	0.60
Ti/V	42.56	13.25
U/Pb	0.04	.00
Ce/Nb	8.01	1.10
Th/Ta	2.56	0.35
Th/Sc	2.56	0.35
Th/Nb	0.13	0.02
Sc/Ni	0.20	0.04
Hf/Ta	9.89	0.51
FeO-T/MgO	1.76	0.29
Sm/Yb	3.03	0.24
Eu/Eu*	0.77	0.07
g(x)	5.40	0.11
Score 1	0.90	0.30
Score 2	-0.28	0.20

Fe2O3-T ==> Total Fe as Fe2O3
NO ENTRY ==> No determination OR below detectability limi
MAJOR ELEMENTS ==> In weight percent
TRACE ELEMENTS ==> In parts per million

Edenville Fm, Klipriviersberg Gp, Ventersdorp SG

SAMPLE	S35E	S34E	S33E	S32E	S31E1
SiO2	52.9	51.9	52.9	51.9	51.1
TiO2	0.4	0.44	0.43	0.43	0.63
Al2O3	9.9	10.5	10.3	10.3	13.4
Fe2O3-T	9.7	10.1	9.6	9.8	11.3
MgO	14.75	13.36	12.97	13.61	8.84
CaO	7.84	7.95	6.41	8.89	9.27
Na2O	1.58	1.99	1.77	2.31	2.83
K2O	0.33	0.41	0.45	0.17	1.29
MnO	0.17	0.16	0.16	0.18	0.18
P2O5	0.04	0.05	0.05	0.05	0.06
LOI	3.66	3.42	3.62	3.65	1.05
TOTAL	101.2	100.2	98.7	101.3	100.0
Rb	18.6	15.8	20.5	6.9	21.7
Ba	87	145	175	85	229
Cs	1.6	0.8	0.8	1.0	1.0
Sr	101	186	115	88	213
Pb	15.4	11.4	11.4	9.7	8.9
Th	0.5	0.6	0.6	0.6	1.1
U	0.2	0.3	0.3	0.2	0.2
Sc	23.8	24.6	24.1	27.4	30.2
V	152	166	165	159	174
Cr	1443	1319	1258	1597	1194
Co	54	55	55	63	63
Ni	412	405	377	397	309
Y	9.0	9.4	10.1	10.6	12.3
Zr	42.3	50.1	49.3	47.0	64.2
Nb	2.2	2.5	2.2	2.2	2.7
Hf	0.9	1.0	1.1	1.2	1.7
Ta	0.10	0.10	0.10	0.10	0.13
La	3.2	4.8	3.9	4.4	8.0
Ce	7.9	11.4	9.2	10.4	17.3
Sm	1.04	1.30	1.22	1.28	1.85
Eu	0.28	0.44	0.34	0.48	0.59
Tb	0.20	0.27	0.24	0.29	0.39
Yb	0.86	0.95	0.98	1.14	1.33
Lu	0.12	0.13	0.14	0.17	0.21
Mg Number	77.4	74.9	75.1	75.7	63.7
K2O/Na2O	0.21	0.21	0.25	0.07	0.46
Na2O+K2O	1.91	2.40	2.22	2.48	4.12
Al2O3/TiO2	24.7	23.8	23.9	24.0	21.3

Edenville Fm, Klipriviersberg Gp, Ventersdorp SG

SAMPLE	S35E	S34E	S33E	S32E	S31E1
CaO/TiO2	19.6	18.1	14.9	20.7	14.7
Zr/TiO2	0.011	0.011	0.011	0.011	0.010
K/Rb	147.3	215.4	182.2	204.5	493.4
Ba/Sr	0.86	0.78	1.52	0.97	1.07
Rb/Sr	0.185	0.085	0.178	0.079	0.102
La/Yb	3.7	5.1	4.0	3.9	6.0
La/Sm	3.1	3.7	3.2	3.4	4.3
Sm/Eu	3.7	3.0	3.6	2.7	3.1
Ti/Zr	56.7	52.7	52.3	54.9	58.9
Zr/Nb	19.2	20.0	22.4	21.4	23.8
Nb/Y	0.24	0.27	0.22	0.21	0.22
Zr/Y	4.7	5.3	4.9	4.4	5.2
Nb/Ta	22.0	25.0	22.0	22.0	20.8
Nb/La	0.69	0.52	0.56	0.50	0.34
La/Ta	32.0	48.0	39.0	44.0	61.5
La/Th	7.0	8.0	6.5	6.9	7.3
Y/Tb	45.0	34.8	42.1	36.6	31.5
Th/Yb	0.53	0.63	0.61	0.56	0.83
Ta/Yb	0.116	0.105	0.102	0.088	0.098
Hf/Th	1.96	1.67	1.83	1.88	1.55
Ti/V	15.8	15.9	15.6	16.2	21.8
U/Pb	0.01	0.02	0.02	0.02	0.03
Ce/Nb	3.59	4.56	4.18	4.73	6.41
Th/Ta	4.60	6.00	6.00	6.40	8.46
Th/Sc	0.02	0.02	0.02	0.02	0.04
Th/Nb	0.21	0.24	0.27	0.29	0.41
Sc/Ni	0.06	0.06	0.06	0.07	0.10
Hf/Ta	9.00	10.00	11.00	12.00	13.08
FeO-T/MgO	0.59	0.68	0.67	0.65	1.15
Sm/Yb	1.21	1.37	1.24	1.12	1.39
Eu/Eu*	0.77	0.95	0.80	1.03	0.89
g(x)	3.84	4.07	3.95	3.89	4.32
Score 1	0.93	1.37	0.96	0.71	1.23
Score 2	-0.18	-0.17	-0.18	-0.16	-0.21

Fe2O3-T ==> Total Fe as Fe2O3
NO ENTRY ==> No determination OR below detectability limi
MAJOR ELEMENTS ==> In weight percent
TRACE ELEMENTS ==> In parts per million

Edenville Fm, Klipriviersberg Gp, Ventersdorp SG

SAMPLE	S30E2	S29E3	S28E4	S27E5	S26E
SiO2	51.8	52.2	51.1	52.2	54.0
TiO2	0.62	0.51	0.5	0.55	0.64
Al2O3	13.1	12.0	12.1	12.4	13.1
Fe2O3-T	10.5	10.0	10.4	8.9	10.2
MgO	8.52	10.33	12.05	8.33	7.93
CaO	8.73	9.57	8.09	13.24	8.36
Na2O	3.38	1.82	2.82	0.35	3.14
K2O	0.82	1.51	0.76	0.02	0.85
MnO	0.17	0.19	0.18	0.17	0.17
P2O5	0.07	0.07	0.05	0.05	0.07
LOI	2.88	1.89	2.89	3.56	1.97
TOTAL	100.6	100.1	100.9	99.8	100.4
Rb	20.6	56.9	58.9	72.8	27.5
Ba	204	948	282	428	382
Cs	0.7	1.8	1.9	1.9	0.3
Sr	311	186	144	186	644
Pb	10.6	9.1	12.2	8.9	8.9
Th	0.9	0.9	0.8	1.0	0.5
U	0.3	0.3	0.3	0.3	0.2
Sc	24.1	23.7	28.0	24.2	23.7
V	155	159	157	161	181
Cr	918	898	1482	894	1394
Co	50	49	65	51	54
Ni	300	299	388	306	430
Y	12.2	13.4	12.8	14.4	10.1
Zr	66.7	60.6	58.3	65.6	52.3
Nb	2.8	2.5	3.2	3.0	2.0
Hf	1.4	1.3	1.4	1.5	1.0
Ta	0.12	0.13	0.13	0.13	0.10
La	6.0	5.2	6.8	6.7	3.6
Ce	14.8	12.0	15.5	13.8	8.4
Sm	1.59	1.55	1.59	1.72	1.15
Eu	0.42	0.43	0.46	0.52	0.57
Tb	0.28	0.29	0.31	0.34	0.26
Yb	1.14	1.15	1.19	1.17	1.07
Lu	0.17	0.16	0.17	0.17	0.16
Mg Number	64.6	69.9	72.3	67.7	63.7
K2O/Na2O	0.24	0.83	0.27	0.06	0.27
Na2O+K2O	4.20	3.33	3.58	0.37	3.99
Al2O3/TiO2	21.1	23.5	24.2	22.5	20.5

Edenville Fm, Kliprivièrsberg Gp, Ventersdorp SG

SAMPLE	S30E2	S29E3	S28E4	S27E5	S26E
CaO/TiO2	14.1	18.8	16.2	24.1	13.1
Zr/TiO2	0.011	0.012	0.012	0.012	0.008
K/Rb	330.4	220.3	107.1	2.3	256.5
Ba/Sr	0.66	5.09	1.96	2.30	0.59
Rb/Sr	0.066	0.306	0.409	0.391	0.043
La/Yb	5.3	4.5	5.7	5.7	3.4
La/Sm	3.8	3.4	4.3	3.9	3.1
Sm/Eu	3.8	3.6	3.5	3.3	2.0
Ti/Zr	55.8	50.5	51.5	50.3	73.4
Zr/Nb	23.8	24.2	18.2	21.9	26.2
Nb/Y	0.23	0.19	0.25	0.21	0.20
Zr/Y	5.5	4.5	4.6	4.6	5.2
Nb/Ta	23.3	19.2	24.6	23.1	20.0
Nb/La	0.47	0.48	0.47	0.45	0.56
La/Ta	50.0	40.0	52.3	51.5	36.0
La/Th	6.5	5.8	8.6	6.9	7.8
Y/Tb	43.6	46.2	41.3	42.4	38.8
Th/Yb	0.82	0.78	0.66	0.83	0.43
Ta/Yb	0.105	0.113	0.109	0.111	0.093
Hf/Th	1.51	1.44	1.77	1.55	2.17
Ti/V	24.0	19.3	19.1	20.5	21.3
U/Pb	0.02	0.03	0.02	0.03	0.03
Ce/Nb	5.29	4.80	4.84	4.60	4.20
Th/Ta	7.75	6.92	6.08	7.46	4.60
Th/Sc	0.04	0.04	0.03	0.04	0.02
Th/Nb	0.33	0.36	0.25	0.32	0.23
Sc/Ni	0.08	0.08	0.07	0.08	0.06
Hf/Ta	11.67	10.00	10.77	11.54	10.00
FeO-T/MgO	1.11	0.87	0.78	0.96	1.15
Sm/Yb	1.39	1.35	1.34	1.47	1.07
Eu/Eu*	0.78	0.80	0.83	0.86	1.36
g(x)	4.42	4.24	4.15	4.30	4.50
Score 1	1.55	1.17	0.98	1.10	2.24
Score 2	-0.18	-0.07	-0.11	-0.08	-0.07

Fe2O3-T ==> Total Fe as Fe2O3
NO ENTRY ==> No determination OR below detectability limi
MAJOR ELEMENTS ==> In weight percent
TRACE ELEMENTS ==> In parts per million

Edenville Fm, Klipriviersberg Gp, Ventersdorp SG

SAMPLE	S25E	S24E	S23E	S22E	S21E
SiO2	51.9	50.9	52.9	53.5	52.9
TiO2	0.41	0.5	0.76	0.64	0.63
Al2O3	11.7	11.4	14.1	13.6	13.3
Fe2O3-T	9.7	9.3	11.5	10.5	10.3
MgO	12.45	10.83	7.93	7.76	8.2
CaO	9.28	8.17	6.69	9.46	8.67
Na2O	0.31	2.85	4.13	2.49	3.73
K2O	0.9	0.93	1.1	0.74	0.86
MnO	0.16	0.17	0.20	0.17	0.20
P2O5	0.04	0.06	0.09	0.07	0.07
LOI	3.48	4.25	1.51	1.9	1.88
TOTAL	100.3	99.3	101.0	100.7	100.8
Rb	8.2	43.5	30.4	33.3	33.3
Ba	101	1690	286	343	275
Cs	0.6	0.5	0.4	0.5	0.7
Sr	124	245	149	212	277
Pb	7.7	9.9	7.7	9.3	9.4
Th	0.5	1.2	1.0	1.1	0.6
U	0.2	0.4	0.4	0.4	0.4
Sc	25.2	24.1	28.3	27.9	31.9
V	178	186	190	201	196
Cr	1484	237	384	345	413
Co	60	39	50	49	55
Ni	459	164	246	224	244
Y	9.7	15.4	13.3	15.0	12.9
Zr	47.2	76.3	65.9	68.5	68.8
Nb	3.1	3.3	3.0	2.8	3.3
Hf	1.1	1.7	1.5	1.6	1.8
Ta	0.10	0.19	0.17	0.16	0.15
La	4.1	6.4	5.6	6.3	6.9
Ce	9.1	13.5	11.4	13.8	14.5
Sm	1.16	1.88	1.67	1.90	1.95
Eu	0.27	0.48	0.42	0.54	0.67
Tb	0.24	0.39	0.32	0.37	0.38
Yb	0.93	1.19	1.12	1.23	1.43
Lu	0.14	0.19	0.18	0.19	0.21
Mg Number	74.4	72.3	60.8	62.5	64.1
K2O/Na2O	2.90	0.33	0.27	0.30	0.23
Na2O+K2O	1.21	3.78	5.23	3.23	4.59
Al2O3/TiO2	28.5	22.7	18.6	21.2	21.2

Edenville Fm, Klipriviersberg Gp, Ventersdorp SG

SAMPLE	S25E	S24E	S23E	S22E	S21E
CaO/TiO2	22.6	16.3	8.8	14.8	13.8
Zr/TiO2	0.012	0.015	0.009	0.011	0.011
K/Rb	911.0	177.4	300.3	184.4	214.4
Ba/Sr	0.81	6.90	1.92	1.62	0.99
Rb/Sr	0.066	0.178	0.204	0.157	0.120
La/Yb	4.4	5.4	5.0	5.1	4.8
La/Sm	3.5	3.4	3.4	3.3	3.5
Sm/Eu	4.3	3.9	4.0	3.5	2.9
Ti/Zr	52.1	39.3	69.2	56.1	54.9
Zr/Nb	15.2	23.1	22.0	24.5	20.8
Nb/Y	0.32	0.21	0.23	0.19	0.26
Zr/Y	4.9	5.0	5.0	4.6	5.3
Nb/Ta	31.0	17.4	17.6	17.5	22.0
Nb/La	0.76	0.52	0.54	0.44	0.48
La/Ta	41.0	33.7	32.9	39.4	46.0
La/Th	8.2	5.3	5.6	5.7	11.5
Y/Tb	40.4	39.5	41.6	40.5	33.9
Th/Yb	0.54	1.01	0.89	0.89	0.42
Ta/Yb	0.108	0.160	0.152	0.130	0.105
Hf/Th	2.20	1.42	1.50	1.45	3.00
Ti/V	13.8	16.2	24.0	19.1	19.3
U/Pb	0.02	0.04	0.05	0.04	0.04
Ce/Nb	2.94	4.09	3.80	4.93	4.39
Th/Ta	5.00	6.32	5.88	6.88	4.00
Th/Sc	0.02	0.05	0.04	0.04	0.02
Th/Nb	0.16	0.36	0.33	0.39	0.18
Sc/Ni	0.05	0.15	0.12	0.12	0.13
Hf/Ta	11.00	8.95	8.82	10.00	12.00
FeO-T/MgO	0.70	0.77	1.30	1.21	1.13
Sm/Yb	1.25	1.58	1.49	1.54	1.36
Eu/Eu*	0.65	0.72	0.72	0.81	0.98
g(x)	3.94	4.40	4.30	4.39	4.41
Score 1	1.05	1.33	0.83	1.14	1.43
Score 2	-0.16	-0.04	-0.29	-0.11	-0.18

Fe2O3-T ==> Total Fe as Fe2O3
NO ENTRY ==> No determination OR below detectability limi
MAJOR ELEMENTS ==> In weight percent
TRACE ELEMENTS ==> In parts per million

Edenville Fm, Klipriviersberg Gp, Ventersdorp SG

SAMPLE	AVG	STD
SiO2	52.3	0.9
TiO2	0.54	0.11
Al2O3	12.1	1.3
Fe2O3-T	10.1	0.7
MgO	10.52	2.39
CaO	8.71	1.51
Na2O	2.37	1.06
K2O	0.74	0.39
MnO	0.18	0.01
P2O5	0.06	0.01
LOI	2.77	0.95
TOTAL	100.4	0.7
Rb	31.26	18.56
Ba	377	406
Cs	0.97	0.54
Sr	212	131
Pb	10.03	1.90
Th	0.79	0.25
U	0.3	0.1
Sc	26.08	2.57
V	172	15
Cr	1017	457
Co	54	6
Ni	331	84
Y	12.04	2.03
Zr	58.87	9.82
Nb	2.72	0.42
Hf	1.35	0.28
Ta	0.13	0.03
La	5.46	1.37
Ce	12.20	2.73
Sm	1.52	0.30
Eu	0.46	0.11
Tb	0.30	0.06
Yb	1.13	0.15
Lu	0.17	0.03
Mg Number	69.27	5.47
K2O/Na2O	0.46	0.68
Na2O+K2O	3.11	1.28
Al2O3/TiO2	22.78	2.25

Edenville Fm, Kliprivierberg Gp, Ventersdorp SG

SAMPLE	AVG	STD
CaO/TiO2	16.70	3.85
Zr/TiO2	0.01	.00
K/Rb	263.12	202.41
Ba/Sr	1.87	1.73
Rb/Sr	0.17	0.11
La/Yb	4.80	0.77
La/Sm	3.55	0.37
Sm/Eu	3.39	0.56
Ti/Zr	55.24	7.67
Zr/Nb	21.78	2.70
Nb/Y	0.23	0.03
Zr/Y	4.90	0.33
Nb/Ta	21.84	3.40
Nb/La	0.52	0.10
La/Ta	43.16	8.11
La/Th	7.17	1.51
Y/Tb	39.88	3.99
Th/Yb	0.70	0.18
Ta/Yb	0.11	0.02
Hf/Th	1.79	0.41
Ti/V	18.80	3.04
U/Pb	0.03	0.01
Ce/Nb	4.49	0.77
Th/Ta	6.16	1.20
Th/Sc	0.03	0.01
Th/Nb	0.29	0.07
Sc/Ni	0.09	0.03
Hf/Ta	10.65	1.22
FeO-T/MgO	0.92	0.23
Sm/Yb	1.35	0.14
Eu/Eu*	0.86	0.16
g(x)	4.21	0.21
Score 1	1.20	0.36
Score 2	-0.15	0.06

Fe2O3-T ==> Total Fe as Fe2O3
NO ENTRY ==> No determination OR below detectability limi
MAJOR ELEMENTS ==> In weight percent
TRACE ELEMENTS ==> In parts per million
==========

Loraine Fm, Kliprivierberg Gp, Ventersdorp SG

SAMPLE	J26L	J27L	J28L	J29L	J30L
SiO2	61.7	54.6	53.4	55.3	59.2
TiO2	1.34	0.67	0.73	1.54	1.42
Al2O3	14.8	12.6	13.6	13.6	15.0
Fe2O3-T	7.4	10.5	10.5	10.1	7.2
MgO	2.8	7.64	7.17	5.41	3.91
CaO	2.52	7.63	9.42	6.93	3.61
Na2O	2.7	2.7	2.47	2.5	3.9
K2O	3.44	1.7	0.99	1.95	2.93
MnO	0.09	0.14	0.15	0.13	0.08
P2O5	0.55	0.1	0.16	0.68	0.61
LOI	2.36	2.04	1.94	2.14	2.04
TOTAL	99.6	100.3	100.5	100.1	99.9
Rb	29.2	47.8	53.7	39.8	33.9
Ba	665	418	229	263	303
Cs	0.7	1.2	2.7	1.9	1.5
Sr	330	295	275	280	345
Pb	9.4	12.0	10.8	13.3	12.4
Th	1.3	1.6	1.2	1.4	1.1
U	0.6	0.6	0.4	0.5	0.4
Sc	31.3	28.9	33.2	36.0	33.4
V	173	191	194	196	185
Cr	341	186	406	389	391
Co	52	52	57	62	58
Ni	185	156	214	185	220
Y	14.4	16.6	13.9	18.2	12.7
Zr	78.0	88.5	71.4	103.8	73.3
Nb	3.0	3.7	3.4	4.1	3.1
Hf	2.0	2.4	2.0	3.1	1.8
Ta	0.22	0.25	0.19	0.29	0.19
La	8.3	9.9	6.6	16.7	7.2
Ce	18.5	21.1	14.9	37.9	15.5
Sm	2.22	2.59	1.99	3.78	2.02
Eu	0.64	0.86	0.62	1.13	0.70
Tb	0.46	0.43	0.40	0.59	0.39
Yb	1.53	1.72	1.41	2.04	1.33
Lu	0.25	0.25	0.23	0.30	0.20
Mg Number	46.1	62.1	60.6	54.7	54.8
K2O/Na2O	1.27	0.63	0.40	0.78	0.75
Na2O+K2O	6.14	4.40	3.46	4.45	6.83
Al2O3/TiO2	11.0	18.8	18.6	8.8	10.6

Loraine Fm, Kliprivbefore, Ventersdorp SG

SAMPLE	J26L	J27L	J28L	J29L	J30L
CaO/TiO2	1.9	11.4	12.9	4.5	2.5
Zr/TiO2	0.006	0.013	0.010	0.007	0.005
K/Rb	977.8	295.2	153.0	406.7	717.4
Ba/Sr	2.02	1.42	0.83	0.94	0.88
Rb/Sr	0.089	0.162	0.195	0.142	0.098
La/Yb	5.4	5.8	4.7	8.2	5.4
La/Sm	3.7	3.8	3.3	4.4	3.6
Sm/Eu	3.5	3.0	3.2	3.3	2.9
Ti/Zr	103.1	45.4	61.3	89.0	116.2
Zr/Nb	26.0	23.9	21.0	25.3	23.6
Nb/Y	0.21	0.22	0.24	0.23	0.24
Zr/Y	5.4	5.3	5.1	5.7	5.8
Nb/Ta	13.6	14.8	17.9	14.1	16.3
Nb/La	0.36	0.37	0.52	0.25	0.43
La/Ta	37.7	39.6	34.7	57.6	37.9
La/Th	6.4	6.2	5.5	11.9	6.5
Y/Tb	31.3	38.6	34.8	30.8	32.6
Th/Yb	0.85	0.93	0.85	0.69	0.83
Ta/Yb	0.144	0.145	0.135	0.142	0.143
Hf/Th	1.54	1.50	1.67	2.21	1.64
Ti/V	46.6	21.1	22.6	47.1	46.1
U/Pb	0.06	0.05	0.04	0.04	0.03
Ce/Nb	6.17	5.70	4.38	9.24	5.00
Th/Ta	5.91	6.40	6.32	4.83	5.79
Th/Sc	0.04	0.06	0.04	0.04	0.03
Th/Nb	0.43	0.43	0.35	0.34	0.35
Sc/Ni	0.17	0.19	0.16	0.19	0.15
Hf/Ta	9.09	9.60	10.53	10.69	9.47
FeO-T/MgO	2.37	1.24	1.32	1.67	1.67
Sm/Yb	1.45	1.51	1.41	1.85	1.52
Eu/Eu*	0.81	0.99	0.88	0.90	0.99
g(x)	4.70	4.57	4.48	4.83	4.68
Score 1	1.24	1.34	1.33	0.94	1.31
Score 2	-0.39	-0.14	-0.19	-0.45	-0.46

Fe2O3-T ==> Total Fe as Fe2O3
NO ENTRY ==> No determination OR below detectability limi
MAJOR ELEMENTS ==> In weight percent
TRACE ELEMENTS ==> In parts per million

Loraine Fm, Klipriviersberg Gp, Ventersdorp SG

SAMPLE	J31L	J32L	J33L	C3L	C4L
SiO2	54.2	52.8	48.6	57.8	54.4
TiO2	0.61	0.61	1.76	0.66	0.62
Al2O3	13.5	13.9	17.8	14.7	13.9
Fe2O3-T	10.1	10.4	12.6	9.1	10.5
MgO	7.5	7.18	6.73	4.79	6.32
CaO	8.52	9.16	3.63	5.89	8.24
Na2O	3	2.92	5.23	3.38	3.97
K2O	0.8	1.1	0.21	1.54	0.91
MnO	0.15	0.16	0.11	0.10	0.16
P2O5	0.09	0.1	0.76	0.12	0.1
LOI	2.17	1.74	1.86	2.84	1.51
TOTAL	100.7	100.1	99.3	100.9	100.7
Rb	47.6	39.7	62.4	53.8	35.1
Ba	417	281	550	408	281
Cs	1.6	1.9	2.1	1.2	1.1
Sr	259	362	192	362	371
Pb	11.8	12.3	8.9	10.3	8.5
Th	1.1	1.2	1.4	1.7	1.6
U	0.4	0.5	0.5	0.6	0.7
Sc	35.6	32.8	29.8	25.8	38.1
V	209	202	173	169	192
Cr	416	301	389	334	285
Co	61	58	57	42	66
Ni	231	180	232	176	179
Y	14.4	14.3	15.5	16.9	15.2
Zr	70.4	76.9	80.6	100.4	76.8
Nb	2.6	3.7	4.5	3.8	3.1
Hf	1.9	2.0	2.2	2.6	2.3
Ta	0.19	0.19	0.21	0.26	0.25
La	7.0	7.7	8.0	11.9	9.9
Ce	16.1	17.0	17.7	25.9	21.5
Sm	2.02	2.14	2.39	3.08	2.44
Eu	0.67	0.75	0.63	0.97	0.91
Tb	0.37	0.41	0.38	0.54	0.50
Yb	1.47	1.46	1.41	1.59	1.77
Lu	0.21	0.22	0.22	0.20	0.27
Mg Number	62.4	60.7	54.5	54.1	57.5
K2O/Na2O	0.27	0.38	0.04	0.46	0.23
Na2O+K2O	3.80	4.02	5.44	4.92	4.88
Al2O3/TiO2	22.1	22.7	10.1	22.2	22.4

Loraine Fm, Klipriviersberg Gp, Ventersdorp SG

SAMPLE	J31L	J32L	J33L	C3L	C4L
CaO/TiO2	14.0	15.0	2.1	8.9	13.3
Zr/TiO2	0.012	0.013	0.005	0.015	0.012
K/Rb	139.5	230.0	27.9	237.6	215.2
Ba/Sr	1.61	0.78	2.86	1.13	0.76
Rb/Sr	0.184	0.110	0.325	0.149	0.095
La/Yb	4.8	5.3	5.7	7.5	5.6
La/Sm	3.5	3.6	3.3	3.9	4.1
Sm/Eu	3.0	2.9	3.8	3.2	2.7
Ti/Zr	52.0	47.6	131.0	39.4	48.4
Zr/Nb	27.1	20.8	17.9	26.4	24.8
Nb/Y	0.18	0.26	0.29	0.22	0.20
Zr/Y	4.9	5.4	5.2	5.9	5.1
Nb/Ta	13.7	19.5	21.4	14.6	12.4
Nb/La	0.37	0.48	0.56	0.32	0.31
La/Ta	36.8	40.5	38.1	45.8	39.6
La/Th	6.4	6.4	5.7	7.0	6.2
Y/Tb	38.9	34.9	40.8	31.3	30.4
Th/Yb	0.75	0.82	0.99	1.07	0.90
Ta/Yb	0.129	0.130	0.149	0.164	0.141
Hf/Th	1.73	1.67	1.57	1.53	1.44
Ti/V	17.5	18.1	60.9	23.4	19.4
U/Pb	0.03	0.04	0.06	0.06	0.08
Ce/Nb	6.19	4.59	3.93	6.82	6.94
Th/Ta	5.79	6.32	6.67	6.54	6.40
Th/Sc	0.03	0.04	0.05	0.07	0.04
Th/Nb	0.42	0.32	0.31	0.45	0.52
Sc/Ni	0.15	0.18	0.13	0.15	0.21
Hf/Ta	10.00	10.53	10.48	10.00	9.20
FeO-T/MgO	1.22	1.31	1.69	1.72	1.50
Sm/Yb	1.37	1.47	1.70	1.94	1.38
Eu/Eu*	0.96	1.01	0.79	0.93	1.05
g(x)	4.42	4.53	4.66	4.65	4.55
Score 1	1.34	1.61	0.66	1.50	1.60
Score 2	-0.11	-0.11	-0.53	-0.16	-0.06

Fe2O3-T ==> Total Fe as Fe2O3
NO ENTRY ==> No determination OR below detectability limi
MAJOR ELEMENTS ==> In weight percent
TRACE ELEMENTS ==> In parts per million

Loraine Fm, Kliprivierberg Gp, Ventersdorp SG

SAMPLE	S20L	S19L	S18L	S17L	S16L
SiO2	51.2	53.5	50.4	52.3	53.5
TiO2	0.43	0.49	0.76	0.65	0.64
Al2O3	10.3	11.8	14.0	13.6	13.7
Fe2O3-T	10.2	9.7	11.4	10.7	9.4
MgO	13.56	11.28	7.38	7.92	9.06
CaO	7.63	7.54	9.77	9.72	7.41
Na2O	2.83	1.84	3.78	2.53	3.52
K2O	0.18	1.81	0.54	1.26	1.15
MnO	0.20	0.17	0.19	0.18	0.20
P2O5	0.05	0.06	0.09	0.07	0.08
LOI	2.81	2.19	2.09	1.73	2.1
TOTAL	99.4	100.4	100.3	100.7	100.8
Rb	33.9	68.2	48.0	5.2	38.3
Ba	197	303	362	19	341
Cs	1.1	1.5	0.6	0.3	0.7
Sr	301	239	263	45	99
Pb	9.7	11.1	10.0	10.6	8.7
Th	1.1	1.2	1.0	0.8	1.3
U	0.4	0.4	0.4	0.3	0.6
Sc	26.0	27.0	30.1	27.2	29.1
V	185	188	203	192	221
Cr	295	313	377	550	246
Co	48	49	53	44	56
Ni	217	220	237	240	209
Y	14.3	15.7	14.3	12.1	17.6
Zr	72.2	70.4	66.6	55.3	77.2
Nb	2.8	2.8	2.5	2.6	3.1
Hf	1.7	1.6	1.6	1.4	1.9
Ta	0.15	0.16	0.15	0.13	0.16
La	6.9	6.5	5.8	6.0	12.9
Ce	14.7	13.8	12.3	13.2	24.4
Sm	1.94	1.84	1.83	1.79	2.46
Eu	0.64	0.55	0.60	0.64	0.67
Tb	0.35	0.34	0.35	0.34	0.40
Yb	1.20	1.18	1.24	1.13	1.46
Lu	0.19	0.19	0.17	0.17	0.22
Mg Number	75.0	72.4	59.3	62.4	68.3
K2O/Na2O	0.06	0.98	0.14	0.50	0.33
Na2O+K2O	3.01	3.65	4.32	3.79	4.67
Al2O3/TiO2	24.0	24.1	18.4	20.9	21.4

Loraine Fm, Klipriviersberg Gp, Ventersdorp SG

SAMPLE	S20L	S19L	S18L	S17L	S16L
CaO/TiO2	17.7	15.4	12.9	15.0	11.6
Zr/TiO2	0.017	0.014	0.009	0.009	0.012
K/Rb	44.1	220.3	93.4	2011.2	249.2
Ba/Sr	0.66	1.27	1.38	0.42	3.45
Rb/Sr	0.113	0.286	0.182	0.116	0.387
La/Yb	5.8	5.5	4.7	5.3	8.8
La/Sm	3.6	3.5	3.2	3.4	5.2
Sm/Eu	3.0	3.3	3.1	2.8	3.7
Ti/Zr	35.7	41.8	68.5	70.5	49.7
Zr/Nb	25.8	25.1	26.6	21.3	24.9
Nb/Y	0.20	0.18	0.17	0.21	0.18
Zr/Y	5.0	4.5	4.7	4.6	4.4
Nb/Ta	18.7	17.5	16.7	20.0	19.4
Nb/La	0.41	0.43	0.43	0.43	0.24
La/Ta	46.0	40.6	38.7	46.2	80.6
La/Th	6.3	5.4	5.8	7.5	9.9
Y/Tb	40.9	46.2	40.9	35.6	44.0
Th/Yb	0.92	1.02	0.81	0.71	0.89
Ta/Yb	0.125	0.136	0.121	0.115	0.110
Hf/Th	1.55	1.33	1.60	1.75	1.46
Ti/V	14.0	15.7	22.5	20.3	17.3
U/Pb	0.04	0.04	0.04	0.03	0.07
Ce/Nb	5.25	4.93	4.92	5.08	7.87
Th/Ta	7.33	7.50	6.67	6.15	8.13
Th/Sc	0.04	0.04	0.03	0.03	0.04
Th/Nb	0.39	0.43	0.40	0.31	0.42
Sc/Ni	0.12	0.12	0.13	0.11	0.14
Hf/Ta	11.33	10.00	10.67	10.77	11.88
FeO-T/MgO	0.68	0.77	1.39	1.22	0.94
Sm/Yb	1.62	1.56	1.48	1.58	1.68
Eu/Eu*	0.96	0.87	0.94	1.03	0.82
g(x)	4.38	4.37	4.47	3.90	4.27
Score 1	1.59	1.31	1.28	-0.06	0.43
Score 2	0.02	0.02	-0.15	-0.40	-0.18

Fe2O3-T ==> Total Fe as Fe2O3
NO ENTRY ==> No determination OR below detectability limi
MAJOR ELEMENTS ==> In weight percent
TRACE ELEMENTS ==> In parts per million
==========

Loraine Fm, Klipriviersberg Gp, Ventersdorp SG

SAMPLE	S15L	S14L	S13L	S12L	AVG
SiO2	53.7	55.4	54.5	55.8	54.3
TiO2	0.46	0.64	0.79	0.82	0.82
Al2O3	10.6	12.8	13.7	13.9	13.6
Fe2O3-T	10.1	11.2	10.7	10.5	10.1
MgO	13.42	7.34	6.82	5.78	7.47
CaO	7.93	8.97	8.56	7.48	7.40
Na2O	1.16	0.25	2.91	3.83	2.92
K2O	1.1	0.14	1.4	0.61	1.25
MnO	0.18	0.14	0.16	0.16	0.15
P2O5	0.06	0.07	0.1	0.1	0.21
LOI	2.02	3.51	1.76	1.59	2.13
TOTAL	100.7	100.5	101.4	100.7	100.4
Rb	23.0	4.3	52.9	24.3	39.01
Ba	354	40	741	159	333
Cs	0.3	0.1	1.0	0.4	1.15
Sr	316	91	305	426	271
Pb	8.4	13.6	12.3	12.5	10.87
Th	1.7	1.3	1.5	1.1	1.29
U	0.7	0.5	0.6	0.4	0.5
Sc	34.2	32.1	23.7	15.1	29.97
V	196	182	202	207	193
Cr	274	289	256	100	323
Co	61	57	49	30	53
Ni	187	179	205	99	197
Y	16.9	13.6	17.7	16.9	15.33
Zr	84.2	64.1	90.8	99.4	78.96
Nb	3.6	3.1	4.0	3.7	3.33
Hf	2.4	1.8	2.1	1.6	2.02
Ta	0.21	0.20	0.23	0.19	0.20
La	8.9	5.9	9.1	7.0	8.54
Ce	20.0	13.5	20.4	15.5	18.63
Sm	2.51	2.13	2.52	1.91	2.29
Eu	0.78	0.71	0.91	0.53	0.73
Tb	0.46	0.44	0.45	0.31	0.42
Yb	1.67	1.47	1.41	0.91	1.44
Lu	0.27	0.21	0.20	0.14	0.22
Mg Number	74.9	59.6	58.9	55.2	60.71
K2O/Na2O	0.95	0.56	0.48	0.16	0.49
Na2O+K2O	2.26	0.39	4.31	4.44	4.17
Al2O3/TiO2	23.1	20.0	17.3	17.0	18.61

Loraine Fm, Klipriviersberg Gp, Ventersdorp SG

SAMPLE	S15L	S14L	S13L	S12L	AVG
CaO/TiO2	17.2	14.0	10.8	9.1	11.06
Zr/TiO2	0.018	0.010	0.011	0.012	0.01
K/Rb	397.0	270.2	219.7	208.4	374.40
Ba/Sr	1.12	0.44	2.43	0.37	1.30
Rb/Sr	0.073	0.048	0.173	0.057	0.16
La/Yb	5.3	4.0	6.5	7.7	5.89
La/Sm	3.5	2.8	3.6	3.7	3.67
Sm/Eu	3.2	3.0	2.8	3.6	3.15
Ti/Zr	32.8	59.9	52.2	49.5	62.85
Zr/Nb	23.4	20.7	22.7	26.9	23.91
Nb/Y	0.21	0.23	0.23	0.22	0.22
Zr/Y	5.0	4.7	5.1	5.9	5.14
Nb/Ta	17.1	15.5	17.4	19.5	16.85
Nb/La	0.40	0.53	0.44	0.53	0.41
La/Ta	42.4	29.5	39.6	36.8	42.57
La/Th	5.2	4.5	6.1	6.4	6.60
Y/Tb	36.7	30.9	39.3	54.5	37.54
Th/Yb	1.02	0.88	1.06	1.21	0.90
Ta/Yb	0.126	0.136	0.163	0.209	0.14
Hf/Th	1.41	1.38	1.40	1.45	1.57
Ti/V	14.1	21.1	23.5	23.7	26.05
U/Pb	0.08	0.04	0.05	0.03	0.05
Ce/Nb	5.56	4.35	5.10	4.19	5.59
Th/Ta	8.10	6.50	6.52	5.79	6.51
Th/Sc	0.05	0.04	0.06	0.07	0.04
Th/Nb	0.47	0.42	0.38	0.30	0.39
Sc/Ni	0.18	0.18	0.12	0.15	0.15
Hf/Ta	11.43	9.00	9.13	8.42	10.12
FeO-T/MgO	0.68	1.37	1.41	1.64	1.36
Sm/Yb	1.50	1.45	1.79	2.10	1.60
Eu/Eu*	0.90	0.94	1.06	0.83	0.93
g(x)	4.49	4.13	4.64	4.75	4.50
Score 1	1.53	0.47	1.28	1.56	1.17
Score 2	0.04	-0.28	-0.16	-0.20	-0.21

Fe2O3-T ==> Total Fe as Fe2O3
NO ENTRY ==> No determination OR below detectability limi
MAJOR ELEMENTS ==> In weight percent
TRACE ELEMENTS ==> In parts per million
==========

Loraine Fm, Klipriviersberg Gp, Ventersdorp SG

SAMPLE	STD
SiO2	2.9
TiO2	0.38
Al2O3	1.6
Fe2O3-T	1.2
MgO	2.72
CaO	2.04
Na2O	1.07
K2O	0.84
MnO	0.03
P2O5	0.23
LOI	0.47
TOTAL	0.5
Rb	16.61
Ba	178
Cs	0.68
Sr	99
Pb	1.62
Th	0.24
U	0.1
Sc	5.13
V	13
Cr	94
Co	8
Ni	33
Y	1.71
Zr	12.53
Nb	0.55
Hf	0.40
Ta	0.04
La	2.72
Ce	5.87
Sm	0.48
Eu	0.15
Tb	0.07
Yb	0.25
Lu	0.04
Mg Number	7.33
K2O/Na2O	0.33
Na2O+K2O	1.35
Al2O3/TiO2	4.84

Loraine Fm, Klipriviersberg Gp, Ventersdorp SG

SAMPLE	STD
CaO/TiO2	4.87
Zr/TiO2	.00
K/Rb	444.12
Ba/Sr	0.82
Rb/Sr	0.09
La/Yb	1.25
La/Sm	0.50
Sm/Eu	0.31
Ti/Zr	27.01
Zr/Nb	2.50
Nb/Y	0.03
Zr/Y	0.45
Nb/Ta	2.46
Nb/La	0.09
La/Ta	10.57
La/Th	1.65
Y/Tb	6.09
Th/Yb	0.13
Ta/Yb	0.02
Hf/Th	0.19
Ti/V	13.11
U/Pb	0.02
Ce/Nb	1.32
Th/Ta	0.79
Th/Sc	0.01
Th/Nb	0.06
Sc/Ni	0.03
Hf/Ta	0.90
FeO-T/MgO	0.40
Sm/Yb	0.19
Eu/Eu*	0.08
g(x)	0.22
Score 1	0.46
Score 2	0.17

Fe2O3-T ==> Total Fe as Fe2O3
NO ENTRY ==> No determination OR below detectability limi
MAJOR ELEMENTS ==> In weight percent
TRACE ELEMENTS ==> In parts per million

Jeannette Fm, Klipriviersberg Gp, Ventersdorp SG

SAMPLE	S11J	S10J	S9J	S8J	S7J
SiO2	55.1	55.0	55.7	55.2	54.5
TiO2	0.97	0.96	0.95	0.94	0.94
Al2O3	15.0	14.9	14.8	14.8	15.0
Fe2O3-T	11.2	11.0	10.8	11.0	11.4
MgO	4.91	4.99	4.69	4.92	5.07
CaO	7.05	7.42	7.53	7.42	6.64
Na2O	3.77	3.55	2.77	3.37	3.24
K2O	1.14	1.27	1.67	1.31	1.64
MnO	0.16	0.15	0.15	0.16	0.14
P2O5	0.11	0.12	0.12	0.12	0.12
LOI	1.82	1.52	1.6	1.7	1.75
TOTAL	101.3	100.9	100.8	100.9	100.5
Rb	50.1	54.1	65.7	53.8	84.4
Ba	415	368	439	425	581
Cs	0.5	0.9	0.8	0.6	1.0
Sr	253	267	395	294	297
Pb	10.0	12.5	11.3	10.3	12.3
Th	1.8	1.8	1.7	1.8	1.8
U	0.8	0.8	0.8	0.8	0.8
Sc	21.3	21.7	20.9	20.6	21.4
V	213	218	215	214	209
Cr	11	12	14	13	23
Co	44	46	44	43	46
Ni	114	120	113	107	131
Y	20.3	20.3	19.6	18.9	19.3
Zr	108.7	109.6	110.6	108.2	103.8
Nb	4.3	5.1	4.2	4.5	4.7
Hf	2.5	2.7	2.5	2.2	2.4
Ta	0.33	0.33	0.33	0.34	0.29
La	10.4	10.7	10.1	10.5	8.1
Ce	23.2	24.4	22.4	22.6	19.6
Sm	2.96	3.13	3.00	3.01	2.76
Eu	0.94	0.93	0.86	0.84	0.74
Tb	0.53	0.50	0.51	0.50	0.47
Yb	1.46	1.51	1.43	1.48	1.51
Lu	0.22	0.23	0.22	0.21	0.21
Mg Number	49.6	50.6	49.4	50.1	50.0
K2O/Na2O	0.30	0.36	0.60	0.39	0.51
Na2O+K2O	4.91	4.82	4.44	4.68	4.88
Al2O3/TiO2	15.5	15.6	15.6	15.7	16.0

Jeannette Fm, Klipriviersberg Gp, Ventersdorp SG

SAMPLE	S11J	S10J	S9J	S8J	S7J
CaO/TiO2	7.3	7.7	7.9	7.9	7.1
Zr/TiO2	0.011	0.011	0.012	0.012	0.011
K/Rb	188.9	194.8	211.0	202.1	161.3
Ba/Sr	1.64	1.38	1.11	1.45	1.96
Rb/Sr	0.198	0.202	0.166	0.183	0.284
La/Yb	7.1	7.1	7.1	7.1	5.4
La/Sm	3.5	3.4	3.4	3.5	2.9
Sm/Eu	3.1	3.4	3.5	3.6	3.7
Ti/Zr	53.5	52.6	51.5	52.1	54.3
Zr/Nb	25.3	21.5	26.3	24.0	22.1
Nb/Y	0.21	0.25	0.21	0.24	0.24
Zr/Y	5.4	5.4	5.6	5.7	5.4
Nb/Ta	13.0	15.5	12.7	13.2	16.2
Nb/La	0.41	0.48	0.42	0.43	0.58
La/Ta	31.5	32.4	30.6	30.9	27.9
La/Th	5.8	5.9	5.9	5.8	4.5
Y/Tb	38.3	40.6	38.4	37.8	41.1
Th/Yb	1.23	1.19	1.19	1.22	1.19
Ta/Yb	0.226	0.219	0.231	0.230	0.192
Hf/Th	1.39	1.50	1.47	1.22	1.33
Ti/V	27.3	26.4	26.5	26.4	26.9
U/Pb	0.08	0.06	0.07	0.08	0.07
Ce/Nb	5.40	4.78	5.33	5.02	4.17
Th/Ta	5.45	5.45	5.15	5.29	6.21
Th/Sc	0.08	0.08	0.08	0.09	0.08
Th/Nb	0.42	0.35	0.40	0.40	0.38
Sc/Ni	0.19	0.18	0.18	0.19	0.16
Hf/Ta	7.58	8.18	7.58	6.47	8.28
FeO-T/MgO	2.06	1.98	2.07	2.02	2.03
Sm/Yb	2.03	2.07	2.10	2.03	1.83
Eu/Eu*	0.93	0.89	0.85	0.83	0.79
g(x)	4.73	4.74	4.83	4.74	4.73
Score 1	0.98	1.03	1.37	1.14	1.15
Score 2	-0.26	-0.25	-0.21	-0.27	-0.23

Fe2O3-T ==> Total Fe as Fe2O3
NO ENTRY ==> No determination OR below detectability limi
MAJOR ELEMENTS ==> In weight percent
TRACE ELEMENTS ==> In parts per million

Jeannette Fm, Klipriviersberg Gp, Ventersdorp SG

SAMPLE	S6J	J34J	AVG	STD
SiO2	54.9	55.4	55.1	0.4
TiO2	0.97	0.85	0.94	0.04
Al2O3	14.8	14.7	14.9	0.1
Fe2O3-T	11.1	10.9	11.1	0.2
MgO	5.22	4.52	4.90	0.22
CaO	7.54	7.75	7.34	0.34
Na2O	3.63	3.04	3.34	0.32
K2O	1.01	1.42	1.35	0.23
MnO	0.16	0.13	0.15	0.01
P2O5	0.13	0.12	0.12	0.01
LOI	1.56	1.39	1.62	0.14
TOTAL	100.9	100.3	100.8	0.3
Rb	49.0	54.0	58.73	11.62
Ba	357	389	425	69
Cs	0.7	1.6	0.87	0.34
Sr	361	419	327	60
Pb	10.9	11.1	11.20	0.87
Th	1.9	2.1	1.84	0.12
U	0.8	0.8	0.8	ERR
Sc	25.6	30.5	23.14	3.38
V	207	209	212	4
Cr	39	27	20	10
Co	53	62	48	6
Ni	146	120	122	12
Y	20.1	18.4	19.56	0.68
Zr	105.3	105.7	107.41	2.32
Nb	4.3	4.6	4.53	0.29
Hf	2.9	3.2	2.63	0.31
Ta	0.36	0.35	0.33	0.02
La	12.4	14.0	10.89	1.72
Ce	27.9	30.4	24.36	3.38
Sm	3.42	3.54	3.12	0.25
Eu	1.07	1.23	0.94	0.15
Tb	0.54	0.58	0.52	0.03
Yb	1.66	1.96	1.57	0.17
Lu	0.27	0.31	0.24	0.03
Mg Number	51.4	48.2	49.89	0.93
K2O/Na2O	0.28	0.47	0.41	0.11
Na2O+K2O	4.64	4.46	4.69	0.18
Al2O3/TiO2	15.2	17.3	15.86	0.64

Jeannette Fm, Kliprivicrsberg Gp, Ventersdorp SG

SAMPLE	S6J	J34J	AVG	STD
CaO/TiO2	7.8	9.1	7.82	0.61
Zr/TiO2	0.011	0.012	0.01	.00
K/Rb	171.1	218.3	192.49	19.08
Ba/Sr	0.99	0.93	1.35	0.34
Rb/Sr	0.136	0.129	0.19	0.05
La/Yb	7.5	7.1	6.91	0.64
La/Sm	3.6	4.0	3.47	0.28
Sm/Eu	3.2	2.9	3.34	0.27
Ti/Zr	55.3	48.2	52.52	2.11
Zr/Nb	24.5	23.0	23.81	1.61
Nb/Y	0.21	0.25	0.23	0.02
Zr/Y	5.2	5.7	5.50	0.19
Nb/Ta	11.9	13.1	13.68	1.43
Nb/La	0.35	0.33	0.43	0.08
La/Ta	34.4	40.0	32.54	3.55
La/Th	6.5	6.7	5.88	0.65
Y/Tb	37.2	31.7	37.88	2.84
Th/Yb	1.14	1.07	1.18	0.05
Ta/Yb	0.217	0.179	0.21	0.02
Hf/Th	1.53	1.52	1.42	0.11
Ti/V	28.1	24.4	26.57	1.04
U/Pb	0.07	0.07	0.07	0.01
Ce/Nb	6.49	6.61	5.40	0.82
Th/Ta	5.28	6.00	5.55	0.37
Th/Sc	0.07	0.07	0.08	0.01
Th/Nb	0.44	0.46	0.41	0.03
Sc/Ni	0.18	0.25	0.19	0.03
Hf/Ta	8.06	9.14	7.90	0.76
FeO-T/MgO	1.91	2.17	2.03	0.08
Sm/Yb	2.06	1.81	1.99	0.11
Eu/Eu*	0.94	1.04	0.90	0.08
g(x)	4.80	4.79	4.77	0.04
Score 1	1.28	1.49	1.21	0.17
Score 2	-0.19	-0.19	-0.23	0.03

Fe2O3-T ==> Total Fe as Fe2O3
NO ENTRY ==> No determination OR below detectability limi
MAJOR ELEMENTS ==> In weight percent
TRACE ELEMENTS ==> In parts per million

Orkney Fm, Klipriviersberg Gp, Ventersdorp SG

SAMPLE	J35o	J36o	J37o	J38o	S5o
SiO2	54.8	54.0	54.6	53.4	53.4
TiO2	0.94	1.01	1.03	0.95	1.03
Al2O3	14.4	15.0	14.9	13.7	15.2
Fe2O3-T	11.1	11.6	10.5	9.1	11.8
MgO	4.98	5.15	5.27	4.14	5.69
CaO	7.19	5.72	6.8	6.88	8.03
Na2O	3.55	2.9	4.53	3.53	3.37
K2O	1.47	2.33	0.62	0.73	0.4
MnO	0.14	0.14	0.11	0.11	0.16
P2O5	0.13	0.13	0.16	0.14	0.13
LOI	1.62	2.04	2.49	7.53	1.61
TOTAL	100.4	100.0	100.9	100.2	100.9
Rb	60.9	89.6	20.6	29.6	18.7
Ba	394	1115	207	1057	169
Cs	1.3	2.1	0.8	2.3	0.3
Sr	352	321	387	596	338
Pb	12.3	10.8	11.8	9.4	13.0
Th	1.9	2.3	2.0	1.9	1.8
U	0.8	1.0	1.0	0.6	0.8
Sc	25.5	29.8	20.1	18.0	23.0
V	203	220	159	161	230
Cr	59	54	66	96	36
Co	50	68	49	43	50
Ni	151	135	170	100	163
Y	19.5	20.2	18.5	15.9	21.2
Zr	110.0	111.6	128.9	121.5	110.3
Nb	4.7	5.1	5.5	4.4	4.3
Hf	2.8	3.6	3.4	3.1	2.5
Ta	0.39	0.45	0.47	0.35	0.39
La	13.1	15.2	14.7	11.4	12.4
Ce	27.9	33.7	32.0	27.4	27.3
Sm	3.43	3.92	3.68	3.39	3.47
Eu	1.08	1.26	1.09	0.90	0.95
Tb	0.52	0.68	0.59	0.54	0.54
Yb	1.67	2.05	1.52	1.40	1.52
Lu	0.25	0.31	0.23	0.22	0.25
Mg Number	50.1	49.9	53.1	50.5	51.9
K2O/Na2O	0.41	0.80	0.14	0.21	0.12
Na2O+K2O	5.02	5.23	5.15	4.26	3.77
Al2O3/TiO2	15.4	14.8	14.4	14.4	14.8

Orkney Fm, Klipriviersberg Gp, Ventersdorp SG

SAMPLE	J35o	J36o	J37o	J38o	S5o
CaO/TiO2	7.6	5.7	6.6	7.2	7.8
Zr/TiO2	0.012	0.011	0.013	0.013	0.011
K/Rb	200.3	215.8	249.8	204.7	177.5
Ba/Sr	1.12	3.48	0.53	1.77	0.50
Rb/Sr	0.173	0.279	0.053	0.050	0.055
La/Yb	7.8	7.4	9.7	8.1	8.2
La/Sm	3.8	3.9	4.0	3.4	3.6
Sm/Eu	3.2	3.1	3.4	3.8	3.7
Ti/Zr	51.3	54.3	47.9	46.9	56.0
Zr/Nb	23.4	21.9	23.4	27.6	25.7
Nb/Y	0.24	0.25	0.30	0.28	0.20
Zr/Y	5.6	5.5	7.0	7.6	5.2
Nb/Ta	12.1	11.3	11.7	12.6	11.0
Nb/La	0.36	0.34	0.37	0.39	0.35
La/Ta	33.6	33.8	31.3	32.6	31.8
La/Th	6.9	6.6	7.4	6.0	6.9
Y/Tb	37.5	29.7	31.4	29.4	39.3
Th/Yb	1.14	1.12	1.32	1.36	1.18
Ta/Yb	0.234	0.220	0.309	0.250	0.257
Hf/Th	1.47	1.57	1.70	1.63	1.39
Ti/V	27.8	27.5	38.9	35.5	26.9
U/Pb	0.07	0.09	0.08	0.06	0.06
Ce/Nb	5.94	6.61	5.82	6.23	6.35
Th/Ta	4.87	5.11	4.26	5.43	4.62
Th/Sc	0.07	0.08	0.10	0.11	0.08
Th/Nb	0.40	0.45	0.36	0.43	0.42
Sc/Ni	0.17	0.22	0.12	0.18	0.14
Hf/Ta	7.18	8.00	7.23	8.86	6.41
FeO-T/MgO	2.01	2.03	1.79	1.98	1.87
Sm/Yb	2.05	1.91	2.42	2.42	2.28
Eu/Eu*	0.96	0.95	0.89	0.80	0.83
g(x)	4.79	4.80	4.87	4.90	4.83
Score 1	1.28	1.16	1.34	1.79	1.18
Score 2	-0.23	-0.25	-0.37	-0.36	-0.21

Fe2O3-T ==> Total Fe as Fe2O3
NO ENTRY ==> No determination OR below detectability limi
MAJOR ELEMENTS ==> In weight percent
TRACE ELEMENTS ==> In parts per million

Orkney Fm, Klipriviersberg Gp, Ventersdorp SG

SAMPLE	S4o	S3o	S2o	S1o	D3o
SiO2	54.2	53.4	51.9	53.7	54.3
TiO2	1.02	1.02	1.07	1.03	0.94
Al2O3	14.6	15.0	15.3	14.6	14.7
Fe2O3-T	11.4	11.2	12.3	11.6	11.2
MgO	5.5	5.13	5.87	5.18	6.04
CaO	7.63	8.77	7.04	7.94	7.38
Na2O	3.31	3.79	3.41	3.74	3.63
K2O	1.21	0.19	1.31	0.56	0.41
MnO	0.16	0.16	0.16	0.16	0.16
P2O5	0.13	0.14	0.14	0.12	0.12
LOI	1.63	1.47	1.81	1.47	2.14
TOTAL	100.7	100.2	100.3	100.0	101.0
Rb	48.8	8.4	78.6	18.8	15.2
Ba	429	129	1020	1265	92
Cs	0.6	0.3	1.0	0.2	0.6
Sr	286	486	254	341	172
Pb	8.6	8.2	8.3	9.6	12.3
Th	1.7	1.7	1.7	1.8	1.6
U	0.8	0.7	0.7	0.8	0.7
Sc	20.9	22.7	21.8	20.9	20.3
V	212	211	223	212	208
Cr	47	39	41	51	46
Co	46	49	47	48	47
Ni	159	140	151	139	148
Y	18.5	19.0	21.3	18.9	18.1
Zr	105.2	110.6	110.3	108.6	101.9
Nb	4.7	4.3	5.0	5.1	4.6
Hf	2.4	2.6	2.6	2.4	2.4
Ta	0.31	0.34	0.35	0.35	0.32
La	9.5	11.0	10.1	10.6	11.6
Ce	21.6	24.7	22.5	23.6	24.7
Sm	2.92	3.21	3.14	3.12	3.16
Eu	0.83	0.96	0.85	0.96	1.00
Tb	0.49	0.50	0.58	0.51	0.54
Yb	1.50	1.60	1.48	1.41	1.45
Lu	0.21	0.25	0.23	0.22	0.23
Mg Number	52.0	50.7	51.8	50.1	54.9
K2O/Na2O	0.37	0.05	0.38	0.15	0.11
Na2O+K2O	4.52	3.98	4.72	4.30	4.04
Al2O3/TiO2	14.3	14.7	14.3	14.1	15.6

Orkney Fm, Klipriviersberg Gp, Ventersdorp SG

SAMPLE	S4o	S3o	S2o	S1o	D3o
CaO/TiO2	7.5	8.6	6.6	7.7	7.9
Zr/TiO2	0.010	0.011	0.010	0.011	0.011
K/Rb	205.8	187.7	138.3	247.2	223.9
Ba/Sr	1.50	0.27	4.01	3.71	0.53
Rb/Sr	0.170	0.017	0.309	0.055	0.088
La/Yb	6.3	6.9	6.8	7.5	8.0
La/Sm	3.3	3.4	3.2	3.4	3.7
Sm/Eu	3.5	3.3	3.7	3.3	3.2
Ti/Zr	58.2	55.3	58.2	56.9	55.3
Zr/Nb	22.4	25.7	22.1	21.3	22.2
Nb/Y	0.25	0.23	0.23	0.27	0.25
Zr/Y	5.7	5.8	5.2	5.7	5.6
Nb/Ta	15.2	12.6	14.3	14.6	14.4
Nb/La	0.49	0.39	0.50	0.48	0.40
La/Ta	30.6	32.4	28.9	30.3	36.3
La/Th	5.6	6.5	5.9	5.9	7.3
Y/Tb	37.8	38.0	36.7	37.1	33.5
Th/Yb	1.13	1.06	1.15	1.28	1.10
Ta/Yb	0.207	0.213	0.236	0.248	0.221
Hf/Th	1.41	1.53	1.53	1.33	1.50
Ti/V	28.8	29.0	28.8	29.1	27.1
U/Pb	0.09	0.09	0.08	0.08	0.06
Ce/Nb	4.60	5.74	4.50	4.63	5.37
Th/Ta	5.48	5.00	4.86	5.14	5.00
Th/Sc	0.08	0.07	0.08	0.09	0.08
Th/Nb	0.36	0.40	0.34	0.35	0.35
Sc/Ni	0.13	0.16	0.14	0.15	0.14
Hf/Ta	7.74	7.65	7.43	6.86	7.50
FeO-T/MgO	1.86	1.97	1.88	2.02	1.66
Sm/Yb	1.95	2.01	2.12	2.21	2.18
Eu/Eu*	0.85	0.91	0.79	0.92	0.94
g(x)	4.74	4.89	4.77	4.80	4.58
Score 1	1.10	1.53	0.93	1.24	0.72
Score 2	-0.30	-0.23	-0.26	-0.28	-0.36

Fe2O3-T ==> Total Fe as Fe2O3
NO ENTRY ==> No determination OR below detectability limi
MAJOR ELEMENTS ==> In weight percent
TRACE ELEMENTS ==> In parts per million

Orkney Fm, Klipriviersberg Gp, Ventersdorp SG

SAMPLE	AVG	STD
SiO2	53.8	0.8
TiO2	1.00	0.04
Al2O3	14.7	0.4
Fe2O3-T	11.2	0.8
MgO	5.30	0.51
CaO	7.34	0.79
Na2O	3.58	0.40
K2O	0.92	0.62
MnO	0.15	0.02
P2O5	0.13	0.01
LOI	2.38	1.74
TOTAL	100.5	0.4
Rb	38.92	27.30
Ba	588	445
Cs	0.95	0.70
Sr	353	112
Pb	10.43	1.74
Th	1.84	0.19
U	0.8	0.1
Sc	22.30	3.14
V	204	23
Cr	54	17
Co	50	6
Ni	146	18
Y	19.11	1.50
Zr	111.89	7.40
Nb	4.77	0.38
Hf	2.78	0.42
Ta	0.37	0.05
La	11.96	1.80
Ce	26.54	3.75
Sm	3.34	0.28
Eu	0.99	0.12
Tb	0.55	0.05
Yb	1.56	0.18
Lu	0.24	0.03
Mg Number	51.50	1.50
K2O/Na2O	0.27	0.21
Na2O+K2O	4.50	0.49
Al2O3/TiO2	14.68	0.45

Orkney Fm, Klipriviersberg Gp, Ventersdorp SG

SAMPLE	AVG	STD
CaO/TiO2	7.32	0.79
Zr/TiO2	0.01	.00
K/Rb	205.12	31.28
Ba/Sr	1.74	1.38
Rb/Sr	0.13	0.10
La/Yb	7.68	0.88
La/Sm	3.56	0.26
Sm/Eu	3.40	0.23
Ti/Zr	54.04	3.82
Zr/Nb	23.56	1.98
Nb/Y	0.25	0.03
Zr/Y	5.90	0.74
Nb/Ta	12.97	1.42
Nb/La	0.41	0.06
La/Ta	32.14	1.98
La/Th	6.49	0.58
Y/Tb	35.03	3.50
Th/Yb	1.18	0.09
Ta/Yb	0.24	0.03
Hf/Th	1.51	0.11
Ti/V	29.95	3.80
U/Pb	0.08	0.01
Ce/Nb	5.58	0.73
Th/Ta	4.98	0.34
Th/Sc	0.08	0.01
Th/Nb	0.39	0.04
Sc/Ni	0.16	0.03
Hf/Ta	7.49	0.63
FeO-T/MgO	1.91	0.11
Sm/Yb	2.16	0.17
Eu/Eu*	0.88	0.06
g(x)	4.80	0.09
Score 1	1.23	0.28
Score 2	-0.28	0.06

Fe2O3-T ==> Total Fe as Fe2O3
NO ENTRY ==> No determination OR below detectability limi
MAJOR ELEMENTS ==> In weight percent
TRACE ELEMENTS ==> In parts per million
==========

Meredale Mb, Westonaria Fm, Klipriviersberg Gp

SAMPLE	1-0	1-M	2-0	2-M	3-0
SiO2	57.6	53.7	58.4	46.1	57.6
TiO2	1	1.15	0.99	1.07	1.06
Al2O3	8.5	8.7	9.0	8.6	10.0
Fe2O3-T	10.6	13.9	10.9	17.5	11.6
MgO	12.64	15.04	11.72	19.23	11.46
CaO	7.42	7.37	6.87	8.61	7.19
Na2O	2.05	0.89	2.78	0.16	1.55
K2O	0.11	0.27	0.13	0.07	0.16
MnO	0.15	0.2	0.17	0.24	0.32
P2O5	0.83	0.11	0.09	0.1	0.1
ORIGINAL TOTAL	100.8	101.3	101.0	101.7	101.1
Rb	1.8	3.4	1.4	1.3	4.9
Ba					
Cs					
Sr	208	68	200	72	274
Pb	10.6	8.5	7.2	4.8	5.1
Th	1.4	1.3	1.2	1.2	1.1
U					
Sc	19.6	21.9	18.5	21.6	22.8
V					
Cr	1637	1751	1348	1475	1611
Co	55	70	68	88	65
Ni	565	717	835	985	830
Y	13	15	13	18	15
Zr	85	89	85	96	80
Nb	4.1	4.4	5.1	4.6	4.9
Hf	1.8	2.3	1.9	2.2	2.6
Ta	0.24	0.26	0.27	0.27	0.32
La	4.9	16.1	5.6	3.2	8.5
Ce	13	32	14	9	22
Sm	2.54	3.32	2.35	1.80	3.31
Eu	0.79	1.10	0.77	0.68	0.98
Tb	0.44	0.57	0.40	0.37	0.48
Yb	1.06	1.07	0.88	1.13	1.16
Lu	0.17	0.16	0.13	0.18	0.17
Mg Number	72.9	70.9	70.8	71.1	68.9
K2O/Na2O	0.05	0.30	0.05	0.44	0.10
Na2O+K2O	2.16	1.16	2.91	0.23	1.71
Al2O3/TiO2	8.5	7.6	9.1	8.0	9.5

Meredale Mb, Westonaria Fm, Klipriviersberg Gp

SAMPLE	1-0	1-M	2-0	2-M	3-0
CaO/TiO2	7.4	6.4	6.9	8.0	6.8
Zr/TiO2	0.009	0.008	0.009	0.009	0.008
K/Rb	507.2	659.1	770.7	446.9	271.0
Ba/Sr	0.00	0.00	0.00	0.00	0.00
Rb/Sr	0.009	0.050	0.007	0.018	0.018
La/Yb	4.6	15.0	6.4	2.8	7.3
La/Sm	1.9	4.8	2.4	1.8	2.6
Sm/Eu	3.2	3.0	3.1	2.6	3.4
Ti/Zr	70.6	77.5	69.9	66.9	79.5
Zr/Nb	20.7	20.2	16.7	20.9	16.3
Nb/Y	0.32	0.29	0.39	0.26	0.33
Zr/Y	6.5	5.9	6.5	5.3	5.3
Nb/Ta	17.1	16.9	18.9	17.0	15.3
Nb/La	0.84	0.27	0.91	1.44	0.58
Ce/Pb	1.23	3.76	1.94	1.92	4.27
Nb/U	ERR	ERR	ERR	ERR	ERR
La/Ta	20.4	61.9	20.7	11.9	26.6
La/Th	3.5	12.4	4.7	2.7	7.7
Y/Tb	29.5	26.3	32.5	48.6	31.3
Th/Yb	1.32	1.21	1.36	1.06	0.95
Th/Sc	0.07	0.06	0.06	0.06	0.05
Th/Nb	0.34	0.30	0.24	0.26	0.22
Sc/Ni	0.03	0.03	0.02	0.02	0.03
Hf/Ta	7.500	8.846	7.037	8.148	8.125
Ta/Yb	0.226	0.243	0.307	0.239	0.276
Hf/Th	1.29	1.77	1.58	1.83	2.36
Ti/V	ERR	ERR	ERR	ERR	ERR
U/Pb	0.00	0.00	0.00	0.00	0.00
Th/Ta	5.83	5.00	4.44	4.44	3.44
FeO-T/MgO	0.75	0.83	0.83	0.82	0.91
Sm/Yb	2.40	3.10	2.67	1.59	2.85
g(x)	4.5122	4.314934	4.499912	4.375706	4.616314
Score 1	0.9986	-0.04815	0.969610	-0.05137	1.154525
Score 2	-0.489	-0.63354	-0.49240	-0.50771	-0.32586

Fe2O3-T ==> Total Fe as Fe2O3
NO ENTRY ==> No determination OR below detectability limi
MAJOR ELEMENTS ==> In weight percent
TRACE ELEMENTS ==> In parts per million

Meredale Mb, Westonaria Fm, Klipriviersberg Gp

SAMPLE	3-M	5-0	5-M	8-0	8-M
SiO2	48.5	57.9	52.3	58.5	53.8
TiO2	1.23	1.03	1.16	0.89	1.04
Al2O3	9.9	9.6	10.0	8.7	8.9
Fe2O3-T	16.0	10.7	13.8	11.1	13.7
MgO	16.8	11.69	15.03	13.07	15.24
CaO	7.84	7.81	7.88	7.04	6.58
Na2O	0.35	1.84	0.81	1.32	1.58
K2O	0.3	0.18	0	0.11	0.17
MnO	0.37	0.15	0.19	0.15	0.17
P2O5	0.13	0.09	0.13	0.08	0.14
ORIGINAL TOTAL	101.4	101.0	101.3	101.0	101.3
Rb	2.8	3.0	7.6	1.5	1.1
Ba					
Cs					
Sr	84	113	70	72	32
Pb	5.4	10.1	3.4	3.3	0.9
Th	2.1	1.2	1.4	0.8	1.4
U					
Sc	27.1	19.4	20.9	16.7	21.1
V					
Cr	2089	1305	1470	1287	1686
Co	82	70	66	67	71
Ni	880	613	634	667	817
Y	16	14	17	12	15
Zr	95	87	99	89	97
Nb	4.6	5.6	6.8	3.7	4.4
Hf	2.6	2.1	2.2	1.6	2.1
Ta	0.27	0.32	0.32	0.22	0.28
La	11.5	8.4	6.9	9.2	6.9
Ce	29	20	18	23	16
Sm	3.63	2.51	2.61	2.40	2.70
Eu	1.18	0.79	0.88	0.69	0.89
Tb	0.61	0.41	0.43	0.37	0.47
Yb	1.38	0.89	1.08	0.81	1.04
Lu	0.22	0.14	0.17	0.13	0.16
Mg Number	70.2	71.0	71.1	72.5	71.4
K2O/Na2O	0.86	0.10	0.00	0.08	0.11
Na2O+K2O	0.65	2.02	0.81	1.43	1.75
Al2O3/TiO2	8.0	9.3	8.6	9.8	8.5

Meredale Mb, Westonaria Fm, Klipriviersberg Gp

SAMPLE	3-M	5-0	5-M	8-0	8-M
CaO/TiO2	6.4	7.6	6.8	7.9	6.3
Zr/TiO2	0.008	0.008	0.009	0.010	0.009
K/Rb	889.3	498.0	0.0	608.7	1282.7
Ba/Sr	0.00	0.00	0.00	0.00	0.00
Rb/Sr	0.033	0.027	0.109	0.021	0.034
La/Yb	8.3	9.4	6.4	11.4	6.6
La/Sm	3.2	3.3	2.6	3.8	2.6
Sm/Eu	3.1	3.2	3.0	3.5	3.0
Ti/Zr	77.7	71.0	70.3	60.0	64.3
Zr/Nb	20.7	15.5	14.6	24.1	22.0
Nb/Y	0.29	0.40	0.40	0.31	0.29
Zr/Y	5.9	6.2	5.8	7.4	6.5
Nb/Ta	17.0	17.5	21.3	16.8	15.7
Nb/La	0.40	0.67	0.99	0.40	0.64
Ce/Pb	5.39	1.95	5.26	6.82	17.67
Nb/U	ERR	ERR	ERR	ERR	ERR
La/Ta	42.6	26.3	21.6	41.8	24.6
La/Th	5.5	7.0	4.9	11.5	4.9
Y/Tb	26.2	34.1	39.5	32.4	31.9
Th/Yb	1.52	1.35	1.30	0.99	1.35
Th/Sc	0.08	0.06	0.07	0.05	0.07
Th/Nb	0.46	0.21	0.21	0.22	0.32
Sc/Ni	0.03	0.03	0.03	0.03	0.03
Hf/Ta	9.630	6.563	6.875	7.273	7.500
Ta/Yb	0.196	0.360	0.296	0.272	0.269
Hf/Th	1.24	1.75	1.57	2.00	1.50
Ti/V	ERR	ERR	ERR	ERR	ERR
U/Pb	0.00	0.00	0.00	0.00	0.00
Th/Ta	7.78	3.75	4.38	3.64	5.00
FeO-T/MgO	0.86	0.83	0.82	0.77	0.81
Sm/Yb	2.63	2.82	2.42	2.96	2.60
g(x)	4.417019	4.391423	4.382257	4.209364	4.122875
Score 1	0.073525	0.446416	-0.08413	0.183620	-0.64693
Score 2	-0.61163	-0.55429	-0.59895	-0.70302	-0.76704

Fe2O3-T ==> Total Fe as Fe2O3
NO ENTRY ==> No determination OR below detectability limi
MAJOR ELEMENTS ==> In weight percent
TRACE ELEMENTS ==> In parts per million

Meredale Mb, Westonaria Fm, Klipriviersberg Gp

SAMPLE	9-0	9-M	12-0	12-M	20-0
SiO2	58.8	54.5	57.6	50.9	55.8
TiO2	0.9	0.92	0.96	1.32	1.27
Al2O3	8.3	7.6	8.5	9.5	10.3
Fe2O3-T	10.3	13.3	10.7	13.9	14.2
MgO	12.21	15.26	13.39	15.96	10.54
CaO	7.57	8.27	7.86	7.99	7.38
Na2O	2.43	0.91	1.65	1.21	1.12
K2O	0.14	0.19	0.12	0.25	0.46
MnO	0.15	0.15	0.13	0.15	0.15
P2O5	0.12	0.11	0.12	0.16	0.14
ORIGINAL TOTAL	100.9	101.2	101.0	101.3	101.4
Rb		2.9	1.1	1.4	
Ba					
Cs					
Sr	112	50	84	56	74
Pb		3.4	4.5	0.8	
Th	1.8	1.3	1.2	1.6	1.5
U					
Sc	24.1	24.2	18.8	24.4	22.6
V					
Cr	1921	1865	1545	1857	1661
Co	66	74	54	66	70
Ni	445	586	523	653	820
Y	12	12	11	17	17
Zr	88	84	91	121	104
Nb		5.7	5.4	6.8	
Hf	2.1	2.2	1.8	2.5	2.3
Ta	0.43	0.35	0.31	0.30	0.39
La	6.0	10.1	4.4	8.2	12.5
Ce	14	24	11	21	28
Sm	2.50	3.10	2.32	3.34	3.41
Eu	0.81	0.94	0.74	1.05	1.13
Tb	0.45	0.46	0.39	0.59	0.57
Yb	0.99	1.17	0.97	1.23	1.19
Lu	0.15	0.18	0.15	0.19	0.17
Mg Number	72.7	72.1	73.8	72.1	62.6
K2O/Na2O	0.06	0.21	0.07	0.21	0.41
Na2O+K2O	2.57	1.10	1.77	1.46	1.58
Al2O3/TiO2	9.2	8.3	8.8	7.2	8.1

Meredale Mb, Westonaria Fm, Klipriviersberg Gp

SAMPLE	9-0	9-M	12-0	12-M	20-0
CaO/TiO2	8.4	9.0	8.2	6.1	5.8
Zr/TiO2	0.010	0.009	0.009	0.009	0.008
K/Rb	ERR	543.8	905.5	1482.1	ERR
Ba/Sr	0.00	0.00	0.00	0.00	0.00
Rb/Sr	0.000	0.058	0.013	0.025	0.000
La/Yb	6.1	8.6	4.5	6.7	10.5
La/Sm	2.4	3.3	1.9	2.5	3.7
Sm/Eu	3.1	3.3	3.1	3.2	3.0
Ti/Zr	61.4	65.7	63.3	65.5	73.3
Zr/Nb	ERR	14.7	16.9	17.8	ERR
Nb/Y	0.00	0.48	0.49	0.40	0.00
Zr/Y	7.3	7.0	8.3	7.1	6.1
Nb/Ta	0.0	16.3	17.4	22.7	0.0
Nb/La	0.00	0.56	1.23	0.83	0.00
Ce/Pb	ERR	6.94	2.49	25.63	ERR
Nb/U	ERR	ERR	ERR	ERR	ERR
La/Ta	14.0	28.9	14.2	27.3	32.1
La/Th	3.3	7.8	3.7	5.1	8.3
Y/Tb	26.7	26.1	28.2	28.8	29.8
Th/Yb	1.82	1.11	1.24	1.30	1.26
Th/Sc	0.07	0.05	0.06	0.07	0.07
Th/Nb	ERR	0.23	0.22	0.24	ERR
Sc/Ni	0.05	0.04	0.04	0.04	0.03
Hf/Ta	4.884	6.286	5.806	8.333	5.897
Ta/Yb	0.434	0.299	0.320	0.244	0.328
Hf/Th	1.17	1.69	1.50	1.56	1.53
Ti/V	ERR	ERR	ERR	ERR	ERR
U/Pb	ERR	0.00	0.00	0.00	ERR
Th/Ta	4.19	3.71	3.87	5.33	3.85
FeO-T/MgO	0.76	0.78	0.72	0.78	1.21
Sm/Yb	2.53	2.65	2.39	2.72	2.87
g(x)	4.319791	4.112036	4.250633	4.408942	4.431117
Score 1	0.549694	-0.12972	0.317662	-0.33203	-0.07454
Score 2	-0.63057	-0.73949	-0.78101	-0.79029	-0.64835

Fe2O3-T ==> Total Fe as Fe2O3
NO ENTRY ==> No determination OR below detectability limi
MAJOR ELEMENTS ==> In weight percent
TRACE ELEMENTS ==> In parts per million

Meredale Mb, Westonaria Fm, Klipriviersberg Gp

SAMPLE	20-M	AVG	STD
SiO2	52.6	54.7	3.7
TiO2	1.01	1.06	0.13
Al2O3	9.6	9.1	0.7
Fe2O3-T	13.8	12.9	2.1
MgO	14.31	13.97	2.23
CaO	8.27	7.62	0.53
Na2O	1.04	1.36	0.68
K2O	0.33	0.19	0.11
MnO	0.14	0.19	0.07
P2O5	0.1	0.16	0.17
ORIGINAL TOTAL	101.2	101.2	0.2
Rb	2.9	2.7	1.7
Ba			
Cs			
Sr	62	103.0	71.0
Pb	2.5	5.0	3.0
Th	1.1	1.4	0.3
U			
Sc	20.1	21.5	2.6
V			
Cr	1354	1616	231
Co	64	69	8
Ni	706	705	141
Y	19	14.6	2.5
Zr	126	95.0	13.6
Nb	6.1	5.2	0.9
Hf	2.1	2.2	0.3
Ta	0.35	0.31	0.05
La	6.9	8.1	3.2
Ce	17	19.3	6.4
Sm	2.42	2.77	0.50
Eu	0.69	0.88	0.16
Tb	0.44	0.47	0.08
Yb	1.00	1.07	0.14
Lu	0.14	0.16	0.02
Mg Number	70.0	70.89	2.45
K2O/Na2O	0.32	0.21	0.21
Na2O+K2O	1.37	1.54	0.67
Al2O3/TiO2	9.5	8.62	0.72

Meredale Mb, Westonaria Fm, Klipriviersberg Gp

=======================================

SAMPLE	20-M	AVG	STD
CaO/TiO2	8.2	7.26	0.93
Zr/TiO2	0.012	0.01	.00
K/Rb	944.5	ERR	ERR
Ba/Sr	0.00	0.00	0.00
Rb/Sr	0.047	0.03	0.03
La/Yb	6.9	7.60	2.87
La/Sm	2.9	2.85	0.78
Sm/Eu	3.5	3.14	0.20
Ti/Zr	48.1	67.81	7.59
Zr/Nb	20.7	ERR	ERR
Nb/Y	0.32	0.31	0.13
Zr/Y	6.6	6.50	0.77
Nb/Ta	17.4	15.46	6.12
Nb/La	0.88	0.66	0.39
Ce/Pb	6.76	ERR	ERR
Nb/U	ERR	ERR	ERR
La/Ta	19.7	27.15	12.36
La/Th	6.3	6.20	2.72
Y/Tb	43.2	32.21	6.27
Th/Yb	1.10	1.26	0.21
Th/Sc	0.05	0.06	0.01
Th/Nb	0.18	ERR	ERR
Sc/Ni	0.03	0.03	0.01
Hf/Ta	6.000	7.17	1.22
Ta/Yb	0.350	0.29	0.06
Hf/Th	1.91	1.64	0.29
Ti/V	ERR	ERR	ERR
U/Pb	0.00	ERR	ERR
Th/Ta	3.14	4.49	1.11
FeO-T/MgO	0.87	0.83	0.11
Sm/Yb	2.42	2.60	0.33
g(x)	4.405397	4.36	0.13
Score 1	-0.19474	0.20	0.49
Score 2	-0.62423	-0.62	0.12

Fe2O3-T ==> Total Fe as Fe2O3
NO ENTRY ==> No determination OR below detectability limi
MAJOR ELEMENTS ==> In weight percent
TRACE ELEMENTS ==> In parts per million
=======================================

Dullstroom Formation, Transvaal Supergroup

SAMPLE	C-33	C-34	C-41	C-42	C-43	C-44	C-45
SiO2	53.5	55.7	55.6	55.2	55.1	55.7	57.1
TiO2	1.46	1.47	1.35	1.53	1.59	1.49	0.64
Al2O3	12.9	13.0	12.1	12.5	13.5	13.3	14.9
Fe2O3-T	11.5	10.8	11.9	12.0	10.9	10.8	10.2
MgO	6.75	5.67	5.59	5.37	4.94	5.18	4.75
CaO	7.45	7.24	8.06	7.64	7.49	7.15	7.52
Na2O	3.52	3.22	2.67	2.58	2.7	2.94	2.32
K2O	1.43	1.63	1.05	1.35	1.56	1.63	1.34
MnO	0.12	0.1	0.13	0.14	0.12	0.13	0.14
P2O5	0.15	0.16	0.14	0.15	0.15	0.14	0.12
LOI	1.48	1.32	1.55	1.41	1.84	1.9	1.24
TOTAL	100.21	100.37	100.21	99.90	99.94	100.29	100.26
Rb	51.3	50.2	61.3	75.7	75.0	69.2	50.2
Ba	335	360	245	268	284	432	398
Cs	1.1	0.7	4.3	2.2	3.0	2.1	2.7
Sr	430	459	374	415	416	448	263
Pb	7.7	3.8	6.5	4.2	4.5	6.2	7.3
Th	3.3	3.5	4.8	5.3	5.6	5.3	6.2
U	0.80	1.40		1.70	1.80	1.90	1.40
Sc	22.2	19.8	24.6	22.9	20.1	20.2	29.7
V	199	202	225	217	228	198	198
Cr	285	255	282	203	213	117	118
Co	48	45	46	42	42	41	39
Ni	187	147	76	76	78	67	59
Y	30.9	33.2	24.6	25.4	26.1	31.7	24.7
Zr	217.0	229.3	148.0	170.2	169.9	194.7	137.0
Nb	14.6	15.3	15.0	15.0	14.7	16.2	8.8
Hf	5.7	5.9	4.2	4.6	5.2	5.1	4.0
Ta	0.85	0.87	0.88	0.88	0.96	0.84	0.48
La	25.9	29.5	20.6	23.1	31.2	27.2	27.3
Ce	60.6	65.1	50.1	52.0	60.8	58.8	58.6
Sm	6.70	6.90	5.27	6.29	7.36	6.89	5.10
Eu	1.83	1.87	1.55	1.72	1.95	2.11	1.14
Tb	1.05	1.02	0.77	0.95	1.05	1.07	0.73
Yb	2.40	2.30	1.70	1.92	2.37	1.89	1.90
Lu	0.36	0.37	0.26	0.30	0.37	0.26	0.27
Mg Number	56.9	54.1	51.3	50.2	50.4	51.8	51.2
K2O/Na2O	0.41	0.51	0.39	0.52	0.58	0.55	0.58
Na2O+K2O	4.95	4.85	3.72	3.93	4.26	4.57	3.66
Al2O3/TiO	8.8	8.9	9.0	8.2	8.5	8.9	23.3

Dullstroom Formation, Transvaal Supergroup

SAMPLE	C-33	C-34	C-41	C-42	C-43	C-44	C-45
CaO/TiO2	5.1	4.9	6.0	5.0	4.7	4.8	11.7
Zr/TiO2	0.015	0.016	0.011	0.011	0.011	0.013	0.021
K/Rb	231.4	269.5	142.2	148.0	172.6	195.5	221.6
Ba/Sr	0.78	0.78	0.66	0.65	0.68	0.96	1.51
Rb/Sr	0.119	0.109	0.164	0.183	0.180	0.154	0.191
La/Yb	10.8	12.8	12.1	12.0	13.2	14.4	14.4
La/Sm	3.9	4.3	3.9	3.7	4.2	3.9	5.4
Sm/Eu	3.7	3.7	3.4	3.7	3.8	3.3	4.5
Ti/Zr	40.4	38.5	54.7	53.9	56.2	45.9	28.0
Zr/Nb	14.9	15.0	9.9	11.3	11.6	12.0	15.6
Nb/Y	0.47	0.46	0.61	0.59	0.56	0.51	0.36
Zr/Y	7.0	6.9	6.0	6.7	6.5	6.1	5.5
Nb/Ta	17.2	17.6	17.0	17.0	15.3	19.3	18.3
Nb/La	0.56	0.52	0.73	0.65	0.47	0.60	0.32
La/Ta	30.5	33.9	23.4	26.3	32.5	32.4	56.9
La/Th	7.8	8.4	4.3	4.4	5.6	5.1	4.4
Y/Tb	29.4	32.5	31.9	26.7	24.9	29.6	33.8
Th/Yb	1.38	1.52	2.82	2.76	2.36	2.80	3.26
Ta/Yb	0.354	0.378	0.518	0.458	0.405	0.444	0.253
Hf/Th	1.73	1.69	0.88	0.87	0.93	0.96	0.65
Ti/V	44.0	43.7	36.0	42.3	41.8	45.2	19.4
U/Pb	0.10	0.37	0.00	0.40	0.40	0.31	0.19
Ce/Nb	4.15	4.25	3.34	3.47	4.14	3.63	6.66
Th/Ta	3.88	4.02	5.45	6.02	5.83	6.31	12.92
Th/Sc	0.15	0.18	0.20	0.23	0.28	0.26	0.21
Th/Nb	0.23	0.23	0.32	0.35	0.38	0.33	0.70
Sc/Ni	0.12	0.13	0.32	0.30	0.26	0.30	0.50
Hf/Ta	6.71	6.78	4.77	5.23	5.42	6.07	8.33
FeO-T/MgO	1.53	1.71	1.92	2.01	1.99	1.88	1.93
Sm/Yb	2.79	3.00	3.10	3.28	3.11	3.65	2.68
Eu/Eu*	0.83	0.83	0.90	0.83	0.82	0.93	0.69
g(x)	5.24	5.29	5.03	5.13	5.15	5.23	4.74
Score 1	1.06	1.08	1.09	1.10	1.08	1.08	1.07
Score 2	-0.39	-0.36	-0.34	-0.42	-0.41	-0.31	-0.09

Fe2O3-T ==> Total Fe as Fe2O3
NO ENTRY ==> No determination OR below detectability limi
MAJOR ELEMENTS ==> In weight percent
TRACE ELEMENTS ==> In parts per million

Dullstroom Formation, Transvaal Supergroup

SAMPLE	C-55	C-40	C-50	AVG1	STD1	AVG2	STD2
SiO2	55.7	65.8	63.3	57.3	3.8	55.5	0.9
TiO2	0.68	0.58	0.58	1.14	0.43	1.28	0.36
Al2O3	14.9	13.8	14.1	13.5	0.9	13.4	1.0
Fe2O3-T	10.8	6.8	6.9	10.3	1.8	11.1	0.6
MgO	4.61	2.65	3.21	4.87	1.13	5.36	0.63
CaO	6.19	4.07	4.97	6.78	1.23	7.34	0.51
Na2O	3.19	2.65	3.18	2.90	0.35	2.89	0.37
K2O	2.48	2.82	2.29	1.76	0.54	1.56	0.39
MnO	0.15	0.06	0.11	0.12	0.02	0.13	0.01
P2O5	0.16	0.13	0.12	0.14	0.01	0.15	0.01
LOI	1.27	1.49	1.38	1.49	0.21	1.50	0.23
TOTAL	100.16	100.77	100.11	100.22	0.23	100.17	0.15
Rb	95.9	90.0	83.8	70.26	15.90	66.10	15.07
Ba	957	678	624	458	216	410	215
Cs	3.0	2.2	1.7	2.30	0.98	2.39	1.07
Sr	258	255	258	358	84	383	74
Pb	21.0	7.8	20.0	8.90	5.96	7.65	5.23
Th	9.3	11.1	8.5	6.29	2.42	5.41	1.74
U	1.80	3.10		1.74	0.61	1.54	0.35
Sc	27.4	15.1	16.7	21.87	4.28	23.36	3.41
V	184	105	105	186	43	206	14
Cr	130	154	144	190	63	200	67
Co	38	20	21	38	9	43	3
Ni	38	22	27	78	49	91	47
Y	29.3	28.1	27.1	28.11	2.90	28.24	3.22
Zr	181.0	197.8	184.9	182.98	27.09	180.89	29.75
Nb	11.4	10.4	10.0	13.14	2.54	13.88	2.32
Hf	5.0	5.4	5.1	5.02	0.58	4.96	0.63
Ta	0.66	0.62	0.58	0.76	0.15	0.80	0.15
La	41.7	37.4	35.7	29.96	6.27	28.31	5.96
Ce	84.4	77.4	73.3	64.11	10.48	61.30	9.84
Sm	6.73	5.91	5.70	6.29	0.72	6.41	0.76
Eu	1.70	1.16	1.22	1.63	0.33	1.73	0.27
Tb	0.89	0.93	0.89	0.94	0.11	0.94	0.12
Yb	2.25	2.58	2.55	2.19	0.29	2.09	0.25
Lu	0.38	0.39	0.36	0.33	0.05	0.32	0.05
Mg Number	48.9	46.9	51.1	51.27	2.58	51.85	2.37
K2O/Na2O	0.78	1.06	0.72	0.61	0.19	0.54	0.11
Na2O+K2O	5.67	5.47	5.47	4.66	0.71	4.45	0.65
Al2O3/TiO	21.9	23.7	24.3	14.54	7.18	12.17	6.02

Dullstroom Formation, Transvaal Supergroup

SAMPLE	C-55	C-40	C-50	AVG1	STD1	AVG2	STD2
CaO/TiO2	9.1	7.0	8.6	6.69	2.27	6.42	2.43
Zr/TiO2	0.027	0.034	0.032	0.02	0.01	0.02	0.01
K/Rb	214.6	260.1	226.8	208.23	41.18	199.42	40.78
Ba/Sr	3.71	2.66	2.42	1.48	1.02	1.22	0.98
Rb/Sr	0.371	0.353	0.325	0.22	0.09	0.18	0.08
La/Yb	18.5	14.5	14.0	13.67	1.99	13.53	2.20
La/Sm	6.2	6.3	6.3	4.80	1.05	4.43	0.82
Sm/Eu	4.0	5.1	4.7	3.96	0.56	3.74	0.34
Ti/Zr	22.5	17.6	18.8	37.66	14.33	42.52	11.76
Zr/Nb	15.9	19.0	18.5	14.36	2.93	13.26	2.16
Nb/Y	0.39	0.37	0.37	0.47	0.09	0.49	0.09
Zr/Y	6.2	7.0	6.8	6.49	0.47	6.38	0.47
Nb/Ta	17.3	16.8	17.2	17.31	0.97	17.38	1.07
Nb/La	0.27	0.28	0.28	0.47	0.16	0.52	0.15
La/Ta	63.2	60.3	61.6	42.08	15.37	37.37	13.57
La/Th	4.5	3.4	4.2	5.21	1.57	5.56	1.55
Y/Tb	32.9	30.2	30.4	30.26	2.66	30.24	2.97
Th/Yb	4.13	4.30	3.33	2.87	0.91	2.63	0.84
Ta/Yb	0.293	0.240	0.227	0.36	0.10	0.39	0.08
Hf/Th	0.54	0.49	0.60	0.93	0.42	1.03	0.41
Ti/V	22.2	33.1	33.1	36.08	8.74	36.82	9.63
U/Pb	0.09	0.40	0.00	0.23	0.16	0.23	0.15
Ce/Nb	7.40	7.44	7.33	5.18	1.69	4.63	1.43
Th/Ta	14.09	17.90	14.66	9.11	4.92	7.32	3.68
Th/Sc	0.34	0.74	0.51	0.31	0.17	0.23	0.06
Th/Nb	0.82	1.07	0.85	0.53	0.29	0.42	0.21
Sc/Ni	0.72	0.69	0.62	0.40	0.21	0.33	0.18
Hf/Ta	7.58	8.71	8.79	6.84	1.40	6.36	1.14
FeO-T/MgO	2.11	2.29	1.93	1.93	0.20	1.89	0.17
Sm/Yb	2.99	2.29	2.24	2.91	0.41	3.07	0.28
Eu/Eu*	0.79	0.59	0.65	0.79	0.10	0.83	0.07
g(x)	4.86	4.83	4.81	5.03	0.19	5.08	0.18
Score 1	0.95	1.01	1.03	1.06	0.04	1.06	0.05
Score 2	-0.15	-0.18	-0.16	-0.28	0.12	-0.31	0.11

Fe2O3-T ==> Total Fe as Fe2O3
NO ENTRY ==> No determination OR below detectability limi
MAJOR ELEMENTS ==> In weight percent
TRACE ELEMENTS ==> In parts per million

Machadodorp Formation, Transvaal Supergroup

SAMPLE	C-23	C-24	C-25	C-26	C-57	C-60
SiO2	51.2	51.2	50.8	50.2	54.3	50.2
TiO2	0.67	0.62	1.41	0.84	1.19	1.48
Al2O3	14.2	14.1	14.1	14.0	14.2	13.9
Fe2O3-T	11.8	11.7	13.1	12.5	13.4	14.5
MgO	7.47	7.52	6.18	7.72	7.88	6.96
CaO	8.4	8.47	10.18	10.32	3.39	8.74
Na2O	2.89	3.62	2.08	3.1	2.21	2.27
K2O	0.82	0.52	0.7	0.13	0.4	0.39
MnO	0.15	0.16	0.2	0.18	0.13	0.19
P2O5	0.1	0.1	0.18	0.1	0.11	0.18
LOI	2.31	2.49	1.66	1.48	3.01	1.34
TOTAL	100.04	100.41	100.60	100.51	100.22	100.07
Rb	40.0	21.4	25.8	2.0	17.6	12.5
Ba	191	142	201	60	86	143
Cs	1.9	0.7	1.2	0.2	2.1	1.4
Sr	93	114	128	118	58	116
Pb	6.0	5.2	12.3	2.9	6.8	5.0
Th	3.2	3.0	2.4	0.3	3.1	2.5
U	0.6	0.6	1.0		0.8	0.7
Sc	58.4	46.7	33.8	42.2	35.1	37.7
V	317	315	230	311	327	221
Cr	291	691	327	726	124	260
Co	55	45	53	42	48	46
Ni	117	141	132	158	93	103
Y	25.8	26.5	46.3	23.8	37.5	49.6
Zr	72.6	70.8	135.8	56.3	113.4	141.6
Nb	4.4	4.6	8.7	3.9	7.6	9.4
Hf	2.3	1.8	3.6	1.5	3.3	3.9
Ta	0.28	0.26	0.45	0.21	0.41	0.44
La	9.4	8.4	11.4	2.7	13.5	11.6
Ce	20.7	18.3	27.2	7.2	26.8	27.0
Sm	2.90	2.40	4.80	2.00	4.25	5.07
Eu	0.95	0.65	1.36	0.78	1.38	1.44
Tb	0.69	0.60	1.11	0.48	0.90	0.98
Yb	2.97	2.56	3.92	2.03	3.03	4.01
Lu	0.47	0.44	0.64	0.34	0.53	0.70
Mg Number	58.8	59.1	51.5	58.2	57.0	52.0
K2O/Na2O	0.28	0.14	0.34	0.04	0.18	0.17
Na2O+K2O	3.71	4.14	2.78	3.23	2.61	2.66
Al2O3/TiO2	21.3	22.7	10.0	16.6	12.0	9.4

Machadodorp Formation, Transvaal Supergroup

SAMPLE	C-23	C-24	C-25	C-26	C-57	C-60
CaO/TiO2	12.5	13.7	7.2	12.3	2.8	5.9
Zr/TiO2	0.011	0.011	0.010	0.007	0.010	0.010
K/Rb	170.2	201.7	225.2	539.5	188.6	259.0
Ba/Sr	2.06	1.25	1.57	0.51	1.49	1.23
Rb/Sr	0.431	0.188	0.201	0.017	0.305	0.108
La/Yb	3.2	3.3	2.9	1.3	4.5	2.9
La/Sm	3.2	3.5	2.4	1.4	3.2	2.3
Sm/Eu	3.1	3.7	3.5	2.6	3.1	3.5
Ti/Zr	55.4	52.5	62.3	89.5	63.0	62.7
Zr/Nb	16.5	15.4	15.6	14.4	14.9	15.1
Nb/Y	0.17	0.17	0.19	0.16	0.20	0.19
Zr/Y	2.8	2.7	2.9	2.4	3.0	2.9
Nb/Ta	15.7	17.7	19.3	18.6	18.5	21.4
Nb/La	0.47	0.55	0.76	1.44	0.56	0.81
La/Ta	33.6	32.3	25.3	12.9	32.9	26.4
La/Th	2.9	2.8	4.8	9.0	4.4	4.6
Y/Tb	37.4	44.2	41.7	49.6	41.7	50.6
Th/Yb	1.08	1.17	0.61	0.15	1.02	0.62
Ta/Yb	0.094	0.102	0.115	0.103	0.135	0.110
Hf/Th	0.72	0.60	1.50	5.00	1.06	1.56
Ti/V	12.7	11.8	36.8	16.2	21.8	40.2
U/Pb	0.10	0.12	0.08	0.00	0.12	0.14
Ce/Nb	4.70	3.98	3.13	1.85	3.53	2.87
Th/Ta	11.43	11.54	5.33	1.43	7.56	5.68
Th/Sc	0.05	0.06	0.07	0.01	0.09	0.07
Th/Nb	0.73	0.65	0.28	0.08	0.41	0.27
Sc/Ni	0.50	0.33	0.26	0.27	0.38	0.37
Hf/Ta	8.21	6.92	8.00	7.14	8.05	8.86
FeO-T/MgO	1.42	1.40	1.91	1.45	1.52	1.87
Sm/Yb	0.98	0.94	1.22	0.99	1.40	1.26
Eu/Eu*	0.88	0.72	0.77	1.05	0.91	0.81
g(x)	4.34	4.37	4.91	4.38	4.57	4.93
Score 1	0.21	0.40	-0.07	0.38	-0.58	-0.20
Score 2	0.11	0.21	-0.01	0.16	-0.13	-0.01

Fe2O3-T ==> Total Fe as Fe2O3
NO ENTRY ==> No determination OR below detectability limi
MAJOR ELEMENTS ==> In weight percent
TRACE ELEMENTS ==> In parts per million

Machadodorp Formation, Transvaal Supergroup

SAMPLE	C-61	C-66	C-208	C-209	C-211	C-212	AVG
SiO2	50.3	55.8	50.3	50.2	50.3	52.6	51.5
TiO2	0.83	0.89	1.54	1.59	0.87	1.05	1.08
Al2O3	14.2	10.9	13.8	14.2	14.3	12.9	13.7
Fe2O3-T	12.6	9.9	14.4	14.2	12.3	12.0	12.7
MgO	9.75	7.02	6.1	6.52	8.28	7.32	7.39
CaO	9.12	12.28	9.21	9.06	9.23	11.55	9.16
Na2O	1.53	1.47	2.52	2.63	2.16	0.68	2.26
K2O	0.11	0.07	0.53	0.22	0.15	0.15	0.35
MnO	0.19	0.17	0.19	0.2	0.17	0.17	0.18
P2O5	0.06	0.08	0.2	0.18	0.1	0.1	0.12
LOI	1.29	1.65	1.55	1.34	2.45	2.67	1.94
TOTAL	100.02	100.19	100.27	100.31	100.27	101.16	100.34
Rb	7.1	2.5	21.3	5.0	4.3	1.4	13.41
Ba	48	72	230	146	67	33	118
Cs	1.1	0.1	2.1	0.2	0.3		1.03
Sr	80	67	127	168	42	72	98
Pb	3.7	3.7	5.6	10.1	6.9	5.9	6.18
Th	0.4	1.3	2.7	2.7	1.1	1.9	2.05
U		0.4	0.9	0.8		0.6	0.7
Sc	44.2	32.5	38.9	38.3	40.0	38.6	40.53
V	294	244	240	239	292	306	278
Cr	361	191	241	254	314	260	337
Co	52	34	42	41	49	44	46
Ni	137	76	75	74	122	98	111
Y	23.1	24.6	52.2	50.8	25.8	24.5	34.21
Zr	58.4	75.4	150.6	147.5	69.2	91.5	98.59
Nb	4.0	4.2	9.5	9.8	4.1	5.1	6.28
Hf	1.6	1.9	4.3	3.9	1.9	2.5	2.71
Ta	0.20	0.24	0.51	0.52	0.19	0.28	0.33
La	2.9	5.3	10.9	10.5	4.4	6.6	8.13
Ce	8.1	12.2	24.6	26.0	12.2	17.7	19.00
Sm	2.11	2.40	5.13	5.08	2.42	3.02	3.47
Eu	0.73	0.71	1.43	1.46	0.75	1.03	1.06
Tb	0.49	0.53	1.18	1.19	0.52	0.61	0.77
Yb	2.09	2.40	4.38	4.24	2.32	2.54	3.04
Lu	0.38	0.41	0.73	0.72	0.42	0.44	0.52
Mg Number	63.5	61.4	48.7	50.8	60.2	57.8	56.59
K2O/Na2O	0.07	0.05	0.21	0.08	0.07	0.22	0.16
Na2O+K2O	1.64	1.54	3.05	2.85	2.31	0.83	2.61
Al2O3/TiO2	17.2	12.2	8.9	8.9	16.4	12.3	13.98

Machadodorp Formation, Transvaal Supergroup

SAMPLE	C-61	C-66	C-208	C-209	C-211	C-212	AVG
CaO/TiO2	11.0	13.8	6.0	5.7	10.6	11.0	9.38
Zr/TiO2	0.007	0.008	0.010	0.009	0.008	0.009	0.01
K/Rb	128.6	232.4	206.5	365.2	289.5	889.3	307.97
Ba/Sr	0.60	1.08	1.81	0.87	1.60	0.46	1.21
Rb/Sr	0.089	0.037	0.167	0.030	0.102	0.020	0.14
La/Yb	1.4	2.2	2.5	2.5	1.9	2.6	2.59
La/Sm	1.4	2.2	2.1	2.1	1.8	2.2	2.31
Sm/Eu	2.9	3.4	3.6	3.5	3.2	2.9	3.24
Ti/Zr	85.3	70.8	61.4	64.7	75.4	68.9	67.65
Zr/Nb	14.6	18.0	15.9	15.1	16.9	17.9	15.85
Nb/Y	0.17	0.17	0.18	0.19	0.16	0.21	0.18
Zr/Y	2.5	3.1	2.9	2.9	2.7	3.7	2.87
Nb/Ta	20.0	17.5	18.6	18.8	21.6	18.2	18.83
Nb/La	1.38	0.79	0.87	0.93	0.93	0.77	0.86
La/Ta	14.5	22.1	21.4	20.2	23.2	23.6	24.02
La/Th	7.3	4.1	4.0	3.9	4.0	3.5	4.60
Y/Tb	47.1	46.4	44.2	42.7	49.6	40.2	44.62
Th/Yb	0.19	0.54	0.62	0.64	0.47	0.75	0.66
Ta/Yb	0.096	0.100	0.116	0.123	0.082	0.110	0.11
Hf/Th	4.00	1.46	1.59	1.44	1.73	1.32	1.83
Ti/V	16.9	21.9	38.5	39.9	17.9	20.6	24.60
U/Pb	0.00	0.11	0.16	0.08	0.00	0.10	0.08
Ce/Nb	2.03	2.90	2.59	2.65	2.98	3.47	3.06
Th/Ta	2.00	5.42	5.29	5.19	5.79	6.79	6.12
Th/Sc	0.01	0.04	0.07	0.07	0.03	0.05	0.05
Th/Nb	0.10	0.31	0.28	0.28	0.27	0.37	0.33
Sc/Ni	0.32	0.43	0.52	0.52	0.33	0.39	0.38
Hf/Ta	8.00	7.92	8.43	7.50	10.00	8.93	8.16
FeO-T/MgO	1.16	1.27	2.13	1.96	1.33	1.48	1.58
Sm/Yb	1.01	1.00	1.17	1.20	1.04	1.19	1.12
Eu/Eu*	0.94	0.82	0.76	0.78	0.86	0.97	0.86
g(x)	4.28	4.33	4.99	5.05	4.20	4.44	4.57
Score 1	0.07	-0.16	-0.16	0.07	-0.55	-0.17	-0.06
Score 2	0.06	-0.09	-0.01	0.02	-0.07	-0.25	.00

Fe2O3-T ==> Total Fe as Fe2O3
NO ENTRY ==> No determination OR below detectability limi
MAJOR ELEMENTS ==> In weight percent
TRACE ELEMENTS ==> In parts per million

Machadodorp Formation, Transvaal Supergroup

SAMPLE	STD
SiO2	1.8
TiO2	0.33
Al2O3	0.9
Fe2O3-T	1.3
MgO	0.96
CaO	2.09
Na2O	0.76
K2O	0.24
MnO	0.02
P2O5	0.04
LOI	0.58
TOTAL	0.30
Rb	11.52
Ba	63
Cs	0.74
Sr	35
Pb	2.58
Th	0.99
U	0.2
Sc	6.66
V	38
Cr	177
Co	6
Ni	27
Y	11.59
Zr	35.18
Nb	2.38
Hf	0.98
Ta	0.12
La	3.51
Ce	7.23
Sm	1.23
Eu	0.32
Tb	0.27
Yb	0.83
Lu	0.14
Mg Number	4.50
K2O/Na2O	0.09
Na2O+K2O	0.89
Al2O3/TiO2	4.57

Machadodorp Formation, Transvaal Supergroup

SAMPLE	STD
CaO/TiO2	3.51
Zr/TiO2	.00
K/Rb	203.53
Ba/Sr	0.50
Rb/Sr	0.12
La/Yb	0.82
La/Sm	0.66
Sm/Eu	0.33
Ti/Zr	10.66
Zr/Nb	1.16
Nb/Y	0.01
Zr/Y	0.32
Nb/Ta	1.55
Nb/La	0.29
La/Ta	6.38
La/Th	1.71
Y/Tb	3.96
Th/Yb	0.30
Ta/Yb	0.01
Hf/Th	1.25
Ti/V	10.53
U/Pb	0.05
Ce/Nb	0.76
Th/Ta	2.92
Th/Sc	0.02
Th/Nb	0.18
Sc/Ni	0.09
Hf/Ta	0.80
FeO-T/MgO	0.30
Sm/Yb	0.14
Eu/Eu*	0.09
g(x)	0.30
Score 1	0.30
Score 2	0.12

Fe2O3-T ==> Total Fe as Fe2O3
NO ENTRY ==> No determination OR below detectability limi
MAJOR ELEMENTS ==> In weight percent
TRACE ELEMENTS ==> In parts per million
==========

Hekpoort Formation, Transvaal Supergroup

SAMPLE	C-31	CDV-6	CDV-7	CDV-8	CDV-9	CDV-10
SiO2	56.7	54.0	53.5	53.5	53.1	56.5
TiO2	0.6	0.72	0.4	0.59	0.54	0.59
Al2O3	15.1	14.6	10.0	14.1	13.6	14.7
Fe2O3-T	10.2	11.4	10.7	10.4	11.1	9.3
MgO	6.17	5.94	13.43	8.21	8.3	6.51
CaO	6.7	7.4	5.27	6.03	7.21	5.1
Na2O	2.33	2.07	0.95	2.56	1.41	2.24
K2O	0.87	1.5	0.32	1.49	1.67	2.29
MnO	0.13	0.15	0.17	0.16	0.14	0.11
P2O5	0.09	0.1	0.06	0.09	0.08	0.09
LOI	1.32	2.39	5.13	3.06	2.91	2.72
TOTAL	100.1	100.3	99.9	100.2	100.1	100.2
Rb	51.3	73.5	17.0	78.4	121.1	160.0
Ba	297	354	102	397	409	452
Cs	2.6	3.9	5.9	1.1	5.0	5.3
Sr	167	120	30	88	180	217
Pb	16.4	11.3	4.6	11.6	11.7	13.2
Th	9.7	8.1	4.1	7.6	6.8	9.2
U	2.60	3.20	1.70	3.50	3.00	4.30
Sc	26.1	35.7	33.2	30.2	29.4	26.3
V	187	235	192	192	190	183
Cr	273	74	1503	909	980	864
Co	39	41	60	49	50	40
Ni	100	78	308	164	178	139
Y	22.6	25.6	13.6	21.3	18.8	20.1
Zr	126.1	117.2	63.7	105.1	97.1	120.6
Nb	10.0	9.6	5.9	9.1	9.1	10.4
Hf	3.6	3.1	1.7	2.9	2.5	3.2
Ta	0.86	0.65	0.35	0.64	0.60	0.80
La	19.6	21.0	11.6	20.1	17.1	20.0
Ce	39.2	43.4	24.0	39.4	35.5	42.6
Sm	3.40	3.70	2.10	3.20	2.90	3.30
Eu	0.82	1.07	0.62	0.88	0.78	0.96
Tb	0.65	0.67	0.40	0.56	0.56	0.56
Yb	2.13	2.15	1.31	1.55	1.45	1.81
Lu	0.34	0.34	0.20	0.24	0.23	0.31
Mg Number	57.7	54.0	73.9	63.9	62.8	61.0
K2O/Na2O	0.37	0.72	0.34	0.58	1.18	1.02
Na2O+K2O	3.20	3.57	1.27	4.05	3.08	4.53
Al2O3/TiO2	25.1	20.3	25.1	23.9	25.2	24.9

Hekpoort Formation, Transvaal Supergroup

SAMPLE	C-31	CDV-6	CDV-7	CDV-8	CDV-9	CDV-10
CaO/TiO2	11.2	10.3	13.2	10.2	13.4	8.6
Zr/TiO2	0.021	0.016	0.016	0.018	0.018	0.020
K/Rb	140.8	169.4	156.2	157.7	114.5	118.8
Ba/Sr	1.78	2.95	3.46	4.53	2.27	2.08
Rb/Sr	0.307	0.613	0.576	0.895	0.671	0.737
La/Yb	9.2	9.8	8.9	13.0	11.8	11.0
La/Sm	5.8	5.7	5.5	6.3	5.9	6.1
Sm/Eu	4.1	3.5	3.4	3.6	3.7	3.4
Ti/Zr	28.5	36.9	37.7	33.7	33.4	29.4
Zr/Nb	12.6	12.2	10.8	11.5	10.7	11.6
Nb/Y	0.44	0.38	0.43	0.43	0.48	0.52
Zr/Y	5.6	4.6	4.7	4.9	5.2	6.0
Nb/Ta	11.6	14.8	16.9	14.2	15.2	13.0
Nb/La	0.51	0.46	0.51	0.45	0.53	0.52
La/Ta	22.8	32.3	33.1	31.4	28.5	25.0
La/Th	2.0	2.6	2.8	2.6	2.5	2.2
Y/Tb	34.8	38.2	34.0	38.0	33.6	35.9
Th/Yb	4.55	3.77	3.13	4.90	4.69	5.08
Ta/Yb	0.404	0.302	0.267	0.413	0.414	0.442
Hf/Th	0.37	0.38	0.41	0.38	0.37	0.35
Ti/V	19.3	18.4	12.5	18.4	17.1	19.3
U/Pb	0.16	0.28	0.37	0.30	0.26	0.33
Ce/Nb	3.92	4.52	4.07	4.33	3.90	4.10
Th/Ta	11.28	12.46	11.71	11.88	11.33	11.50
Th/Sc	0.37	0.23	0.12	0.25	0.23	0.35
Th/Nb	0.97	0.84	0.69	0.84	0.75	0.88
Sc/Ni	0.26	0.46	0.11	0.18	0.17	0.19
Hf/Ta	4.19	4.77	4.86	4.53	4.17	4.00
FeO-T/MgO	1.48	1.72	0.71	1.14	1.20	1.29
Sm/Yb	1.60	1.72	1.60	2.06	2.00	1.82
Eu/Eu*	0.69	0.84	0.85	0.81	0.77	0.86
g(x)	4.57	4.54	3.73	4.34	4.45	4.59
Score 1	0.76	0.37	-0.29	0.26	0.95	1.03
Score 2	-0.16	-0.14	-0.29	-0.20	-0.11	-0.18

Fe2O3-T ==> Total Fe as Fe2O3
NO ENTRY ==> No determination OR below detectability limi
MAJOR ELEMENTS ==> In weight percent
TRACE ELEMENTS ==> In parts per million

Hekpoort Formation, Transvaal Supergroup

SAMPLE	CDV11d	CDV11e	WBK-6	WBK-9	D-105	AVG-1	STD-1
SiO2	56.3	55.1	53.5	56.3	71.4	56.4	4.9
TiO2	0.58	0.59	0.59	0.58	0.43	0.56	0.08
Al2O3	14.8	14.8	14.5	14.9	10.7	13.8	1.7
Fe2O3-T	10.1	10.0	10.4	10.0	9.1	10.2	0.6
MgO	5.47	6.05	8.19	5.54	1.53	6.85	2.75
CaO	5.96	6.29	5.72	6.78	0.35	5.71	1.83
Na2O	2.21	2.1	2.66	1.39	2.67	2.05	0.54
K2O	1.95	2.62	1.07	1.81	1.87	1.59	0.62
MnO	0.14	0.14	0.14	0.12	0.04	0.13	0.03
P2O5	0.09	0.09	0.08	0.09	0.07	0.08	0.01
LOI	2.96	2.35	3.42	2.42	1.86	2.78	0.93
TOTAL	100.5	100.1	100.2	100.0	100.1	100.1	0.1
Rb	114.7	165.0	47.9	98.4	60.3	89.78	44.78
Ba	478	589	247	322	1292	449	293
Cs	3.8	5.1	3.7	3.8	2.8	3.91	1.33
Sr	187	239	71	271	165	158	71
Pb	19.5	16.9	10.1	14.8	7.0	12.46	4.16
Th	9.5	9.3	7.4	9.7	17.4	8.98	3.11
U	4.20	3.50	3.00	4.00	5.90	3.54	1.03
Sc	25.1	24.9	28.8	25.4	7.2	26.57	6.98
V	176	176	191	183	71	180	38
Cr	436	508	479	452	126	600	405
Co	39	40	45	39	7	41	12
Ni	104	114	143	109	22	133	69
Y	22.3	22.2	20.9	21.9	26.2	21.41	3.21
Zr	121.6	121.5	103.7	122.4	257.6	123.33	45.78
Nb	10.3	9.9	8.7	10.5	14.0	9.77	1.81
Hf	3.3	3.1	2.7	3.3	7.7	3.37	1.45
Ta	0.84	0.90	0.66	0.84	1.00	0.74	0.17
La	21.9	22.6	19.1	21.9	49.8	22.25	9.18
Ce	45.6	46.4	37.3	46.6	101.5	45.59	18.73
Sm	3.60	3.70	3.39	3.60	6.36	3.57	0.99
Eu	0.86	0.82	0.79	0.88	0.97	0.86	0.11
Tb	0.53	0.57	0.65	0.61	0.80	0.60	0.10
Yb	1.79	1.86	1.90	1.96	2.52	1.86	0.33
Lu	0.29	0.29	0.29	0.31	0.38	0.29	0.05
Mg Number	55.0	57.6	64.0	55.4	27.5	57.53	10.94
K2O/Na2O	0.88	1.25	0.40	1.30	0.70	0.80	0.34
Na2O+K2O	4.16	4.72	3.73	3.20	4.54	3.64	0.93
Al2O3/TiO2	25.5	25.1	24.5	25.7	24.9	24.56	1.43

Hekpoort Formation, Transvaal Supergroup

SAMPLE	CDV11d	CDV11e	WBK-6	WBK-9	D-105	AVG-1	STD-1
CaO/TiO2	10.3	10.7	9.7	11.7	0.8	10.00	3.20
Zr/TiO2	0.021	0.021	0.018	0.021	0.060	0.02	0.01
K/Rb	141.1	131.8	185.4	152.7	257.4	156.89	37.51
Ba/Sr	2.55	2.46	3.50	1.19	7.83	3.15	1.72
Rb/Sr	0.612	0.690	0.679	0.363	0.365	0.59	0.17
La/Yb	12.2	12.2	10.1	11.2	19.8	11.73	2.84
La/Sm	6.1	6.1	5.6	6.1	7.8	6.09	0.60
Sm/Eu	4.2	4.5	4.3	4.1	6.6	4.13	0.85
Ti/Zr	28.6	29.1	34.1	28.4	10.0	29.98	7.10
Zr/Nb	11.8	12.3	11.9	11.7	18.4	12.32	2.00
Nb/Y	0.46	0.45	0.42	0.48	0.53	0.46	0.04
Zr/Y	5.5	5.5	5.0	5.6	9.8	5.66	1.38
Nb/Ta	12.3	11.0	13.2	12.5	14.0	13.51	1.63
Nb/La	0.47	0.44	0.46	0.48	0.28	0.46	0.07
La/Ta	26.1	25.1	28.9	26.1	49.8	29.92	7.03
La/Th	2.3	2.4	2.6	2.3	2.9	2.47	0.25
Y/Tb	42.1	38.9	32.2	35.9	32.8	36.03	2.88
Th/Yb	5.31	5.00	3.89	4.95	6.90	4.74	0.93
Ta/Yb	0.469	0.484	0.347	0.429	0.397	0.40	0.06
Hf/Th	0.35	0.33	0.36	0.34	0.44	0.37	0.03
Ti/V	19.8	20.1	18.5	19.0	36.3	19.89	5.57
U/Pb	0.22	0.21	0.30	0.27	0.84	0.32	0.17
Ce/Nb	4.43	4.69	4.29	4.44	7.25	4.54	0.89
Th/Ta	11.31	10.33	11.21	11.55	17.40	12.00	1.78
Th/Sc	0.38	0.37	0.26	0.38	2.42	0.49	0.62
Th/Nb	0.92	0.94	0.85	0.92	1.24	0.90	0.13
Sc/Ni	0.24	0.22	0.20	0.23	0.33	0.24	0.09
Hf/Ta	3.93	3.44	4.09	3.93	7.70	4.51	1.08
FeO-T/MgO	1.65	1.49	1.14	1.63	5.34	1.71	1.18
Sm/Yb	2.01	1.99	1.78	1.84	2.52	1.90	0.25
Eu/Eu*	0.73	0.67	0.67	0.73	0.48	0.74	0.11
g(x)	4.57	4.64	4.28	4.66	4.70	4.46	0.26
Score 1	0.87	1.07	0.09	1.19	0.76	0.64	0.45
Score 2	-0.12	-0.09	-0.24	-0.08	-0.34	-0.18	0.08

Fe2O3-T ==> Total Fe as Fe2O3
NO ENTRY ==> No determination OR below detectability limi
MAJOR ELEMENTS ==> In weight percent
TRACE ELEMENTS ==> In parts per million

Hekpoort Formation, Transvaal Supergroup

SAMPLE	AVG-2	STD-2
SiO2	54.8	1.4
TiO2	0.58	0.07
Al2O3	14.1	1.4
Fe2O3-T	10.3	0.6
MgO	7.38	2.28
CaO	6.25	0.74
Na2O	1.99	0.53
K2O	1.56	0.64
MnO	0.14	0.02
P2O5	0.09	0.01
LOI	2.87	0.93
TOTAL	100.1	0.2
Rb	92.73	45.94
Ba	365	128
Cs	4.02	1.34
Sr	157	74
Pb	13.01	3.97
Th	8.14	1.68
U	3.30	0.75
Sc	28.51	3.50
V	191	16
Cr	648	395
Co	44	7
Ni	144	62
Y	20.93	2.97
Zr	109.90	17.94
Nb	9.35	1.29
Hf	2.94	0.51
Ta	0.71	0.16
La	19.49	3.04
Ce	40.00	6.47
Sm	3.29	0.46
Eu	0.85	0.11
Tb	0.58	0.07
Yb	1.79	0.26
Lu	0.28	0.04
Mg Number	60.53	5.69
K2O/Na2O	0.81	0.36
Na2O+K2O	3.55	0.93
Al2O3/TiO2	24.52	1.50

Hekpoort Formation, Transvaal Supergroup

SAMPLE	AVG-2	STD-2
CaO/TiO2	10.92	1.40
Zr/TiO2	0.02	.00
K/Rb	146.84	20.90
Ba/Sr	2.68	0.92
Rb/Sr	0.61	0.16
La/Yb	10.92	1.33
La/Sm	5.91	0.24
Sm/Eu	3.89	0.38
Ti/Zr	31.98	3.41
Zr/Nb	11.71	0.58
Nb/Y	0.45	0.04
Zr/Y	5.24	0.43
Nb/Ta	13.46	1.70
Nb/La	0.48	0.03
La/Ta	27.93	3.31
La/Th	2.44	0.23
Y/Tb	36.36	2.82
Th/Yb	4.53	0.66
Ta/Yb	0.40	0.07
Hf/Th	0.37	0.02
Ti/V	18.24	2.08
U/Pb	0.27	0.06
Ce/Nb	4.27	0.25
Th/Ta	11.46	0.51
Th/Sc	0.29	0.08
Th/Nb	0.86	0.08
Sc/Ni	0.23	0.09
Hf/Ta	4.19	0.40
FeO-T/MgO	1.35	0.29
Sm/Yb	1.84	0.16
Eu/Eu*	0.76	0.07
g(x)	4.44	0.26
Score 1	0.63	0.47
Score 2	-0.16	0.06

Fe2O3-T ==> Total Fe as Fe2O3
NO ENTRY ==> No determination OR below detectability limi
MAJOR ELEMENTS ==> In weight percent
TRACE ELEMENTS ==> In parts per million

Abel Erasmus Formation, Transvaal Supergroup

SAMPLE	D-37	D-38	D-39	D-40	AVG
SiO2	50.2	46.7	47.5	49.7	48.5
TiO2	2.02	2.1	2.25	1.66	2.01
Al2O3	13.5	12.9	13.2	15.1	13.7
Fe2O3-T	14.6	12.3	15.8	12.3	13.8
MgO	7.26	6.42	7.35	4.98	6.50
CaO	5.16	8.58	6.61	8.82	7.29
Na2O	2.77	0.94	0.09	2.18	1.50
K2O	1.01	1.79	1.31	1.88	1.50
MnO	0.18	0.11	0.1	0.13	0.13
P2O5	0.42	0.4	0.43	0.23	0.37
LOI	3.43	7.98	5.34	2.91	4.92
TOTAL	100.5	100.2	100.1	100.0	100.2
Rb	31.6	42.0	30.9	43.0	36.88
Ba	245	705	465	330	436
Cs	6.1	0.7	1.1	4.4	3.08
Sr	96	51	34	390	143
Pb	3.1	2.8	3.0	5.3	3.55
Th	4.2	4.0	4.5	2.8	3.88
U	1.0	0.8	1.5	0.8	1.0
Sc	31.9	14.7	32.8	31.6	27.75
V	315	319	323	296	313
Cr	111	80	84	70	86
Co	50	26	65	34	44
Ni	58	47	55	54	54
Y	51.4	55.4	31.0	44.6	45.60
Zr	297.1	306.7	317.8	200.3	280.48
Nb	19.6	20.0	20.0	12.6	18.05
Hf	7.6	4.4	9.9	5.1	6.75
Ta	1.04	0.48	1.43	0.65	0.90
La	29.2	30.3	9.3	22.1	22.73
Ce	69.1	62.2	22.5	50.1	50.98
Sm	8.03	5.00	3.11	6.27	5.60
Eu	1.98	1.45	0.49	2.12	1.51
Tb	1.28	0.73	0.68	1.29	1.00
Yb	4.84	1.92	5.08	4.19	4.01
Lu	0.77	0.29	0.88	0.64	0.65
Mg Number	52.7	53.9	51.1	47.6	51.33
K2O/Na2O	0.36	1.90	14.56	0.86	4.42
Na2O+K2O	3.78	2.73	1.40	4.06	2.99
Al2O3/TiO2	6.7	6.1	5.9	9.1	6.94

Abel Erasmus Formation, Transvaal Supergroup

SAMPLE	D-37	D-38	D-39	D-40	AVG
CaO/TiO2	2.6	4.1	2.9	5.3	3.72
Zr/TiO2	0.015	0.015	0.014	0.012	0.01
K/Rb	265.3	353.7	351.9	362.9	333.45
Ba/Sr	2.56	13.93	13.52	0.85	7.71
Rb/Sr	0.330	0.830	0.898	0.110	0.54
La/Yb	6.0	15.8	1.8	5.3	7.23
La/Sm	3.6	6.1	3.0	3.5	4.05
Sm/Eu	4.1	3.4	6.3	3.0	4.20
Ti/Zr	40.8	41.1	42.5	49.7	43.52
Zr/Nb	15.2	15.3	15.9	15.9	15.57
Nb/Y	0.38	0.36	0.65	0.28	0.42
Zr/Y	5.8	5.5	10.3	4.5	6.51
Nb/Ta	18.8	41.7	14.0	19.4	23.47
Nb/La	0.67	0.66	2.15	0.57	1.01
La/Ta	28.1	63.1	6.5	34.0	32.93
La/Th	7.0	7.6	2.1	7.9	6.12
Y/Tb	40.2	75.9	45.6	34.6	49.05
Th/Yb	0.87	2.08	0.89	0.67	1.13
Ta/Yb	0.215	0.250	0.281	0.155	0.23
Hf/Th	1.81	1.10	2.20	1.82	1.73
Ti/V	38.5	39.5	41.8	33.6	38.35
U/Pb	0.32	0.29	0.50	0.15	0.31
Ce/Nb	3.53	3.11	1.13	3.98	2.93
Th/Ta	4.04	8.33	3.15	4.31	4.96
Th/Sc	0.13	0.27	0.14	0.09	0.16
Th/Nb	0.21	0.20	0.23	0.22	0.22
Sc/Ni	0.55	0.31	0.60	0.59	0.51
Hf/Ta	7.31	9.17	6.92	7.85	7.81
FeO-T/MgO	1.81	1.73	1.94	2.22	1.93
Sm/Yb	1.66	2.60	0.61	1.50	1.59
Eu/Eu*	0.74	0.89	0.44	0.95	0.76
g(x)	5.15	5.03	4.81	5.32	5.08
Score 1	-0.54	-1.12	-1.24	0.79	-0.53
Score 2	-0.53	-0.61	-1.14	-0.13	-0.60

Fe2O3-T ==> Total Fe as Fe2O3
NO ENTRY ==> No determination OR below detectability limi
MAJOR ELEMENTS ==> In weight percent
TRACE ELEMENTS ==> In parts per million

Abel Erasmus Formation, Transvaal Supergroup

SAMPLE	STD
SiO2	1.5
TiO2	0.22
Al2O3	0.9
Fe2O3-T	1.5
MgO	0.95
CaO	1.50
Na2O	1.05
K2O	0.36
MnO	0.03
P2O5	0.08
LOI	1.99
TOTAL	0.2
Rb	5.64
Ba	174
Cs	2.26
Sr	144
Pb	1.02
Th	0.65
U	0.3
Sc	7.55
V	10
Cr	15
Co	15
Ni	4
Y	9.27
Zr	46.87
Nb	3.15
Hf	2.17
Ta	0.37
La	8.37
Ce	17.79
Sm	1.80
Eu	0.64
Tb	0.29
Yb	1.25
Lu	0.22
Mg Number	2.36
K2O/Na2O	5.88
Na2O+K2O	1.04
Al2O3/TiO2	1.28

Abel Erasmus Formation, Transvaal Supergroup

SAMPLE	STD
CaO/TiO2	1.08
Zr/TiO2	.00
K/Rb	39.57
Ba/Sr	6.04
Rb/Sr	0.33
La/Yb	5.18
La/Sm	1.18
Sm/Eu	1.30
Ti/Zr	3.64
Zr/Nb	0.33
Nb/Y	0.14
Zr/Y	2.21
Nb/Ta	10.71
Nb/La	0.66
La/Ta	20.22
La/Th	2.37
Y/Tb	15.98
Th/Yb	0.56
Ta/Yb	0.05
Hf/Th	0.40
Ti/V	2.97
U/Pb	0.12
Ce/Nb	1.09
Th/Ta	2.00
Th/Sc	0.07
Th/Nb	0.01
Sc/Ni	0.12
Hf/Ta	0.85
FeO-T/MgO	0.19
Sm/Yb	0.71
Eu/Eu*	0.20
g(x)	0.18
Score 1	0.80
Score 2	0.36

Fe2O3-T ==> Total Fe as Fe2O3
NO ENTRY ==> No determination OR below detectability limi
MAJOR ELEMENTS ==> In weight percent
TRACE ELEMENTS ==> In parts per million

Ngwanedzi Fm, Soutpansberg Group

SAMPLE	C-132	C-137	C-189	C-190	C-191
SiO2	47.3	48.5	49.3	48.6	49.5
TiO2	1.40	0.73	1.49	1.54	1.63
Al2O3	15.7	15.7	14.9	15.5	14.7
Fe2O3-T	14.9	11.0	14.0	14.2	14.3
MgO	7.60	9.52	6.45	6.90	6.57
CaO	7.14	9.95	8.30	8.83	9.17
Na2O	2.51	1.86	2.54	2.14	2.05
K2O	0.51	0.44	0.24	0.54	0.54
MnO	0.28	0.15	0.18	0.18	0.18
P2O5	0.15	0.04	0.15	0.13	0.14
LOI	2.45	3.38	2.87	1.56	1.72
TOTAL	100.05	101.32	100.40	100.12	100.45
Rb	16.3	10.4	8.2	12.4	12.3
Ba	291	320	285	301	300
Cs	0.1	0.2	0.2	0.1	0.2
Sr	126	146	186	161	193
Pb	8.5	6.5	5.6	6.7	7.0
Th	3.4	0.6	2.1	2.2	2.1
U	0.9		0.4		0.2
Sc	51.3	31.9	34.7	41.2	38.4
V	357	237	304	289	325
Cr	205	293	118	91	136
Co	62	52	48	61	49
Ni	86	185	106	109	89
Y	40.4	14.4	35.6	32.2	33.3
Zr	133.2	55.9	137.4	125.0	130.3
Nb	9.2	5.2	9.6	9.5	9.6
Hf	4.4	1.4	3.6	3.9	3.8
Ta	0.48	0.11	0.47	0.53	0.49
La	15.2	4.7	13.6	15.7	12.7
Ce	33.5	10.8	32.3	37.1	28.4
Sm	5.29	2.04	4.92	5.04	4.72
Eu	1.52	0.68	1.46	1.75	1.45
Tb	1.05	0.45	0.97	0.99	0.89
Yb	3.96	1.33	2.89	3.25	2.98
Lu	0.65	0.20	0.47	0.53	0.50
Mg Number	53.4	66.1	50.8	52.2	50.8
K2O/Na2O	0.20	0.24	0.09	0.25	0.26
Na2O+K2O	3.02	2.30	2.78	2.68	2.59
Al2O3/TiO2	11.2	21.5	10.0	10.0	9.0

Ngwanedzi Fm, Soutpansberg Group

SAMPLE	C-132	C-137	C-189	C-190	C-191
CaO/TiO2	5.1	13.6	5.6	5.7	5.6
Zr/TiO2	0.010	0.008	0.009	0.008	0.008
K/Rb	259.7	351.2	242.9	361.5	364.4
Ba/Sr	2.30	2.20	1.53	1.87	1.55
Rb/Sr	0.129	0.071	0.044	0.077	0.064
La/Yb	3.8	3.5	4.7	4.8	4.3
La/Sm	2.9	2.3	2.8	3.1	2.7
Sm/Eu	3.5	3.0	3.4	2.9	3.3
Ti/Zr	63.1	78.4	65.1	73.9	75.1
Zr/Nb	14.5	10.8	14.3	13.2	13.6
Nb/Y	0.23	0.36	0.27	0.30	0.29
Zr/Y	3.3	3.9	3.9	3.9	3.9
Nb/Ta	19.2	47.3	20.4	17.9	19.6
Nb/La	0.61	1.11	0.71	0.61	0.76
La/Ta	31.7	42.7	28.9	29.6	25.9
La/Th	4.5	7.8	6.5	7.1	6.0
Y/Tb	38.5	32.0	36.7	32.5	37.4
Th/Yb	0.86	0.45	0.73	0.68	0.70
Ta/Yb	0.121	0.083	0.163	0.163	0.164
Hf/Th	1.29	2.33	1.71	1.77	1.81
Ti/V	23.5	18.5	29.4	32.0	30.1
U/Pb	0.11	0.00	0.07	0.00	0.03
Ce/Nb	3.64	2.08	3.36	3.91	2.96
Th/Ta	7.08	5.45	4.47	4.15	4.29
Th/Sc	0.07	0.02	0.06	0.05	0.05
Th/Nb	0.37	0.12	0.22	0.23	0.22
Sc/Ni	0.60	0.17	0.33	0.38	0.43
Hf/Ta	9.17	12.73	7.66	7.36	7.76
FeO-T/MgO	1.77	1.04	1.96	1.85	1.96
Sm/Yb	1.34	1.53	1.70	1.55	1.58
Eu/Eu*	0.82	0.92	0.85	0.99	0.89
g(x)	4.87	4.27	4.96	4.88	4.96
Score 1	-0.03	0.80	0.32	0.24	0.35
Score 2	-0.10	-0.13	-0.17	-0.22	-0.21

Fe2O3-T ==> Total Fe as Fe2O3
NO ENTRY ==> No determination OR below detectability limi
MAJOR ELEMENTS ==> In weight percent
TRACE ELEMENTS ==> In parts per million

Ngwanedzi Fm, Soutpansberg Group

SAMPLE	C-192	C-194	C-195	AVG	STD
SiO2	49.1	48.3	49.8	48.8	0.7
TiO2	1.61	1.59	1.51	1.44	0.28
Al2O3	15.1	15.0	14.6	15.1	0.4
Fe2O3-T	14.0	14.5	14.4	13.9	1.1
MgO	6.52	6.87	6.52	7.12	0.97
CaO	9.64	8.89	9.18	8.89	0.81
Na2O	1.79	2.15	2.02	2.13	0.25
K2O	0.61	0.31	0.75	0.49	0.15
MnO	0.19	0.19	0.18	0.19	0.04
P2O5	0.15	0.14	0.16	0.13	0.04
LOI	1.64	2.43	1.51	2.20	0.65
TOTAL	100.34	100.47	100.57	100.47	0.36
Rb	13.6	9.0	16.0	12.28	2.80
Ba	335	406	371	326	40
Cs	0.2	0.1	0.3	0.18	0.07
Sr	203	203	170	174	26
Pb	8.4	7.0	6.3	7.00	0.94
Th	2.0	2.1	2.7	2.15	0.73
U	0.3	0.1	0.6	0.4	0.3
Sc	35.3	44.8	36.8	39.30	5.88
V	301	329	361	313	37
Cr	124	116	100	148	64
Co	50	61	49	54	6
Ni	97	107	90	109	30
Y	35.2	34.4	36.7	32.78	7.32
Zr	139.6	126.5	150.9	124.85	27.18
Nb	9.9	9.7	11.1	9.23	1.61
Hf	3.9	4.1	4.1	3.65	0.88
Ta	0.52	0.49	0.53	0.45	0.13
La	15.1	16.3	16.6	13.74	3.63
Ce	33.9	34.8	36.8	30.95	8.03
Sm	4.96	5.42	5.17	4.70	1.02
Eu	1.56	1.80	1.59	1.48	0.32
Tb	0.96	1.09	1.02	0.93	0.19
Yb	3.05	3.39	3.09	2.99	0.70
Lu	0.50	0.58	0.54	0.50	0.12
Mg Number	51.1	51.5	50.5	53.30	4.90
K2O/Na2O	0.34	0.14	0.37	0.24	0.09
Na2O+K2O	2.40	2.46	2.77	2.63	0.22
Al2O3/TiO2	9.3	9.5	9.7	11.29	3.93

Ngwanedzi Fm, Soutpansberg Group

SAMPLE	C-192	C-194	C-195	AVG	STD
CaO/TiO2	6.0	5.6	6.1	6.66	2.65
Zr/TiO2	0.009	0.008	0.010	0.01	.00
K/Rb	372.3	285.9	389.1	328.36	52.85
Ba/Sr	1.65	2.00	2.18	1.91	0.29
Rb/Sr	0.067	0.044	0.094	0.07	0.03
La/Yb	5.0	4.8	5.4	4.54	0.57
La/Sm	3.0	3.0	3.2	2.88	0.27
Sm/Eu	3.2	3.0	3.3	3.18	0.19
Ti/Zr	69.2	75.4	60.0	70.01	6.25
Zr/Nb	14.1	13.0	13.6	13.38	1.10
Nb/Y	0.28	0.28	0.30	0.29	0.03
Zr/Y	4.0	3.7	4.1	3.82	0.23
Nb/Ta	19.0	19.8	20.9	23.02	9.21
Nb/La	0.66	0.60	0.67	0.71	0.16
La/Ta	29.0	33.3	31.3	31.56	4.70
La/Th	7.6	7.8	6.1	6.68	1.06
Y/Tb	36.7	31.6	36.0	35.17	2.53
Th/Yb	0.66	0.62	0.87	0.70	0.13
Ta/Yb	0.170	0.145	0.172	0.15	0.03
Hf/Th	1.95	1.95	1.52	1.79	0.29
Ti/V	32.1	29.0	25.1	27.46	4.42
U/Pb	0.04	0.01	0.10	0.04	0.04
Ce/Nb	3.42	3.59	3.32	3.28	0.52
Th/Ta	3.85	4.29	5.09	4.83	0.98
Th/Sc	0.06	0.05	0.07	0.05	0.02
Th/Nb	0.20	0.22	0.24	0.23	0.07
Sc/Ni	0.36	0.42	0.41	0.39	0.11
Hf/Ta	7.50	8.37	7.74	8.53	1.68
FeO-T/MgO	1.93	1.90	1.98	1.80	0.29
Sm/Yb	1.63	1.60	1.67	1.58	0.11
Eu/Eu*	0.90	0.94	0.88	0.90	0.05
g(x)	5.00	4.96	4.97	4.86	0.23
Score 1	0.37	0.39	0.22	0.34	0.22
Score 2	-0.20	-0.15	-0.21	-0.17	0.04

Fe2O3-T ==> Total Fe as Fe2O3
NO ENTRY ==> No determination OR below detectability limi
MAJOR ELEMENTS ==> In weight percent
TRACE ELEMENTS ==> In parts per million

Sabasa Fm, Soutpansberg Group

SAMPLE	D-10	D-12	C-108	C-109	C-111
SiO2	50.3	50.9	49.3	49.4	49.2
TiO2	1.65	1.01	1.11	1.12	1.18
Al2O3	14.0	14.0	15.0	14.8	15.5
Fe2O3-T	14.7	13.2	13.7	13.2	13.5
MgO	6.01	6.83	7.06	6.75	7.29
CaO	8.43	7.82	8.96	9.04	7.39
Na2O	2.1	2.81	2.66	2.85	3.05
K2O	0.44	0.1	0.13	0.25	0.88
MnO	0.18	0.17	0.19	0.17	0.2
P2O5	0.19	0.1	0.11	0.11	0.11
LOI	2.18	3.27	2.46	2.47	1.86
TOTAL	100.12	100.21	100.59	100.20	100.11
Rb	19.5	2.8	6.5	9.3	38.5
Ba	231	25	85	113	426
Cs	0.1	0.1	0.1	0.7	0.3
Sr	171	81	149	173	145
Pb	9.7	9.2	10.8	4.2	7.2
Th	5.4	4.6	2.1	2.1	2.7
U	1.3	1.2	0.5	0.6	0.4
Sc	32.7	32.7	36.9	37.1	37.6
V	359	274	287	304	297
Cr	76	63	195	205	236
Co	49	61	51	56	58
Ni	73	127	102	110	114
Y	39.2	25.9	28.1	25.9	27.5
Zr	160.7	104.6	102.5	103.3	102.7
Nb	12.2	8.4	8.5	7.6	8.1
Hf	4.1	3.1	2.7	2.7	2.6
Ta	0.62	0.40	0.30	0.34	0.34
La	19.7	15.3	10.6	11.5	11.5
Ce	43.3	32.3	23.4	24.1	24.3
Sm	5.56	3.96	3.51	3.65	3.57
Eu	1.59	1.10	1.13	1.00	1.15
Tb	1.00	0.73	0.77	0.69	0.76
Yb	3.25	2.17	2.49	2.37	2.45
Lu	0.53	0.33	0.40	0.37	0.38
Mg Number	47.9	53.7	53.7	53.4	54.9
K2O/Na2O	0.21	0.04	0.05	0.09	0.29
Na2O+K2O	2.54	2.91	2.79	3.10	3.93
Al2O3/TiO2	8.5	13.9	13.5	13.2	13.1

Sabasa Fm, Soutpansberg Group

SAMPLE	D-10	D-12	C-108	C-109	C-111
CaO/TiO2	5.1	7.7	8.1	8.1	6.3
Zr/TiO2	0.010	0.010	0.009	0.009	0.009
K/Rb	187.3	296.4	166.0	223.1	189.7
Ba/Sr	1.35	0.31	0.57	0.65	2.94
Rb/Sr	0.114	0.034	0.044	0.054	0.266
La/Yb	6.1	7.1	4.3	4.9	4.7
La/Sm	3.5	3.9	3.0	3.2	3.2
Sm/Eu	3.5	3.6	3.1	3.7	3.1
Ti/Zr	61.6	57.9	65.0	65.1	68.9
Zr/Nb	13.2	12.5	12.1	13.6	12.7
Nb/Y	0.31	0.32	0.30	0.29	0.29
Zr/Y	4.1	4.0	3.6	4.0	3.7
Nb/Ta	19.7	21.0	28.3	22.4	23.8
Nb/La	0.62	0.55	0.80	0.66	0.70
La/Ta	31.8	38.3	35.3	33.8	33.8
La/Th	3.6	3.3	5.0	5.5	4.3
Y/Tb	39.2	35.5	36.5	37.5	36.2
Th/Yb	1.66	2.12	0.84	0.89	1.10
Ta/Yb	0.191	0.184	0.120	0.143	0.139
Hf/Th	0.76	0.67	1.29	1.29	0.96
Ti/V	27.6	22.1	23.2	22.1	23.8
U/Pb	0.13	0.13	0.05	0.14	0.06
Ce/Nb	3.55	3.85	2.75	3.17	3.00
Th/Ta	8.71	11.50	7.00	6.18	7.94
Th/Sc	0.17	0.14	0.06	0.06	0.07
Th/Nb	0.44	0.55	0.25	0.28	0.33
Sc/Ni	0.45	0.26	0.36	0.34	0.33
Hf/Ta	6.61	7.75	9.00	7.94	7.65
FeO-T/MgO	2.20	1.74	1.74	1.76	1.66
Sm/Yb	1.71	1.82	1.41	1.54	1.46
Eu/Eu*	0.84	0.81	0.89	0.79	0.90
g(x)	5.02	4.50	4.69	4.72	4.70
Score 1	0.17	-0.08	0.36	0.51	0.32
Score 2	-0.23	-0.25	-0.11	-0.16	-0.15

Fe2O3-T ==> Total Fe as Fe2O3
NO ENTRY ==> No determination OR below detectability limi
MAJOR ELEMENTS ==> In weight percent
TRACE ELEMENTS ==> In parts per million

Sabasa Fm, Soutpansberg Group

SAMPLE	C-112	C-113	C-114	C-115	C-116
SiO2	49.4	49.0	50.1	49.9	50.0
TiO2	1.09	1.16	1.11	1.09	1.1
Al2O3	15.1	14.7	14.5	15.0	14.8
Fe2O3-T	13.7	13.5	13.4	13.1	13.0
MgO	8.31	7.59	7.55	6.79	6.86
CaO	7.33	8.72	7.64	9.86	9.75
Na2O	2.29	2.61	2.83	2.09	2.25
K2O	0.43	0.38	0.59	0.48	0.32
MnO	0.21	0.19	0.21	0.2	0.18
P2O5	0.11	0.11	0.11	0.1	0.11
LOI	2.35	2.26	2.2	1.71	1.75
TOTAL	100.26	100.13	100.30	100.30	100.14
Rb	15.4	14.5	17.9	18.3	12.5
Ba	149	139	330	249	129
Cs	0.7	0.4	0.9	0.7	0.3
Sr	180	114	191	161	122
Pb	6.3	4.7	24.2	5.6	10.1
Th	2.2	2.0	2.2	2.0	2.1
U	0.5	0.6	0.5	0.4	0.6
Sc	37.6	43.1	39.5	37.2	37.4
V	266	284	277	287	276
Cr	195	150	202	192	197
Co	57	63	54	55	52
Ni	118	105	112	117	105
Y	27.5	29.2	29.4	28.9	38.1
Zr	100.7	101.7	99.8	98.7	101.7
Nb	8.0	7.7	8.1	8.1	8.0
Hf	2.7	3.0	2.7	2.5	2.7
Ta	0.32	0.42	0.37	0.31	0.30
La	9.5	11.8	10.7	10.1	10.2
Ce	23.4	25.9	24.8	21.7	24.8
Sm	3.54	3.93	3.69	3.42	3.61
Eu	1.04	1.33	1.08	1.13	1.10
Tb	0.71	0.87	0.78	0.73	0.79
Yb	2.54	2.80	2.52	2.46	2.53
Lu	0.41	0.45	0.41	0.38	0.41
Mg Number	57.6	55.9	55.8	53.8	54.3
K2O/Na2O	0.19	0.15	0.21	0.23	0.14
Na2O+K2O	2.72	2.99	3.42	2.57	2.57
Al2O3/TiO2	13.8	12.7	13.1	13.8	13.5

Sabasa Fm, Soutpansberg Group

SAMPLE	C-112	C-113	C-114	C-115	C-116
CaO/TiO2	6.7	7.5	6.9	9.0	8.9
Zr/TiO2	0.009	0.009	0.009	0.009	0.009
K/Rb	231.8	217.5	273.6	217.7	212.5
Ba/Sr	0.83	1.22	1.73	1.55	1.05
Rb/Sr	0.086	0.127	0.094	0.114	0.102
La/Yb	3.7	4.2	4.2	4.1	4.0
La/Sm	2.7	3.0	2.9	3.0	2.8
Sm/Eu	3.4	3.0	3.4	3.0	3.3
Ti/Zr	64.9	68.4	66.7	66.3	64.9
Zr/Nb	12.6	13.2	12.3	12.2	12.7
Nb/Y	0.29	0.26	0.28	0.28	0.21
Zr/Y	3.7	3.5	3.4	3.4	2.7
Nb/Ta	25.0	18.3	21.9	26.1	26.7
Nb/La	0.84	0.65	0.76	0.80	0.78
La/Ta	29.7	28.1	28.9	32.6	34.0
La/Th	4.3	5.9	4.9	5.1	4.9
Y/Tb	38.7	33.6	37.7	39.6	48.2
Th/Yb	0.87	0.71	0.87	0.81	0.83
Ta/Yb	0.126	0.150	0.147	0.126	0.119
Hf/Th	1.23	1.50	1.23	1.25	1.29
Ti/V	24.6	24.5	24.0	22.8	23.9
U/Pb	0.08	0.13	0.02	0.07	0.06
Ce/Nb	2.93	3.36	3.06	2.68	3.10
Th/Ta	6.88	4.76	5.95	6.45	7.00
Th/Sc	0.06	0.05	0.06	0.05	0.06
Th/Nb	0.28	0.26	0.27	0.25	0.26
Sc/Ni	0.32	0.41	0.35	0.32	0.36
Hf/Ta	8.44	7.14	7.30	8.06	9.00
FeO-T/MgO	1.49	1.60	1.60	1.74	1.70
Sm/Yb	1.39	1.40	1.46	1.39	1.43
Eu/Eu*	0.83	0.93	0.82	0.92	0.84
g(x)	4.73	4.65	4.76	4.71	4.72
Score 1	0.53	0.11	0.55	0.42	0.08
Score 2	-0.08	-0.14	-0.02	-0.05	0.09

Fe2O3-T ==> Total Fe as Fe2O3
NO ENTRY ==> No determination OR below detectability limi
MAJOR ELEMENTS ==> In weight percent
TRACE ELEMENTS ==> In parts per million

Sabasa Fm, Soutpansberg Group

SAMPLE	C-118	C-125	C-126	C-127	C-138
SiO2	50.1	52.9	51.3	50.3	52.0
TiO2	1.05	1.2	1.15	1.77	1.5
Al2O3	14.9	13.8	14.0	13.8	13.7
Fe2O3-T	13.2	13.2	13.3	15.3	14.0
MgO	7.25	5.25	5.52	5.6	4.14
CaO	9.15	7.02	8.97	8.3	7.92
Na2O	2.1	2.47	2.92	2.74	1.88
K2O	0.31	2.29	0.58	0.37	2.74
MnO	0.21	0.16	0.18	0.2	0.15
P2O5	0.1	0.14	0.13	0.23	0.17
LOI	2.24	1.98	2.24	1.68	1.85
TOTAL	100.62	100.36	100.22	100.36	100.03
Rb	13.2	108.1	23.7	15.5	101.3
Ba	189	640	225	210	640
Cs	0.3	1.5	0.4	0.5	0.8
Sr	159	197	133	171	57
Pb	301.8	16.6	17.2	7.7	15.6
Th	2.1	8.0	7.0	5.8	7.7
U	0.6	1.8	1.6	1.4	1.9
Sc	35.3	28.4	29.1	34.6	26.4
V	285	280	290	402	316
Cr	301	33	25	79	23
Co	54	48	53	49	48
Ni	129	78	97	71	67
Y	26.2	33.2	30.9	43.6	39.0
Zr	96.7	171.2	153.4	177.8	202.4
Nb	8.3	10.9	10.6	12.5	12.1
Hf	2.7	4.6	4.1	4.9	5.5
Ta	0.33	0.57	0.59	0.63	0.65
La	10.1	27.1	24.0	21.9	29.3
Ce	23.5	57.6	51.2	50.9	63.6
Sm	3.40	5.72	5.23	6.35	6.63
Eu	1.05	1.42	1.36	1.73	1.67
Tb	0.76	0.92	0.91	1.24	1.16
Yb	2.33	2.73	2.48	3.92	3.25
Lu	0.35	0.43	0.39	0.63	0.48
Mg Number	55.2	47.2	48.2	45.1	39.9
K2O/Na2O	0.15	0.93	0.20	0.14	1.46
Na2O+K2O	2.41	4.76	3.50	3.11	4.62
Al2O3/TiO2	14.2	11.5	12.1	7.8	9.1

Sabasa Fm, Soutpansberg Group

SAMPLE	C-118	C-125	C-126	C-127	C-138
CaO/TiO2	8.7	5.9	7.8	4.7	5.3
Zr/TiO2	0.009	0.014	0.013	0.010	0.013
K/Rb	194.9	175.8	203.1	198.1	224.5
Ba/Sr	1.19	3.26	1.69	1.23	11.25
Rb/Sr	0.083	0.550	0.178	0.091	1.780
La/Yb	4.3	9.9	9.7	5.6	9.0
La/Sm	3.0	4.7	4.6	3.4	4.4
Sm/Eu	3.2	4.0	3.8	3.7	4.0
Ti/Zr	65.1	42.1	45.0	59.7	44.5
Zr/Nb	11.7	15.7	14.5	14.2	16.7
Nb/Y	0.32	0.33	0.34	0.29	0.31
Zr/Y	3.7	5.2	5.0	4.1	5.2
Nb/Ta	25.2	19.1	18.0	19.8	18.6
Nb/La	0.82	0.40	0.44	0.57	0.41
La/Ta	30.6	47.5	40.7	34.8	45.1
La/Th	4.8	3.4	3.4	3.8	3.8
Y/Tb	34.5	36.1	34.0	35.2	33.6
Th/Yb	0.90	2.93	2.82	1.48	2.37
Ta/Yb	0.142	0.209	0.238	0.161	0.200
Hf/Th	1.29	0.58	0.59	0.84	0.71
Ti/V	22.1	25.7	23.8	26.4	28.5
U/Pb	.00	0.11	0.09	0.18	0.12
Ce/Nb	2.83	5.28	4.83	4.07	5.26
Th/Ta	6.36	14.04	11.86	9.21	11.85
Th/Sc	0.06	0.28	0.24	0.17	0.29
Th/Nb	0.25	0.73	0.66	0.46	0.64
Sc/Ni	0.27	0.36	0.30	0.49	0.39
Hf/Ta	8.18	8.07	6.95	7.78	8.46
FeO-T/MgO	1.64	2.26	2.17	2.47	3.05
Sm/Yb	1.46	2.10	2.11	1.62	2.04
Eu/Eu*	0.85	0.75	0.77	0.78	0.74
g(x)	4.67	4.95	4.80	5.09	4.78
Score 1	0.47	0.46	0.19	0.09	-0.73
Score 2	-0.10	-0.26	-0.30	-0.23	-0.50

Fe2O3-T ==> Total Fe as Fe2O3
NO ENTRY ==> No determination OR below detectability limi
MAJOR ELEMENTS ==> In weight percent
TRACE ELEMENTS ==> In parts per million

Sabasa Fm, Soutpansberg Group

SAMPLE	C-140	C-141	C-143	C-145	C-146
SiO2	49.4	49.4	49.7	50.2	49.5
TiO2	1.3	1.4	0.9	1.34	1.65
Al2O3	14.9	15.3	15.5	14.6	13.9
Fe2O3-T	13.6	13.6	10.7	14.8	14.8
MgO	7.54	7.6	9.13	5.55	6
CaO	8.62	8.77	10.17	8.93	8.98
Na2O	2	1.49	1.59	1.54	2.26
K2O	0.86	0.52	0.56	1.37	1.08
MnO	0.18	0.17	0.15	0.18	0.18
P2O5	0.12	0.13	0.1	0.13	0.2
LOI	1.75	2.14	1.71	2.62	2.05
TOTAL	100.20	100.61	100.25	101.24	100.58
Rb	32.5	29.6	79.0	86.8	41.0
Ba	259	203	147	648	409
Cs	1.0	0.4	1.1	0.3	0.3
Sr	134	191	183	135	198
Pb	9.0	8.7	5.9	16.4	11.8
Th	2.9	2.8	0.8	6.1	5.5
U	0.6	0.7	0.2	1.5	1.4
Sc	35.5	34.9	37.0	33.2	33.8
V	292	310	237	385	366
Cr	195	135	351	44	99
Co	51	50	48	57	47
Ni	92	109	135	96	67
Y	31.7	34.2	19.8	32.0	40.9
Zr	115.8	120.9	69.2	136.2	164.8
Nb	9.5	9.6	6.0	10.6	11.7
Hf	3.0	3.2	1.6	3.8	4.6
Ta	0.48	0.50	0.21	0.45	0.57
La	12.2	13.2	6.0	21.4	20.0
Ce	28.9	29.8	13.9	44.6	46.4
Sm	4.06	4.41	2.47	4.96	5.83
Eu	1.24	1.36	0.82	1.34	1.69
Tb	0.81	0.95	0.50	0.93	1.06
Yb	2.53	3.00	1.82	2.83	3.33
Lu	0.43	0.48	0.29	0.45	0.55
Mg Number	55.6	55.6	65.7	45.8	47.7
K2O/Na2O	0.43	0.35	0.35	0.89	0.48
Na2O+K2O	2.86	2.01	2.15	2.91	3.34
Al2O3/TiO2	11.4	10.9	17.3	10.9	8.4

Sabasa Fm, Soutpansberg Group

SAMPLE	C-140	C-141	C-143	C-145	C-146
CaO/TiO2	6.6	6.3	11.3	6.7	5.4
Zr/TiO2	0.009	0.009	0.008	0.010	0.010
K/Rb	219.6	145.8	58.8	131.0	218.6
Ba/Sr	1.93	1.07	0.80	4.80	2.07
Rb/Sr	0.242	0.155	0.431	0.643	0.207
La/Yb	4.8	4.4	3.3	7.6	6.0
La/Sm	3.0	3.0	2.4	4.3	3.4
Sm/Eu	3.3	3.2	3.0	3.7	3.4
Ti/Zr	67.4	69.5	78.0	59.0	60.1
Zr/Nb	12.2	12.6	11.5	12.8	14.1
Nb/Y	0.30	0.28	0.30	0.33	0.29
Zr/Y	3.7	3.5	3.5	4.3	4.0
Nb/Ta	19.8	19.2	28.6	23.6	20.5
Nb/La	0.78	0.73	1.00	0.50	0.59
La/Ta	25.4	26.4	28.6	47.6	35.1
La/Th	4.2	4.7	7.5	3.5	3.6
Y/Tb	39.1	36.0	39.6	34.4	38.6
Th/Yb	1.15	0.93	0.44	2.16	1.65
Ta/Yb	0.190	0.167	0.115	0.159	0.171
Hf/Th	1.03	1.14	2.00	0.62	0.84
Ti/V	26.7	27.1	22.8	20.9	27.0
U/Pb	0.07	0.08	0.03	0.09	0.12
Ce/Nb	3.04	3.10	2.32	4.21	3.97
Th/Ta	6.04	5.60	3.81	13.56	9.65
Th/Sc	0.08	0.08	0.02	0.18	0.16
Th/Nb	0.31	0.29	0.13	0.58	0.47
Sc/Ni	0.39	0.32	0.27	0.35	0.50
Hf/Ta	6.25	6.40	7.62	8.44	8.07
FeO-T/MgO	1.62	1.62	1.06	2.39	2.22
Sm/Yb	1.60	1.47	1.36	1.75	1.75
Eu/Eu*	0.87	0.86	0.94	0.78	0.84
g(x)	4.77	4.90	4.51	4.82	5.08
Score 1	0.16	0.39	0.78	0.14	0.27
Score 2	-0.16	-0.10	-0.05	-0.25	-0.19

Fe2O3-T ==> Total Fe as Fe2O3
NO ENTRY ==> No determination OR below detectability limi
MAJOR ELEMENTS ==> In weight percent
TRACE ELEMENTS ==> In parts per million

Sabasa Fm, Soutpansberg Group

SAMPLE	C-147	C-148	C-149	C-150	C-151
SiO2	49.4	50.1	48.6	49.0	50.3
TiO2	1.53	1.21	1.09	1.08	1.29
Al2O3	14.4	14.3	14.7	15.1	14.0
Fe2O3-T	14.3	13.7	13.9	13.8	14.5
MgO	6.71	7.24	7.61	7.79	6.29
CaO	8.75	9.18	9.45	9.09	9.71
Na2O	2.11	1.42	1.63	1.16	1.49
K2O	0.45	0.59	0.53	0.57	0.69
MnO	0.18	0.19	0.18	0.19	0.19
P2O5	0.15	0.12	0.1	0.1	0.13
LOI	2.01	1.34	2.33	2.31	1.46
TOTAL	99.94	99.29	100.12	100.16	99.99
Rb	15.9	30.6	20.7	18.7	22.2
Ba	199	297	210	258	422
Cs	0.2	0.6	0.2	0.2	0.3
Sr	119	123	132	134	180
Pb	14.8	6.7	6.9	6.2	9.6
Th	3.6	2.8	2.0	1.9	3.3
U	0.9	0.7	0.5	0.6	1.0
Sc	38.3	34.2	36.2	36.8	39.1
V	337	300	269	287	300
Cr	161	215	205	229	124
Co	48	48	54	56	53
Ni	73	93	117	128	78
Y	37.4	29.7	30.7	26.5	31.7
Zr	141.0	116.8	100.6	95.0	121.6
Nb	10.6	9.1	7.8	7.3	8.6
Hf	3.8	3.1	2.6	2.5	3.4
Ta	0.48	0.41	0.34	0.32	0.42
La	16.1	13.3	10.3	9.6	13.8
Ce	36.4	28.5	22.7	22.1	30.5
Sm	4.92	3.97	3.37	3.41	4.21
Eu	1.52	1.15	1.19	1.06	1.42
Tb	0.99	0.81	0.82	0.69	0.83
Yb	3.37	2.61	2.40	2.31	3.21
Lu	0.53	0.43	0.40	0.37	0.48
Mg Number	51.3	54.3	55.2	56.0	49.4
K2O/Na2O	0.21	0.42	0.33	0.49	0.46
Na2O+K2O	2.56	2.01	2.16	1.73	2.18
Al2O3/TiO2	9.4	11.8	13.5	14.0	10.8

Sabasa Fm, Soutpansberg Group

SAMPLE	C-147	C-148	C-149	C-150	C-151
CaO/TiO2	5.7	7.6	8.7	8.4	7.5
Zr/TiO2	0.009	0.010	0.009	0.009	0.009
K/Rb	234.9	160.0	212.5	253.0	258.0
Ba/Sr	1.67	2.42	1.59	1.92	2.35
Rb/Sr	0.133	0.250	0.157	0.139	0.123
La/Yb	4.8	5.1	4.3	4.2	4.3
La/Sm	3.3	3.4	3.1	2.8	3.3
Sm/Eu	3.2	3.5	2.8	3.2	3.0
Ti/Zr	65.1	62.2	65.0	68.2	63.7
Zr/Nb	13.3	12.8	12.9	13.0	14.1
Nb/Y	0.28	0.31	0.25	0.28	0.27
Zr/Y	3.8	3.9	3.3	3.6	3.8
Nb/Ta	22.1	22.2	22.9	22.8	20.5
Nb/La	0.66	0.68	0.76	0.76	0.62
La/Ta	33.5	32.4	30.3	30.0	32.9
La/Th	4.5	4.8	5.2	5.1	4.2
Y/Tb	37.8	36.7	37.4	38.4	38.2
Th/Yb	1.07	1.07	0.83	0.82	1.03
Ta/Yb	0.142	0.157	0.142	0.139	0.131
Hf/Th	1.06	1.11	1.30	1.32	1.03
Ti/V	27.2	24.2	24.3	22.6	25.8
U/Pb	0.06	0.10	0.07	0.10	0.10
Ce/Nb	3.43	3.13	2.91	3.03	3.55
Th/Ta	7.50	6.83	5.88	5.94	7.86
Th/Sc	0.09	0.08	0.06	0.05	0.08
Th/Nb	0.34	0.31	0.26	0.26	0.38
Sc/Ni	0.52	0.37	0.31	0.29	0.50
Hf/Ta	7.92	7.56	7.65	7.81	8.10
FeO-T/MgO	1.92	1.70	1.64	1.59	2.07
Sm/Yb	1.46	1.52	1.40	1.48	1.31
Eu/Eu*	0.88	0.82	0.95	0.88	0.96
g(x)	4.87	4.71	4.68	4.63	4.85
Score 1	-0.08	0.13	0.23	0.31	0.40
Score 2	-0.22	-0.20	-0.05	-0.12	-0.14

Fe2O3-T ==> Total Fe as Fe2O3
NO ENTRY ==> No determination OR below detectability limi
MAJOR ELEMENTS ==> In weight percent
TRACE ELEMENTS ==> In parts per million
==========

Sabasa Fm, Soutpansberg Group

SAMPLE	C-153	C-154	C-155	C-156	AVG
SiO2	52.0	52.0	50.2	49.3	50.1
TiO2	1.14	0.89	1	1.24	1.22
Al2O3	14.2	14.0	14.4	14.7	14.5
Fe2O3-T	12.1	11.8	13.0	13.8	13.5
MgO	5.48	6.27	6.69	7.8	6.78
CaO	9.48	10.32	10.27	8.21	8.84
Na2O	2.98	2.38	2.03	1.75	2.19
K2O	0.58	0.56	0.54	0.64	0.68
MnO	0.16	0.17	0.17	0.19	0.18
P2O5	0.12	0.1	0.1	0.13	0.13
LOI	2.49	2.21	1.9	2.36	2.11
TOTAL	100.73	100.65	100.32	100.17	100.28
Rb	19.3	21.7	26.3	22.2	30.47
Ba	283	227	175	263	268
Cs	0.4	0.7	1.0	0.3	0.51
Sr	152	125	162	133	148
Pb	12.0	9.7	9.1	5.6	20.11
Th	6.7	4.8	5.0	2.3	3.74
U	1.6	0.9	1.2	0.5	0.9
Sc	28.2	32.0	35.8	35.8	35.05
V	280	254	272	281	298
Cr	42	110	76	184	150
Co	48	48	64	52	53
Ni	100	93	129	139	103
Y	28.6	25.2	25.7	31.8	30.98
Zr	141.5	120.9	107.4	110.8	122.08
Nb	9.3	8.6	8.3	8.4	9.12
Hf	4.1	3.2	3.4	3.0	3.31
Ta	0.51	0.37	0.40	0.32	0.42
La	22.9	19.6	17.9	12.4	15.24
Ce	48.8	40.2	39.4	28.8	33.65
Sm	5.04	4.17	4.32	4.03	4.31
Eu	1.37	1.06	1.42	1.28	1.27
Tb	0.90	0.73	0.87	0.83	0.85
Yb	2.32	2.25	2.45	2.80	2.67
Lu	0.35	0.37	0.40	0.45	0.43
Mg Number	50.4	54.5	53.6	56.0	52.67
K2O/Na2O	0.19	0.24	0.27	0.37	0.34
Na2O+K2O	3.56	2.94	2.57	2.39	2.87
Al2O3/TiO2	12.4	15.7	14.4	11.9	12.29

Sabasa Fm, Soutpansberg Group

SAMPLE	C-153	C-154	C-155	C-156	AVG
CaO/TiO2	8.3	11.6	10.3	6.6	7.51
Zr/TiO2	0.012	0.014	0.011	0.009	0.01
K/Rb	249.4	214.2	170.4	239.3	206.13
Ba/Sr	1.86	1.82	1.08	1.97	2.01
Rb/Sr	0.127	0.174	0.162	0.166	0.24
La/Yb	9.9	8.7	7.3	4.4	5.68
La/Sm	4.5	4.7	4.1	3.1	3.44
Sm/Eu	3.7	3.9	3.0	3.1	3.38
Ti/Zr	48.3	44.2	55.9	67.1	61.37
Zr/Nb	15.2	14.1	12.9	13.2	13.26
Nb/Y	0.33	0.34	0.32	0.26	0.30
Zr/Y	4.9	4.8	4.2	3.5	3.93
Nb/Ta	18.2	23.2	20.8	26.3	22.23
Nb/La	0.41	0.44	0.46	0.68	0.65
La/Ta	44.9	53.0	44.7	38.8	35.47
La/Th	3.4	4.1	3.6	5.4	4.47
Y/Tb	31.8	34.5	29.5	38.3	36.77
Th/Yb	2.89	2.13	2.04	0.82	1.39
Ta/Yb	0.220	0.164	0.163	0.114	0.16
Hf/Th	0.61	0.67	0.68	1.30	1.04
Ti/V	24.4	21.0	22.1	26.5	24.41
U/Pb	0.13	0.09	0.13	0.09	0.09
Ce/Nb	5.25	4.67	4.75	3.43	3.60
Th/Ta	13.14	12.97	12.50	7.19	8.42
Th/Sc	0.24	0.15	0.14	0.06	0.11
Th/Nb	0.72	0.56	0.60	0.27	0.39
Sc/Ni	0.28	0.34	0.28	0.26	0.35
Hf/Ta	8.04	8.65	8.50	9.38	7.89
FeO-T/MgO	1.99	1.69	1.75	1.59	1.85
Sm/Yb	2.17	1.85	1.76	1.44	1.61
Eu/Eu*	0.80	0.75	0.93	0.89	0.85
g(x)	4.79	4.61	4.68	4.74	4.76
Score 1	0.34	0.33	0.50	0.17	0.26
Score 2	-0.29	-0.24	-0.16	-0.12	-0.17

Fe2O3-T ==> Total Fe as Fe2O3
NO ENTRY ==> No determination OR below detectability limi
MAJOR ELEMENTS ==> In weight percent
TRACE ELEMENTS ==> In parts per million

Sabasa Fm, Soutpansberg Group

SAMPLE	STD
SiO2	1.0
TiO2	0.22
Al2O3	0.5
Fe2O3-T	0.9
MgO	1.04
CaO	0.87
Na2O	0.53
K2O	0.56
MnO	0.02
P2O5	0.03
LOI	0.38
TOTAL	0.33
Rb	27.00
Ba	157
Cs	0.34
Sr	33
Pb	53.42
Th	1.99
U	0.5
Sc	3.62
V	37
Cr	83
Co	5
Ni	21
Y	5.35
Zr	29.94
Nb	1.60
Hf	0.85
Ta	0.11
La	5.84
Ce	12.26
Sm	0.98
Eu	0.22
Tb	0.15
Yb	0.44
Lu	0.07
Mg Number	4.80
K2O/Na2O	0.29
Na2O+K2O	0.71
Al2O3/TiO2	2.17

Sabasa Fm, Soutpansberg Group

SAMPLE	STD
CaO/TiO2	1.69
Zr/TiO2	.00
K/Rb	45.92
Ba/Sr	1.96
Rb/Sr	0.32
La/Yb	2.00
La/Sm	0.66
Sm/Eu	0.32
Ti/Zr	8.64
Zr/Nb	1.17
Nb/Y	0.03
Zr/Y	0.59
Nb/Ta	2.99
Nb/La	0.15
La/Ta	6.96
La/Th	0.91
Y/Tb	3.23
Th/Yb	0.72
Ta/Yb	0.03
Hf/Th	0.33
Ti/V	2.06
U/Pb	0.04
Ce/Nb	0.83
Th/Ta	2.91
Th/Sc	0.07
Th/Nb	0.16
Sc/Ni	0.07
Hf/Ta	0.73
FeO-T/MgO	0.38
Sm/Yb	0.25
Eu/Eu*	0.06
g(x)	0.14
Score 1	0.27
Score 2	0.11

Fe2O3-T ==> Total Fe as Fe2O3
NO ENTRY ==> No determination OR below detectability limi
MAJOR ELEMENTS ==> In weight percent
TRACE ELEMENTS ==> In parts per million
==========

Pongola Supergroup CIPW Norms

S#	P1	P2	P16	P17	P18	P19	P20	P22	P23	P24
qtz	7.5	4.8	4.2	14	7	4.5	21	5.5	3.4	19
or	6.7	5.3	1.7	0.3	0.5	1.5	2.8	5.9	3.6	1.6
ab	27	18	18	22	27	33	28	25	29	28
an	22	29	29	19	25	23	16	23	23	14
di	13	26	20		6.5	9.6		16	14	
hy	18	11	20	33	25	20	21	20	21	28
ol										
mgt	3.8	3.9	4.4	4.7	4.9	4.8	5.1	3.6	3.5	3.8
il	2	2.1	2.9	3.1	3.4	3.2	3.7	1.8	1.6	1.9
ap	0.5	0.5	0.3	0.6	0.8	0.7	0.8	0.4	0.4	0.4
c				3.1			1.8			4.5

S#	MS34	WR1	MS32	HK28	MS37	WR9	WR2	MS33	WR7	WR6
qtz	4.5	2.8	5.3	2.8	1.4	4.9	11	1.9	4.3	9.3
or	9	4.7	2.5	5.8	6	2.7	1	3.6	13	10
ab	15	26	25	19	22	23	21	36	24	21
an	28	26	26	26	24	28	34	21	21	24
di	12	17	15	20	14	8.9	8.6	14	6.1	5.8
hy	24	18	19	22	28	28	19	17	2.5	22
ol										
mgt	4.3	3.8	4	3.1	3.1	3.1	3.8	4.1	3.8	4.1
il	2.7	2.1	2.4	1.2	1.1	1.2	2.1	2.5	2	2.5
ap	0.7	0.2	0.6	0.3	0.3	0.3	0.8	0.5	0.5	0.6
c										

S#	HK30	AS25	OS44	WR15	KB48	AS24	AS23	WR5	WR14	WR12
qtz	13	5	11	9.2	7.8	7.6	9.9	8	12	19
or	4.3	6	3.5	9	9	6.6	7.8	7.2	1.1	6
ab	23	21	20	25	31	22	19	30	27	21
an	29	28	28	18	15	25	25	19	25	18
di	13	16	14			13	14	14	13	
hy	14	18	18	28	27	19	19	15	15	26
ol										
mgt	3	3.7	3.5	3.9	4.1	3.6	3.7	3.8	3.6	3.2
il	1.1	1.9	1.7	2.3	2.5	1.9	2	2.1	1.9	1.4
ap	0.3	0.5	0.5	0.9	0.6	0.5	0.5	0.5	0.5	0.4
c				3.4	3.8			0.01		5.1

Pongola Supergroup CIPW Norms

S#	AS22	OS42	WR17	D38	HK31	NS47	NS46	OS39	WR4	WR13
qtz	13	16	15	11	26	27	24	28	38	30
or	7.8	14	1.3	11	11	20	19	15	20	23
ab	25	27	35	37	18	14	25	18	7.8	14
an	22	14	20	14	24	12	15	21	18	18
di	12	3.5	3.7	10	0.1			7.3	0.2	
hy	15	18	19	12	16	20	11	5.3	12	9.6
ol							3.6			
mgt	3.7	4.6	3.7	3.1	3.7	3.6	1.8	3.6	3.1	3.2
il	2	3.1	2	1.1	1.9	1.9	0.5	1.8	1.2	1.3
ap	0.4	0.8	0.5	0.8	0.6	0.5	0.3	0.5	0.5	0.4
c						1.7				0.2

S#	PK18	HK27	WR3	WR11	MS35	WR10	OS40	WR16	C19	OS41
qtz	30	31	37	38	37	42	32	34	33	35
or	18	22	15	26	30	26	34	24	31	27
ab	24	20	25	20	19	15	20	25	23	28
an	13	12	12	6.8	5.9	8.9	3.8	6.2	7.2	2.7
di	0.2	1.7	0.5							
hy	10	9.5	5.9	5.2	4.4	4.3	4.8	5.4	2.2	2.7
ol										
mgt	3.4	3.2	3	2.9	2.8	2.9	2.9	3.1	2.9	2.8
il	1.6	1.4	1.1	0.9	0.9	0.9	1	1.2	0.9	0.9
ap	0.4	0.5	0.4	0.3	0.2	0.2	0.3	0.4	0.3	0.2
c				1.5	0.01	0.6	2.1	0.6	0.1	0.9

S#	OS43	AS21
qtz	47	40
or	31	43
ab	7.9	12
an	4	1.8
di		
hy	22	0.1
ol		
mgt	2.8	0.9
il	0.7	0.6
ap	0.1	0.1
c	4.3	0.4

Dominion Group CIPW Norms

S#	BTF3	BTF4	BTF5	BTF6	BTF8	BTF9	BT10	BT11	BT15	BT2D
qtz	0.8		1.7	4.5	18	12			4.1	5.1
or	6.8	0.6	4.1	5.8	1.1	0.3	1.4	0.4	1.4	0.7
ab	25	44	27	22	29	42	60	33	18	19
an	23	6	24	26	7.5	8	5.4	21	28	27
di	15		11	16				15	15	14
hy	25	34	28	22	34	28	21	22	29	29
ol		3					1.7	4.1		
mgt	3.1	3.3	3.2	3.2	3.2	3.2	3.5	3.3	3.3	3.3
il	1.1	1.3	1.3	1.2	1.2	1.2	1.6	1.4	1.4	1.3
ap	0.3	0.5	0.4	0.4	0.7	1.3	1	0.4	0.4	0.4
c		7.2			6	4	5			

S#	BSF3	BSF5	BSF6	BSF8	BS12	BS14	BS15	BS17	BBS2	BBS4
qtz			3.6	0.7				25	1.7	1.6
or	11	1	7.4	1.6	5.7	6.1	3.2	1.9	5.9	5.2
ab	20	51	25	45	32	32	35	8.4	33	32
an	23	20	25	15	19	17	19	26	20	20
di	17	5.5	14	16	17	16	15		12	18
hy	19	1.1	20	18	9	16	4.4	25	21	17
ol	5.3	15			12	6.7	18			
mgt	3.2	3.5	3.1	3.2	3.5	3.6	3.5	3.6	3.8	3.7
il	1.3	1.7	1.2	1.2	1.6	1.7	1.6	1.7	2	1.9
ap	0.3	0.5	0.4	0.4	0.5	0.5	0.5	0.5	0.3	0.4
c								7.1		

S#	BBS5	BBS8	BBS9	BB16	BB18	BTF2	BSF2	BSF9	BS10	BS11
qtz	2.3	4.1			15	21	7.9	4.7	8	1.4
or	6.8	5.5	6.9	3.7	27	1.3	3.7	3.2	1.7	7.4
ab	32	33	43	43	34	33	36	38	44	37
an	18	18	16	15	2.5	9.6	20	19	15	18
di	13	11	6.9	11			6	9		7.9
hy	21	23	11	10	13	24	20	19	23	21
ol			12	12						
mgt	3.7	3.7	3	3.5	3.1	4.1	4	4	4	4
il	2	2	1.1	1.6	1.1	2.4	2.3	2.3	2.3	2.3
ap	0.4	0.4	0.3	0.5	0.3	0.7	0.7	0.9	0.9	0.9
c					4	4.2				

Dominion Group CIPW Norms

S#	BB11	BB13
qtz	22	4.8
or	4.6	7.5
ab	33	35
an	18	15
di	1	
hy	15	28
ol		
mgt	3.8	4.1
il	2.1	2.4
ap	0.8	0.9
c		2

S#
qtz
or
ab
an
di
hy
ol
mgt
il
ap
c

S#
qtz
or
ab
an
di
hy
ol
mgt
il
ap
c

Ventersdorp Supergroup CIPW Norms

S#	J1A	J2A	J3A	J4A	J5A	J6A	J7A	J8A	C5A	J13R
qtz	6.5	12	12	11	21	2	8	16	6.7	14
or	1.9	10	10	9.2	15	3.7	6.8	21	6.9	12
ab	34	43	44	30	25	43	42	2.3	36	24
an	17	12	12	21	11	19	14	30	15	22
di		8.8	8.6	6.1			11	3.7	13	16
hy	29	7.7	7.9	18	19	22	12	20	15	3.9
ol										
mgt	4.7	4	4	3.3	3.9	4.8	4	4.3	4	4.4
il	3.1	2.3	2.2	1.3	2.2	3.3	2.2	2.4	2.3	2.6
ap	1.7	0.5	0.5	0.3	0.5	2.1	0.5	0.5	0.5	1.5
c	2.5				2.6	0.5				

S#	J14R	J15R	J16R	J17R	J18M	J19M	J20M	C1M	C2M	D6M
qtz	0.9	5.7	14	7.3	46	2	42	40	34	29
or	5	1.9	8.2	7.3	16	8.8	19	35	29	23
ab	44	35	30	35	19	33	16	11	28	31
an	16	18	16	16	5	19	4.9	4.4	2.1	8.7
di	12			12		12				0.5
hy	12	28	23	16	5.5	20	7.6	5.5	2.8	2.9
ol										
mgt	4.9	4.7	4.3	4.1	3.6	3.3	3.7	1.4		2.7
il	3.4	3.1	2.6	2.3	1.9	1.4	2	0.6	0.1	1.3
ap	1.9	1.6	0.5	0.5	1	0.3	1	0.2	0.1	0.5
c		2.2	2.9		2.3				1.9	
hem								0.9	1.8	0.4
rut									0.2	

S#	J21G	J22G	J23G	J24G	J25G	S35E	S34E	S33E	S32E	S31E
qtz	12		12	2.5	5.8	3.2	1.3	6.2		
or	9.2	1.3	9.1	6.8	11	2	2.5	2.8	1	7.8
ab	24	47	24	22	33	14	18	16	20	24
an	24	13	24	22	18	20	19	20	18	21
di	7.6		7.5	19	6.4	16	17	11	22	21
hy	15	13	14	24	16	42	38	41	33	12
ol		11							1.7	9.3
mgt	4.5	5	4.5	3.1	4.7	2.9	2.9	3	2.9	3.2
il	2.9	3.5	2.9	1.2	3.1	0.8	0.9	0.9	0.8	1.2
ap	1.6	1.9	1.6	0.2	1.7	0.1	0.1	0.1	0.1	0.1
c		4.4								

Ventersdorp Supergroup CIPW Norms

S#	S30E	S29E	S28E	S27E	S26E	S25E	S24E	S23E	S22E	S21E
qtz		6.7		13	2.8	7.5			4.5	
or	5	10	4.6	0.1	5.1	5.5	5.8	6.6	4.5	5.2
ab	30	17	25	3.1	27	2.7	26	36		32
an	19	23	19	34	20	29	16	17	22	17
di	21	23	18	28	18	15	21	13	24	21
hy	16	18	19	18	23	36	22	13	19	13
ol	5.5		11				5.2	9.4	22	6.2
mgt	3.2		3	3.1	3.2	2.9	3.1	3.3		3.2
il	1.2	0.5	1	1.1	1.2	0.8	1	1.5	3.1	1.2
ap	0.2	0.2	0.1	0.1	0.2	0.1	0.2	0.2	1.2	0.2
c									0.2	

S#	J26L	J27L	J28L	J29L	J30L	J31L	J32L	J33L	C3L	S20L
qtz	24	4.3	4.8	12	13	4.2	1.5		11	
or	21	10	6	12	18	4.8	6.7	1.3	9.3	1.1
ab	24	23	21	22	34	26	25	46	29	25
an	9.2	18	24	21	14	22	22	14	21	16
di		17	19	8.3		17	20		6.9	19
hy	10	23	20	17	13	22	20	17	18	28
ol								8		7.4
mgt	4.2	3.2	3.3	4.5	4.3	3.1	3.1	4.9	3.2	2.9
il	2.6	1.3	1.4	3	2.8	1.2	1.2	3.5	1.3	0.9
ap	1.3	0.2	0.4	1.6	1.5	0.2	0.2	1.8	0.3	0.1
c	3.5				0.3			4.4		
hem										
rut										

S#	S19L	S18L	S17L	S16L	S15L	S14L	S13L	S12L	S11J	S10J
qtz	2.4		0.7		4.8	21	3.7	5.9	4.7	5
or	11	3.3	7.6	6.9	6.6	0.9	8.4	3.7	6.8	7.6
ab	16	33	22	30	10	2.2	25	33	32	31
an	19	20	22	19	21	35	20	19	21	21
di	15	24	21	15	15	9.1	18	15	11	13
hy	32	1.5	22	22	39	28	20	18	18	17
ol		14		2.7						
mgt	3	3.4	3.2	3.2	2.9	3.2	3.4	3.4	3.6	3.6
il	1	1.5	1.3	1.2	0.9	1.3	1.5	1.6	1.9	1.9
ap	0.1	0.2	0.2	0.2	0.1	0.2	0.2	0.2	0.3	0.3
c										

Ventersdorp Supergroup CIPW Norms

S#	S9J	S8J	S7J	S6J	J34J	J35o	J36o	J37o	S5o	S4o
qtz	8.7	5.9	5	4.8	7.7	4.5	5	2.7	4.6	4.5
or	10	7.9	9.9	6.1	8.6	8.9	14	3.8	2.4	7.3
ab	24	29	28	31	26	31	25	39	29	29
an	24	22	22	21	23	20	22	19	26	22
di	11	12	8.9	13	13	13	5.6	12	12	13
hy	17	18	20	18	16	17	22	17	21	19
ol										
mgt	3.6	3.6	3.6	3.6	3.5	3.6	3.8	3.8	3.7	3.7
il	1.8	1.8	1.8	1.9	1.7	1.8	2	2	2	2
ap	0.3	0.3	0.3	0.3	0.3	0.3	0.3	0.4	0.3	0.3
c										

S#	S3o	S2o	S1o	D3o	J38o	1-O	1-M	2-O	2-M	3-O
qtz	3.8	0.4	4	5.1	9.9	12	6.5	9.7		14
or	1.2	7.9	3.4	2.5	4.7	0.7	1.6	0.8	0.4	0.9
ab	33	30	32	31	33	17	7.5	24	1.4	13
an	24	23	22	23	21	14	19	12	22	20
di	16	9.6	15	11	12	14	14	17	16	12
hy	16	23	18	21	14	34	46	31	35	34
ol									19	
mgt	3.7	3.8	3.8	3.6	3.9	3.6	3.8	3.6	3.7	3.7
il	2	2.1	2	1.8	2	1.9	2.2	1.9	2	2
ap	0.3	0.3	0.3	0.3	0.4	1.9	0.3	0.2	0.2	0.21
c										
hem										
rut										

S#	3-M	5-O	5-M	8-O	8-M	9-O	9-M	12-O	12-M	20-O
qtz		12	5.2	15	4	11	6.9	11		13
or	1.8	1.1		0.7	1	0.8	1.1	0.7	1.5	2.7
ab	3	16	6.8	11	13	21	7.7	14	10	10
an	25	17	24	18	17	11	16	15	20	22
di	11	17	12	14	12	20	19	18	15	11
hy	49	31	46	37	47	30	43	35	46	35
ol	4.3								1.4	
mgt	4	3.7	3.9	3.5	3.7	3.5	3.5	3.6	3.6	4
il	2.3	2	2.2	1.7	2	1.7	1.8	1.8	1.8	2.4
ap	0.3	0.2	0.3	0.2	0.3	0.3	0.3	0.3	0.4	0.3
c										

Ventersdorp Supergroup CIPW Norms

S#	
qtz	
or	
ab	
an	
di	
hy	
ol	
mgt	
il	
ap	
c	

S#	
qtz	
or	
ab	
an	
di	
hy	
ol	
mgt	
il	
ap	
c	
hem	
rut	

S#	20-M
qtz	4
or	2
ab	8.8
an	20
di	16
hy	43
ol	
mgt	3.6
il	1.9
ap	0.2
c	

Transvaal Supergroup CIPW Norms

S#	C33	C34	C41	C42	C43	C44	C45	C55	C40	C50
qtz	2.2	7.7	11	11	11	9.7	13	5.1	26	20
or	8.6	9.8	6.4	8.2	9.5	9.9	8.1	15	17	14
ab	30	28	23	22	24	26	20	28	23	27
an	15	17	18	19	21	19	27	19	18	18
di	17	15	18	15	14	14	8.6	9	1.7	5.3
hy	18	15	16	16	14	15	19	19	11	11
ol										
mgt	4.4	4.4	4.2	4.5	4.6	4.4	3.2	3.2	3.1	3.1
il	2.8	2.8	2.6	3	3.1	2.9	1.2	1.3	1.1	1.1
ap	0.4	0.4	0.3	0.4	0.4	0.3	0.3	0.4	0.3	0.3
c										

S#	C23	C24	C25	C26	C57	C60	C61	C66	C208	C209
qtz	0.2		4.8		16	3.8	3.6	15	3.2	3.2
or	5	3.2	4.2	0.8	4.4	2.4	0.7	0.4	3.2	1.3
ab	25	32	18	27	2.5	20	13	13	22	23
an	24	21	28	24	20	27	32	23	25	27
di	15	18	19	22	17	13	11	31	17	15
hy	26	15	19	15	34	26	34	12	22	23
ol		7.1		5.9						
mgt	3.3	3.2	4.3	3.5	4.1	4.4	3.5	3.5	4.5	4.6
il	1.3	1.2	2.7	1.6	2.4	2.9	1.6	1.7	3	3.1
ap	0.2	0.2	0.4	0.2	0.3	0.4	0.1	0.2	0.5	0.4
c										

S#	C211	C212	c31	CDV6	CDV7	CDV8	CDV9	CD10	C11d	C11e
qtz	2.9	13	13	8.6	12	4.4	7.5	11	12	7.5
or	0.9	0.9	5.3	9.1	2	9.1	10	14	12	16
ab	19	5.9	20	18	8.6	23	12	20	19	18
an	30	32	29	27	24	23	27	24	26	24
di	14	21	3.9	8.5	3.1	5.7	8	1.2	3.7	6.2
hy	28	21	25	24	48	30	31	26	23	24
ol										
mgt	3.6	3.8	3.1	3.3	2.9	3.2	3.1	3.1	3.1	3.1
il	1.7	2	1.2	1.4	0.8	1.2	1.1	1.2	1.1	1.2
ap	0.2	0.2	0.2	0.2	0.2	0.2	0.2	0.2	0.2	0.2
c										

Transvaal Supergroup CIPW Norms

S#	WBK6	WBK9	D105	D37	D38	D39	D40
qtz	5.6	15	43	4.3	7.6	13	3.3
or	6.6	11	11	6.2	12	8.3	12
ab	24	12	23	24	8.7	0.8	19
an	25	30	1.3	22	28	32	27
di	3	3.4		1.3	13		14
hy	32	24	14	31	20	34	16
ol							
mgt	3.2	3.1	2.9	5.3	5.7	5.8	4.8
il	1.2	1.1	0.8	4	4.4	4.6	3.3
ap	0.2	0.2	0.2	1	1	1.1	0.6
c			3.9			0.7	

S#
qtz
or
ab
an
di
hy
ol
mgt
il
ap
c

S#
qtz
or
ab
an
di
hy
ol
mgt
il
ap
c

Soutspansberg Group CIPW Norms

S#	C132	C137	C189	C190	C191	C192	C194	C195	D10	D12
qtz			3.1	1.6	3.7	3.9	2.2	3.3	6.5	3.9
or	3.1	2.7	1.5	3.3	3.3	3.7	19	4.5	2.7	0.6
ab	22	16	22	19	18	16	19	18	18	25
an	31	34	30	32	30	32	31	29	28	26
di	3.6	13	10	10	13	13	11	13	11	11
hy	28	25	26	27	24	24	27	24	25	27
ol	4.7	3.5								
mgt	4.4	3.3	4.5	4.5	4.7	4.6	4.6	4.5	4.7	3.8
il	2.8	1.4	2.9	3	3.2	3.1	3.1	2.9	3.2	2
ap	0.4	0.1	0.4	0.3	0.3	0.4	0.3	0.4	0.5	0.2
c										

S#	C108	C109	C111	C112	C113	C114	C115	C116	C118	C125
qtz	0.6	0.2		1.2		0.2	2.6	2.8	3.3	4.3
or	0.8	1.5	5.4	2.6	2.3	3.6	2.9	1.9	1.9	14
ab	23	25	27	20	23	25	18	20	18	22
an	29	28	27	31	28	26	31	30	31	20
di	13	15	8.4	5.1	13	10	15	15	12	12
hy	27	25	19	34	26	29	24	24	27	21
ol			7		1.4					
mgt	3.9	3.9	4	3.9	4	3.9	3.9	3.9	3.8	4
il	2.2	2.2	2.3	2.1	2.3	2.2	2.1	2.2	2.1	2.3
ap	0.3	0.3	0.3	0.3	0.3	0.3	0.2	0.3	0.2	0.3
c										

S#	C126	C127	C138	C140	C141	C143	C145	C146	C147	C148
qtz	3.2	4.2	5.7	1.8	5	1.9	5.3	2.2	3.8	6.2
or	3.5	2.2	17	5.2	3.2	3.4	8.3	6.6	2.8	3.6
ab	26	24	16	17	13	14	13	20	18	12
an	24	25	21	30	35	34	30	25	29	32
di	17	13	15	11	7.6	13	13	16	12	12
hy	20	23	17	28	30	28	24	22	26	28
ol										
mgt	4	4.9	4.5	4.2	4.3	3.6	4.2	4.7	4.5	4.1
il	2.3	3.5	2.9	2.5	2.7	1.8	2.6	3.2	3	2.4
ap	0.3	0.6	0.4	0.3	0.3	0.2	0.3	0.5	0.4	0.3
c										

Soutspansberg Group CIPW Norms

S#	C149	C150	C151	C153	C154	C155	C156
qtz	2.3	4.9	6.3	3.9	4.7	3.1	3.5
or	3.2	3.5	4.2	3.5	3.4	3.3	3.9
ab	14	10	13	26	21	18	15
an	32	35	30	24	26	29	32
di	13	8.6	15	19	21	18	8
hy	29	31	24	17	19	22	31
ol							
mgt	3.9	3.9	4.2	3.9	3.6	3.7	4.1
il	2.1	2.1	2.5	2.2	1.7	2	2.4
ap	0.2	0.2	0.3	0.3	0.2	0.2	0.3
c							

S#
qtz
or
ab
an
di
hy
ol
mgt
il
ap
c

S#
qtz
or
ab
an
di
hy
ol
mgt
il
ap
c

APPENDIX D

Core Correlation

Part 1.

The BSF and BBS cores which sample the Rhenosterhoek Formation, Dominion Group are located within a few kilometers of each other. Similar textural and features, along with comparable geochemistry, strongly suggests that these cores are indeed sampling the same unit. The BTF core, however, is located several kilometers to the northeast. Textural similarities and comparable geochemistry are noted between the BTF and the BSF-BBS cores but the distance between these cores restricts a simplistic comparison. In an attempt to more rigorously evaluate the cores and give a statistical probability to their similarity (geochemical in this case), a T-Test was used (Levine and Rubin, 1980). Using the T-Test an upper and/or lower acceptance limit (as needed) was calculated for the BTF core at the 95% confidence level for several immobile, compatible and incompatible trace elements. An average value for the corresponding trace element in the BSF core is shown for comparison. If the trace element abundance in the BSF core is within the limit (a lower value if an upper [+] limit and a higher value if a lower [-] limit) calculated for the

BTF core then, with 95% confidence, the cores have similar geochemistry with respect to that trace element. Test failures are marked with a star (*).

Formulas used:

Sp= square root $[(N-1)(S1)^2 + (N-1)(S2)^2/N + N - 2]$ (D-1)

Sx= Sp X square root $[1/N_1 + 1/N_2]$ (D-2)

Hypothesized value of BTF mean + T X Sx= upper or lower limit. (D-3)

Where:

Sp= pooled standard deviation of data points.

Sx= estimated standard error of difference between two means.

N= number of samples

T= T value from Table for desired probability and N-2.

S= standard deviation of the mean.

Example:

	BTF (N= 10)	BSF (N= 8)
Ni =	297 + 49	309 + 55

Sp= square root $(10-1)(49)^2 + (8-1)(55)^2/10+8-2=$ = 51.7

Sx= 51.7 X square root 1/10 + 1/8= 24.5

T= 2.12 at N= 16 (ie. N-2) and 95% confidence level.

Upper limit test: 297 + 2.12 X 24.5= 322 ppm Ni.

Test results: 322 ppm is greater than the mean Ni abundance in the BSF core of 309 ppm; ie. the mean BSF Ni abundance falls within the upper limit at a 95% confidence interval and the two cores have significantly similar Ni abundances.

Table D-1
Core Mean Comparison Test

BTF-BSF Cores

	BTF MEAN	Calculated BTF Upper and Lower Limit	BSF MEAN
Ni	297 ppm	+322; -273	309 ppm
Sc	25.0	+29.4; -20.7	25.6
Zr	91	+102; -79	101
Y	16.9	+21.8; -12.1	20.5
Ta	0.15	+0.2; -0.1	0.16
Yb	1.46	+1.88; -1.04	1.56

Part 2.

Most Ventersdorp Supergroup samples are from the J and S cores. Initial stratigraphic correlations between the two cores was based on textural similarities. The distance between these two cores is approximately 120 km. Thus, as with Appendix D, Part 1, there is a need to statistically confirm the Loraine Formation in the J core is the same as the Loraine Formation in the S core, and conversely, that the Loraine Formation is different from the formations stratigraphically above and below it. A core mean comparison test (the former) was performed for all formations present in both cores. A core mean difference test (the latter) was performed on all formations present. A T-Test was used. The formulas used are the same as in Appendix C, Part 1. All tests are at the 95% confidence level. Test failures are marked with a star (*).

Table D-2
Core Mean Comparison Test

a) Loraine Formation

	J Core	Calculated J Core Upper and Lower Limit		S Core
Ni	200 ppm	+238;	-163	199 ppm
Zr	80	+94;	-67	76
Y	15.0	+16.9;	-13.1	15.5
Ta	0.22	+0.25;	-0.18	0.18
Yb	1.55	+1.79;	-1.31	1.30 *
Th	1.3	+1.5;	-1.1	1.2

b) Orkney Formation

	J Core	Calculated J Core Upper and Lower Limit		S Core
Ni	139 ppm	+173;	-106	150
Zr	118	+128;	-108	109
Y	18.5	+21.1;	-15.9	19.8
Ta	0.42	+0.49;	-0.35	0.35
Yb	1.66	+1.96;	-1.36	1.50
Th	2.0	+2.2;	-1.8	1.7 *

Table D-3
Core Mean Difference Test

a) Edenville vs. Loraine Formation

	Edenville	Calculated Edenville Upper or Lower Limit	Loraine
Ni	331 ppm	-295	197
Zr	59	+66	79
Y	12.0	+13.1	15.3
Ta	0.13	+0.15	0.20
Yb	1.13	+1.25	1.44
Sc	26	+29	30

b) Loraine vs. Jeanette Formation

	Loraine	Calculated Loraine Upper or Lower Limit	Jeanette
Ni	197 ppm	-175	122
Zr	79	+87	107
Y	15.3	+16.5	19.6
Ta	0.20	+0.23	0.33
Yb	1.44	+1.62	1.57 *
Sc	30	-26	23

c) Jeanette vs. Orkney Formation

	Jeanette	Calculated Jeanette Upper or Lower Limit	Orkney
Ni	122 ppm	+136	146
Zr	107	+113	112 *
Y	19.6	-18.5	19.1 *
Ta	0.33	+0.37	0.37
Yb	1.57	-1.42	1.56 *
Sc	23	-20	22 *

Summary.

1) Despite the distance between the BTF and BSF cores, statistical analyses suggest the two cores are similar at the 95% confidence level and the cores are sampling the same unit.

2) The Ventersdorp Supergroup core comparison test suggests (note two test failures), with 95% confidence, that the Loraine and Orkney Formations in J core are geochemically similar to the same formations in the S core.

3) Core mean difference tests on the Ventersdorp Supergroup demonstrate, at the 95% confidence level, that the Edenville and Loraine Formations are significantly different, and the Loraine and Jeanette Formations are significantly different (not one test failure). Numerous test failures in the Jeanette-Orkney test, however, suggests that these formations are not significantly different dispite textural evidence to the contrary.

Appendix E

Modeling

A quantitative evaluation of the petrogenesis within volcanic suites is performed with the aid of computer programs. For volcanic rock suites that no longer contain primary phenocryst phases (due to metamorphism), a program modified after Wright and Doherty (1970)(a least-squares mixing model) is employed to estimate phenocryst proportions for fractional crystallization. Trace element models are made using partial melting and closed- and open-system fractional crystallization equations (DePaolo, 1981; Allegre and Minster, 1978; O'Hara, 1977) in the computer program MODULUS (Knoper, 1988). MODULUS (MODeling-Using-LotUS) is written on a LOTUS spreadsheet with separate files for each geochemical model and Kd-file. The geochemical model to be examined (batch melting, fractional crystallization) is called-up from memory and the appropriate Kd file is attached. Data and temperature are then input and the modeling equation (see below) is solved for the desired unknown. An example of a spreadsheet, as viewed on the computer screen, is given in Table E-1.

Geochemical models are based on simple relationships. For partial melting, the equation used

Table E-1

Non-Modal Equilibrium (Batch) PM
Comment:

	Givn Co	Calc Cl	Calc Cs	Bulk D	Bulk P	Mineral	Melt Mode	Source Mode
Na	0	NA	NA	NA	NA		0.0000	0.0000
K	0	NA	NA	NA	NA		0.0000	0.0000
Rb	0	NA	NA	NA	NA		0.0000	0.0000
Sr	0	NA	NA	NA	NA		0.0000	0.0000
Cs	0	NA	NA	NA	NA		0.0000	0.0000
Ba	0	NA	NA	NA	NA		0.0000	0.0000
Th	0	NA	NA	NA	NA		0.0000	0.0000
U	0	NA	NA	NA	NA		0.0000	0.0000
							0.0000	0.0000
La	0	NA	NA	NA	NA		0.0000	0.0000
Ce	0	NA	NA	NA	NA		0.0000	0.0000
Nd	0	NA	NA	NA	NA		0.0000	0.0000
Sm	0	NA	NA	NA	NA		0.0000	0.0000
Eu	0	NA	NA	NA	NA		0.0000	0.0000
Tb	0	NA	NA	NA	NA		0.0000	0.0000
Yb	0	NA	NA	NA	NA		0.0000	0.0000
Lu	0	NA	NA	NA	NA		0.0000	0.0000
							0.0000	0.0000
P	0	NA	NA	NA	NA		0.0000	0.0000
Sc	0	NA	NA	NA	NA		0.0000	0.0000
Ti	0	NA	NA	NA	NA		0.0000	0.0000
Y	0	NA	NA	NA	NA			
Zr	0	NA	NA	NA	NA	Total	0.0000	0.0000
Nb	0	NA	NA	NA	NA			
Hf	0	NA	NA	NA	NA			
Ta	0	NA	NA	NA	NA			
V	0	NA	NA	NA	NA			
Cu	0	NA	NA	NA	NA			
Zn	0	NA	NA	NA	NA			
Pb	0	NA	NA	NA	NA			
Ga	0	NA	NA	NA	NA			
Cr	0	NA	NA	NA	NA			
Mg	0	NA	NA	NA	NA			
Mn	0	NA	NA	NA	NA			
Fe	0	NA	NA	NA	NA			
Co	0	NA	NA	NA	NA			
Ni	0	NA	NA	NA	NA			

M. F. Liquid
F = NA

M. F. Xtals
(1-F) = 0.000

(NA = "not available", ERR = "error")

Dated:

is:

$$C_l/C_o = 1/D_o + F(1-P_o) \qquad \text{(E-1)}$$

(Allegre and Minster, 1978) where the bulk distribution coefficient, D_o = Kd x X and the bulk distribution coefficient for melting, P_o = Kd x Y. Also:

Kd = distribution coefficent = concentration in the solid/concentration in the liquid.

X = weight fraction of a phase in the mode.

Y = weight fraction of the liquid contributed by each phase during melting.

C_l = trace element concentration in the liquid after a given amount of partial melting.

C_o = initial trace element concentration in the solid.

F = the fraction melted.

Equation E-1 can be solved for C_l (liquid composition) or C_o (solid composition). In most geochemical models of this dissertation, a mantle source composition is assumed (C_o) and a model liquid composition (C_l) is calculated. Liquid trajectories are then drawn (at even increments of batch melting) through the data points on various plots.

The equation for fractional crystallization (Rayleigh distillation law, Allegre and Minster, 1978) is:

$$C_1/C_o = F^{D-1} \qquad \text{(E-2)}$$

where:

F = the fraction of the liquid remaining (1-F = the amount of fractional crystallization).

C_1 = trace element concentration in a magma after a given amount of fractionation.

C_o = initial concentration in the magma.

Similar to the liquid trajectories calculated for batch melting above, liquid trajectories for fractional crystallization are calculated so as to pass through the data points on various plots. Both equations (E-1 and E-2) can be modified to apply to special situations but in most instances the simple equations presented here are sufficient. An exception is open-system fractional crystallization. Open-system fractional crystallization is a modification of the above closed-system fractional crystallization equation (E-2) which allows for the injection of new magma into the fractionation chamber (O'Hara, 1977). For each new magma injection a new value of C_o (C_o') is calculated and substituted for the C_o in the closed-system fractional crystallization equation above where:

$$C_o' = FC_1 + JC_o/F + J \qquad \text{(E-3)}$$

where:

J is the weight fraction of primary magma added back to the residual liquid (C_1) after some amount of fractional crystallization.

Evaluation of simultaneous fractional crystallization and wallrock assimilation (AFC) is performed with the equation of DePaolo (1981; 1985). The equation is:

$$du/dt = M_aC_a - M_cDC_m \quad \text{(E-4)}$$

$$= C_m \times dM_m/dt + M_m \times dC_m/dt \quad \text{(E-5)}$$

where:

u = mass of an element in the magma.

M_a = rate of wallrock assimilation in mass/unit time.

M_m = mass of the magma body.

M_c = crystallization rate.

C_a = element concentration in wallrock.

C_m = element concentration in magma.

DC_m = element concentration in crystallizing phases.

The equation above can be solved in the form of a concentration equation (Reagan et al., 1987) such that:

$$C_m = C_oF^{-z} + (xC_a + yC_i/z)(1-F^{-z}) \quad \text{(E-6)}$$

where:

C_i = element concentration of intruded magma.

C_o = element concentration of initial magma.

F = ratio of initial to final magma mass.

$x = r_1/r_1-r_2+r_3-1$

$y = r_3/r_1-r_2+r_3-1$

$z = r_1+r_3+D-1/r_1-r_2+r_3-1$

D = the bulk distribution coefficient for crystals being separated.

$r_1 = R_a/R_c$

$r_2 = R_e/R_c$

$r_3 = R_i/R_c$

R_a = rate of assimilation.

R_c = rate of crystallization.

R_e = rate of extrusion.

R_i = rate of intrusion.

There are four assumptions in the equation above (Reagan et al., 1987):

1) rate ratios are constant.
2) elemental concentrations in intruded magma and assimilant do not change over time.
3) distribution coefficients are constant.
4) modeled magma systems remain homogeneous and in equilibrium.

Appendix F

Distribution Coefficients

A distribution coefficient (Kd)(also called partition coefficient) represents the concentration ratio of a trace element between two equilibrated phases. In the case of a magmatic system, Kds reflects the distribution of a trace element between a magma and the solid phases with which it coexists. The usual form of a distribution coefficient is as a ratio of solid/liquid such that ratios greater than one represent trace elements which prefer the solid and ratios less than one represent trace elements which prefer the liquid. The Kds used in this dissertation are divided into three groups: 1) mafic, 2) intermediate and 3) felsic. As a general rule, mafic Kds are used in models which involve batch melting of mantle material and fractional crystallization (FXL) of basaltic rocks to intermediate compositions. Intermediate Kds are used for FXL of andesitic rocks to rocks of dacitic composition, and felsic Kds are used for rhyolite models. Kds are compiled from Arth and Barker (1976), Dostal et al. (1983), Drake and Weill (1975), Fujimaki and Tatsumoto (1984), Green and Pearson (1985), Harrison (1981), Irving and Frey

(1984), Nash and Crecraft (1985), Nicholls and Harris (1980), Villemant et al. (1°81) and Watson (1980).

Distribution coefficients for Ni in olivine and clinopyroxene are temperature dependent and are calculated with the following mineral-melt linear least-squares regression equations (Nielsen, 1985; Nielsen and Dungan, 1983):

$$\ln K = a/T(K) + b \qquad \text{(F-1)}$$

Where:

K = equilibrium constant.

T = temperature in degrees Kelvin.

a = constant.

b = constant.

For olivine:

a = 11230

b = -5.74

For clinopyroxene:

a = 22719

b= -14.65

Equation F-1 is in MODULUS (see Appendix E). When modeling, a geologically reasonable temperature is placed in MODULUS and all temperature dependent Kds are calculated for that temperature automatically using equation F-1.

Abbreviations used in Table F-1, below, are: ol=

olivine, opx= orthopyroxene, cpx= clinopyroxene, plag= plagioclase, amp= amphibole, grn= garnet, mgt= magnetite, ilm= ilmenite, zir= zircon, apa= apatite, sph= sphene, rut= rutile, bio= biotite, ksp= potassium feldspar, qtz= quartz, crd= cordierite and aln= allanite.

Table F-1

Partition Coefficients	MAFIC				
	-----> (primary phases):				
	oli 1	opx 1	cpx 1	plg	amp
Na	0.02	0.02	0.27	50	0.75
K	0.007	0.014	0.011	0.17	0.96
Rb	0.01	0.02	0.02	0.13	0.2
Sr	0.015	0.02	0.1	2	0.6
Cs	0.0004	0.02	0.01	0.025	0.1
Ba	0.01	0.013	0.005	0.25	0.7
Th	0.02	0.13	0.02	0.05	0.05
U	0.04	0.007	0.05	0.06	0.15
La	0.00001	0.007	0.07	0.15	0.2
Ce	0.00001	0.008	0.1	0.12	0.26
Nd	0.00007	0.01	0.22	0.08	0.4
Sm	0.0006	0.02	0.4	0.067	0.7
Eu	0.001	0.02	0.4	0.35	0.8
Tb	0.002	0.05	0.5	0.06	0.8
Yb	0.02	0.15	0.6	0.07	0.6
Lu	0.016	0.18	0.6	0.06	0.5
P	0.043	0.014	0.009	0	0
Sc	0.3	1	2	0.04	1.5
Ti	0.02	0.1	0.4	0.04	1.5
Y	0.01	0.2	0.5	0.03	1
Zr	0.01	0.03	0.1	0.01	1.5
Nb	0.01	0.15	0.1	0.01	0.8
Hf	0.01	0.03	0.1	0.01	1.5
Ta	0.01	0.15	0.1	0.01	0.8
V	0.05	0.3	1.2	0	3.5
Cu	0.37	0.8	2	0.01	0.5
Zn	0.95	0.5	0.41	0.43	0.55
Pb	0	0	0	0.45	0
Ga	0	0	0	0	0
Cr	1	0	0	0.001	15
Mg	0	0	0	0	10
Mn	0	2	0	0	1
Fe	0	0	0	0	10
Co	0	3	0	0.001	7
Ni	0	3	0	0.001	7

Table F-1 continued

Partition Coefficients	MAFIC			<-----	-----> (accessory phases)		
	grn	apa	sph	rut 1,2,4	mgt 1	ilm 1	zir 1,3
Na	0.01	0	0	0	0	0	0
K	0.02	0	0	0	0	0	0
Rb	0.04	0	0	0	0	0	0
Sr	0.012	5	100	0	0	0	0
Cs	0.03	0	0	0	0	0	0
Ba	0.02	0	1	0	0	0	0
Th	0.001	1.5	130	0	0	0	50
U	0.001	0.4	0	0	0	0	10
La	0.03	7	32	0	0	0	0.08
Ce	0.03	15	60	0	0	0	0.1
Nd	0.087	12	180	0	0	0	0.2
Sm	0.22	14	200	0	0	0	0.4
Eu	1	13	120	0	0	0	1.25
Tb	3	11	210	0	0	0	50
Yb	5	7	190	0	0	0	138
Lu	5.5	5	115	0	0	0	170
P	0.15	1000	0	0			
Sc	5	0.04	40	0	2	0	1
Ti	0.3	0	0	0	7.5	0	0
Y	2	3	30	0	0.2	0	60
Zr	0.3	0.12	65	0	0.1	0	0
Nb	0.1	0	6	20	0.7	2.3	0.6
Hf	0.3	0.12	65	0	0.1	0	0
Ta	0.1	0	17	20	0.8	2.7	0.6
V	0.27	0	0	10	25	0	0
Cu	0	0	0	0	4.2	0	0
Zn	0	0	0	0	12	0	0
Pb	0	0	0	0	0	0	0
Ga	0	0	0	0	0	0	0
Cr	17.5	0	0	1	0	0	0
Mg	0	0	0	0	0	0	0
Mn	0	0	0	0	2	1	0
Fe	0	0	0	1	0	0	0
Co	0	0	0	0	10	10	0
Ni	0	0	0	0	10	10	0

Table F-1 continued

Partition Coefficients	INTERMEDIATE					
-----> (primary phases):	oli 1	opx 1	cpx 1	plg	amp	bio
Na	0.02	0.06	0.11	1.5	0.08	0.1
K	0.007	0.001	0.01	0.19	0.01	3.5
Rb	0.01	0.003	0.03	0.05	0.01	3.3
Sr	0.015	0.01	0.52	3	0.02	0.12
Cs	0.0004	0.3	0.01	0.05	0.02	2.4
Ba	0.01	0.003	0.13	0.4	0.04	10
Th	0.02	0.15	0.03	0.05	0.01	0.3
U	0.04	0.006	0.03	0.006	0.4	0.02
La	0.00001	0.1	0.2	0.08	0.23	0.03
Ce	0.00001	0.15	0.4	0.2	0.9	0.04
Nd	0.00007	0.22	1.1	0.17	2.8	0.04
Sm	0.0006	0.25	1.67	0.1	4	0.06
Eu	0.001	0.17	1.5	0.8	3.5	0.15
Tb	0.002	0.65	2.4	0.085	6	0.16
Yb	0.02	0.85	2	0.08	5	0.18
Lu	0.016	0.9	1.5	0.06	4.5	0.2
P	0.043	0	0	0	0	0
Sc	0.3	7	22	0.1	10	10
Ti	0.02	0.25	0.4	0.05	3	1.5
Y	0.01	0.45	1.5	0.06	2.5	0.03
Zr	0.04	0.08	0.25	0.03	1.4	2
Nb	0.01	0.35	0.3	0.03	1.3	5
Hf	0.04	0.08	0.25	0.03	1.4	2
Ta	0.01	0.35	0.3	0.03	1.3	5
V	0.05	6	1.1	0.01	32	50
Cu	0.37	0	0	0	0	0
Zn	0.95	0.9	0	0	7	20
Pb	0	0	0	0.6	0	0.7
Ga	0	0	0	0	0	0
Cr	1	0	0	0.001	15	0
Mg	0	0	0	0	10	0
Mn	0	2	0	0	1	0
Fe	0	0	0	0	10	0
Co	0	3	0	0.001	7	0
Ni	0	3	0	0.001	7	0

Table F-1 continued

Partition Coefficients INTERMEDIATE	grn	qtz	<----- crd	-----> mgt 1	(accessory phases) ilm 1	zir 1,3
Na	0	0	0	0	0	0
K	0	0	0	0	0	0
Rb	0.01	0	0	0	0	0
Sr	0.15	0	1.3	0	0	0
Cs	0.01	0	0	0	0	0
Ba	0.015	0	0.62	0	0	0
Th	0.02	0	1.85	0.4	0.4	100
U	0	0	1	0.1	0	0
La	0.35	0	0.9	0	0	2
Ce	0.35	0	0.85	0	0	2.5
Nd	0.5	0	0.92	0	0	2.2
Sm	2.6	0	0.86	0	0	3.1
Eu	1.5	0	0.32	0	0	3.5
Tb	35	0	0.45	0.1	0.1	100
Yb	40	0	0.97	0.1	0.1	200
Lu	30	0	1.19	0.1	0.1	200
P	0	0	0	0	0	0
Sc	11	0	0.47	8	8	60
Ti	0.5	0	1	9	50	50
Y	11	0	1	0.5	0.1	60
Zr	0.5	0	1	0.5	0.6	0
Nb	0.5	0	1	0.7	2.3	50
Hf	0.5	0	1.2	0.5	0.7	0
Ta	0.5	0	1	0.8	2.7	50
V	8	0	5.5	30	12	0
Cu	0	0	1	0	0	0
Zn	0	0	4	0	0	0
Pb	0	0	1	0	0	0
Ga	0	0	1	0	0	0
Cr	17.5	0	1.66	0	0	0
Mg	0	0	500	0	0	0
Mn	0	0	5	2	1	0
Fe	0	0	100	0	0	0
Co	0	0	13.33	10	10	0
Ni	0	0	1.9	10	10	0

Table F-1 continued

Partition Coefficients	INTERMEDIATE				
	aln	apa	sph	rut 1,2,4	ksp
Na	0	0	0	0	1
K	0	0	0	0	1.4
Rb	0	0	0	0	0.35
Sr	0	0	100	0	4
Cs	0	0	0	0	0.2
Ba	0	0	1	0	5
Th	1500	2	130	0	0.01
U	0	0	0	0	0.005
La	2500	20	32	0	0.05
Ce	2000	35	60	0	0.04
Nd	1700	57	180	0	0.025
Sm	1300	63	200	0	0.02
Eu	800	30	120	0	1.1
Tb	500	20	210	0	0.006
Yb	100	25	190	0	0.01
Lu	100	25	115	0	0.006
P	0	1000	0	0	0
Sc	60	0	40	0	0.02
Ti	50	0.1	0	0	0.05
Y	100	20	30	0	0.1
Zr	2	0.1	65	0	0.03
Nb	2	0.1	6	20	0.05
Hf	2	0.1	65	0	0.03
Ta	2	0.1	17	20	0.05
V	0	0	0	10	0.01
Cu	0	0	0	0	0
Zn	0	0	0	0	0
Pb	0	0	0	0	2.5
Ga	0	0	0	0	0
Cr	0	0	0	1	0
Mg	0	0	0	0	0
Mn	0	0	0	0	0
Fe	0	0	0	1	0
Co	0	0	0	0	0
Ni	0	0	0	0	0

Table F-1 continued

Partition Coefficients FELSIC					
-----> (primary phases):	opx 1	cpx 1	plg	amp	bio
Na	0.06	0.11	1.5	0.08	0.1
K	0.001	0.01	0.19	0.01	3.5
Rb	0.003	0.03	0.04	0.01	2.2
Sr	0.01	0.52	4	0.02	0.12
Cs	0.3	0.01	0.05	0.02	2.4
Ba	0.003	0.13	0.3	0.04	6
Th	0.15	0.03	0.05	0.01	0.5
U	0.006	0.01	0.006	0.4	0.02
La	0.1	0.3	0.3	0.33	0.11
Ce	0.15	0.5	0.25	1.5	0.32
Nd	0.22	1.1	0.2	4.3	0.3
Sm	0.25	1.67	0.13	7.8	0.25
Eu	0.17	1.5	1.5	5	0.25
Tb	0.65	1.8	0.6	12	0.35
Yb	0.85	1.5	0.05	8	0.44
Lu	0.9	1.5	0.05	5.5	0.3
P	0	0	0	0	0
Sc	7	22	0.04	10	15
Ti	0.4	0.7	0.05	7	2.5
Y	1	4	0.1	6	0.03
Zr	0.2	0.6	0.04	1.4	2
Nb	0.15	0.4	0.05	1.5	5
Hf	0.2	0.6	0.04	1.4	2
Ta	0.15	0.4	0.05	1.5	5
V	6	1.1	0.01	32	50
Cu	0	0	0	0	0
Zn	0.9	0	0	7	20
Pb	0	0	0.6	0	0.7
Ga	0	0	0	0	0
Cr	0	0	0.2	0	19
Mg	0	0	0	0	0
Mn	2	0	0	0	0
Fe	0	0	0	0	0
Co	3	0	0	0	51
Ni	3	0	0	0	5

Table F-1 continued

Partition Coefficients FELSIC	gnt	qtz	<----- crd	-----> mgt 1	(accessory phases) ilm 1	zir 1,3
Na	0	0	0	0	0	0
K	0	0	0	0	0	0
Rb	0.01	0	0	0	0	0
Sr	0.15	0	1.3	0.15	0	0
Cs	0.01	0	0	0	0	0
Ba	0.015	0	0.62	0	0	0
Th	0.02	0	1.85	0.4	0.4	100
U	0	0	1	0.1	0	0
La	0.35	0	0.9	0	0	2
Ce	0.35	0	0.85	0	0	2.5
Nd	0.5	0	0.92	0	0	2.2
Sm	2.6	0	0.86	0	0	3.1
Eu	1	0	0.32	0	0	3.5
Tb	35	0	0.45	0.1	0.1	100
Yb	40	0	0.97	0.1	0.1	200
Lu	30	0	1.19	0.1	0.1	200
P	0	0	0	0	0	0
Sc	20	0	0.47	8	8	60
Ti	1.2	0	1	12.5	50	50
Y	35	0	1	2	0.1	60
Zr	1.2	0	1	0.8	0.7	0
Nb	0.5	0	1	5	3	50
Hf	1.2	0	1.2	0.8	0.7	0
Ta	0.5	0	1	5	3	50
V	8	0	5.5	30	12	0
Cu	0	0	1	0	0	0
Zn	0	0	4	0	0	0
Pb	0	0	1	0	0	0
Ga	0	0	1	0	0	0
Cr	0	0	1.66	0	0	0
Mg	0	0	500	0	0	0
Mn	0	0	5	20	1	0
Fe	0	0	100	0	0	0
Co	0	0	13.33	20	10	0
Ni	0	0	1.9	20	10	0

Table F-1 continued

Partition Coefficients FELSIC	aln	apa	sph	rut 1,2,4	ksp
Na	0	0	0	0	1
K	0	0	0	0	1.4
Rb	0	0	0	0	0.35
Sr	100	2	100	0	4
Cs	0	0	0	0	0.2
Ba	0	2	1	0	6
Th	1500	0	130	0	0.01
U	0	0	0	0	0.005
La	2500	20	32	0	0.05
Ce	2000	35	60	0	0.04
Nd	1700	57	180	0	0.025
Sm	1300	63	200	0	0.02
Eu	800	30	120	0	1.1
Tb	500	20	210	0	0.006
Yb	100	25	190	0	0.01
Lu	100	25	115	0	0.006
P	0	1000	0	0	0
Sc	60	0	40	0	0.02
Ti	50	0.1	0	0	0.05
Y	100	40	150	0	0.1
Zr	2	0.1	65	0	0.1
Nb	2	0.1	500	20	0.05
Hf	10	0.1	65	0	0.1
Ta	2	0.1	800	20	0.05
V	0	0	0	10	0.01
Cu	0	0	0	0	0
Zn	0	0	0	0	0
Pb	0	0	0	0	2.5
Ga	0	0	0	0	0
Cr	0	0	0	1	0
Mg	0	0	0	0	0
Mn	0	0	0	0	0
Fe	0	0	0	1	0
Co	0	0	0	0	0
Ni	0	0	0	0	0

References

Allegre, C.J. and Minster, J.F., 1978. Quantitative models of trace element behavior in magmatic processes. Earth Planet. Sci. Lett. 38: 1-25.

Arculus, R.J., 1987. The significance of source versus process in the tectonic controls of magma genesis. J. Volc. Geotherm. Res. 32: 1-12.

Armstrong, R.A., Compston, W., Retief, E.A. and Welke, H.J., 1986. Ages and isotopic evolution of the Ventersdorp volcanics. Geocongress '86, Extended Abstracts, Geol. Soc. S. Africa, Johannesburg: 89-92.

Armstrong, N.V., Hunter, D.R. and Wilson, A.H., 1982. Stratigraphy and petrology of the Archean Nsuze Group, northern Natal and southeastern Transvaal, South Africa. Precamb. Res. 19: 75-107.

Armstrong, N.V., Wilson, A.H. and Hunter, D.R., 1986. The Nsuze Group, Pongola Sequence, South Africa: geochemical evidence for Archean volcanism in a continental setting. Precamb. Res. 34: 175-203.

Arth, J.G. and Barker, F., 1976. Rare-earth partitioning between hornblende and dactic liquid and implications for the genesis of trondhjemitictonalitic magmas. Geology, 4: 534-536.

Atherton, M.P., Sanderson, M.L., Warden, V. and McCourt, W.J., 1985. The volcanic cover: chemical composition and the origin of the magmas of the Calipuy Group: In: W. S. Pitcher and M. P. Atherton (Editors), Magmatism At A Plate Edge, The Peruvian Andes. Halsted Press, New York: pp 273-284.

Ballard, S. and Pollack H.N., 1988. Modern and ancient geotherms beneath southern Africa. Earth Planet. Sci. Lett., 88: 132-142.

Ballard, S. and Pollack, H.N., 1987. Diversion of heat by Archean cratons: A model for southern Africa. Earth Planet. Sci. Lett., 85: 253-264.

Barker, O.B., 1979. A contribution to the geology of the Soutpansberg Group, Waterberg Supergroup, northern Transvaal. M.S. Thesis, University of Witwatersrand, South Africa (unpublished): 116 pp.

Barton, J.M., 1979. The chemical compositions, Rb-Sr isotopic systematics and tectonic setting of certain post-kinematic mafic igneous rocks, Limpopo Mobile Belt, southern Africa. Precambrian Res., 9: 57-80.

Basaltic Volcanism on the Terrestrial Planets, 1981, Pergamon Press, New York: 1286 pp.

Beswick, A.E. and Soucie, G., 1978. A correction procedure for metasomatism in an Archean greenstone belt. Precamb. Res, 6: 235-248.

Boryta, M.D., 1988. Geochemistry of granulite facies meta--igneous rocks from the central zone of the Limpopo Mobile Belt, South Africa. New Mexico Institute of Mining and Technology, M.S. Thesis (unpublished).

Bowen, M.P., 1984. The petrogenesis of the volcanic rocks of the Witwatersrand Triad in the Klerksdorp area, Transvaal. Unpublished M.S. thesis, Rhodes University, Grahamstown, South Africa: 204 pp.

Bowen, T.B., Marsh, J.S., Bowen, M.P. and Eales, H.V., 1986. Volcanic rocks of the Witwatersrand Triad, South Africa, I. Precambrian Res., 31: 297-324.

Boyd, F.R., 1987. High- and low-temperature garnet peridotite xenoliths and their possible relation to the lithosphere-asthenosphere boundary beneath southern Africa. In: P.H.Nixon (Editor), Mantle Xenoliths. John Wiley and Sons, New York.

Boyd, F.R. and Gurney, J.J., 1986. Diamonds and the African lithosphere. Science, 232: 472-476.

Burger, A.J. and Walraven, F., 1976. Summary of age determinations carried out during the period April 1975 to March 1976. Ann. Geol. Surv. S. Africa, 11: 323-329.

Burke, K. and Kidd, W.S.F., 1978. Were Archean continental geothernal gradients much steeper than those of today? Nature, 272: 240-241.

Burke, K., Kidd, W. F. S. and Kusky, T. M., 1986. Archean foreland basin tectonics in the Witwatersrand, South Africa. Tectonics, 5: 439-456.

Burke, K., Kidd, W.S.F., and Kusky, T., 1985. The Pongola structure of southeastern Africa: The world's oldest preserved rift?. J. Geodyn, 2: 35-49.

Burke, K., Kidd, W.S.F., and Kusky, T., 1985. Is the Ventersdorp rift system of southern Africa related to a continental collision between the Kaapvaal and Zimbabwe Cratons at 2.64 Ga ago? Tectonophys., 115: 1-24.

Butler, J.C. and Woronow, A., 1986. Discrimination amoung tectonic settings using trace element abundances of basalts. Jour. Geophys. Res., 91, B10: 10289-10300.

Button, A., 1981. The Pongola Supergroup. In: Precambrian of the Southern Hemisphere (Edited by Hunter, D.R.). Elsivier, Amsterdam: 882 pp.

Button, A., 1974. Low-potash pillow basalts in the

Pretoria Group, Transvaal Supergroup. Trans. Geol. Soc. S. Afr., 77: 99-104.

Button, A., 1973. A regional study of the stratigraphy and development of the Transvaal basin in the eastern and northeastern Transvaal. Ph.D. Dissertation, University of Witwatersrand, South Africa (unpublished): 352 pp.

Button, A. and Tyler, N., 1981. The character and economic significance of Precambrian paleoweathering and erosion surfaces in Southern Africa. Econ. Geol., 75: 676-699.

Cawthorn, R.G., Strong, D.F. and Brown, P.A., 1976. Origin of corundum-normative intrusive and extrusive magmas. Nature, 259: 102-104.

Clendenin, C.W., Charlesworth, E.G. and Maske, S., 1988. An early Proterozoic three-stage rift system, Kaapvaal craton, South Africa. Tectonophy., 145: 73-86.

Cocherie, A., 1986. Systematic use of trace element distribution patterns in log-log diagrams for plutonic suites. Geochim. Cosmochim. Acta, 50: 2517-2522.

Cole, J.N., 1984. Taupo-Rotura depression: an ensialic marginal basin of North Island, New Zealand. In: B. P. Kokelaar and M. F. Howells (Editors), Marginal Basin Geology. Blackwell Scient. Pubishers, Palo Alto, California: pp. 109-119.

Condie, K.C., 1985. Secular variation in the composition of basalts: an index to mantle evolution. Jour. Petrol., 26: 545-563.

Condie, K.C. and Allen, P., 1984. Origin of Archean charnockites from southern India. In: A. Kroner, G. N. Hanson and A. M. Goodwin (Editors), Archean Geochemistry. Springer-Verlag, New York: pp 182-203.

Condie, K.C. and Hunter, D.R., 1976. Trace element geochemistry of Archean granitic rocks from the Barberton Region, South Africa. Earth Planet. Sci. Lett., 29: 389-400.

Coertze, F.J. Burger, A.J., Walraven, F., Marlow, A.G. and MacCaskie, D.R., 1978. Field relations and age determinations in the Bushveld Complex. Trans. Geol. Soc. S. Africa, 81: 1-11.

DePaolo, D.J., 1985. Isotopic studies of processes in mafic magma chambers: I. The Kiglapait intrusion, Labrador. Jour. Petrol., 26: 925-951.

DePaolo, D.J., 1981. Trace element and isotopic effects of combined wall rock assimilation and fractional crystallization. Earth Planet. Sci. Letters, 53: 189-202.

Dostal, J., Dupuy, C., Carron, J.P., Le Guen de Kerneizon, M. and Maury, R.C., 1983. Partition coefficients of trace elements: application to volcanic rocks of St. Vincent, Wesst Indies. Geochem. Cosmochim. Acta, 47: 525-533.

Drake, M.J. and Weill, D.F., 1975. Partition of Sr, Ba, Ca, Y, Eu^{+2}, Eu^{+3}, and other REE between plagioclase feldspar and magmatic liquid: an experimental study. Geochim. Cosmochim. Acta, 39: 689-712.

Duncan, A.R., 1987. The Karoo Igneous Province - A problem area for inferring tectonic setting from basalt geochemistry. Jour. Volc. Geotherm. Res., 32: 13-34.

Dungan, M.A., Lindstrom, M.M., McMillan, N.J., Moorbath, S., Hoefs, J. and Haskin, L.A., 1986. Open system magmatic evolution of the Taos Plateau volcanic field, Northern New Mexico, 1. The petrology and geochemistry of the Servilleta basalt. J. Geophys. Res., 91: 5999-6028.

Dupuy, C., Marsh, J., Dostal, J., Michard, A. and Testa, S., 1988. Asthenospheric and lithospheric sources for Mesozoic dolerites from Liberia (Africa): Trace element and isotopic evidence. Earth Planet. Sci. Lett., 87: 100-110.

Elthon, D., 1983. Isomolar and isostructural pseudo-liquidus phase diagrams for oceanic basalts. Amer. Mineral., 68: 506-511.

Elthon, D. and Scarfe, C.M., 1984. High-pressure phase equilibria of a high-magnesia basalt and the genesis of primary oceanic basalts. Amer. Mineral., 69: 1-15.

Eriksson, P.G. and Twist, D., 1986. A note on a lahar deposit in the Hekpoort Formation, Transvaal sequence, near Pretoria. Trans. Geol. Soc. S. Afr., 89: 415-418.

Erlank, A.J., Marsh, J.S., Duncan, A.R., Miller, R.M., Hawkesworth, C.J., Betton, P.J. and Rex, D.C., 1984. Geochemistry and petrogenesis of the Etendeka Volcanic rocks from SWA/Namibia. Geol. Soc. S. Africa, Spec. Publ. 13: 195-245.

Floyd, P.A. and Winchester, J.A., 1978. Identification and discrimination of altered and metamorphosed volcanic rocks using immobile elements. Chem. Geol., 21: 291-306.

Fujimaki, H. and Tatsumoto, M. 1984. Partition coefficients of Hf, Zr, and REE between phenocrysts and groundmass. J. Geophys. Res., 89 (Supp): B662-B672.

Gill, J. B., 1981. Orogenic Andesites and Plate

Tectonics. Springer-Verlag, New York: 390 pp.

Gladney, E.S., 1980. Compilation of elemental concentration data for Nbs biological and environmental standard reference materials. Anal. Chim. Acta, 118: 385-396.

Gordon, M.B. and Hempton, M.R., 1986. Collision-induced rifting: The Grenville orogney and the Keweenawan rift of North America. Tectonophy., 127: 1-25.

Gorton, M.P., 1977. The geochemistry and origin of Quaternary volcanism in the New Hebrides. Geochim. Cosmochim. Acta, 41: 1257-1270.

Govindaraju, K., 1984. 1984 compilation of working values and sample descriptions for 170 international reference samples of mainly silicate rocks and minerals. Geostand. Newslett., 8: Special Issue.

Govindaraju, K., 1980. Report (1980) on three GIT-IWG rock reference samples: anorthosite form Greenland, AN-G: basalte d'Essey-la Cote, BE-N; granite de Beauvoir, MA-N: Geostand. Newslett., 4: 49-138.

Grandstaff, D.E., Edelman, M.J., Foster, R.W., Zbinden, E. and Kimberly, M.M., 1986. Chemistry and mineralogy of Precambrian paleosols at the base of the Dominion and Pongola Groups (Transvaal, South Africa). Precamb. Res., 32: 97-131.

Green, T.H. and Pearson, N.J., 1985. Experimental determination of REE partition coefficients between amphibole and basaltic to andesitic liquids at high pressure. Geochim. Cosmochim. Acta, 49: 1465-1468.

Grobler, N.J., Kleynhaus, E.P.J., Botha, P.J. and DeBruiyn, H., 1982. Distinction between lavas of the Allanridge Andesite and Rietgat Formations in the northern Cape and western Transvaal. Trans. Geol. Soc. S. Africa, 85: 117-126.

Grove, T.L. and Baker, M.B., 1984. Phase equilibrium controls on the tholeiitic versus calc-alkaline differentiation trends. Jour. Geophys. Res., 89: 3253-3274.

Groves, D.I., Ho, S.E., Rock, N.M.S., Barley, M.E. and Muggeridge, M.T., 1987. Archean cratons, diamonds and platinum: Evidence for coupled long-lived crust-mantle systems. Geology, 15: 801-805.

Hamilton, J.O., 1977. Sr isotope and trace element studies of the Great Dyke and Bushveld mafic phase and their relation to early Proterozoic magma genesis in southern Africa. Jour. Petro., 18: 24-52.

Hargraves, R.B., 1986. Faster spreading or greater ridge length in the Archean?. Geology, 14: 750-

752.

Harrison, W.J., 1981. Partitioning of REE between minerals and coexissting melts during partial melting of a garnet lherzolite. Amer. Mineral., 66: 242-259.

Hawkesworth, C.J., Marsh, J.S., Duncan, A.R., Erlank, A.S. and Norry, M. J., 1984. The role of continental lithosphere in the generation of the Karoo volcanic rocks: evidence from combined Nd and Sr isotope studies. Geol. Soc. S. Africa, Spec. Publ. 13: 341-354.

Hawkesworth, C.J., Rogers, N.W., van Calsteren, P.W.C. and Menzies, M.A., 1984. Mantle enrichment processes. Nature, 311: 331-335.

Hegner, E., Kroner, A. and Hofmann, A.W., 1984. Age and isotope geochemistry of the Archaean Pongola and Usushwana suites in Swaziland, southern Africa: A case for crustal contamination of mantle derived magma. Earth Planet. Sci. Letters, 70: 267-279.

Hole, M.J., Saunders, A.D., Marriner, G.F. and Tarney, J., 1984. Subduction of pelagic sediments: implications for the origin of Ce-anomalous basalts from the Mariana Islands. J. Geol. Soc. London, 141: 453-472.

Humphris, S.E., Morrison, M.A. and Thompson, R.N., 1978. Influence of rock crystallization history upon subsequent lanthanide mobility during hydrothermal alteration of basalts. Chem. Geol., 23: 125-137.

Hunter, D.R., 1981. Precambrian of the Southern Hemisphere. Elsevier, New York, 882 pp.

Hunter, D.R., 1974. Crustal development in the Kaapvaal Craton, II. The Proterozoic. Precam. Res., 1: 295-326.

Irvine, T.N. and Baragar, W.R.A., 1971. A guide to the chemical classification of the common volcanic rocks. Can. J. Earth. Sci., 8: 523-548.

Irving, A.J. and Frey, F., 1984. Trace element abundances in megacrysts and their host basalts: constraints on partition coefficients and megacryst genesis. Geochim. Cosmochim. Acta, 48: 1201-1221.

Jacobs, J.W., Korotev, R.L., Blanchard, D.P. and Haskins, L.A., 1977. A well-tested procedure for instrumental neutron activation analysis of silicate rocks and minerals. Radioanalyt. Chem., 40: 93-114.

Jensen, H., 1975. The Soutpansberg trough (northern Transvaal)- An aulacogen. Trans. Geol. Soc. S.

Afr., 78: 129-136.

Jensen, L.S., 1976. A new cation plot for classifying subalkaline volcanic rocks. Ont. Div. Mines, Misc. Paper, 66: 22 pp.

Kay, S.M., Kay, R.W. and Citron, G.P., 1982. Tectonic controls on tholeiitic and calc-alkaline magmatism in the Aleutian arc. Jour. Geophys. Res., 87: 4051-4072.

Knoper, M., 1988. MODULUS: Spreadsheet modeling program using Lotus. (Manuscript in prep.).

Levine, R.I. and Rubin, D.S., 1980. Applied Elementary statistics. Printice-Hall, Englewood, N.J.: 579 pp.

Lindstrom, D.J. and Korotev, R.L., 1982. TEABAGS: computer programs for instrumental neutron activation analysis. Radioanalyt. Chem., 70: 439-458.

Ludden, J. and Gelinas, L., 1982. Archean metavolcanics from the Rouyn-Noranda district, Abitibi Greenstone Belt, Quebec. Mobility of trace elements and petrographic constraints. Can. J. Earth Sci., 19: 2276-2287.

Ludden, J. and Thompson, G., 1979. An evaluation of the behavior of the rare earth elements during the weathering of sea-floor basalt. Earth Planet.

Sci. Lett., 43: 85-92.

MacGregor, I.D. and Manton, W.I., 1986. Roberts Victor Eclogite: Ancient oceanic crust. Jour Geophy. Res., 91: 14063-14079.

Menzies, M., Seyfried, W.E. and Blanchard, K., 1979. Experimental evidence of rare earth element immobility in greenstones. Nature, 282: 398-399.

Marsh, J.S., 1987. Basalt geochemistry and tectonic discrimination within continental flood basalt provinces. Jour. Volc. Geogtherm. Res., 32: 35-49.

McIver, J.R., Cawthorn, R.G. and Wyatt, B.A., 1982. The Ventersdorp Supergroup-the youngest komatiitic sequence in southern Africa. In: N.T. Arndt and E.G. Nisbet (Editors), Komatiites. Allen and Unwin, Boston: pp 81-90.

Merriman, R.J., Bevins, R.E. and Ball, T.K., 1986. Petrological and geochemical variations within the Tal y Fan intrusion: a study of element mobility during low-grade metamorphism with implications for petrotectonic modeling. J. Petrol., 27: 1409-1436.

Miyashiro, A., 1974. Volcanic rock series in island arcs and active continental margins. Amer. Jour. Sci., 274: 321-355.

Myers, R.E., Palmer, K., McCarthy, T.S., Cawthorn, R.G., Myers, M., Moloi, N. and Hewitt, T., 1987. Geochemical stratigraphy of the Klipriviersberg flood basalts, South Africa: insight into the mechanisms of flood basalts generation and eruption. Abstract vol., Intern. Conference on Proterozoic Geochemistry, Lund, Sweden, 1987: 66.

Nash, W.P. and Crecraft, H.R., 1985. Partition coefficients for trace elements in silicic magmas. Geochim. Cosmochim. Acta, 49: 2309-2322.

Nicholls, I.A. and Harris, K.L., 1980. Experimental rare earth element partition coefficients for garnet, clinopyroxene and amphibole coexisting with andesitic and basaltic liquids. Geochim. Cosmochim. Acta, 44: 287-308.

Nielsen, R.L., 1985. EQUIL: a program for the modeling of low-pressure differentiation process in natural mafic bodies. Comput. Geoscience, 11: 531-546.

Nielsen, R.L. and Dungan, M.A., 1983. Low pressure mineral-melt equilibria in natural anhydrous mafic systems. Contrib. Mineral. Petro., 84: 310-326.

Norrish, K. and Chappel, B.W., 1977. X-ray fluorescence. In: J. Zussman (Editor), Physical Methods in Determitive Mineralogy. Academic Press, New York: pp 235-262.

Norrish, K. and Hutton, J.T., 1969. An accurate X-ray spectrographic method for analysis of a wide range of geological samples. Geochim. Cosmochim. Acta, 33: 431-453.

O'Hara, M.J., 1977. Geochemical evolution during fractional crystallization of a periodically refilled magma chamber. Nature, 266: 503-507.

Paces, T.B., Bornhorst, T.J. and Bell, K., 1986. Primitive continental rift tholeiites (abs.). Geol. Soc Amer. Abstr. with Prog., 18: 713.

Pearce, J.A., 1983. Role of the sub-continental lithosphere in magma genesis at active continental margins. In: C.J. Hawkesworth and M.J. Norry (Editors), Continental Basalts and Mantle Xenoliths. Shiva Press, Nantwich, U.K.: pp 230-249.

Pearce, J.A., 1982. Trace element characteristics of lavas from destructive plate boundaries. In: R.S. Thorpe (Editor), Andesites. John Wiley and Sons, New York, N.Y.: pp 525-548.

Pearce, J.A. and Cann, J.R., 1973. Tectonic setting of basic volcanic rocks determined using trace-element analysis. Earth Planet. Sci. Letters, 19: 290-300.

Peccerillo, A. and Taylor, S.R., 1976. Geochemistry of

Eocene calc-alkaline volcanic rocks from the Kastasmonu area, northern Turkey. Contrib. Mineral. Petrol., 58: 63-81.

Pharaoh, T.C. and Pearce, J.A., 1984. Geochemical evidence for the geotectonic setting of early Proterozoic metavolcanic sequences in Lapland. Precambrian Res., 25: 283-308.

Phillips, G.N., 1986. Metamorphism of shales in the Witwatersrand Goldfields. Information Circ. No. 192, Econ. Geol. Res. Unit, Univ. Witwatersrand, Johannesburg: 25 pp.

Pretorius, D.A., 1976. The nature of the Witwatersrand gold-uranium deposits. In: K. H. Wold (Editor), Handbook of Strata-bound and Stratiform Ore Deposits, 77. Elsevier, Amsterdam: pp 29-88.

Reagan, M.K., Gill, J.B., Malavassi, E. and Garcia, M.O., 1987. Changes in magma composition at Arenal volcano, Costa Rica, 1968-1985: Real-time monitoring of open-system differentiation. Bull. Volcanol., 49: 415-434.

Richardson, S.H. Gurney, J.J., Erlank, A.J. and Harris, J.W., 1984. Origin of diamonds in old enriched mantle. Nature, 310: 198-202.

Schweitzer, J. and Kroner, A., 1985. Geochemistry and petrogenesis of early Proterozoic intracratonic volcanic rocks of the Ventersdorp Supergroup, South Africa. Chem. Geol., 51: 265-288.

Shervais, J.W., 1982. Ti-V plots and the petrogenesis of modern and ophiolitic lavas. Earth Planet. Sci. Lett., 59: 101-118.

Shervais, J.W., Taylor, L.A., Lugmair, G.W., Clayton, R.N., Mayeda, T.K. and Korotev, R.L., 1988. Early Proterozoic oceanic crust and the evolution of subcontinental mantle: Eclogites and related rocks from southern Africa. Bull. Geol. Soc. Amer., 100: 411-423.

South African Committee for Stratigraphy (SACS), 1981. Stratigraphy of South Africa. Part 1 (Comp. L.E. Kent). Lithostratigraphy of the Republic of South Africa, South West Africa/Namibia, and the Republics of Bophuthatswana, Transkei and Venda. Handb. Geol. Survey S. Africa, 8: 690 pp.

Stanistreet, I.G., McCarthy, T.S., Charlesworth, E.G., Myers, R.E. and Armstrong, R.A., 1986. Pre-Transvaal wrench tectonics along the northern margin of the Witwatersrand basin, South Africa. Tectonophys., 131: 53-74.

Tankard, A.J., Jackson, M.P.A., Eriksson, K.A., Hobday, O.K., Hunter, D.R. and Minter, W.E.L., 1982. Crustal evolution of southern Africa. Springer-

Verlag, New York: 523 pp.

Taylor, S.R. and McClennan, S.M., 1985. The continental crust: its composition and evolution. Blackwell Sci. Publ., Boston: 312 pp.

Thompson, R.N., 1982. Magmatism of British Tertiary Volcanic Province. Scot. J. Geol., 18: 49-107.

Thompson, R.N., Morrison, M.A., Dickin, A.P. and Hedry, G.L., 1983. Continental flood basalts... arachnids rule OK? In: C.J. Hawkesworth and M.J. Norry (Editors), Continental Basalts and Mantle Xenoliths. Shiva Press, Nantwich, U. K.: pp 230-249.

Thompson, R.N., Dickin, A.P., Gibson, I.L. and Morrison, 1982. Elemental fingerprints of isotopic contamination of Hebridean Palaeocene mantle-derived magmas by Archean sial. Contrib. Mineral. Petrol., 79: 159-168.

Thornton, C.P. and Tuttle, O.F., 1960. Chemistry of igneous rocks: part 1, Differentiation index. Amer. Jour. Sci., 258: 664-684.

Tyler, N., 1979. Stratigraphy, geochemistry and correlation of the Ventersdorp Supergroup in the Derdepoort area, west-central Transvaal. Trans. Geol. Soc. S. Africa, 82: 133-147.

Tyler, N., 1979. The stratigraphy of the early

Proterozoic Buffalo Springs Group in th Thabazimbi area, west-central Transvaal. Trans. Geol. Soc. S. Afr., 82: 215-226.

Van Niekerk, C.B. and Burger, A.J., 1969. Lead isotopic data relating to the age of the Dominion Reef Lava. Trans. Geol. Soc. S. Africa., 72: 37-45.

Villemant, B., Jaffrezic, H., Joron, J.L. and Treuil, M., 1981. Distribution coefficients of major and trace elements; fractional crystallization in the alkali basalt series of Chaine des Puys (Massif Central, France). Geochim. Cosmochim. Acta, 45: 1997-2016.

Visser, J.N.J., Grobler, N.J., Joubert, C.W., Putgietor, C.D., McLaren, C.H. and Liebenberg, J., 1976. The Ventersdorp Group between Taung and Britstown, northern Cape Province. Ann. Geol. Surv. S. Africa, 11: 15-28.

Watchorn, M.B., 1980. The stratigraphic and sedimentological development of the Witwatersrand West Rand Basin in the Klerksdorp area. Econ. Geol. Res. Unit, Information Circ. No. 148: 9 pp.

Watchorn, M.B., 1981. Continental sedimentation and volcanism in the Dominion Group of the Western Transvaal: A review. Trans. Geol. Soc. S. Africa, 84: 67-73.

Watson, E.B., 1980. Some experimentally determined zircon/liquid partition coefficients for the rare earth elements. Geochim. Cosmochim. Acta, 44: 895-897.

Weaver, B.L. and Tarney, J., 1983. Chemistry of the sub-continental mantle: inferences from Archean and Proterozoic dykes and continental flood basalts. In: C. J. Hawkesworth and M. J. Norry (Editors), Continental Basalts and Mantle Xenoliths. Shiva Press, Nantwich, U. K.: pp 111-138.

Whitford, D.J., Nicholls, I.A. and Taylor, S.R., 1979. Spatial Variations in the geochemistry of Quaternary lavas across the Sunda Arc in Java and Bali. Contrib. Mineral. Petrol., 70: 341-356.

Whiteside, H.C.M., 1970. Volcanic rocks of the Witwatersrand Triad. In: T.N. Clifford and I.G. Gass (Editors), African Magmatism and Tectonics. Oliver and Boyd, Edinburgh: pp 78-87.

Wilks, M.E., 1988. The Himalayas - a modern analogue for Archean crustal evolution. Earth Planet. Sci. Lett., 87: 127-136.

Winchester, J.A. and Floyd, P.A., 1977. Geochemical discrimination of different magma series and their differentiation products using immobile elements. Chem. Geol., 20: 325-343.

Windley, B.F., 1984. The Archean-Proterozoic boundary. Tectonophys., 105: 43-53.

Winter, H. de la R., 1976. A lithostratigraphic classification of the Ventersdorp succession. Trans. Geol. Soc S. Africa, 79: 31-48.

Winter, H. de la R., 1986. A cratonic-foreland model for Witwatersrand basin-development in a continental, back-arc, plate tectonic setting. Information Circ. No. 193, Econ. Geol. Res. Unit, Univ. Witwatersrand, Johannesburg: 36 pp.

Wood, D.A., 1980. The application of a Th-Hf-Ta diagram to problems of tectonomagmatic classification and to establishing the nature of crustal contamination of basaltic lavas of the British Tertiary volcanic province. Earth Planet. Sci. Letters, 50: 11-30.

Wood, D.A., 1979. A variably veined suboceanic upper mantle-Genetic significance for mid-ocean ridge basalts from geochemical evidence. Geology, 7: 499-503.

Wright, T.L. and Doherty, P.C., 1970. A linear-programming and least squares computer method for solving petrologic mixing problems. Geol. Soc.

Amer. Bull., 81: 1995-2007.

Wronkiewicz, D.J. and Condie, K.C., 1988. Geochemistry of sediments from the Pongola Supergroup, South Africa: Evidence for a 3.0Ga continental craton. (in press).

Wronkiewicz, D. and Condie, K.C., 1987. Geochemistry and Provenance of Archean shales from the Witwatersrand Supergroup, Southern Transvaal, South Africa. Geochim. Cosmochim. Acta, (in press).

Wyatt, B.A., 1976. The geology and geochemistry of the Klipriviersberg volcanics, Ventersdorp Supergroup, south of Johannesburg. M.S. thesis, University of Witwatersrand, Johannesburg, South Africa: 178pp.

This dissertation is accepted on behalf of the faculty of the Institute by the following committee:

Advisor

25 July 1988

Date